[redacted]

NASA TECHNICAL MEMORANDUM

NASA TM X-1108

NASA TM X-1108

POSTFLIGHT EVALUATION OF ATLAS-CENTAUR AC-4 (Launched December 11, 1964)

by Staff of the Lewis Research Center

Lewis Research Center
Cleveland, Ohio

NATIONAL AERONAUTICS AND SPACE ADMINISTRATION • WASHINGTON, D. C. • JULY 1965

[redacted]

[redacted]

NASA TM X-1108

POSTFLIGHT EVALUATION OF ATLAS-CENTAUR AC-4

(Launched December 11, 1964)

By Staff of the Lewis Research Center

Lewis Research Center
Cleveland, Ohio

NATIONAL AERONAUTICS AND SPACE ADMINISTRATION

[redacted]

[redacted]

CONTENTS

[redacted]

[redacted]

[redacted]

[redacted]

I. SUMMARY

The Atlas-Centaur AC-4 vehicle (Atlas 146D, Centaur 4C) was successfully launched at 0925:02:548 EST on December 11, 1964 from ETR Complex 36A. Included on board the Centaur stage was a mass model Surveyor of 2090 pounds. The major mission objectives (see II. INTRODUCTION) were satisfied; however, because of the inability to control the position of the hydrogen propellant within the tank under near weightless conditions, some of the secondary test objectives were not accomplished.

The AC-4 Atlas-Centaur vehicle was launched on an azimuth of 105° East of true North and was programed to a flight azimuth of 102.5° East of true North. The Centaur guidance system injected the AC-4 upper stage into a near perfect 90-nautical-mile circular orbit (94.92 n. mi. apogee altitude, 88.20 n. mi. perigee altitude). This was the first flight with the inertial guidance system operating as closed loop; velocity errors were well within nominal values. To ensure structural integrity of the nosecone during higher atmospheric heating than on Centaur flights AC-2 and AC-3, thermal insulation was applied to the forward section of the AC-4 vehicle. This Thermalag insulation maintained the maximum skin temperatures well within prescribed limits. No structural difficulties or serious vibration levels were experienced by the vehicle; the altitude wind loadings at the time of launch were relatively low.

During the coast phase of the AC-4 Centaur flight, the 4-pound thrust of the ullage motors was insufficient to position the remaining liquid hydrogen in the bottom of the propellant tank. During the first vent, liquid hydrogen instead of ullage gas was bled from the tank; consequently, uncontrollable vehicle forces were set in motion. Excessive hydrogen vent losses and vehicle tumbling precluded successful restarting of the Centaur main engines. An important result of the flight is the realization that, on main engine cutoff after orbital flight has been obtained, kinetic energies may be present within the propellant that far overshadow the intermolecular forces within the fluid. This finding has considerable significance not only to future Centaur two-burn vehicles but to other space vehicles where propellant management in a near-weightless condition may be a requirement.

Trajectory analysis of the AC-4 flight has indicated a deficiency in the models used in the computation of the predicted thrust acceleration. This deficiency was similar to the results obtained from the AC-2 and AC-3 flights and appears to be related to the estimate of the base drag. The significance of this discrepancy is that the payload at injection for an operational Centaur vehicle (AC-15) may be increased approximately 45 pounds.

[redacted]

II. INTRODUCTION

The AC-4 Atlas-Centaur vehicle, which was successfully launched from ETR on December 11, 1964 at 9:25 a.m. EST was the fourth in a series of developmental flights. Ultimately the Atlas-Centaur vehicle will be used to place a Surveyor spacecraft on the moon. A payload of 2090 pounds was carried aboard AC-4, making it the first Atlas-Centaur to date to carry a mock payload of the Surveyor. The objectives of the flight were as follows.

PRIMARY TEST OBJECTIVES

(1) To demonstrate the structural integrity of the Atlas and Centaur vehicles during all powered phases of flight

(2) To demonstrate the system integrity of the guidance system

(3) To obtain data on the measuring accuracy of the guidance system during closed-loop flight

(4) To demonstrate that the guidance system provides proper discrete and steering signals to Atlas and Centaur flight control systems

(5) To verify the structural and thermal integrity of the Centaur nose fairings and insulation panels

(6) To verify the satisfactory performance of the insulation-panel and nose-fairing-jettison systems

SECONDARY TEST OBJECTIVES

(1) To demonstrate the restart capabilities of the Centaur main engine system in flight environment

(2) To obtain data on the following flight environments: pressures, temperatures, and vibration levels

(3) To verify the satisfactory operation of the Atlas-Centaur separation system

(4) To verify that the flight control system supplies the proper signal for attitude control and dynamic stability of the Centaur vehicle

(5) To demonstrate the capabilities of the coast motors and the attitude control system to retain the propellants in the proper attitude for engine restart

(6) To obtain data on the vehicle acceleration, propellant behavior and heat transfer, and propellant tank ullage temperatures and pressure histories during coast phase

(7) To obtain data on the performance of the H_2O_2 attitude control system, hydraulic system, pneumatic system, electrical system, radio-frequency systems (telemetry, Azusa, and C-band beacon), Centaur main engine system and all of the Atlas systems

(8) To obtain data on the launch-on-time capability (fixed launch azimuth of the Atlas-Centaur

(9) To demonstrate that the guidance equations and the associated trajectory parameters are satisfactory

(10) To obtain data on the capability of the Centaur to perform a retromaneuver

(11) To obtain data on the spacecraft environment during the launch-to-spacecraft separation phase of flight

(12) To verify the ability of the Centaur propulsion system to start in the flight environment and burn to guidance cutoff

(13) To obtain data on the orbital environments, terminal behavior, and general postmission performance of vehicle systems until loss of all data links

The coast motors in item (5) of the secondary objectives are two 2-pound thrust H_2O_2 propellant settling motors that burn continuously throughout the coast period. The spacecraft separation in item (11) of the secondary objectives was only a simulated event, which provided a terminal point for obtaining spacecraft environmental data.

The flight events and the Centaur, sustainer, and booster-stage weights are presented in tables II-I and II, respectively. A schematic diagram of the AC-4 flight is shown in figure II-1, and an illustration of the general arrangement of the Centaur stage is presented in figure II-2.

TABLE II-I. - SEQUENCE OF FLIGHT EVENTS[a]

Event	Nominal time (b)	Actual time
Lock LH_2 vent valve	T - 7	[c]T - 7.32
Programer start; 2-in. rise	T + 0	T + 0
Open LH_2 vent valve	T + 74	T + 74.5
BECO discrete	T + 150.36	[c]T + 148.81
Booster engine cutoff; close LH_2 vent valve	T + 150.46	T + 149.05
Jettison booster package	T + 153.46	T + 151.75
Open LH_2 vent valve	T + 160.36	T + 159.4
Jettison insulation panels	T + 200.36	T + 198.47
Start Centaur boost pumps	T + 209.36	T + 208.2
Unlatch nose fairings	T + 213.86	T + 211.89
Jettison nose fairing	T + 214.36	T + 212.38
SECO/VECO	T + 226.36	T + 224.25
Close LOX and LH_2 vent valves; start hydraulic recirculating pump	T + 226.46	T + 225.6
Atlas-Centaur separation	T + 228.86	T + 226.76
Fire retrorockets	T + 228.96	T + 226.86
LOX and LH_2 prestart; admit guidance for attitude control	T + 229.96	T + 227.9
First main engine start	T + 235.96	T + 233.8
Admit guidance for steering control	T + 239.96	T + 237.6
Main engine cutoff (MECO); ullage control engines on; admit guidance for attitude control	T + 573.4	T + 572.65
Open LH_2 vent valve	T + 615.4	T + 615.2
Close LH_2 vent valve	T + 2006.4	[c]T + 2005.47
Start boost pumps	T + 2010.4	T + 2010.1
LH_2 prestart; LOX prestart	T + 2045.4	T + 2044.8
Second MES; ullage control engines off; inhibit guidance	T + 2050.4	[c]T + 2049.75
Admit guidance for steering control	T + 2054.4	
Second MECO; inhibit fixed vector 2	T + 2104.4	T + 2103.8
Separate spacecraft	T + 2152.9	
Begin 180° turn	T + 2157.9	
End 180° turn; start retromaneuver thrust	T + 2387.9	
H_2O_2 "All Off"; open LOX and LH_2 vent valves	T + 3517.9	
End retromaneuver thrust	T + 3519.9	

[a]All symbols and abbreviations are defined in appendix A.

[b]Ref. 1.

[c]Ref. 2.

TABLE II-II. - WEIGHT SUMMARY

Centaur stage	Weight, lb
Basic hardware	
Body group	1159
Propulsion group	1284
Guidance group	328
Control group	136
Pressurization group	163
Electrical group	223
Separation equipment	185
Flight instrumentation	605
Miscellaneous equipment	380
Payload	2090
Total	6553
Jettisonable hardware	
Nose fairing	2052
Tank insulation	1278
Total	3330
Residuals	
Unburned LH_2	978
Unburned LOX	4712
GH_2	106
GO_2	143
H_2O_2	198
He	9
Ice	[a]12
Total	6158
Expendables	
Main impulse LH_2	3 906
Main impulse LOX	19 550
Ground vent, H_2	[a]15
Ground vent, O_2	[a]92
Inflight chill, LH_2	19
Inflight chill, LOX	19
Boost-phase vent, H_2	72
Boost-phase vent, O_2	[a]36
H_2O_2	[a]38
He	10
Ablated ice	50
Total	23 807
Total tanked weight	39 848
Ground vent[a]	- 107
Total Centaur weight at lift-off	39 741

Sustainer stage	Weight, lb
Basic hardware	
Interstage adapter	1537
Body group	2308
Separation and destruct systems	319
Propulsion group	1905
Prime power system	47
Hydraulic and pneumatic group	123
Electrical group	242
Guidance	235
Environmental control group	33
Instrumentation group	428
Total	7177
Residuals	
Trapped RP-1	496
Trapped LOX	515
Unburned main impulse RP-1	845
Unburned main impulse LOX	2537
Unburned lubrication oil	19
GN_2	2
GO_2	603
He	85
Total	5102
Total jettison	12 279
Flight expendables	
Main impulse RP-1	74 589
Main impulse LOX	169 013
Lubrication oil	176
Gaseous oxidizer vent	15
Sustainer thrust decay	73
Total	243 866
Ground expendables (2.63 sec)	
RP-1 expended	683
LOX expended	2278
Lubrication oil expended	3
Exterior frost dumped	50
LN_2 dumped	140
LOX overboard vent	40
Preignition GO_2 loss	450
Total	3644

Atlas booster stage	Weight, lb
Basic hardware	
Body group	1811
Separation and destruct systems	102
Propulsion group	4017
Hydraulic and pneumatic group	122
Electrical group	49
Instrumentation group	90
Total	6191
Residuals	
Trapped RP-1	500
Trapped LOX	558
He	84
Unburned lubrication oil	24
Total	1166
Total tanked weight	267 146
Ground run	- 3 644
Total Atlas weight at lift-off	263 502

[a]Ref. 2.

[redacted]

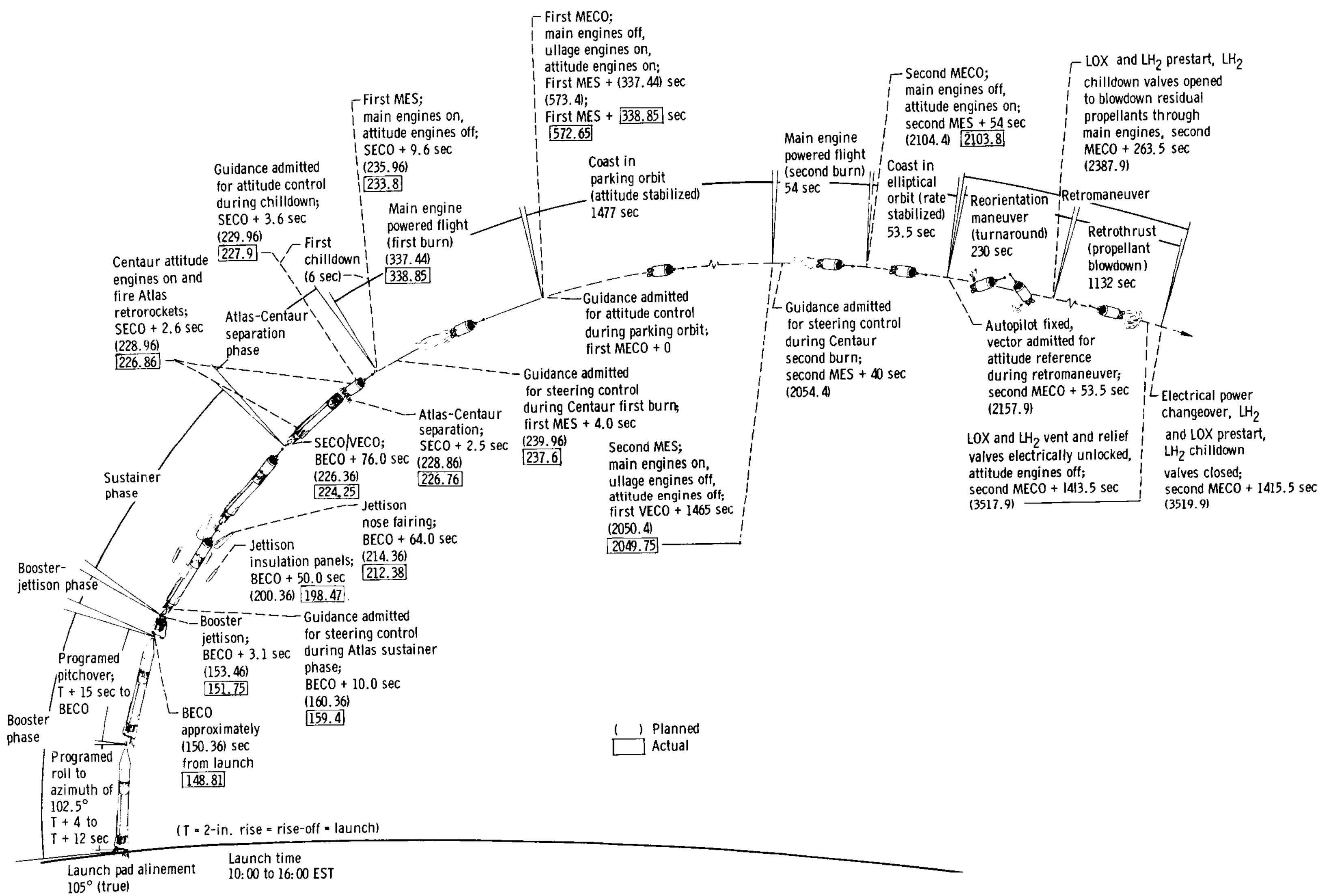

Figure II-1. - AC-4 flight compendium (ref. 3).

[redacted]

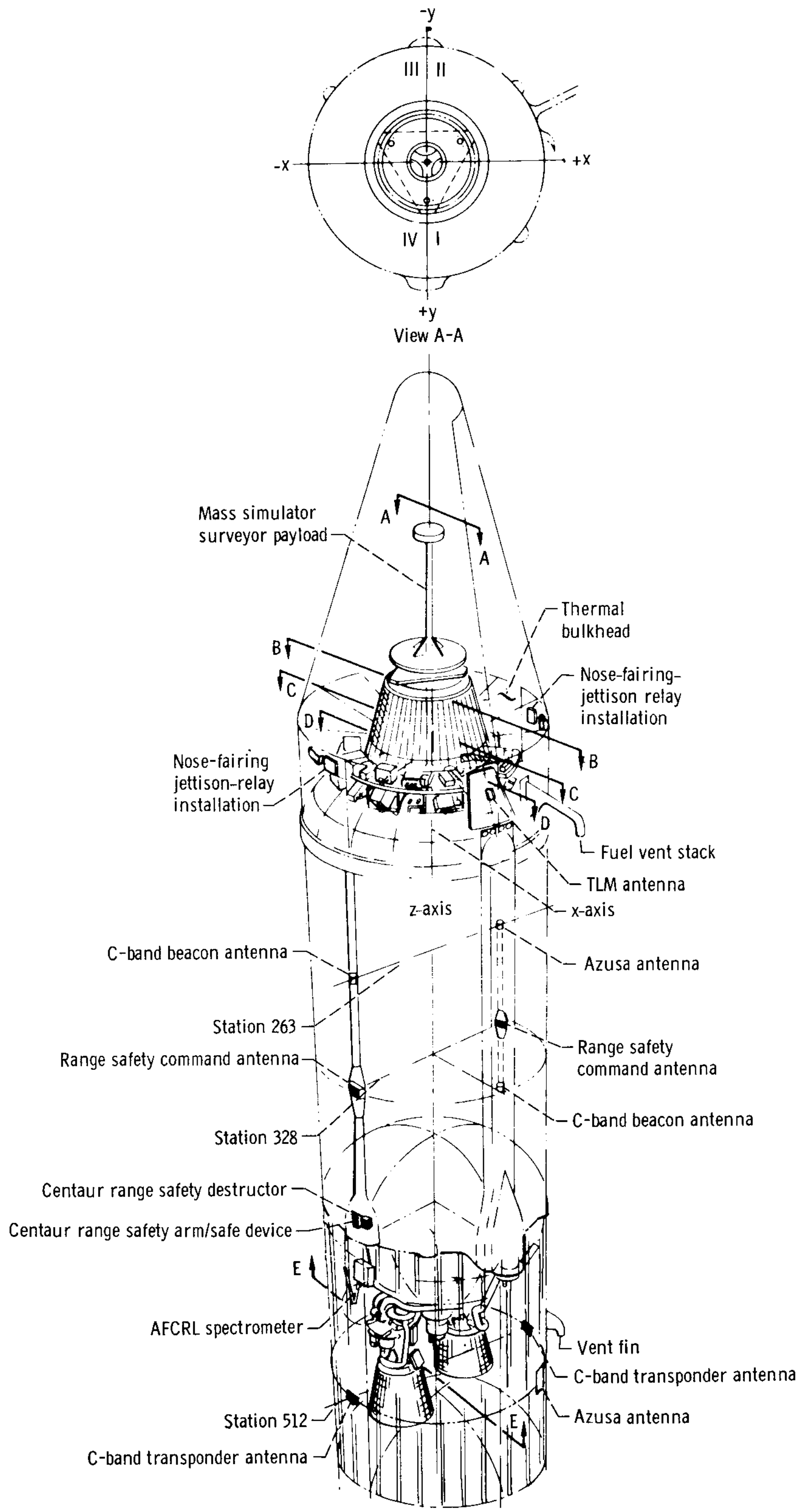

Figure II-2. - Centaur 4C general

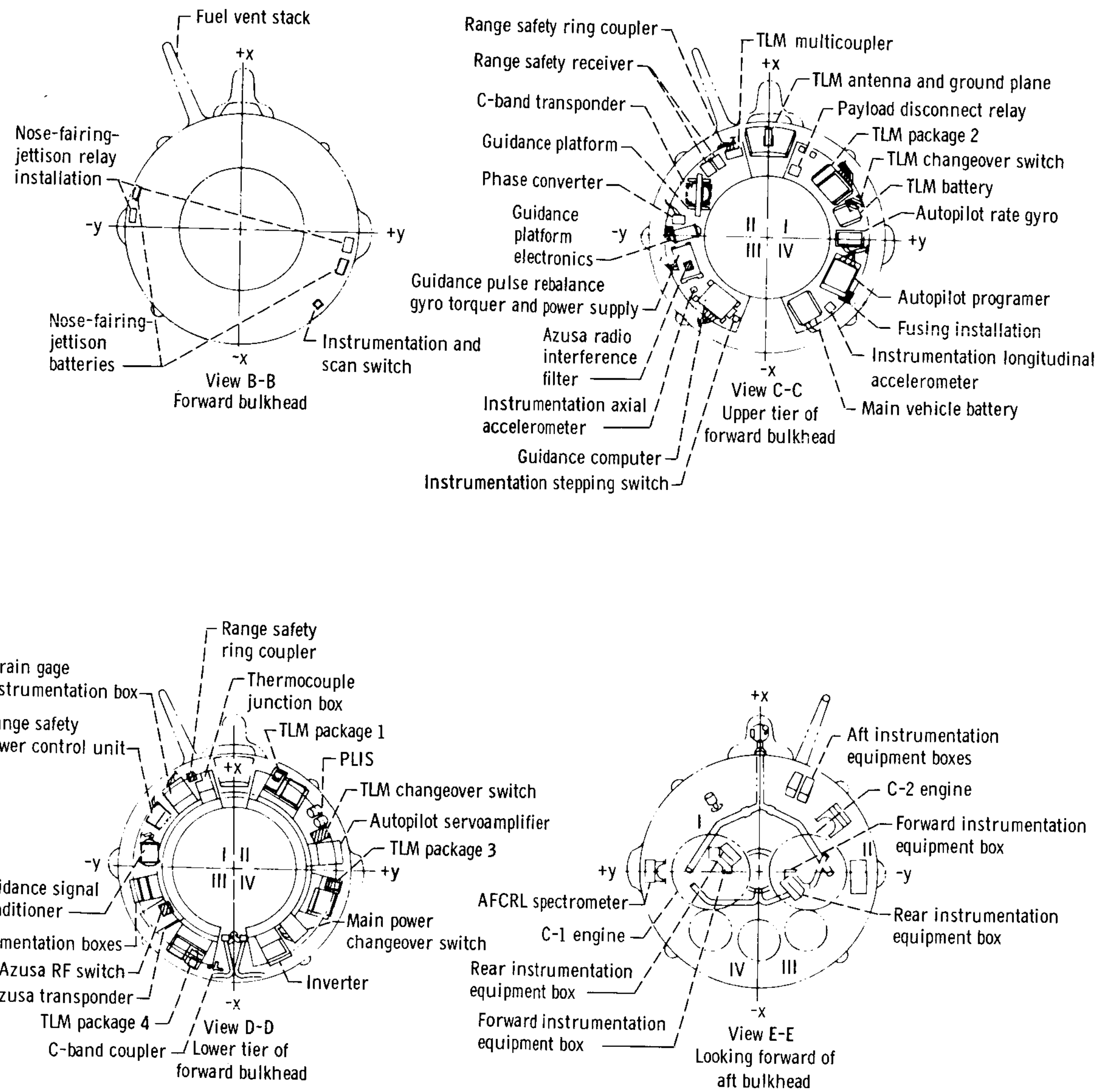

arrangement (ref. 3).

III. LAUNCH OPERATIONS

ARRIVAL AND ERECTION

The Atlas 146D booster arrived at ETR on July 23, 1964 followed by the interstage adapter (I/A) on July 28. The Atlas booster was erected on Complex 36A on July 30 and the I/A was mated to the Atlas on August 4. The Centaur 4C arrived at ETR on August 14 and was mated with the Atlas on August 20.

The Atlas-Centaur launch vehicle was deerected and returned to the hangar on September 8 due to forecasts of Hurricane Dora approaching the coast of Florida. Reerection of the launch vehicle on Complex 36A began on September 14 with the Atlas, I/A on September 15, and Centaur 4C on September 16.

AUTOPILOT AND GUIDANCE INTEGRATED TEST

The initial test was conducted on October 16 and was completed, but because of a discrepancy that occurred, the Centaur programer was sent back to San Diego for rework. The problem involved a resistor of the wrong value in the timing circuit. (For additional information see section XII. FLIGHT CONTROL SYSTEM.) The second test was conducted on October 22. The test was completed and all results were satisfactory.

FLIGHT CONTROL AND PROPELLANT TANKING TEST (QUAD TANKING)

The first tanking test was conducted on October 27 (ref. 4). The test was proceeding normally until an indication of overpressurization was noted in the Centaur LOX tank during the LOX tanking phase. The overpressurization was due to a failure in the propellant level indicating system (PLIS) and the human error to acknowledge the 100-percent-propellant-level indicator light. (For additional information see section X. VEHICLE STRUCTURES.) The propellants were detanked and the test was scrubbed.

Prior to the second tanking test conducted on November 6 (ref. 5), a Stokes gage was installed on the intermediate bulkhead to check for leaks that might have occurred as a result of the overpressurization. A leak found in one of the PLIS sensing lines was also corrected. The test was completed after two holds, one at T - 80 minutes and the other at T - 45 minutes. The holds were due to a faulty heater circuit in the air-conditioning system.

The third and final tanking test was conducted on November 16 (ref. 6) and was completed with satisfactory results. Prior to this test, the insulation panels were removed to permit X-rays of the station 408 area. The X-ray results showed no defects from overpressurization of the Centaur LOX tank.

A special Centaur LOX tanking test was conducted on November 27 (ref. 7) to verify the modifications to increase the temperatures of the H_2O_2 system. The results of this test were satisfactory.

FLIGHT ACCEPTANCE COMPOSITE TEST

The flight acceptance composite test (FACT) was successfully accomplished on November 24 with only minor discrepancies encountered (ref. 8).

COMPOSITE READINESS TEST

The composite readiness test (CRT) was successfully accomplished on November 30 with no significant discrepancies encountered (ref. 7).

ENCAPSULATION

The first encapsulation of the mass model was accomplished on October 19 and was mated to Centaur prior to the first flight control and propellant tanking test. The encapsulated payload was demated and returned to Hangar AM on November 25 for final preparations for flight. The encapsulated mass model was remated to Centaur on December 1.

LAUNCH

The first launch attempt was conducted on December 4. After a hold for 5 hours and 13 minutes at T - 200 minutes, because of a short in the airborne side of the Atlas umbilical plug, P1002, the countdown proceeded normally until T - 84 minutes. The launch attempt was scrubbed at this time due to a severe weather warning.

The second launch attempt was conducted on December 5. The countdown proceeded normally to T - 5 minutes for the scheduled 10-minute built-in hold. The hold was extended for weather and subsequently the launch attempt was scrubbed due to adverse weather conditions.

The third and successful attempt to launch was accomplished on December 11 at 0925:02:548 a.m. EST. The countdown proceeded normally to T - 90 minutes and the 60-minute built-in hold. This hold time was extended 35 minutes because of a problem in the launch stabilization system. After a total hold time of 95 minutes the count was resumed and proceeded normally to lift-off. The 10-minute built-in hold at T - 5 minutes was omitted due to the extended hold time at T - 90 minutes.

WEATHER

The weather conditions on launch day were favorable except for surface winds. The wind velocity recorded at the 90-foot level was 15 knots with gusts

[redacted]

up to 19 knots. The maximum critical allowable winds for Atlas-Centaur (AC-4) was 16.0 knots when fully tanked and at flight pressure.

Location of optical coverage	Percent coverage
Patrick Air Force Base	60
Cocoa Beach	60
Grand Bahama Island	60
False Cape	80
Melbourne	90
Vero Beach	90

AC-4 MILESTONES

Event	Date (1964)
Arrival of Atlas 146D booster	July 23
Arrival of interstage adapter	July 28
Erection of Atlas 146D booster	July 30
Erection of interstage adapter	August 4
Arrival of Centaur 4C	August 14
Erection of Centaur 4C	August 20
Arrival of insulation panels	September 8
Deerection of Atlas-Centaur (Hurricane Dora)	September 8
Erection of Atlas 146D booster	September 14
Erection of interstage adapter	September 15
Erection of Centaur 4C	September 16
Erection of insulation panels	October 1
Arrival of nose fairing and mass model	October 6
A/P and guidance integrated test	October 16
Encapsulation of mass model	October 19
Mating of mass model	October 19
A/P and guidance integrated test	October 22
Flight control and propellant tanking test	October 27
Flight control and propellant tanking test	November 6
Flight control and propellant tanking test	November 16
Flight acceptance composite test	November 24
Demate encapsulated mass model	November 25
Centaur special LOX tanking	November 27
Composite readiness test	November 30
Mating of encapsulated mass model	December 1
Attempted launch	December 4
Attempted launch	December 5
Launch	December 11

[redacted]

AC-4 COUNTDOWN (REF. 9)

F - 2 Days

Atlas tanked with fuel (RP-1)

F - 1 Day

Atlas-Centaur A/P readiness test
Atlas-Centaur TLM/RF system test
Nose-fairing bottles storage
H_2O_2 tanking and passivation
Insulation panel jettison reservoir storage
Engine trich auto flushing
Main engine Hypergol purge
Boost-pump and attitude-engine firing
Installation of pyrotechnic devices

F - 0 (Launch) Day

	Starting time	Completion time
Atlas and Centaur range safety command destruct boxes installation	T - 360 min	T - 300 min
Atlas-Centaur A/P testing	T - 335 min	T - 300 min
Range safety command test	T - 230 min	T - 215 min
Guidance A/P integrated test	T - 145 min	T - 70 min
Tower removal	T - 120 min	T - 80 min
Guidance final alinement	T - 80 min	T - 45 min
Centaur LOX tanking (55 percent)	T - 70 min	T - 60 min
Atlas LOX tanking	T - 60 min	T - 40 min
Centaur LH_2 tanking	T - 40 min	T - 1 min 30 sec
Centaur LOX topping	T - 22 min	T - 6 min
Atlas LOX topping	T - 15 min	T - 2 min 35 sec
Guidance to flight mode	T - 4 min	----------------
Programers to arm	T - 60 sec	----------------
Guidance to internal	T - 8 sec	----------------
Engine start - automatic sequence	T - 8 sec	----------------
2-Inch rise	T - 0	----------------

LAUNCH-ON-TIME CAPABILITY ANALYSIS

On the third launch attempt on December 11, 1964, lift-off occurred at 9:25:02.548 a.m. EST. This obviously did not meet a 20-minute minimum lunar window opening at 9:00 a.m. The planned hold of 60 minutes at T - 90 minutes was extended to 95 minutes by weather and by problems in the Centaur main power changeover switch and in the launcher stabilization regulator. Utilization of the 10-minute absorbing hold at T - 5 minutes permitted launch at 9:25 a.m.; launch would have been at 9:35 a.m. without the availability of the 10-minute planned hold.

The second launch attempt on December 5, 1964 was scrubbed at T - 5 minutes by rapidly approaching thunderstorms; the vehicle was ready and holding at T - 5 minutes, but Range Safety did not permit launch because the ceiling was then below Range standards. The count proceeded normally to T - 5 minutes at 8:45 a.m. and held at this point, fully tanked, for 29 minutes prior to the initiating of abort procedures at 9:14 a.m. EST. Had weather not dictated an abort, this launch attempt apparently could have met the minimum lunar window on time.

The first launch attempt on December 4, 1964 was 313 minutes late at T - 90 minutes because of autopilot and instrumentation problems and was aborted at T - 84 minutes because of excessive ground winds. The first delay occurred at T - 200 minutes because of a problem in the autopilot system and lasted for 258 minutes. The hold at T - 200 minutes was extended an additional 55 minutes by telemetry instrumentation. There was a delay of 47 minutes at T - 90 minutes to catch up on procedures. After this, there was an additional hold at T - 90 minutes for 41 minutes because weather predictions at this time indicated possible decreasing winds. The count proceeded down from T - 90 minutes, and when the winds increased, launch was aborted at T - 84 minutes.

NOSE-FAIRING RECOVERY ATTEMPT

The objective of the recovery operation was to retrieve the nose fairing flown on the Atlas-Centaur AC-4 launch vehicle to evaluate the Thermolag effect on the structural integrity of the nose fairing. Recovery aids were three yellow-green fluorescein dye markers installed in each half of the fairing. Since the nose fairing is constructed of lightweight materials, it was expected to float on impact. Separation of the fairing occurred at 358 306 feet, and impact occurred 1026 seconds after lift-off.

Specific items of interest	
Predicted impact point	25°50.4' N, 70°33.6' W
Flight azimuth	102° True of North
Scheduled launch time	9:00 a.m. EST
Actual launch time	9:25.02 a.m. EST

Recovery force

Unit	Position	Altitude, ft
RIS Kilo	25°50' N, 70°30' W	----
RIS Victor	25°37' N, 69°35' W	----
Aircraft Silver 3 (JC-130)	26°15' N, 70°26' W	1000
Aircraft Silver 4 (SC-131)	25°26' N, 70°41' W	500

Impact area weather

Clouds	3/10 Cumulus at 2200 ft; cirrus, height unknown
Wind	60° True of North, 20 knots
Sea	Code 4-5 (8- to 10-ft waves)

Sequence of events

Time, EST	Event
0925.02	Lift-off
0941	RIS Victor reported visual sighting of large charred-black rectangular object bearing 285° true of North, elevation 30°, range approximately 4 n. mi. Victor proceeded toward splash point.
0948	RIS Kilo reported negative visual sighting.
1000	RIS Kilo released from the recovery attempt. Silver 3 and 4 conducting visual search.
1040	RIS Victor reported unable to locate object that was sighted. Aircraft reported negative results.
1230	Recovery attempt terminated, negative results.

CONCLUDING REMARKS

After a successful launch and separation, a large charred-black rectangular object believed to be a section of the nose fairing impacted approximately 4 nautical miles, bearing 285° true of North, from RIS Victor. Victor and the aircraft went immediately to the impact area and made a thorough visual search. No dye marker or fairing was sighted and it was assumed that it had sunk on impact. Victor and the aircraft searched the predicted impact area with negative results. The recovery attempt was terminated at 12:30 p.m. EST.

[redacted]

IV. FACILITIES AND GROUND SUPPORT EQUIPMENT

SUMMARY

The facility and ground support systems performed satisfactorily for the launch attempts and launch. A faulty regulator valve on launch day and a slow LH_2 tanking rate on the launch attempt December 5 were the only problems. The environmental control system performed within the prescribed limits. Gas and propellant supplies were adequate. The propellant loading systems performed without problems, and the Atlas LOX red-line temperature was met without a hold to dump LOX as was necessary on AC-2 and AC-3.

PROPELLANT LOADING SYSTEMS

During the launch attempt on December 5 the LH_2 vehicle tanking rate started normally then dropped to about one-half the normal transfer rate. This decrease in flow rate was attributed to contamination clogging the 150-micron filter in the LH_2 fill and drain valve. After detanking, samples were taken from the LH_2 storage tank.

Date	Remarks	Results
December 8, 1964	The liquid was agitated by pressurizing and venting the tank then dumping approximately 500 gallons before sampling.	100 ppm N_2 5 ppm O_2
December 9, 1964 (a.m.)	This sample was taken after the tank was topped off.	190 ppm N_2 0.8 ppm O_2
December 9, 1964 (p.m.)	This sample was taken after the tank was topped off.	29 ppm N_2 0.7 ppm O_2

In addition, the LH_2 transfer line was purged and sampled for GN_2 and O_2.

The normal transfer line helium purge consists of a 1-hour purge at F - 2 days with no sample taken or further purge until LH_2 loading. At F - 2 days for the AC-4, the line was purged with helium from the fill and drain valve to the storage tank outlet valve for 1 hour and then sampled. The results showed 1.4 percent GN_2 and 0.38 percent O_2. The purge was continued for an additional hour and sampled again. The results showed 0.045 percent GN_2 and 0.004 percent O_2. These results indicated a lack of adequate purging of the transfer line in the past. On launch day, the line was purged for 1 hour and sampled prior to the start of LH_2 loading. The results showed 2.84 percent GN_2 and 0.74 percent O_2. These results indicated an air leak into the LH_2 transfer line. The

[redacted]

tanking rate on launch day started at 11 percent per minute and leveled out at 8 percent per minute with the flow control valve wide open. This rate of flow is considered normal.

On AC-2 and AC-3, it was necessary to hold and dump Atlas LOX to meet the -284° F maximum redline on breakaway valve temperature. Low boiloff caused a low topping rate to maintain the LOX level between topping-low and topping-high probes allowing the LOX temperature in the topping line to exceed -284° F. On AC-4 the topping procedure was changed so that the topping-low probe was not reached until approximately T - 4 minutes. Since Atlas LOX is secured at T - 2:35 minutes, the LOX in the topping line does not have time to warm up. The breakaway valve temperature at LOX securing on AC-4 was -308° F (CN1165T).

PRESSURIZATION SYSTEM

All pneumatic systems performed within the limits. The only problem was a leaking regulator in the launch booster unit (P/N 27-8225-2). This valve regulates 6700 psig GN_2 from storage bottles to 2000 psig for the launcher stabilization system. During the hold at T - 90 minutes, this valve allowed the pressure to rise above 2000 psig. The valve was replaced, and the system was reported ready approximately 23 minutes prior to picking up the count at T - 90 minutes.

ENVIRONMENTAL CONTROL SYSTEMS

The air-conditioning-system temperatures and pressures were within the specified limits for launch. Some changes were required between the final tanking test and launch to achieve these limits. The tanking test and launch data are as follows:

Upper stage cooling limits	
Temperature, $^{\circ}$F	45 to 60
Pressure (minimum), psig	0.433
Final tanking test A/C duct temperature, $^{\circ}$F	45.3 to 36.6
F - 1 day A/C duct temperatures, $^{\circ}$F	44 to 46
F - 1 day A/C duct pressures, psig	0.85 to 0.90
Launch morning A/C duct temperatures, $^{\circ}$F	44 to 46
Launch morning A/C duct pressures, psig	0.75 to 0.80

At T - 90 minutes (GN_2 flow start) the duct temperature increased from 46° to 50° F and remained steady to lift-off at a duct pressure of 0.82 psig. During the tanking test, the temperature was 8.4° F below the lower limit. This problem was solved by circumventing the dehumidifier cooling coils when proceeding to GN_2 flow (T - 90 min) since the dehumidifier is not required for GN_2. The blower and the heater in this unit were still used. The temperature recorded at the dehumidifier showed a variation of 48° to 56° F; however, this measurement is not considered as reliable as that obtained by the duct transducer.

The land-line temperature measurements taken on the payload adapter and correlated with the duct temperature readings are shown in the following table.

Time, min	Air-conditioning duct (CN1191T), °F	Payload adapter ring at station 171 (CA1468T), °F	Separation latches at station 127 (CA1461T, CA1462T, CA1463T, avg), °F
T - 90 hold	44 to 46	50 to 60	57 to 57.6
T - 40 (LH_2 chill-down complete)	50	75	87 to 89
T - 25	50	0	84 to 85.5
T - 10	50	-25	83.5 to 84
T - 0	50	-25	84.2 to 87

Centaur Thrust Section Heating

Limits.

Temperature, °F . . . . 130±5
Pressure (minimum), psig 0.47
Final tanking test duct temperature, °F . . . . 127 to 130

The launch day duct temperature of 119° F gradually increased to 122° F, then to 125° F, then remained steady to lift-off. The duct pressure was 0.85 to 0.975 psig.

Atlas Pod Cooling

Limits.

Temperature (maximum), °F 50
Pressure, psig . . . . 0.83 to 1.44
Final tanking test duct temperature, °F . . . . 47.5 to 50

The launch day duct temperature was steady at 43.4° F then decreased to 39.4° F at lift-off with a duct pressure of 1.02 psig. The temperature recorded at the A/C unit was 38° F for air and 34° F for GN_2 at launch. During the daytime tests, it is usual to gain 5° to 6° F temperature from the A/C unit to the vehicle as a result of duct warming.

Atlas Thrust Section Heater

Limits.

LOX temperature (minimum), $^{\circ}F$	147
Final tanking test duct temperature, $^{\circ}F$	183 to 179
Launch day duct temperature, $^{\circ}F$	176 and steady

Boom Retraction Times

Limits (2.2 to 3.5 sec to within 10° of vertical).

Upper boom (2-in. rise switch actuation)

Retraction start, sec	T + 0.20
10° from vertical time, sec	T + 2.90
Total time, sec	2.70

Lower boom (8-in. rise switch or TDPU relay K-4 actuated)

Retraction start, sec	T + 0.24
10° from vertical, sec	T + 2.69
Total time, sec	2.45

The boom accumulator pressures were 2655 psig (redline is 2425 psig, minimum).

Launcher Holddown and Release System

The theoretical vehicle release point occurs when the holddown cylinders blow down from 5750 to 2480 psig. The parameter on blowdown time to 2480 psig is 0.45 second maximum. The release signal was sent at T - 0.81 second.

Blowdown start, sec	T - 0.59
B_1 cylinder at 2480 psig, sec	T - 0.41
B_2 cylinder at 2480 psig, sec	T - 0.39

Gas and Propellants

Air-conditioning GN_2 supply.

Total water volume including 28 tube bank trailers, cu ft	11 607
Total available, scf	1 360 000
Total used, scf	244 000
Total available at lift-off, scf	1 116 000
Hold time available at lift-off, min	200

This 200 minutes is in addition to the 70 minutes required after start of detanking. The total time for GN_2 flow was 90 minutes.

Helium insulation panel and engine purge.

Total water volume from 12 tube bank trailers, cu ft	4164
Total available at 6:45 a.m., lb	2400
Total available at T - 0, lb	1848
Hold time available at T - 0, min	234

This 234 minutes does not include the 4 hours required for warmup after detanking.

Helium for LOX transfer.

Total water volume available from three tube bank trailers, cu ft	1 041
Total available at 6:45 a.m., scf	123 381
Total used, scf	38 940

Atlas thrust section heater GN_2.

Total water volume available from one tube bank trailer, cu ft	273.9
Total available, scf	34 200
Total used, scf	6 300

The total time for GN_2 flow was 6 minutes.

Launcher booster unit GN_2.

Starting pressure, psig	6700
Ending pressure, psig	5700
Minimum pressure required, psig	5400

Facility GN_2 (3000 psig).

Starting pressure, psig	2300
Ending pressure, psig	1860
Minimum pressure, psig	1100

Facility helium (3000 psig).

Starting pressure, psig	2800
Ending pressure, psig	2610
Minimum pressure, psig	1500

Facility helium (6000 psig).

Starting pressure, psig	5600
Ending pressure, psig	4500
Minimum pressure, psig	3550

Liquid oxygen.

Storage tank level at start, gal	30 650
Storage tank level at end, gal	7 350
Amount used, gal	23 300

The level gage transducers on both storage tanks were rejected after inspection, therefore, the preceding figures are an approximation.

Liquid helium.

Storage tank level at start, gal	1005
Storage tank level at end, gal	755
Amount used, gal	250
Approximate hold time remaining, min	42

Liquid hydrogen.

Storage tank level at start, gal	21 000
Storage tank level at end, gal	11 100
Amount used, gal	9 900

V. TRAJECTORY

SUMMARY

The AC-4 trajectory deviated only slightly from the preflight estimate. The major cause of these deviations was that the actual flight winds had more of a head-wind characteristic than did the nominal wind profile used in the preflight simulation. The thrust acceleration was also greater than that predicted during the atmospheric portion of the flight. The resultant trajectory was thus lofted, and BECO occurred approximately 1.5 seconds early. The actual trajectory was also slightly to the right of the predicted trajectory probably as the result of a small Atlas autopilot yaw drift and/or a deficiency in establishing the pitch over azimuth.

Subsequent to closing the Centaur guidance loop following BECO, the actual trajectory began to approach the predicted trajectory, and at MECO (parking orbit injection) the altitude error was approximately 1200 feet.

Reconstruction of the Atlas portion of the flight indicated that the reference specific impulse for the booster was 0.1 percent greater than nominal and for the sustainer was essentially as predicted. The reference thrusts were 0.4 percent greater than those predicted for the booster and essentially nominal for the sustainer. These values of thrust correspond to a lift-off weight of 302 954 pounds. In order to match the observed trajectory, it was also necessary to introduce a yaw drift of 0.21 degree per minute into the autopilot and to decrease the pitch rates by 0.2 percent.

Reconstruction of the Centaur phase resulted in an overall Centaur specific impulse of 431.9 seconds (+0.2 percent, table V-I), which is equivalent to an average engine specific impulse of 432.4 seconds. A deficiency in the calculated thrust acceleration has been noted in this and previous Atlas-Centaur postflight trajectory analyses. A possible cause of these discrepancies was the lack of an altitude sensitive term in the base drag calculation. The computed payload of an operational mission, such as AC-15, would be increased approximately 45 pounds if the modified AC-4 drag coefficients were used instead of the current nominal values.

TRAJECTORY EVALUATION

The AC-4 trajectory data were analyzed to obtain vehicle performance based on the observed trajectory. The "best estimate of trajectory," hereinafter called BET, obtained from the Data Processing Section AFETR (ref. 10) is a weighted combination of the outputs of the various tracking devices (see appendix B). A second objective was to evaluate further the capabilities of the preflight simulation techniques to predict the details of the flights. Also, it may be possible to improve the accuracy of the various models used in the simulation and to refine the flight performance reserve propellant allotment on the basis of an analysis of the results of a number of flights.

Atmospheric Conditions

The atmospheric conditions that will exist at the time of launch cannot be accurately predicted, and therefore the deviation of the actual conditions from those assumed for the preflight simulation are the first items evaluated. The actual atmospheric conditions as determined by a Rawinsonde run made at 09:05 EST are presented in figure V-1. The temperature and pressure profiles (fig. V-1(a)) show relatively small deviations from the standard atmosphere used in the simulation. The measured wind profile is compared with the nominal seasonal profile used in the preflight simulation. The shift from the predicted tail wind to a head wind during the first 10 000 feet of altitude together with the lower velocity above this altitude tended to loft the trajectory. The Atlas pitch program was tailored to minimize the angles of attack with the assumed seasonal winds. Since the actual wind velocity was somewhat less than predicted, the angles of attack presented in figure V-2 resulted.

The dynamic pressure and flight Mach number histories presented in figure V-3 were generally greater than those predicted by the preflight simulation. This resulted in slightly higher drag forces than predicted; the drag at T + 72 seconds was approximately 2300 pounds greater than predicted.

Trajectory Parameters

The planned trajectory for AC-4 consisted of a powered boost flight to a 90-nautical-mile circular parking orbit with a coast phase of 1465 seconds. A second burn was then to be used to change the circular orbit into an eccentric orbit followed by a simulated payload separation sequence. As mentioned in section I and discussed elsewhere in this report, however, a second main engine start was not achieved. The trajectory analysis will be limited to the powered portion of the flight from launch to parking orbit.

The preflight simulation was generally a satisfactory prediction of the actual flight. Comparisons of the predicted and actual trajectories are presented in tables V-II and III and in figures V-4 to 6. The actual trajectory was higher during the atmospheric portion of the flight by approximately 0.4 nautical mile (fig. V-5). During this time, the vehicle was controlled by the Atlas autopilot, which was not designed to correct for changes in the wind profile or in engine performance. The error in altitude was gradually reduced by the Centaur guidance system, following its activation at BECO, so that the altitude error was only 0.2 nautical mile at orbit injection.

The actual flight path was up to 3 nautical miles to the right of the predicted flight path (fig. V-4). This error was probably the result of the vehicle pitching over at an azimuth slightly greater than planned and/or as a result of a slight yaw drift of the Atlas autopilot.

[redacted]

The energy added to the vehicle is indicated by the thrust acceleration $(F - D)/W$ (fig. V-5). There is generally good agreement between the actual and predicted values except for the time period from T + 70 seconds to BECO. During this time, the thrust acceleration was approximately 0.1 g greater than predicted. This discrepancy is similar to ones noted in the AC-2 and AC-3 analyses (ref. 11). The higher acceleration resulted in BECO occurring about 1.5 seconds early. A probable cause of this acceleration difference will be discussed later in this section.

The actual velocities were about 200 feet per second greater than those predicted during the boost phase (fig. V-6) as a result of the greater thrust acceleration. The velocity at BECO, however, was slightly less than the planned velocity due to premature BECO. There was good agreement between the actual and predicted velocities from BECO to first MECO.

The AC-4 Centaur stage was injected into a nearly nominal parking orbit (table V-III). The errors in perigee altitude, period, and eccentricity were 0.77 nautical mile, 0.02 minute, and 0.0005, respectively, which is indicative of satisfactory guidance system performance.

Vehicle Performance

Two techniques were used to evaluate the performance of the AC-4 vehicle. The most detailed was the trajectory reconstruction. In this method the preflight simulation program was used to find, by a process of iterations, those performance parameters which resulted in an analytical trajectory that best matched the observed positions and velocities. The second and more direct method was used to obtain the Centaur specific impulse. This method makes use of the relation between the observed thrust acceleration and specific impulse.

Centaur Specific Impulse

The overall specific impulse of a vehicle operating in a vacuum may be determined directly from the observed trajectory provided that the thrust is constant. As derived in reference 12, the overall specific impulse $\bar{I}$ is defined as

$$\bar{I} = \frac{\text{Total vehicle thrust}}{\text{Total vehicle flow}} = \left[\frac{d}{dt}\,\frac{1}{\left(\frac{F - D}{W}\right)}\right]^{-1}$$

The inverse of the thrust acceleration $W/(F - D)$ is a linear function of time if both the thrust-drag and the flow rates are constant. The Centaur stage operated in essentially a vacuum (zero drag), and the RL-10 engines were controlled to provide constant thrust and flow. Therefore it was possible to estimate from the BET a vehicle specific impulse $\bar{I}$ of 431.8 seconds. This value was based on the time period from T + 300 seconds to first MECO. Prior to T + 300 seconds, the RL-10 engines had not reached equilibrium thrust, and therefore this method was not usable.

[redacted]

The average engine specific impulse of 432.3 seconds was obtained from the vehicle impulse by reducing the thrust 8.72 pounds and the flow 0.103 pound per second, which represent the contribution of the turbopump system.

Trajectory Reconstruction

A good estimate of vehicle performance can be obtained by reconstructing the trajectory based on tracking data. This method makes use of a detailed trajectory simulation to determine a set of performance parameters, that is, thrust, weight flow, etc., that will yield a computed trajectory which will best fit the BET in a weighted least-square sense. The velocity and position residuals (differences between the reconstructed trajectory and the BET) may represent combined errors in the tracking data and in the simulation including the mathematical models describing engine and vehicle performance, for example, thrust, weight flow, and drag. If the residuals are small, there is a high probability that the derived values of the performance variables are a good estimate of those having occurred during the flight. If a consistent pattern in the residuals is observed over a series of flights, it may be possible to deduce the source of the error and improve the models used in the vehicle simulation.

The reconstruction of the AC-4 flight differed from that of AC-3 (ref. 11) in several ways. The Centaur guidance system supplied the steering signals for the flight following BECO, whereas, for the AC-3 flight, the guidance system was passive. Thus, for the AC-4 trajectory simulation it was necessary to simulate the guidance system. For this analysis, however, no attempt was made at a detailed evaluation of the guidance system. Secondly the sustainer residual propellant weight was used to determine the lift-off thrust and weight for the Atlas. In a similar manner, the estimated Centaur propellant weights (see section VII) were used to establish the Centaur thrust level.

The values of position, thrust acceleration, and velocity obtained from the reconstruction are compared with the preflight nominal trajectory and the BET in figures V-4 to 6, respectively, and tables V-II and III. The reconstruction agrees closely with the BET in all cases. The time of BECO, MES, and MECO listed as Reconstruction in table V-II are those times required to best fit the BET data using the preflight transient thrust and flow models. No attempt was made in the AC-4 reconstruction to tailor these thrust and flow transient models to the observed data. Therefore, the reconstruction times are not directly comparable to the observed times. A summary of the propellant and vehicle weights used in the trajectory analysis are presented in table V-IV. The hardware, or dry, weights were based on the summation of the weights of individual components. The weight at SECO was calculated from the dry weight plus the propellant residuals calculated from the measured propellant heads at SECO. The Centaur weight at SECO was based on the propellant loading calculated in section VII. The gross weight at lift-off was 302 954 pounds based on the preceding assumptions, which is approximately 290 pounds less than the estimate from the loading calculations (table II-II).

The derived propulsion parameters are presented in two forms in table V-I. The reference values are those values used in the propulsion models and correspond to the values that would have been obtained at the standard engine inlet conditions. Since the engine inlet conditions are not generally at the standard values, a second ("specific") set of parameters is presented that are the values calculated to exist at the times specified.

The Atlas performance was essentially nominal. Booster and sustainer reference specific impulse was less than 0.2 percent greater than the nominal reference values. The booster reference thrust was about 0.4 percent above nominal, whereas the sustainer was nominal. It was necessary to decrease the pitch attenuation factor of the Atlas autopilot from 1.020 to 1.018. This reduction in pitch rates is well within the predicted autopilot accuracy and may result from not simulating the time lags of the actual system. This factor was applied to all 10 pitch rates and no attempt was made to adjust individual rates to improve the match.

It was necessary in the reconstruction of the Centaur phase of the flight to simulate the operation of the guidance system. A simplified model of this system was employed in the trajectory reconstruction, which, although not accurately simulating the guidance system, permitted an otherwise satisfactory match of the trajectory. An analytical model of the Centaur propulsion was used in the postflight reconstruction that compensated for (1) the startup transients as reported in section VI, (2) the measured propellant temperatures and pressures, and (3) the observed nonequilibrium performance prior to T + 300 seconds. This nonequilibrium performance model agreed with the data in the engine specification (ref. 13). The preflight simulation, however, used constant values of thrust and specific impulse throughout the Centaur phase. Inclusion of the postflight model in the simulation of a typical operational mission, for instance, AC-15, will not change the payload at injection significantly (less than 1 lb increase); however, use of the postflight propulsion model improved the fit of the thrust acceleration data (fig. V-7). The apparent points of disagreement are due to the scatter in the tracking data. The component velocities were matched to within 10 feet per second and the positions to within 800 feet. The nonrandom patterns observed in these residuals (figs. V-8 and 9) are attributed to the simplified model used in the reconstruction since the thrust acceleration residuals (fig. V-7(b)) do not exhibit the same trends. The Centaur had a specific impulse slightly better than predicted; the vehicle specific impulse $\bar{I}$ was approximately 0.2 percent above, and the thrust was about 0.2 percent below the values predicted by the acceptance data.

A detailed trajectory listing is presented in appendix E. A modified set of drag coefficients was used in the calculation of these data. A discussion of the problems associated in achieving this match and its significance follows.

THRUST ACCELERATION DISCREPANCY

The magnitude and distribution of the position, velocity, and thrust acceleration residuals indicates how well the computed trajectory duplicates the actual flight. The reconstruction is considered satisfactory if the residuals are small and apparently random. A systematic pattern of these residuals would indicate a deficiency in one or more of the mathematical models used in the simulation or, some unaccounted for deviation in vehicle performance.

The residuals in position, velocity, and thrust acceleration for the AC-4 reconstruction are presented in figures V-7 to 9. There is a deficiency in the calculated thrust acceleration indicated during the time period from T + 60 to T + 110 seconds when the nominal models are used. There is a corresponding variation in the velocity residuals. This pattern is similar to that noted in the AC-2 reconstruction (ref. 14) and in the AC-3 analysis (ref. 11).

The deficiency in calculated thrust acceleration could result from computing too low a level of thrust and/or flow, or too high a drag force. A maximum error of 10 000 pounds would be required in either thrust (5σ) or drag. A probable source of error in the thrust and flow calculations would be the LOX density. An error in LOX density of approximately 3 percent (14° F in LOX temperature) would be required, and this is not considered probable. Another possibility is the propulsion models themselves. These models assume linear variations of thrust and flow with inlet conditions. Nonlinearities amounting to 5 percent in thrust or 8 percent in flow would be required to satisfy the observed thrust acceleration, which again does not appear probable.

The time period during which the discrepancy occurs corresponds to the period of maximum dynamic pressure and thus to maximum drag (figs. V-3 and 10). The cause of the observed discrepancy in the AC-2 analysis was considered by STL (ref. 14) to be an error in the drag model. They derived a new drag curve (fig. V-11) that eliminated the observed thrust acceleration deficiency. This same curve was satisfactory for the AC-3 trajectory reconstruction and provided a better fit for the AC-4 data.

The drag on a vehicle may be divided into two parts: (1) the drag due to the air flow over the forebody and (2) the drag associated with the base area. The forebody drag is a function of flight Mach number and dynamic pressure and was evaluated for the Atlas-Centaur in the Lewis Research Center 8- by 6-foot supersonic wind tunnel.

The base drag, however, is not only a function of the Mach number and dynamic pressure but also of the effects of the jet interaction and the resulting mass recirculation at the vehicle base (refs. 15 and 16). For this configuration, in a supersonic free-stream Mach number regime, the recirculation of mass is directly proportional to the ratio of the jet to ambient pressure. Therefore the base pressure force will be less (i.e., the base drag is greater) for an Atlas-Centaur vehicle flying at a lower altitude than for one flying at the same Mach number but at a higher altitude.

The AC-4 vehicle flew a lower altitude trajectory than did the AC-2 and the AC-3. It would be anticipated that the base drag should be somewhat greater for the AC-4 flight than for the AC-2 and the AC-3. Examination of the AC-4 thrust acceleration residuals (fig. V-7) shows that the use of the drag coefficients derived by STL for the higher altitude trajectory did result in the calculation of too small an apparent drag force. A new set of drag coefficients shown in figure V-11 as modified AC-4 was used and a satisfactory match was obtained.

Use of the modified drag coefficients in the reconstruction resulted in reducing the thrust attenuation factor from 1.006 to 1.004 and improved the specific impulse for the booster approximately 0.2 percent. These are relatively small changes in performance parameters and the modified coefficients were therefore used in this analysis.

It is not possible at this time to determine if the error is solely due to base drag and not to the propulsion model or other unknown causes. The desired result, however, could be achieved by incorporating any nonlinear altitude-dependent aspects of the propulsion model with the base drag coefficients. The significance of this is that, if the base drag model remains predictable from flight to flight, the computed payload of an operational vehicle, for instance, AC-15, would be increased by approximately 45 pounds.

TABLE V-I. - PROPULSION PARAMETERS AS DERIVED BY TRAJECTORY RECONSTRUCTION

Stage	Parameter	Reference values[a]			Specific values[b]	
		Preflight	Derived		Preflight	Derived
			Ratio[c]	Value		
Booster	Thrust (sea level), lb	309 000	1.0040	310 236.0	306 083.6	306 270.5
	Weight flow, lb/sec	1234.0	1.0032	1238.0	1225.3	1225.6
	Specific impulse (sea level), sec	250.4	1.0008	250.6	249.7	249.9
	Mixture ratio, O/F	2.283	1.0000	2.283	2.244	2.215
Sustainer plus vernier	Thrust (sea level), lb	59 000	1.0003	59 017.7	58 352.2	58 238.2
	Weight flow, lb/sec	275.1	1.0003	275.2	273.6	275.1
	Specific impulse (sea level), sec	214.4	1.0000	214.4	213.2	211.7
	Mixture ratio, O/F	2.270	1.0000	2.270	2.328	2.546
Centaur[d]	Thrust (vacuum), lb	29 952.7	0.9976	29 880.8	29 952.7	30 206.8
	Weight flow,[e] lb/sec	69.498	.9955	69.185	69.498	70.166
	Specific impulse[f] (vacuum), sec	431.5	1.0021	432.4	431.5	431.0
	Vehicle specific impulse,[e] sec	431.0	1.0021	431.9	431.0	[f]430.5
	Mixture ratio,[f] O/F	5.005	1.0000	5.005	5.005	5.062

[a]Values of the parameters specified for the propulsion models corrected to specified engine inlet conditions (appendix B of ref. 1, source of preflight data).

[b]Uncorrected values at T + 4 sec for the Atlas stage and T + 300 sec for the Centaur stage.

[c]Ratio of derived to preflight nominal.

[d]Values for combined C-1 and C-2 engines.

[e]Includes minor flow of 0.103 lb/sec and associated thrust of 8.72 lb.

[f]Vehicle specific impulse obtained from the slope method was 431.8 sec.

TABLE V-II. - TRAJECTORY PARAMETER COMPARISON

Parameter	BECO[a]	Insulation jettison	Nose-fairing jettison	SECO	Separation[a]	MES	MECO[a]
Time from lift-off,[b] sec							
Planned[c] Actual Reconstruction	150.46 149.06 [d]149.06	200.36 198.47 198.47	214.36 212.38 212.38	226.36 224.25 224.25	228.96 226.65 226.65	235.96 233.87 [d]235.20	573.41 572.65 [e]573.09
Altitude, n. mi.							
Planned Tracking[f] Reconstruction	30.102 30.425 30.398	52.566 53.033 53.028	58.127 58.607 58.597	62.704 63.146 63.137	63.666 64.037 64.028	66.121 66.602 67.013	90.791 90.990 90.998
Range, n. mi.							
Planned Tracking Reconstruction	44.950 43.666 43.703	112.93 110.494 110.509	134.67 131.928 131.944	154.410 151.292 151.312	158.80 155.315 155.338	170.62 167.407 169.676	1039.270 1035.055 1036.778
Relative velocity,[g] ft/sec							
Planned Tracking Reconstruction	8099 8070 8069	9622 9561 9559	10 168 10 106 10 096	10 704 10 618 10 622	10 694 10 611 10 622	10 650 10 567 10 569	24 267 24 254 24 284
Inertial velocity, ft/sec							
Planned Tracking Reconstruction	9343 9307 9306	10 916 10 852 10 850	11 471 11 409 11 397	12 014 11 926 11 930	12 004 11 921 11 931	11 966 11 881 11 884	25 607 25 596 25 625
Axial load factor, g							
Planned Tracking Reconstruction	5.520 [h]5.49 5.523	1.383 1.38 1.370	1.510 1.51 1.497	1.672 1.65 1.656	0.004 ----- .049	0 --- 0	2.316 2.33 2.340

[a]Referenced to beginning of thrust decay or weight separation.
[b]Time from 2-in. motion (0925:02:548 EST).
[c]Ref. 1.
[d]Effective time compatible with the transient model used in reconstruction.
[e]Time compatible with guidance simulation model.
[f]Data from best estimate of trajectory (ref. 10).
[g]Velocity relative to the Earth.
[h]Accelerometer (CM101A) indicated 5.52 g's maximum at 149.06 sec from 2-in. motion (ref. 2).

TABLE V-III. - ORBITAL PARAMETERS

Parameter	Preflight[a]	Postflight[b]
Time of injection[c]	573.56	572.7
Perigee altitude,[d] n. mi.	88.9067	88.1341
Eccentricity	0.000461	0.00095
Semimajor axis, n. mi.	3534.536	3535.493
Period, min	87.845	87.86
Inclination, deg	30.7303	30.69
Longitude of ascending node,[e] deg	243.983	243.96
Argument of perigee,[f] deg	116.865	179.5

[a]Data obtained from ref. 1.
[b]Data obtained from ref. 2.
[c]Time from 2-in. motion (from 0925:02:548 EST).
[d]Measured above spherical Earth, R_o = 3444 n. mi.
[e]Measured East from launch meridian.
[f]Measured in direction of motion from ascending node.

TABLE V-IV. - WEIGHT SUMMARY FOR TRAJECTORY ANALYSIS

Weight, lb	Preflight estimate[a]	Postflight estimate[b]	Trajectory reconstruction
Total at lift-off	304 002	303 243	302 958
At BECO	79 399	-------	79 905
Booster,[c] wet	7 410	7 357	[d]7 357
Insulation jettison	1 219	1 278	[d]1 278
Nose fairing	1 990	2 052	[d]2 052
Total at SECO	48 204	48 672	48 724
Total at separation	48 165	-------	48 684
Sustainer,[c] wet	9 006	9 028	[d]9 028
Unburned Atlas propellant at SECO	2 781	3 401	3 409
Centaur at lift-off[e]	39 698	39 741	[d]39 741
Boost-phase vent	71	168	[d]168
Boost-phase jettison	3209	3 330	[d]3 330
Centaur at separation	36 418	36 243	[d]36 243
At MECO[e]	12 932	12 713	12 794
Centaur,[c] wet plus payload	7 166	7 155	[d]7 155
Unburned Centaur propellants	5 766	5 558	5 639
Payload (simulated mass)	2 091	2 090	[d]2 090

[a]Appendix B of ref. 1.
[b]Data from section II.
[c]Dry hardware weight plus residuals (not including unburned propellant).
[d]Assumed for purposes of reconstruction.
[e]Includes payload weight.

[redacted]

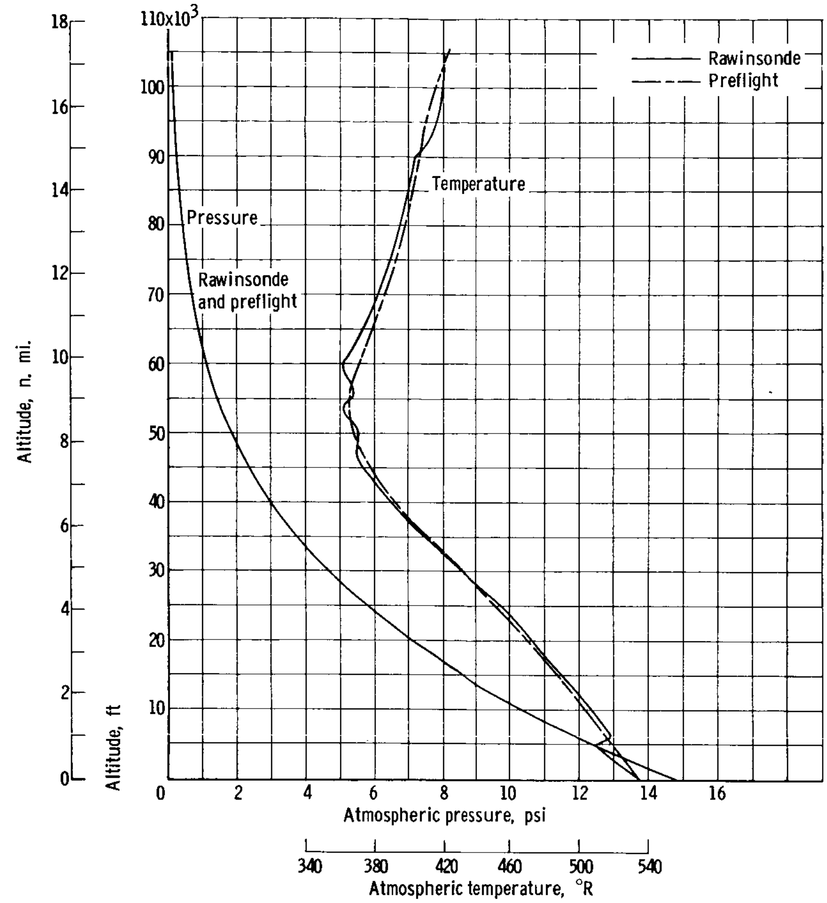

(a) Pressure and temperature.

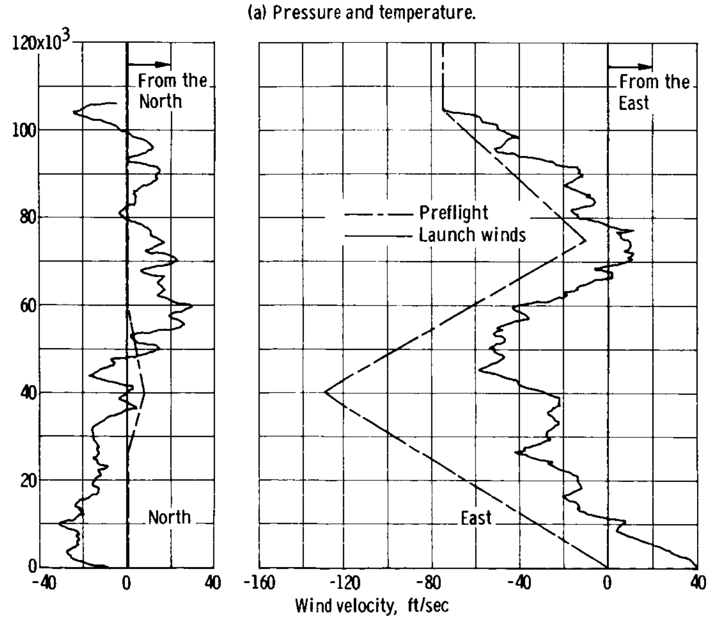

(b) Wind components.

Figure V-1. - Atmospheric conditions at time of launch. Rawinsonde run 1594 at 9:05 EST, December 11, 1964.

[redacted]

[redacted]

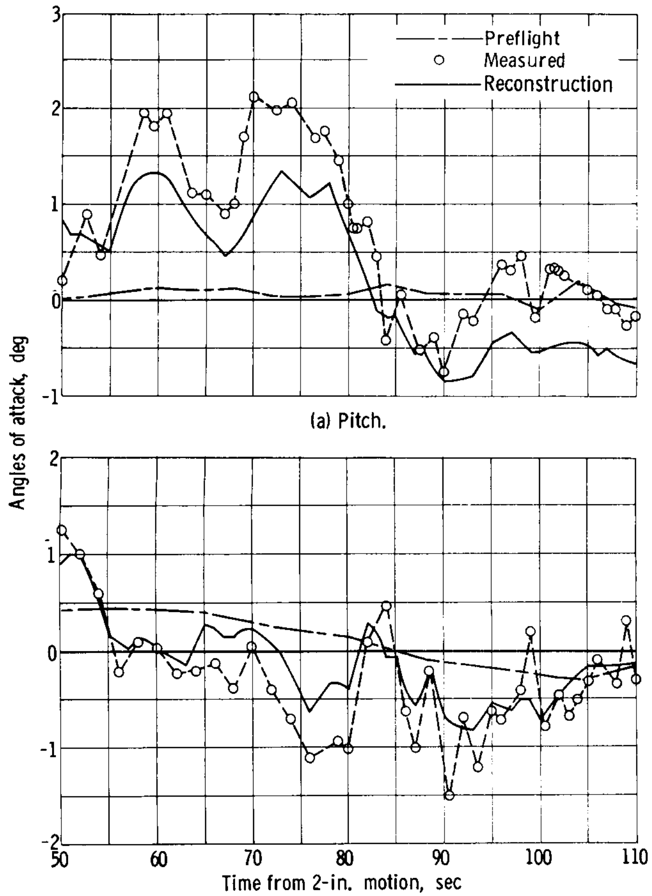

(a) Pitch.

(b) Yaw.

Figure V-2. - Comparison of pitch and yaw angles of attack.

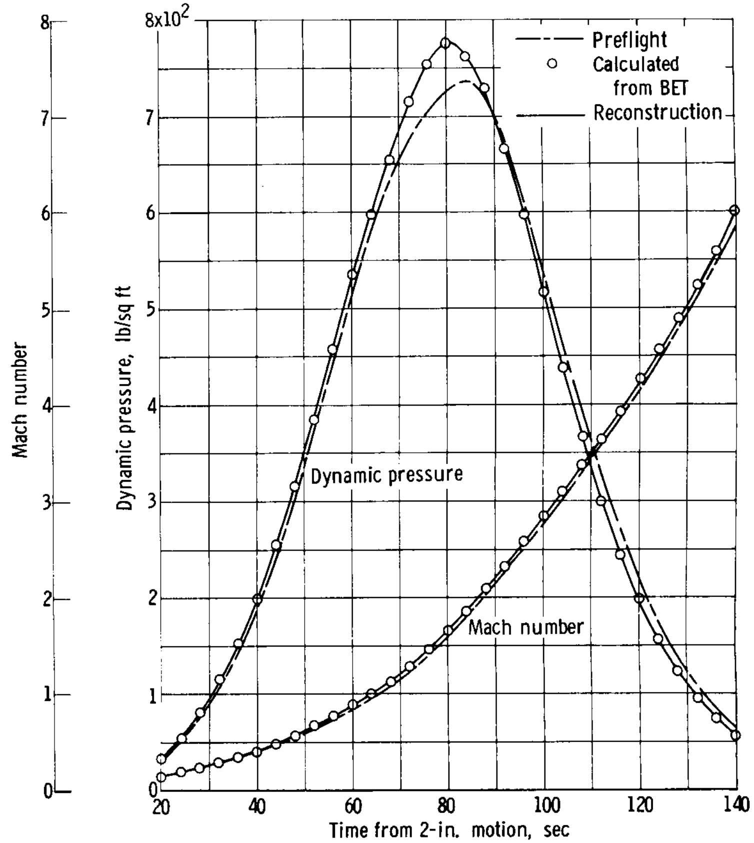

Figure V-3. - Comparison of aerodynamic parameters for AC-4.

[redacted]

[redacted]

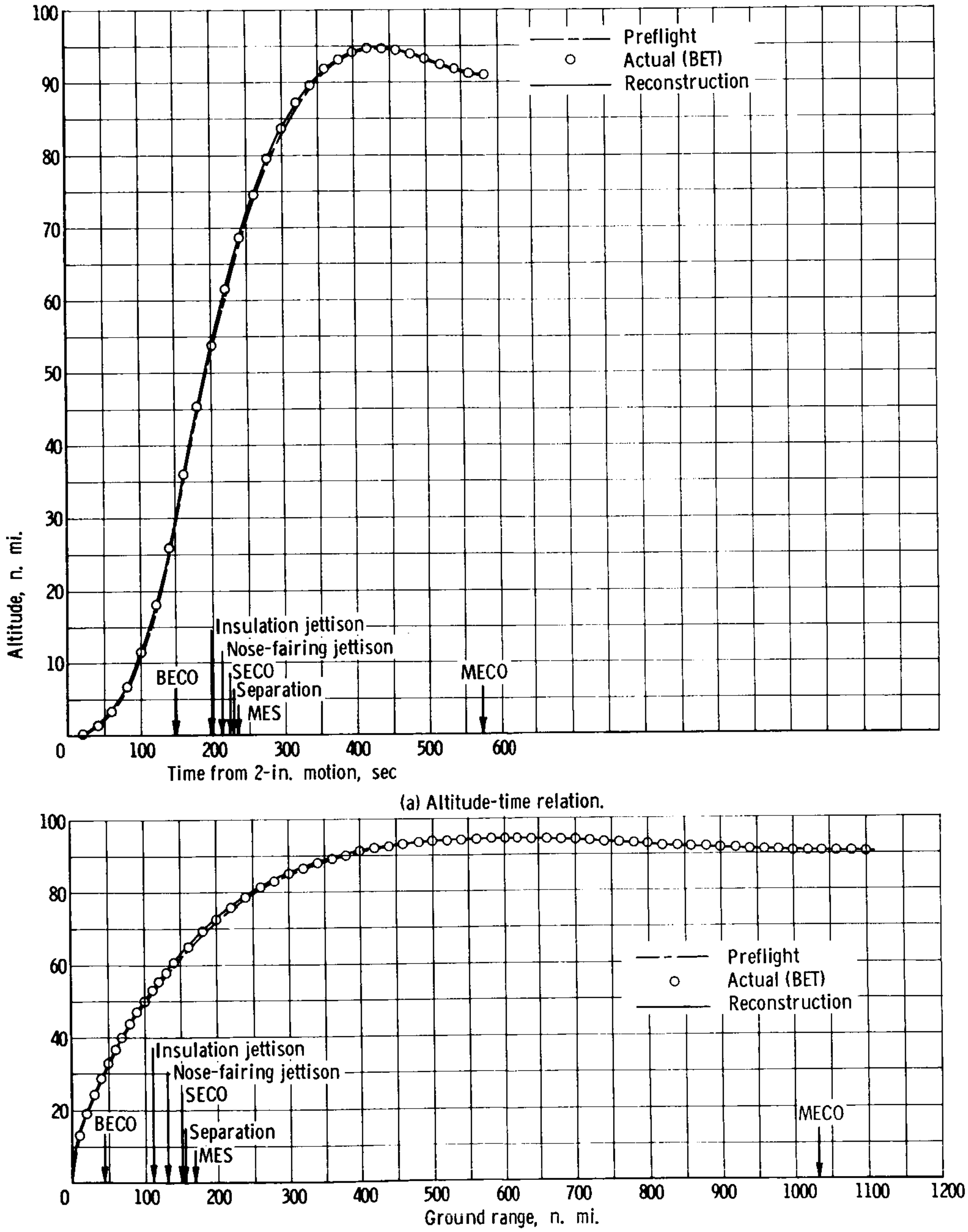

(a) Altitude-time relation.

(b) Vertical plane.

Figure V-4. - Trajectory position comparison.

[redacted]

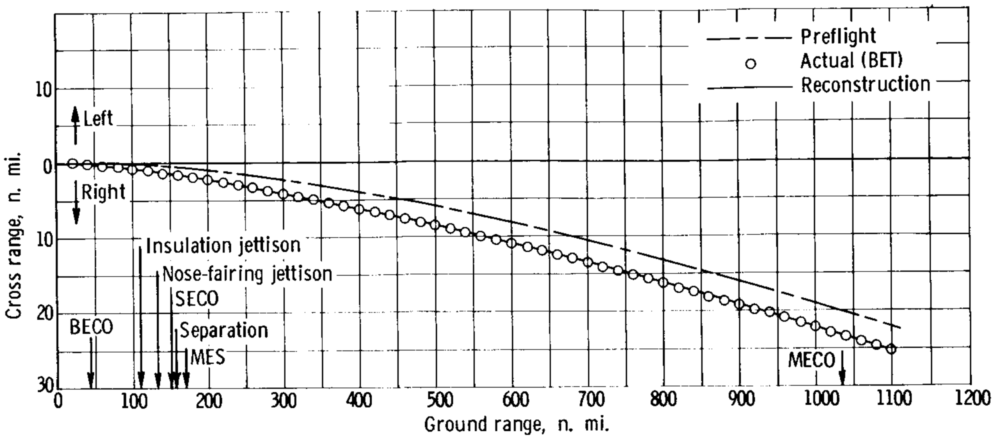

(c) Horizontal plane.

Figure V-4. - Concluded.

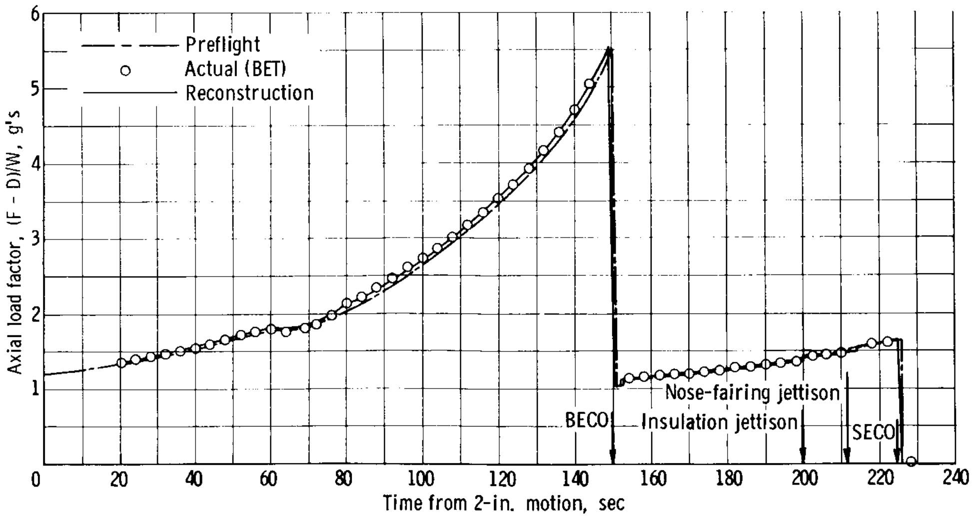

(a) Atlas phase.

Figure V-5. - Trajectory comparison. Thrust acceleration (axial load factor).

[redacted]

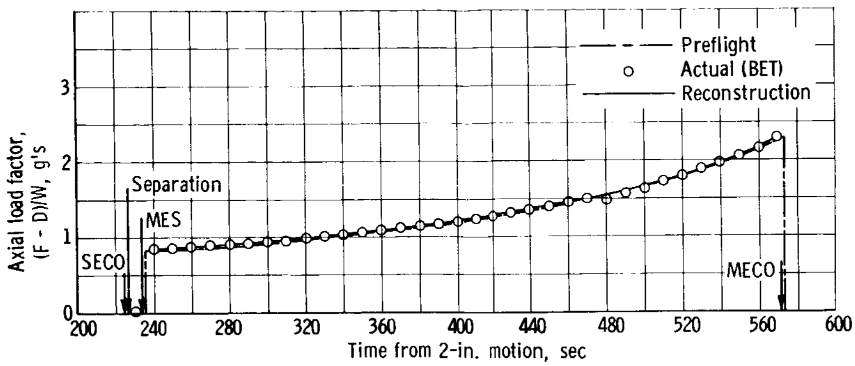

(b) Centaur phase.

Figure V-5. - Concluded.

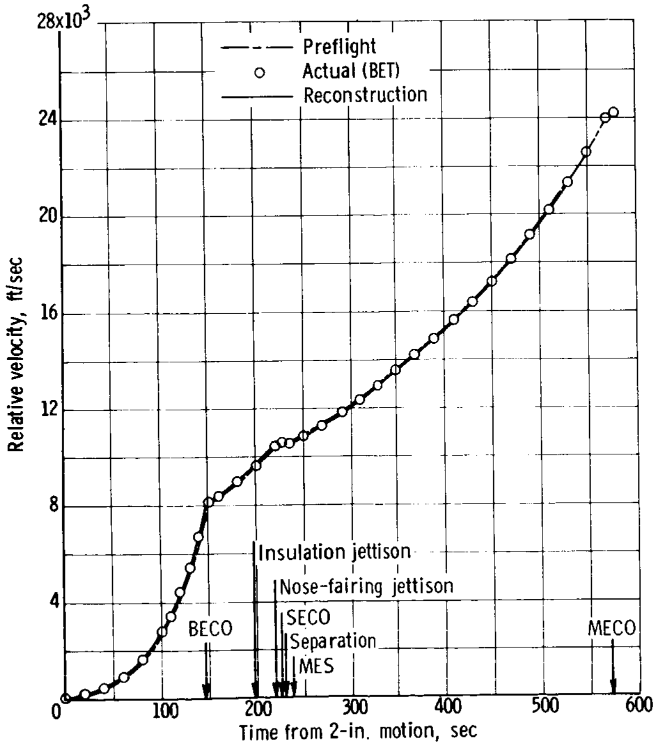

Figure V-6. - Trajectory comparison. Velocity relative to atmosphere including wind effects.

[redacted]

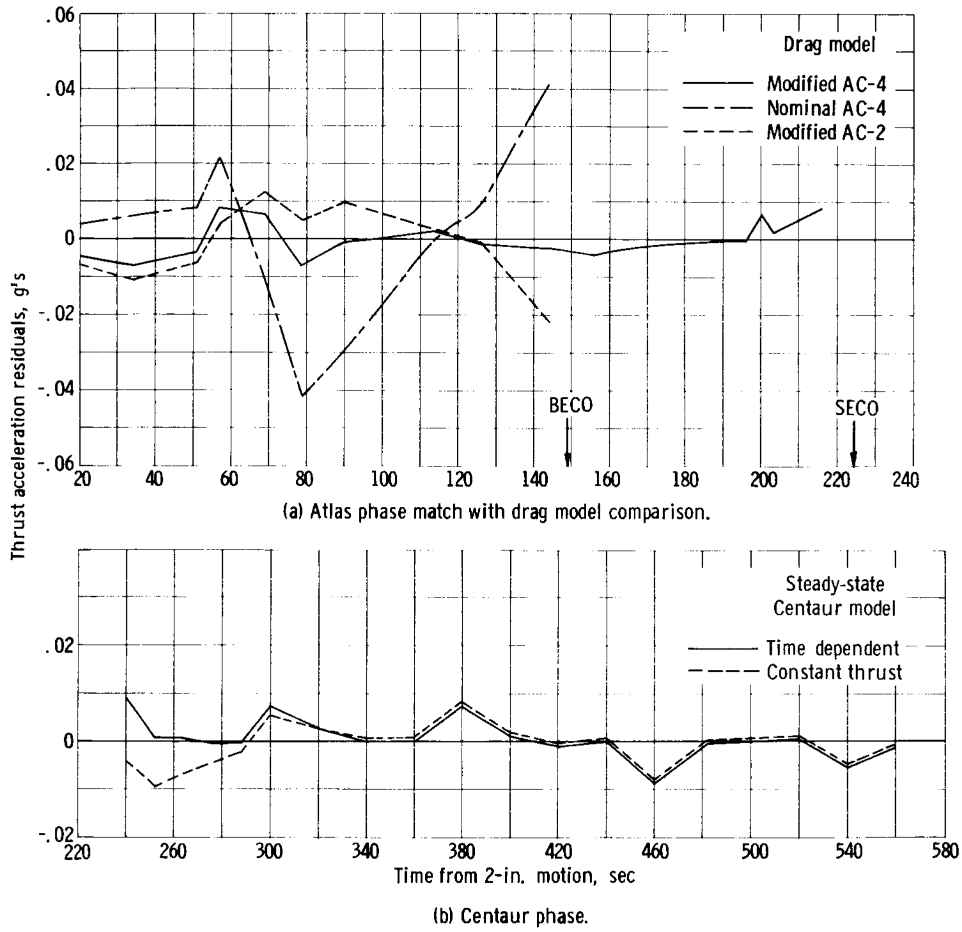

Figure V-7. - Thrust acceleration residuals (computed minus tracking) from AC-4 trajectory reconstruction.

[redacted]

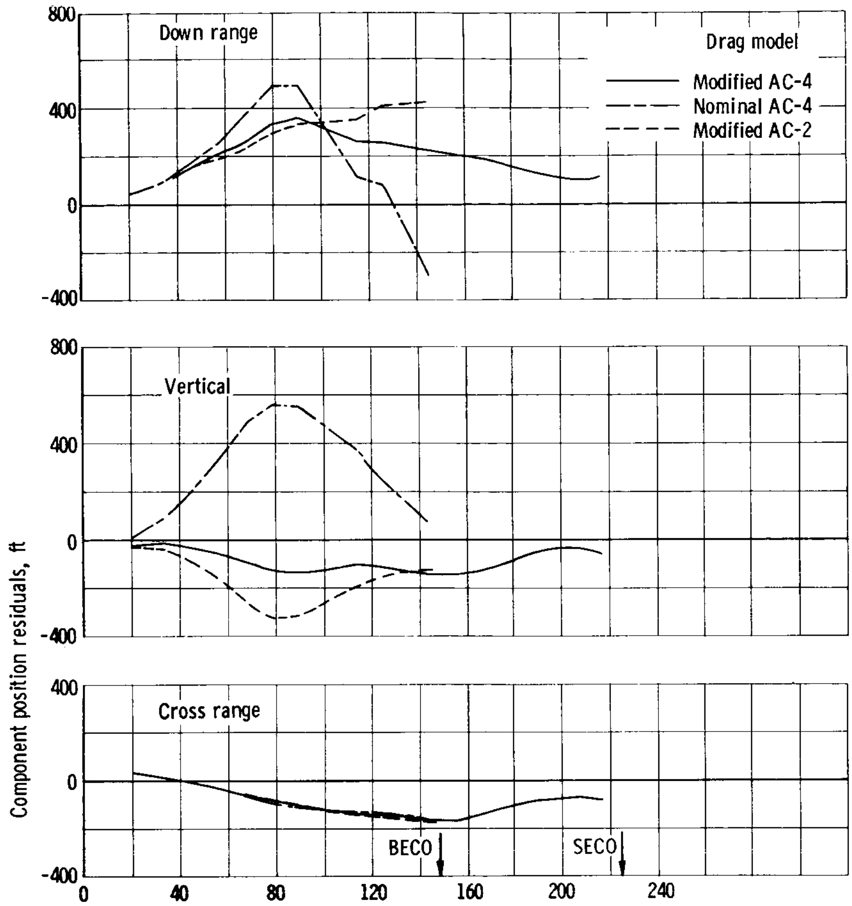

(a) Atlas phase.

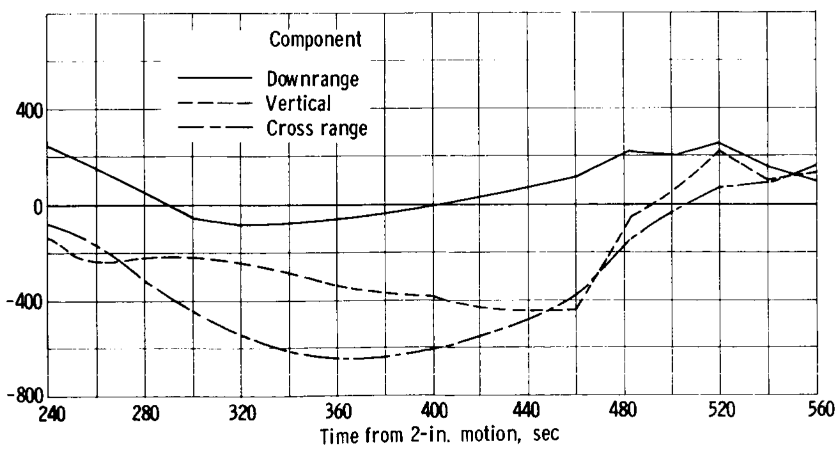

(b) Centaur phase.

Figure V-8. - Component position residuals (computed minus tracking) for AC-4.

[redacted]

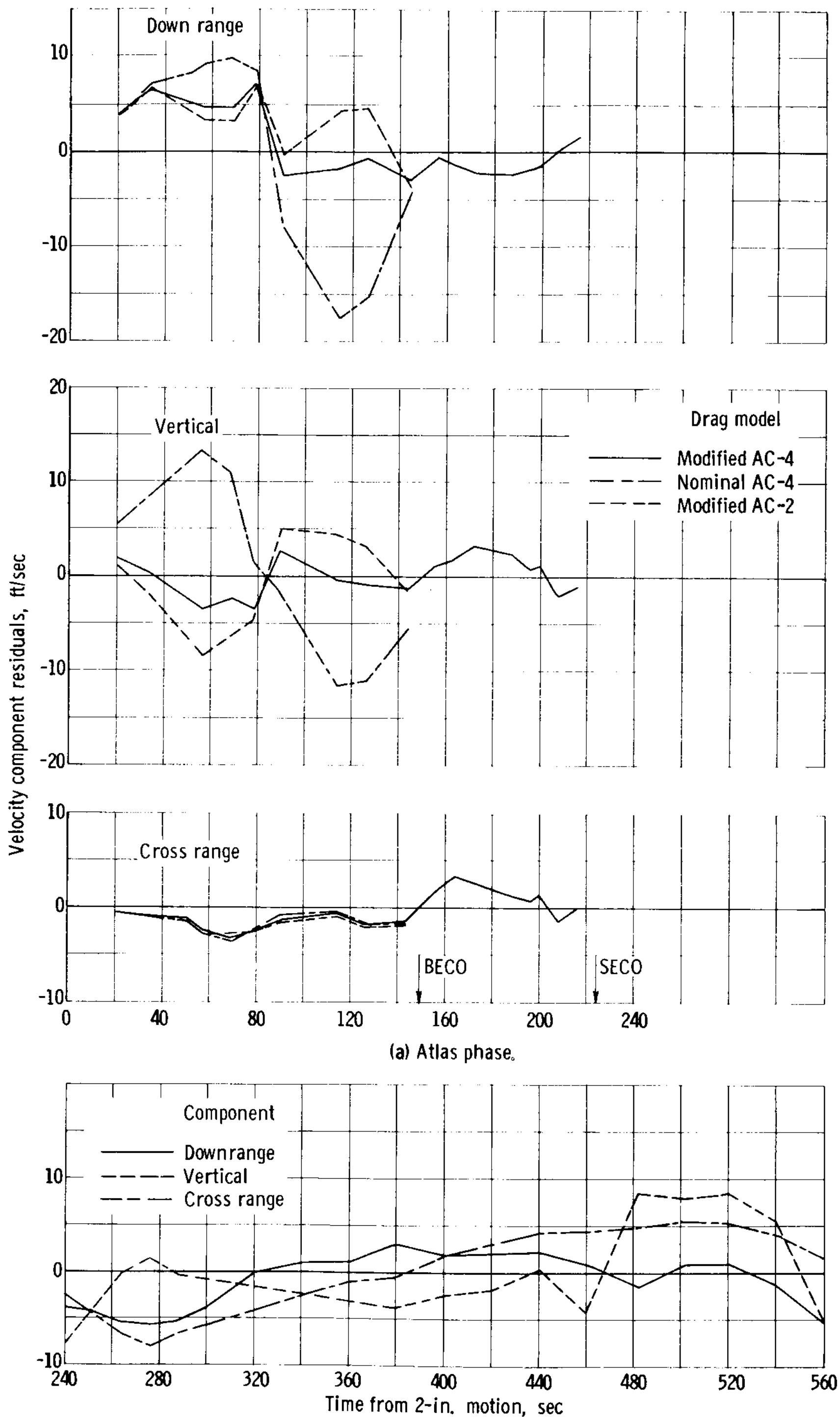

(b) Centaur phase.

Figure V-9. - Component velocity residuals (computed minus tracking) for AC-4.

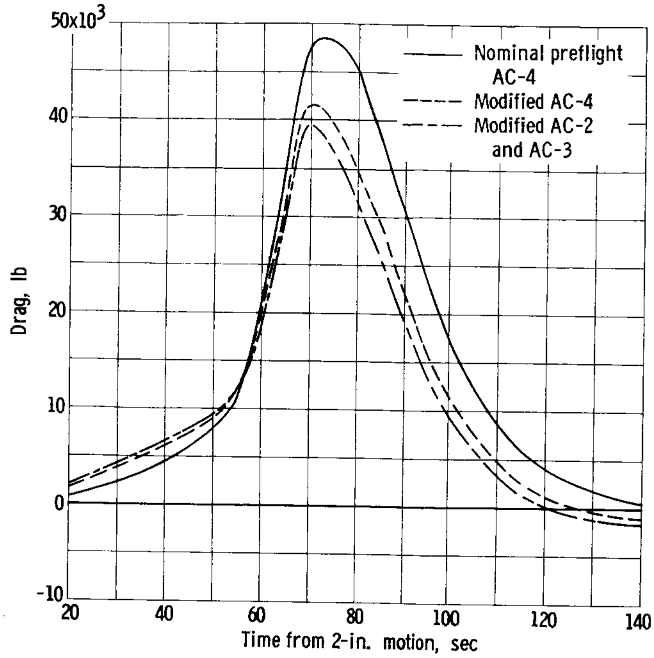

Figure V-10. - Comparison of drag computed with various drag coefficients and AC-4 BET data.

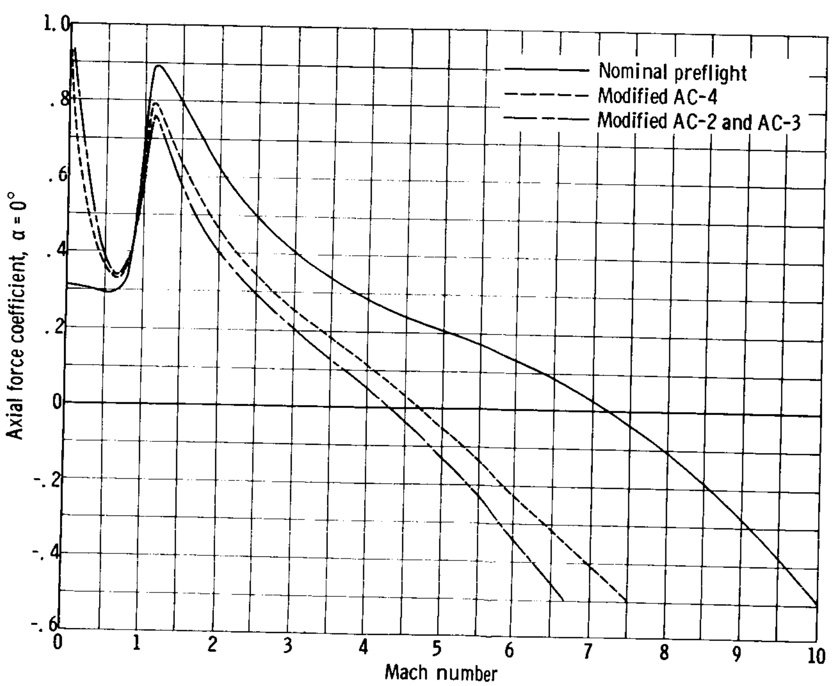

Figure V-11. - Comparison of drag curves used in AC-4 trajectory reconstruction.

VI. PROPULSION

SUMMARY

Atlas performance was almost as predicted throughout the booster phase of flight. The propulsion system operated satisfactorily during the Centaur first burn, but Centaur second burn was not obtained as planned.

ATLAS

Performance of the Atlas propulsion system in terms of thrust, specific impulse and mixture ratio at lift-off, booster engine cutoff, and sustainer engine cutoff is given in table VI-I. The DEPRO program (see appendix C) prediction is compared with values obtained using the DEPRO program based on flight data. The primary cause of values differing from those predicted is attributed to the different setting of the PU system. Previous Centaur boosters had been orificed to provide a mixture ratio of 2.359, whereas AC-4 (Atlas 146D) was orificed to 2.28. The PU valve positions were 1.8° below the nominal 26.7° setting at lift-off and 5.1° low (closed limit) at both BECO and SECO. Other factors causing values to be different from predicted are data inaccuracy and 146D having slightly hot boosters. All other Atlas propulsion values were nominal.

CENTAUR

Centaur first burn was obtained as planned. AC-4 was the first Centaur flight utilizing a pre-SECO boost-pump start and a reduced-power fuel boost pump. The hydraulic system modifications incorporated since AC-3 proved to be adequate.

Although the ullage settling rockets fired as planned during the coast phase and the attitude control system functioned properly, the effect of vehicle tumbling and the lack of fuel at the boost-pump inlet prevented the second burn from being obtained as programed.

All valves actuated properly for the Centaur reorientation and retromaneuver; however, this experiment lost its effect because of vehicle tumbling.

MAIN ENGINES

Main engine performance during the start-transient, steady-state, and shutdown periods for the first burn were satisfactory. Performance compared favorably with acceptance and ground testing and with previous flight data.

The chamber pressure and pump inlet conditions during the start-transient period were normal and are illustrated in figures VI-1 to 3. The start total impulse (valued up to 90 percent of rated thrust) for the C-1 and C-2 engines was 3840 and 3900 pound-seconds, respectively.

Steady-state values in terms of thrust, specific impulse, and mixture ratio are listed in table VI-II. Off-nominal values in the Lewis method for determining performance are a result of the sensitivity of this method, data accuracy, and accuracy of some of the engine constants. Specification requirements for the engine are 15 000±300 pounds for thrust, 430 seconds for specific impulse (nominal), and 5.0±2.00 percent for mixture ratio. Engine measurements obtained during steady-state operation and nominal operating values are shown in table VI-III.

At main engine cutoff (MECO), the chamber pressure for both engines started to drop simultaneously. Both engines required approximately 0.04 second to reach 5 percent of rated thrust, which is well within the normal differential impulse shutdown range.

Figures VI-4 and 5 illustrate fuel and LOX pump housing temperatures, respectively, from lift-off through the first orbit. The temperature variations noted between the C-1 and C-2 engines are characteristic; however, the magnitude of the temperature difference for both the fuel and LOX pumps appears to be greater during the first burn than that experienced on previous flights. There is no apparent reason for the increase in temperature differential of the two engines. Figure VI-6 illustrates the turbopump skin temperature during the first burn and also indicates that the C-2 engine is warmer.

Thrust chamber skin temperatures from lift-off through the first orbit are illustrated in figure VI-7.

For the attempted second-burn portion of flight, the C-1 chamber pressure started to rise at MES + 0.25 second and the C-2 engine at 3.7 seconds. This rise in chamber pressure indicates that the engines ignited and burned at a very low level. The chamber pressure for both engines never exceeded 10 psia. Because of the longer time lag for ignition of the C-2 engine, the differential pressure across the turbine was sufficient to rotate the turbopump. The C-2 hydraulic pressure momentarily reached a normal operating level during this time period. The lack of fuel at the pump inlet did not allow the engines to develop rated thrust. Second-burn operating conditions are given in table VI-IV. The fuel-pump-housing and thrust-chamber-skin temperatures were within engine specification requirements prior to second MES. The engine specification requires that the fuel-pump-housing temperature be 150° R or lower and the thrust-chamber-skin temperature be above 300° R. Figures VI-4(b) and 7(b) illustrate the flight temperatures prior to the second burn. Temperature excursions noted for the second burn, the retromaneuver, and the subsequent times followed engine programed activity.

BOOST PUMPS

AC-4 was the first Centaur flight that utilized a pre-SECO boost-pump start in support of the first main-engine start sequence. Resulting flight data indicated that this sequence is entirely satisfactory with no detrimental effects on boost-pump or engine performance. This was also the first Centaur flight in which a reduced-power fuel boost pump was used. The fuel unit flown was orificed to operate at a steady-state turbine speed of 45 955 rpm with a corresponding headrise of 15.15 psid.

The LOX boost pump was orificed to provide 27.3 psid headrise with a corresponding steady-state turbine speed of 32 580 rpm.

The first-burn start sequence was very close to the planned times with the boost-pump-start signal initiated 16.2 seconds prior to SECO. The time from boost-pump start to prestart was 19.8 seconds, and from boost-pump start to main-engine start was 25.8 seconds. Flight data indicated a normal start and acceleration of both LOX and fuel boost pumps. Except for CP28P (fuel-boost-pump turbine nozzlebox pressure) the time from start signal to first indication of gas-generator and nozzlebox pressures was approximately 0.8 second for both the LOX and fuel boost pumps. CP28P failed to rise until 9 seconds after the start signal. The delay is attributed to a failure of the transducer since the upstream gas-generator pressure, headrise, and turbine speed rose immediately.

First-burn performance data are presented in table VI-V, together with the steady-state acceptance data for comparison purposes. The fuel-boost-pump turbine speed appears to be approximately 900 rpm higher than expected. This does not correlate with the flight headrise data, which show a value slightly lower than the acceptance test value. With a higher turbine speed, the headrise should be correspondingly higher. These differences are the result of inaccuracies involved in interpreting the data. Fuel-boost-pump gas-generator and nozzlebox pressures were normal with minor oscillations less than ±10 psia peak to peak. LOX-boost-pump gas-generator and nozzlebox pressures were slightly lower than the acceptance values, but had no significant effect on performance. These values were expected to be slightly low in flight because of an error during the acceptance test in which a hydrogen peroxide inlet pressure of 309 psia was used instead of the nominal inflight value of 296 psia. Preflight predictions estimated a reduction of nozzlebox pressure of approximately 3 psi and a corresponding reduction in LOX-boost-pump headrise of 1 to 1.5 psid. Minor oscillations of less than ±10 psi were also noted on the LOX-boost-pump gas-generator and nozzlebox pressures, with no noticeable effect on performance.

Following first MECO, the fuel-boost-pump headrise essentially decayed to zero for 2 seconds before ΔP was reestablished, and normal decay resumed during coastdown of the boost pump (see fig. VI-8). Simultaneously with headrise going to zero, the turbine speed trace flattens out to a constant value (see fig. VI-9). This phenomenon has been noted on previous flights as well as in ground tests and is attributed to a combination "water-hammer" effect, due to sudden valve closing downstream, and backflow of gaseous and/or liquid hydrogen through the boost pump. The backflow through the boost pump is believed to be a result of relieving the high-pressure liquid hydrogen downstream of the main-engine fuel pump after the main fuel shutoff valve closes at MECO. The valve sequencing is such that the engine inlet valve remains open for approximately 0.4 second after MECO. Turbine speed coastdown for the LOX boost pump was 115 seconds, and became linear at approximately MECO + 20 seconds, which corresponds with the time that LOX-boost-pump headrise becomes zero (approx. MECO + 19 sec).

Turbine speed coastdown for the fuel boost pump was 65 seconds, and became linear at approximately MECO + 20 seconds, which again corresponds with the time that fuel-boost-pump headrise goes to zero (MECO + 20 sec). It is felt that this phenomenon is due to loss of liquid at the boost-pump inlet under zero-gravity conditions and is of no significance provided adequate thrust is available to resettle the propellants prior to the second start attempt. Calculations were made which indicate that approximately 20 pounds of liquid hydrogen were pumped through the boost-pump volute bypass line during the post-MECO coastdown. This contributed to the propellant disturbances within the fuel tank during the coast phase.

During the coast phase, at lift-off + 610 seconds, the fuel-boost-pump turbine nozzle temperature transducer (CP29T) failed completely. The fuel-boost-pump discharge temperature (CP884T) began a gradual rise and eventually went off scale (high) indicating gaseous hydrogen in the propellant ducts. This was anticipated prior to flight, and 35 seconds of boost-pump deadhead operation were programed at the second start to ensure liquid in the ducts.

The fuel-boost-pump electrical-distribution-box and control-valve temperatures (CP336T and CP337T, respectively) went off scale (high) sometime after lift-off + 1080 seconds at a time when there was no telemetry coverage. (Schematic drawings of the fuel-boost-pump and oxidizer systems are shown in fig. VI-10.) The upper range capabilities of these transducers were 147.1° and 146.9° F, respectively. The temperature limit for the electrical distribution box is specified at 200° F maximum. The maximum operating temperature for the valve is specified at 160° F. The electrical distribution box is not considered a problem, but the valve temperature must be evaluated for future two-burn missions, since the maximum specification limit for hydrogen peroxide is 140° F. It should be noted, however, that the AC-4 second boost-pump start showed a normal gas-generator and nozzlebox pressure rise for both LOX and fuel with no indications of a vapor lock condition.

Second boost-pump start was initiated at lift-off + 2010.1±0.5 seconds followed by prestart at 2044.8 seconds and main-engine start signal at 2049.8 seconds.

The first indication of gas-generator and nozzlebox pressures was 0.6 and 0.2 second for the LOX and fuel boost pumps, respectively. Oscillations of ±20 psi were noted in the LOX-boost-pump gas generator, beginning at BPS + 32 seconds and continuing until cutoff. Similar oscillations of ±15 psi were evident in the LOX nozzlebox pressure, beginning at BPS + 32 seconds but ending at BPS + 55 seconds. Oscillations occurred in the fuel-boost-pump gas-generator and nozzlebox pressures (approx. ±20 psi) from BPS until over-speed trip-out occurred. Oscillations of similar magnitudes have been observed on several ground tests with no detrimental effects on boost-pump performance. The LOX boost pump started and operated successfully during the second-burn attempt (see table VI-VI).

The fuel-boost-pump performance for the attempted second start was not

[redacted]

normal. A detailed explanation is given in section XV. <u>COAST-PHASE PROPELLANT AND VEHICLE BEHAVIOR</u>.

HYDRAULIC SYSTEM PERFORMANCE

The analysis of data obtained from the AC-3 C-1 engine hydraulic system failure strongly indicated that the system remained intact and that the prime suspect trouble area was that of the interface between the RL-10 engine and the hydraulic power package. Schematic drawings of the AC-3 Centaur hydraulic system and the modified AC-4 system are shown in figure VI-11.

The hydraulic power package main pump assembly is driven by the engine LOX turbopump drive shaft, which is near liquid-hydrogen temperature during engine operation and prelaunch liquid-helium childown. The drive coupling interface therefore must provide an adequate thermal barrier through all phases of prelaunch and flight so that the hydraulic system temperature remains above -30° F at all times. The most significant failure modes that could have caused the hydraulic system loss are

(1) Excessive cooling of the nylon drive coupling

(2) Pump or pump shaft failure

(3) Large-particle contamination of the pump

(4) Engine accessory drive failure

(5) Interface structural failure

Redesign of the hydraulic system and the new preflight testing program philosophy have been adapted to eliminate completely the possible failure modes. The redesigned system encompasses the following additions and changes:

(1) Incorporation of ambient helium gas purges to the accessory drive cavity of the engine and the coupling area between the power package main pump and the open hydraulic power package adapter

(2) Incorporation of a metallic bellows coupling to replace the nylon coupling; this new coupling provides greater flexibility, thermal isolation, and shielding between the engine drive and the power package

(3) Incorporation of an open adapter to disperse any leakage from the hydraulic or engine system

(4) Incorporation of a return line and main pump inlet filters

(5) Incorporation of a main pump with a larger shaft and a face-type seal

(6) Incorporation of a phenolic insulation block with more uniform distribution of expected loads

[redacted]

Associated changes were made to the remaining portions of the system to adapt to the modifications, but for the most part the basic schematic representation is the same as shown in figure VI-11(b).

Evaluation of the data received from the AC-4 flight shows that both C-1 and C-2 hydraulic systems operated properly. Full system pressure was achieved in 1.5 seconds on both systems and held steady throughout main engine burn (figs. VI-12 and 13). At SECO + 0.1 second, the circulation systems of C-1 and C-2 engine hydraulics came up to their proper values. The C-1 and C-2 pressures were 111 and 110 psia, respectively. Both engines moved to null under circulation system power at a rate of approximately 0.3 degree per second. From SECO + 0.1 to MES + 0 second, the pressure profiles and the pitch and yaw feedbacks were quite similar to those of AC-2 and AC-3. Thrust buildup and the associated rate transients were such that, at MES + 4 seconds, the vehicle attitude was very close to that required by guidance when it was readmitted. Consequently, engine gimbal requirement and hydraulic demand were very low. The usual dip in pressure at MES + 4 seconds was nonexistent. C-1 and C-2 main-system pressures were steady at 1167 and 1188 psia, respectively.

The ambient helium purges to the accessory drive and coupling cavities during liquid helium ground chilldown were effective in thermally isolating the power packages from the engine accessory drive pad. Temperatures of the oil in the power packages and manifolds were maintained at 70° F prior to lift-off. The expected drop in temperatures through booster phase and the subsequent rise during engine operation were realized equally on both systems: the minimum and maximum were 60° and 155° F, respectively. The only discrepancy at this point of operation can be seen on the traces of hydraulic power package adapter temperatures as a function of time (fig. VI-12). The temperature drop of the C-1 adapter was more rapid than that of the C-2, and it is suspected that this was caused by a cooler C-1 engine or greater dynamic seal leakage from the accessory cavity of the engine. In any event, this temperature discrepancy was not reflected to the power package indicating that thermal isolation in space was adequately effective through coast and the second main-engine start. At main-engine cutoff, the manifold temperatures were as expected and approximately 25° higher than those of the power package pump discharge (fig. VI-14). Minimum temperatures of the power packages and manifolds throughout coast were above 80° F. Therefore, thermostatic activation of the recirculation pump was not commanded.

Temperature profiles of the power packages and the manifolds showed a dipping and separation at approximately T + 1260 seconds. An associated engine movement without hydraulic power occurred at this same point of flight. Engine movements (fig. VI-15) were more pronounced in pitch to the toed-in position and can be attributed to the predominance of tumble and acceleration forces that resulted. Manifold temperature profile separation, which started at this same time, is attributed possibly to the movement of hydraulic fluid by the actuator pistons. These combined with the effect of sun radiation and manifold shading due to vehicle tumble and roll provide the only positive explanation at this time. Other heating or cooling environments near either manifold could also cause such a temperature dispersion, but no evidence of any extraneous source exists at this time.

ATTITUDE CONTROL AND HYDROGEN PEROXIDE SYSTEMS

A schematic diagram of the attitude control and H_2O_2 supply systems is shown in figure VI-16. The H_2O_2 system temperatures were normal during the first portion of the flight (fig. VI-17). The abrupt temperature change in the two fuel supply lines at T - 194 seconds was caused by pressurizing the bottle. Normally, any change at this time would be an increase in temperature caused by warmer H_2O_2 from the bottle entering the lines. A possible explanation for the drop in the P-2 fuel-supply-line temperature is that the line was not completely purged prior to pressurization, and when the system was pressurized, colder H_2O_2 in the upstream line moved to the location of the temperature probe. The drop in all temperatures at lift-off is the result of discontinuing the ground air conditioning at this time. The temperature rise in both cluster manifolds at approximately T + 75 seconds is attributed to aerodynamic heating. Both fuel-supply-line temperatures increased after first MECO because of H_2O_2 flow in the lines as the attitude control and ullage settling engines were fired. Shortly after T + 1300 seconds, the P-2 cluster manifold temperature decreased sharply. Since flight data show that H_2O_2 is flowing to this cluster almost constantly during this period, there is no reason for a temperature drop. Therefore, it is assumed that the temperature patch separated from the manifold and came close to the tank bulkhead. The P-1 cluster manifold temperature went off scale (high) some time after T + 2340 seconds. This is attributed to instrumentation failure since there is no change in system operation before or after this time.

Figure VI-18 shows the combustion chamber temperatures on the ullage control engines. These temperatures are considered inaccurate from a quantitative standpoint. Their prime purpose was to confirm ullage engine firing. The sharp increase in temperature at first MECO and decrease after second MES show that the engines operated as programed.

The H_2O_2 bottle pneumatic pressure was normal throughout the flight (fig. VI-19). After pressurizing the bottle on the ground, the pressure remained at 317 psia until the boost pumps started at T + 208 seconds when the pressure dropped to about 302 psia. This drop is normal and is explained by the fact that the bottle pressure regulator is referenced to ambient pressure and is set to give a nominal pressure of 300 psia in space. Therefore, it will regulate to a nominal 315 psia on the ground and will gradually decrease as the vehicle rises. The bottle pressure did not drop gradually because a check valve between the regulator and the bottle traps the initial pressure in the bottle until H_2O_2 is first used at boost-pump start. The pressure remained at approximately 302 psia for the remainder of the flight.

Data that indicate attitude control engine firing times are shown in figure VI-20. Figures VI-20(a) to (b-3) show A-3 and A-4 engines firing with an almost constant duty cycle of 0.9 second on and 1.7 seconds off from shortly after first MECO to first MECO + 267 seconds. There are several possibilities or combinations of possibilities that could have caused this yaw error. If the propellants moved to the forward end of the tank after MECO, the center of gravity of the vehicle would move forward and the ullage control engines could create a couple about the center of gravity. A second possible cause could be exhaust gas impingement from the ullage control engines on the main engines. Another cause could be a leak in any pressure line on the vehicle. At first MECO + 267 seconds when the LH_2 tank started venting, the A-3 and A-4 engines remained on almost constantly until sometime after MECO + 484 seconds (area of no data coverage). It is evident that the venting of LH_2 caused a yaw torque on the vehicle above the recovery capability of the attitude control engines. By MECO + 784 seconds, the error had changed to a pitch-roll-yaw error, and the P-1 and A-3 engines came on and remained on for most of the remaining portion of flight. This type of error is attributed to a differential thrust from the two exhaust ducts of the LH_2 vent valve (see section VII. CENTAUR PROPELLANT SYSTEMS).

[redacted]

TABLE VI-I. - ATLAS PERFORMANCE - DEPRO PROGRAM[a]

	Flight value	Predicted value
Thrust at lift-off + 10 seconds, lb		
Boosters	307 320	306 940
Sustainer	56 600	56 650
Verniers, axial	1 710	1 710
Total	365 630	365 300
Thrust at BECO, lb		
Boosters	357 810	356 600
Sustainer	79 710	79 760
Verniers, axial	1 970	1 970
Total	439 490	438 330
Thrust at SECO, lb		
Sustainer	76 910	79 100
Verniers, axial	1 460	1 460
Total	78 370	80 560
Specific impulse at lift-off, sec		
Boosters	250.1	250.4
Sustainer	216.1	207.2
Total	244.5	243.6
Specific impulse at BECO, sec		
Booster	287.7	288.1
Sustainer	302.3	297.8
Total	289.9	291.4
Specific impulse at SECO, sec		
Total	295.7	303.2
LOX to fuel ratio		
Lift-off	2.321	2.240
BECO	2.356	2.336
SECO	2.035	2.228

[a]See appendix C for explanation.

[redacted]

TABLE VI-II. - CENTAUR PERFORMANCE[a]

(a) C-1 engine (1847)

	Acceptance test, P_c = 293.5	Time from MES, sec							
		5	50	100	150	200	250	300	338
Thrust, lb	14 990								
Lewis Venturi		14 736	14 855	14 799	14 725	14 748	14 729	14 746	14 721
PWA Regression		15 021	14 949	14 954	14 882	14 880	14 881	14 890	14 882
PWA C*		14 966	15 070	15 031	14 948	14 972	14 951	14 971	14 947
Specific impulse, sec	432.0								
Lewis Venturi		425.3	421.9	425.1	423.7	424.3	423.4	424.5	424.5
PWA Regression		430.4	431.6	431.6	432.8	432.8	432.8	432.6	432.8
PWA C*		431.3	430.6	430.5	431.0	430.8	430.9	430.9	431.1
Mixture ratio	4.97								
Lewis Venturi		4.977	5.113	5.068	5.036	5.045	5.054	5.036	5.018
PWA Regression		5.212	5.051	5.059	4.893	4.890	4.893	4.913	4.898
PWA C*		5.040	5.132	5.143	5.079	5.099	5.094	5.093	5.073

(b) C-2 engine (1858)

	Acceptance test, P_c = 299.3	Time from MES, sec							
		5	50	100	150	200	250	300	338
Thrust, lb	15 018								
Lewis Venturi		14 889	15 220	14 982	14 961	14 952	14 905	14 944	14 940
PWA Regression		15 087	15 048	15 046	14 965	14 957	14 956	14 959	14 955
PWA C*		15 028	15 366	15 109	15 085	15 071	15 020	15 064	15 061
Specific impulse, sec	431.0								
Lewis Venturi		419.9	419.1	412.5	413.2	411.3	411.1	412.4	412.8
PWA Regression		429.8	430.4	430.5	431.9	432.0	432.0	432.0	432.0
PWA C*		433.8	432.5	433.1	432.9	432.8	433.1	433.0	433.0
Mixture ratio	5.0								
Lewis Venturi		4.985	5.190	5.208	5.227	5.274	5.245	5.238	5.221
PWA Regression		5.157	5.074	5.067	4.882	4.867	4.868	4.875	4.869
PWA C*		4.656	5.856	4.765	4.794	4.809	4.774	4.789	4.780

[a]See appendix C for explanation of techniques.

TABLE VI-III. - CENTAUR ENGINE STEADY-STATE OPERATING CONDITIONS

	Nominal	MES + 50 sec	MES + 338 sec
C-1 engine			
LH_2 pump total inlet pressure, psia	38.4	33.85	31.76
LH_2 pump inlet temperature, $^{\circ}R$	38.8	39.2	36.7
LOX pump total inlet pressure, psia	59.8	58.6	58.8
LOX pump inlet temperature, $^{\circ}R$	176.6	177.0	174.8
LOX pump speed, rpm	11 350	-----	11 040
LOX pump discharge pressure, psia	464	446	438
LH_2 pump discharge pressure, psia	922	892	875
Fuel Venturi upstream pressure, psia	649	659.8	655.0
Turbine inlet temperature, $^{\circ}R$	331	340.3	335.1
Chamber pressure, psia	293.5	291.7	289.5
C-2 engine			
LH_2 pump total inlet pressure, psia	38.4	35.75	33.29
LH_2 pump inlet temperature, $^{\circ}R$	38.8	37.35	36.8
LOX pump total inlet pressure, psia	59.8	59.6	57.6
LOX pump inlet temperature, $^{\circ}R$	176.6	177.2	175.0
LOX pump speed, rpm	11 350	-----	11 390
LOX pump discharge pressure, psia	464	438	438
LH_2 pump discharge pressure, psia	922	920	937
Fuel Venturi upstream pressure, psia	649	688.2	683.8
Turbine inlet temperature, $^{\circ}R$	331	338.0	339.7
Chamber pressure, psia	299.3	302.0	296.3

TABLE VI-IV. - CENTAUR SECOND-BURN OPERATING CONDITIONS

	Time, sec			
	MES	+5	+30	+50
C-1 engine				
LH_2 pump inlet pressure, psia	15.7	-----	14.9	14.4
LH_2 pump inlet temperature, °R	-----	-----	~37.5	-----
LOX pump inlet pressure, psia	108.0	-----	108.4	108.4
LOX pump inlet temperature, °R	-----	-----	~177	-----
Turbine inlet temperature, °R	275	505	505	505
Chamber pressure, psia	0	8.0	7.2	7.2
C-2 engine				
LH_2 pump inlet pressure, psia	15.8	15.6	15.0	14.5
LH_2 pump inlet temperature, °R	-----	-----	37.5	-----
LOX pump inlet pressure, psia	113.3	108.8	109.0	108.8
LOX pump inlet temperature, °R	-----	-----	~177	-----
Turbine inlet temperature, °R	260	505	505	505
Chamber pressure, psia	0	9.9	7.0	5.8

[redacted]

TABLE VI-V. - AC-4 FIRST-BURN BOOST-PUMP PERFORMANCE

Parameter	Prestart[a]	MES[a]	MES + 60 sec[a]	MECO[b]	Initial acceptance test (steady state)
Fuel boost pump					
Turbine speed, rpm	49 650	47 950	46 650	46 830	45 955
Gas-generator pressure, psia	148.6	149.6	151.6	152.1	153.5
Nozzlebox pressure, psia	140.0	140.0	-----	141.9	136.5
Headrise, psid	24.95	22.9	14.6	14.9	15.15
Oxidizer boost pump					
Turbine speed, rpm	37 705	36 555	32 000	32 500	32 580
Gas-generator pressure, psia	97.1	98.1	100.1	[c]100.9	107.0
Nozzlebox pressure, psia	84.4	85.0	90.0	[c]112.5	95.0
Headrise, psid	66.9	64.9	25.7	26.2	27.3

[a]Data source, TEL II replay and Grand Bahama Island.
[b]Data source, Antigua.
[c]Data are questionable; nozzlebox pressure cannot exceed gas-generator pressure.

TABLE VI-VI. - AC-4 SECOND-BURN LOX-BOOST-PUMP PERFORMANCE[a]

Parameter	Prestart	MES	MECO
Oxidizer boost pump			
Speed, rpm	37 890	37 440	38 140
Gas-generator pressure, psia	[b]92.5	[b]96.5	[b]96.5
Nozzlebox pressure, psia	92.3	92.3	94.5
Headrise, psid	76.2	72.3	73.5

[a]Fuel boost pump cavitated prior to prestart.
[b]Data are questionable; do not correlate with turbine speed, nozzlebox pressure, and headrise.

[redacted]

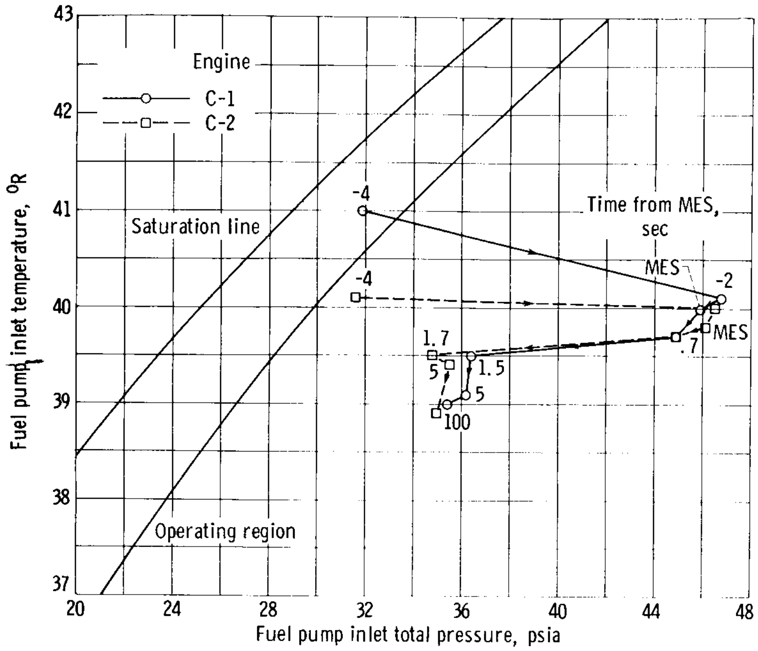

Figure VI-1. - Fuel pump inlet conditions near engine start.

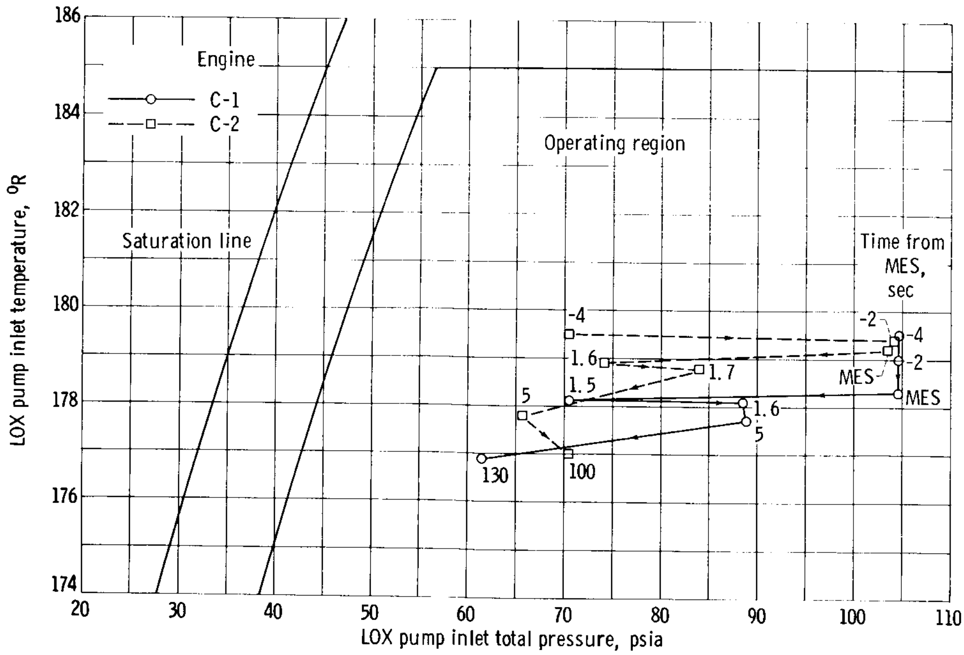

Figure VI-2. - LOX pump inlet conditions near engine start.

[redacted]

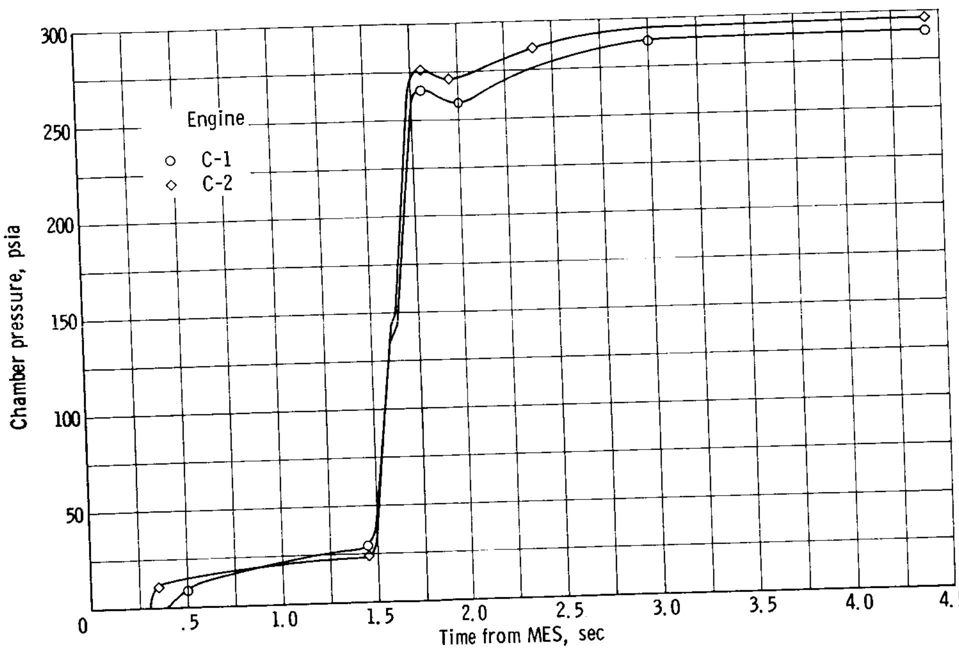

Figure VI-3. - Start transient chamber pressure.

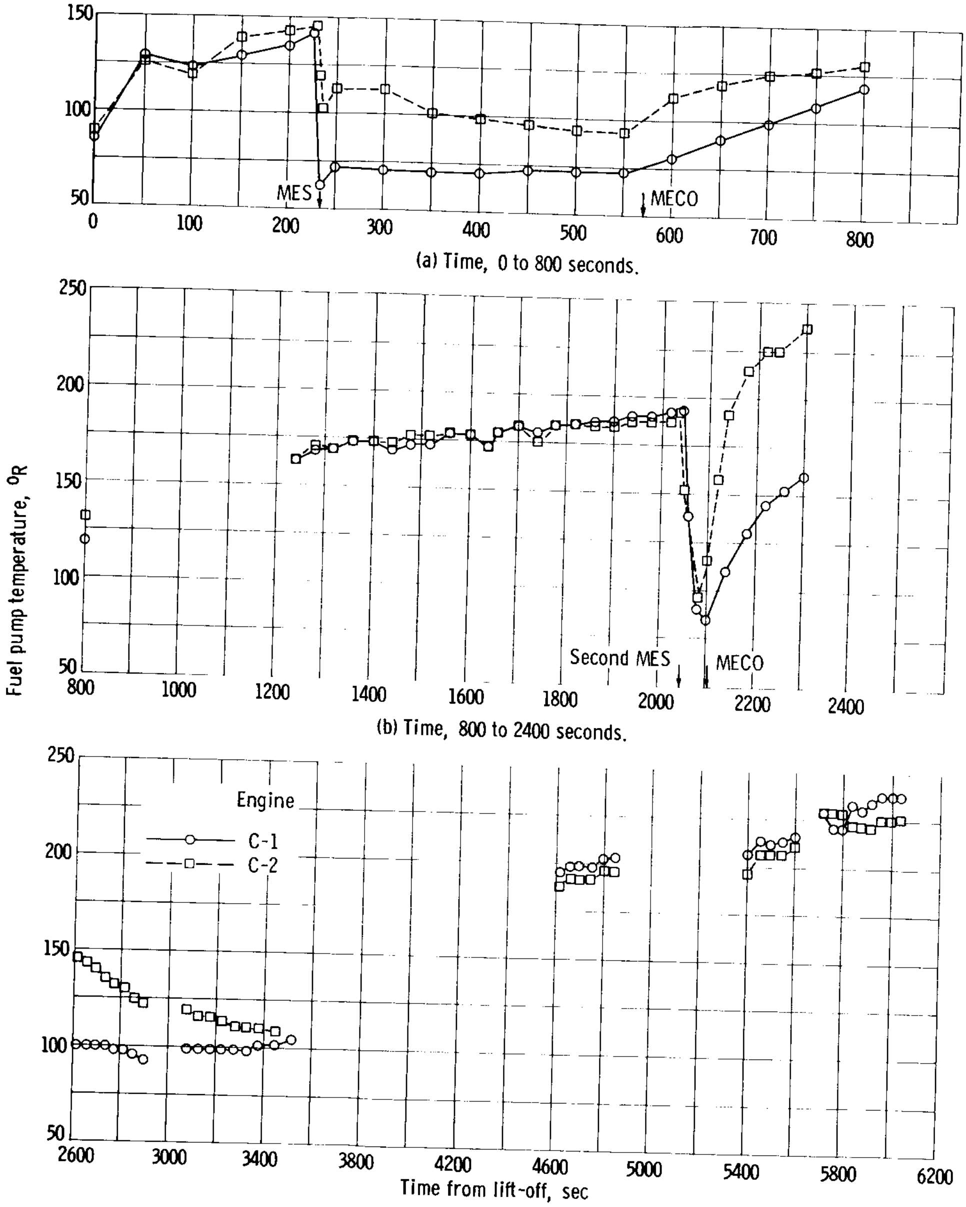

(a) Time, 0 to 800 seconds.

(b) Time, 800 to 2400 seconds.

(c) Time, 2600 to 6200 seconds.

Figure VI-4. - Fuel pump housing temperature.

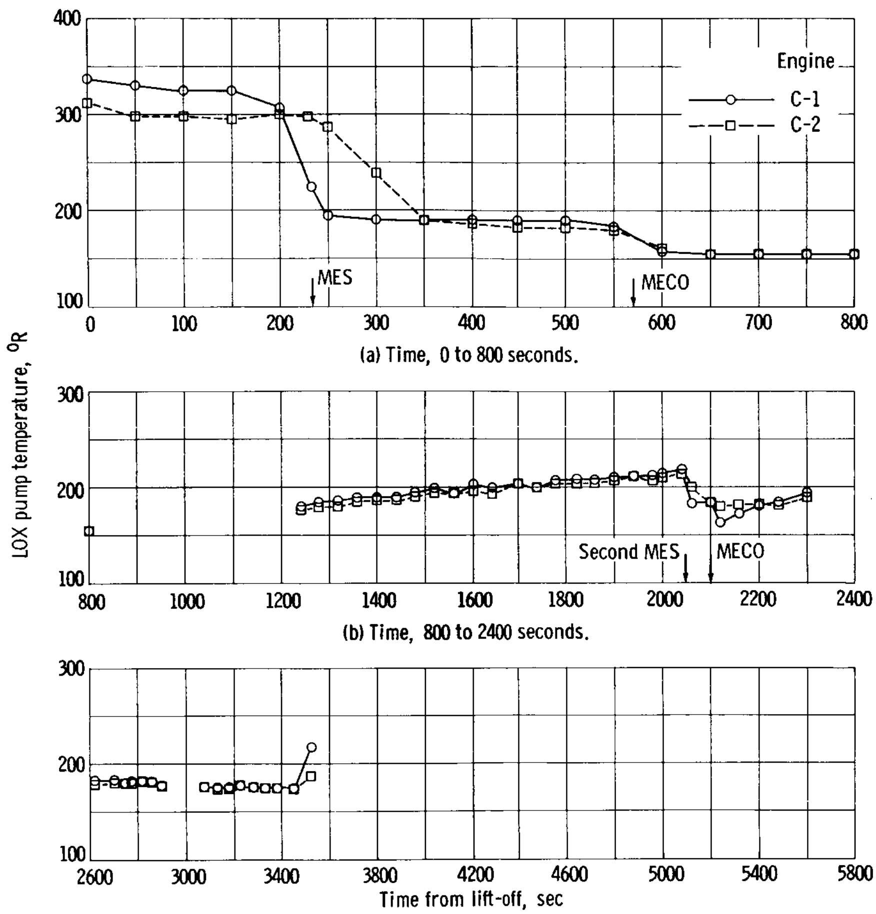

(c) Time, 2600 to 5800 seconds.

Figure VI-5. - LOX pump housing temperature.

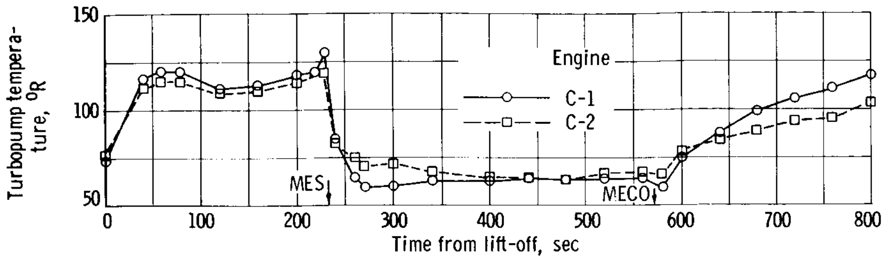

Figure VI-6. - Turbopump housing temperature.

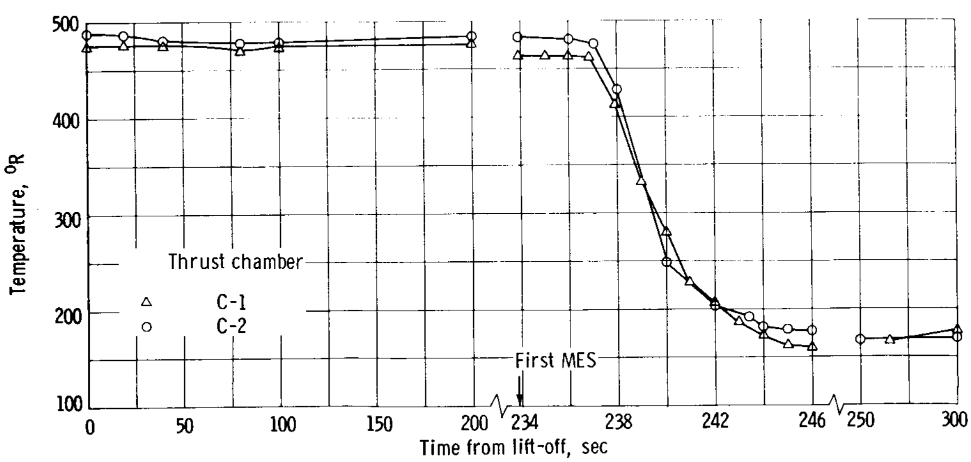

(a) Time, 0 to 300 seconds.

Figure VI-7. - Thrust chamber skin temperature.

[redacted]

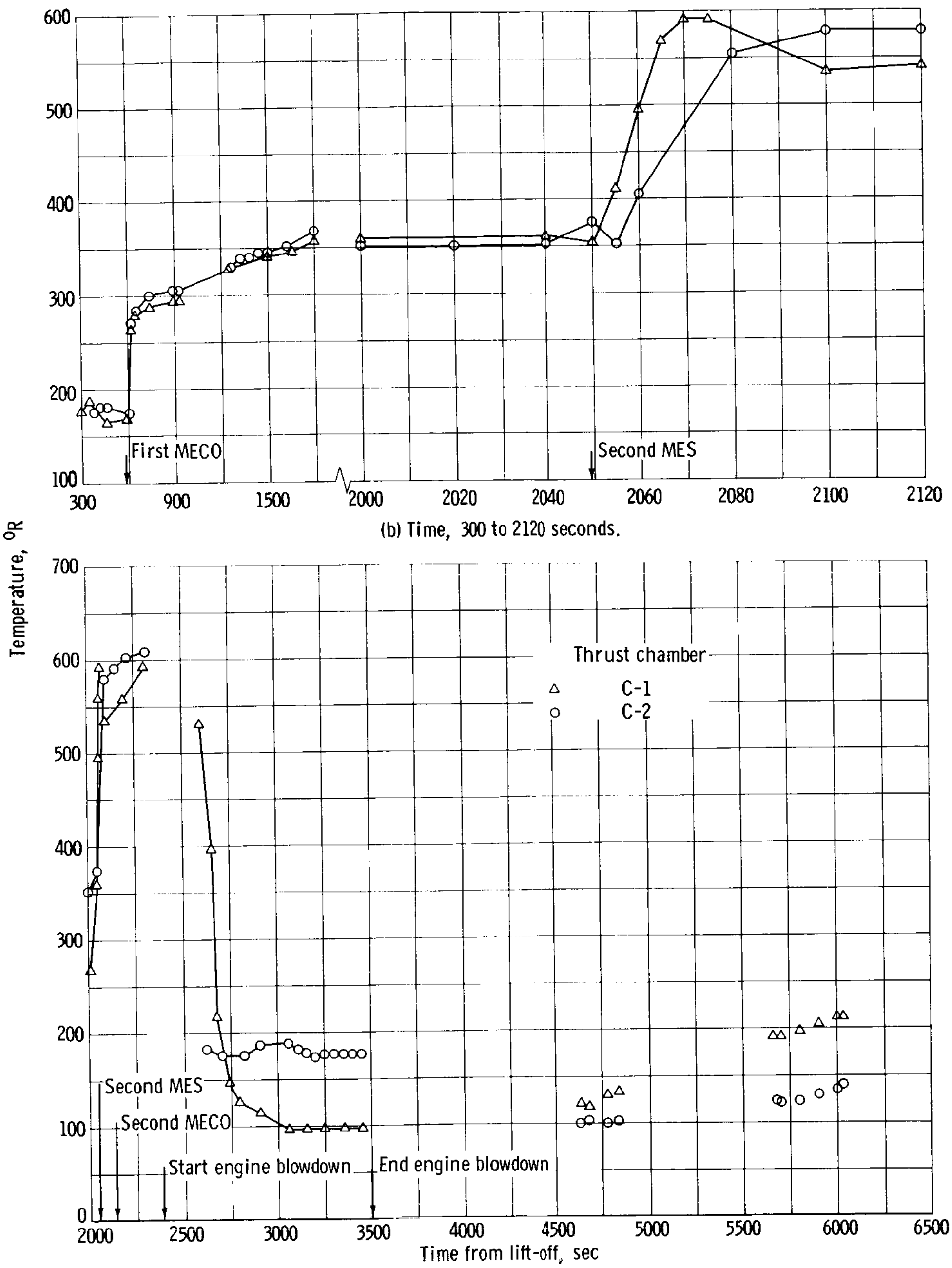

(b) Time, 300 to 2120 seconds.

(c) Time, 2000 to 6500 seconds.

Figure VI-7. - Concluded.

[redacted]

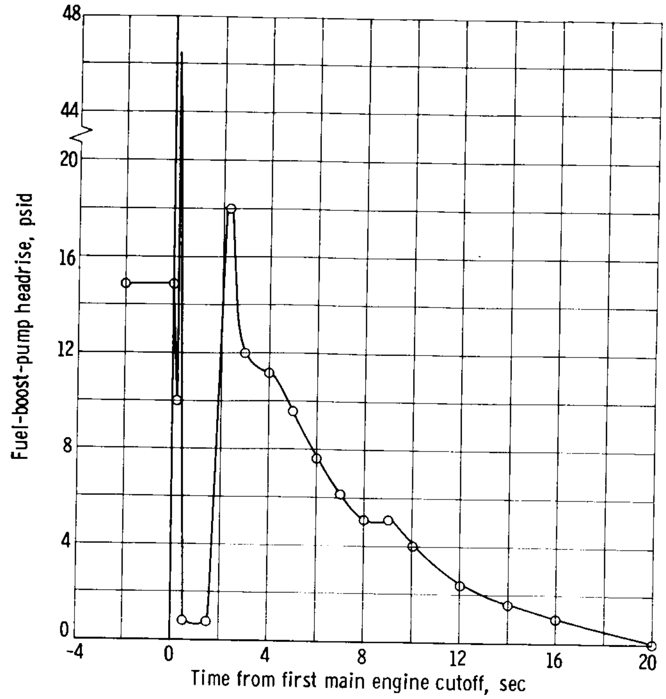

Figure VI-8. - Fuel-boost-pump headrise decay after first main engine cutoff.

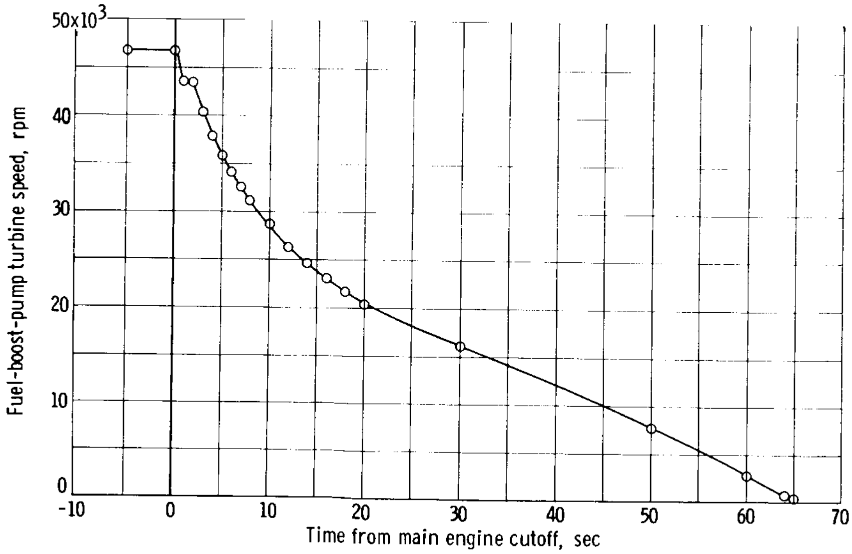

Figure VI-9. - Fuel boost pump turbine speed tail-off after MECO.

[redacted]

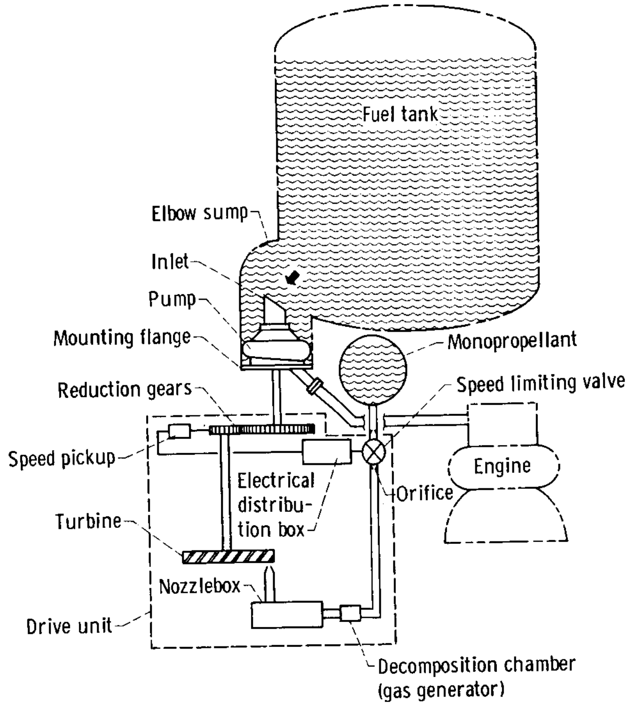

(a) Fuel system.

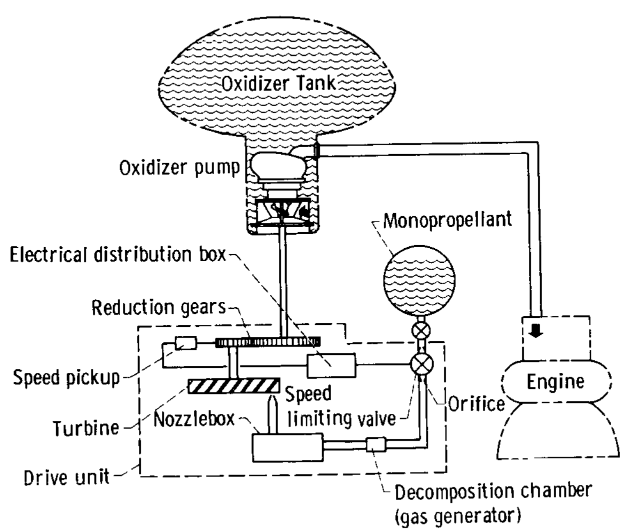

(b) Oxidizer system.

Figure VI-10. - Fuel-boost-pump system and oxidizer system schematic drawings.

[redacted]

[redacted]

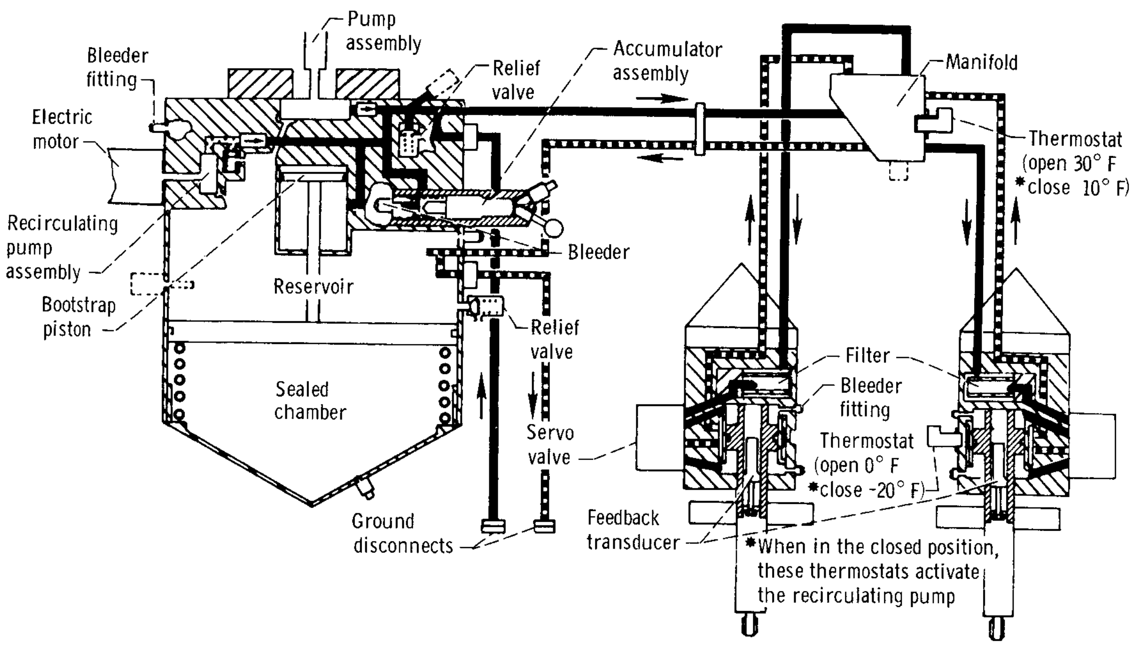

(a) AC-3 Centaur hydraulic system.

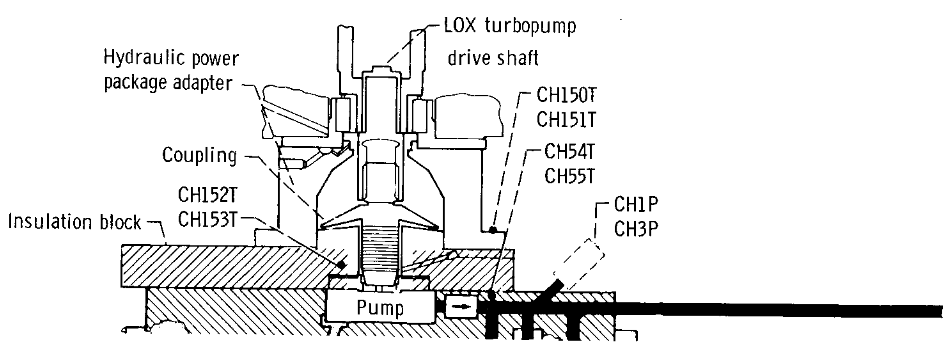

(b) AC-4 modified Centaur hydraulic system.

Figure VI-11. - Schematic drawing of AC-3 Centaur hydraulic system and AC-4 modified hydraulic system.

[redacted]

[redacted]

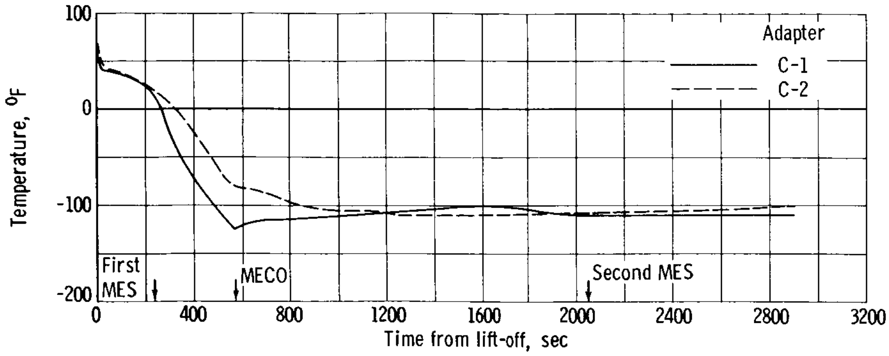

Figure VI-12. - Hydraulic power package adapter temperature.

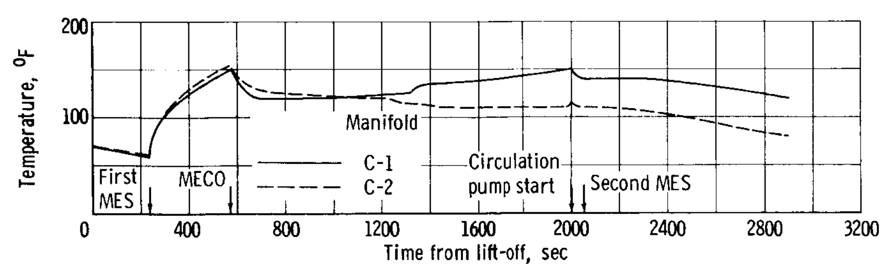

Figure VI-13. - Hydraulic manifold temperature.

[redacted]

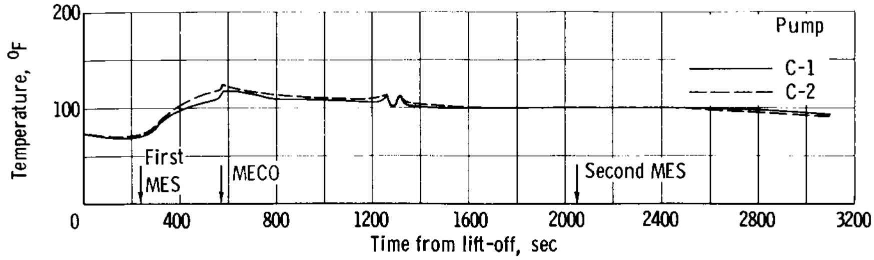

Figure VI-14. - Hydraulic power package pump discharge temperature.

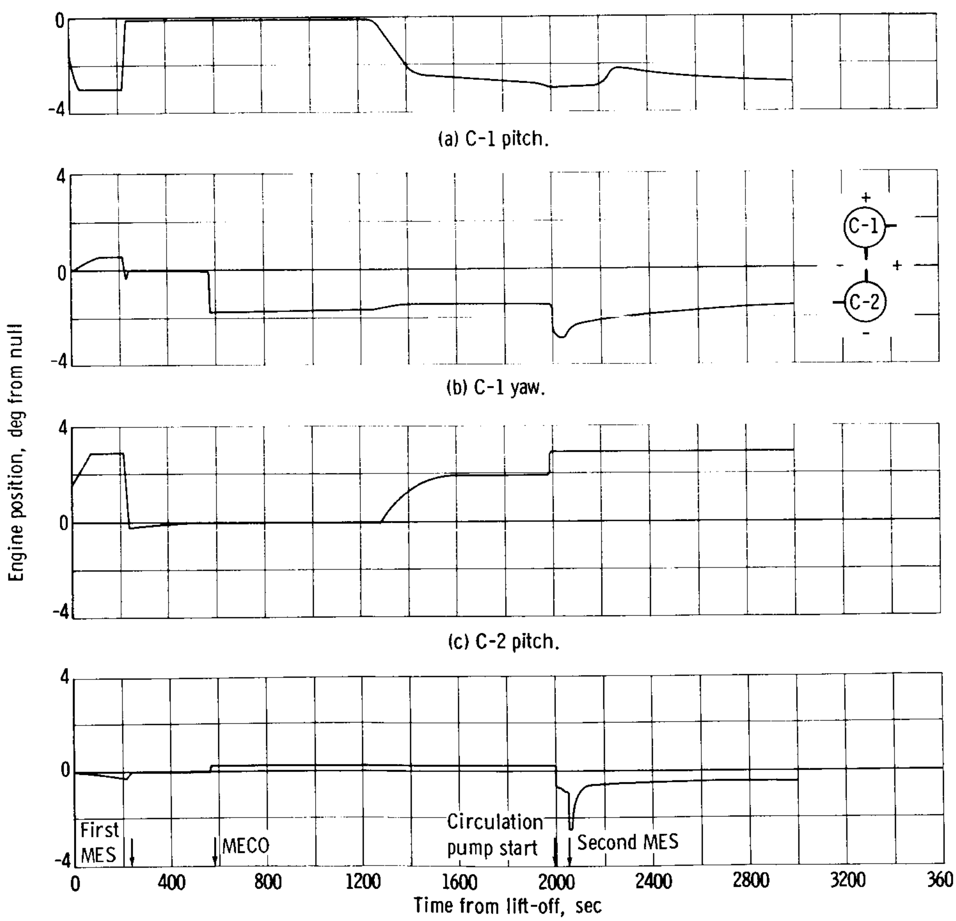

(a) C-1 pitch.

(b) C-1 yaw.

(c) C-2 pitch.

(d) C-2 yaw.

Figure VI-15. - Engine positions.

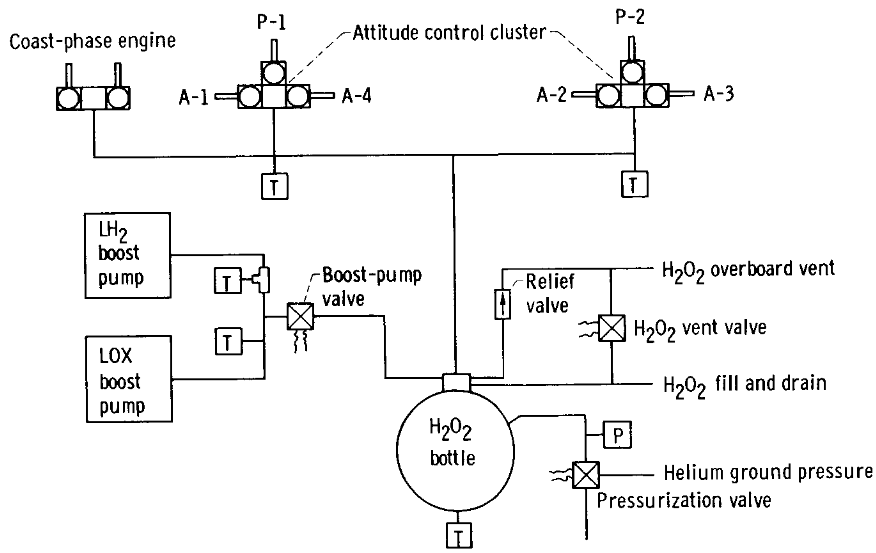

Figure VI-16. - Attitude control and hydrogen peroxide supply systems.

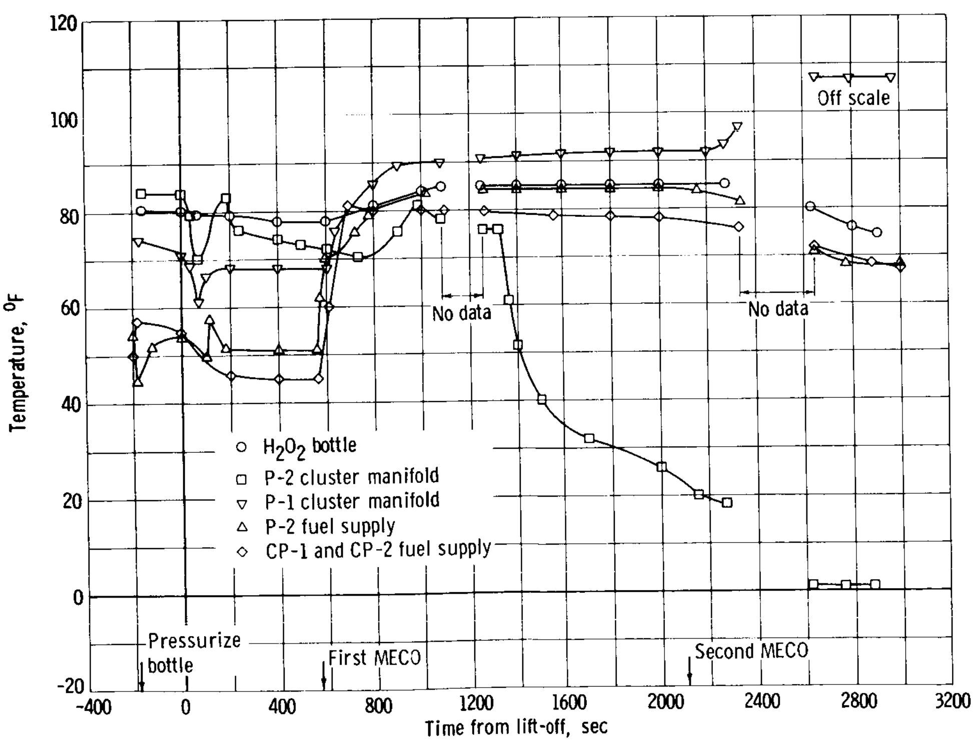

Figure VI-17. - Hydrogen peroxide system temperatures.

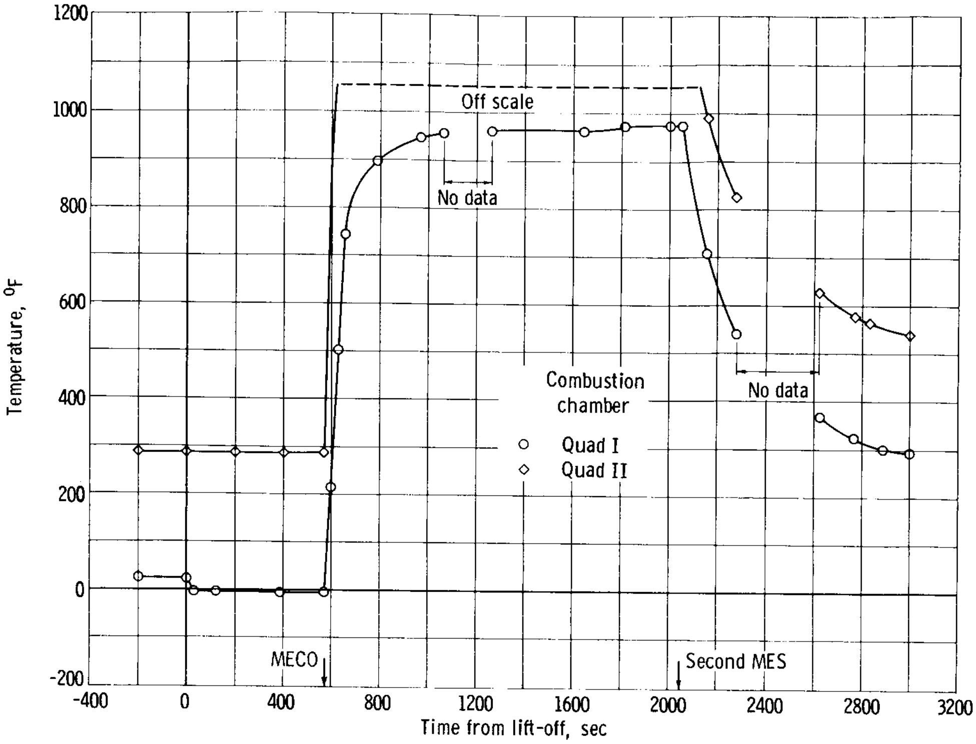

Figure VI-18. - Ullage control engine temperatures.

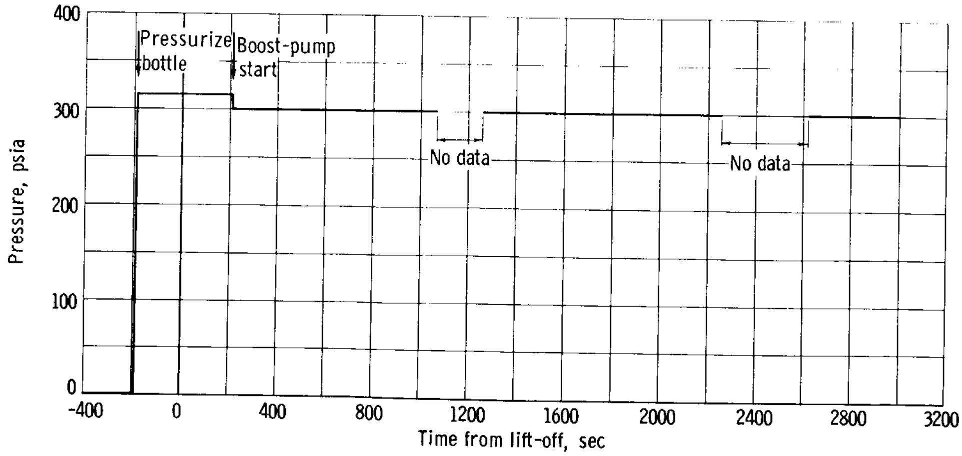

Figure VI-19. - Hydrogen peroxide bottle pressure.

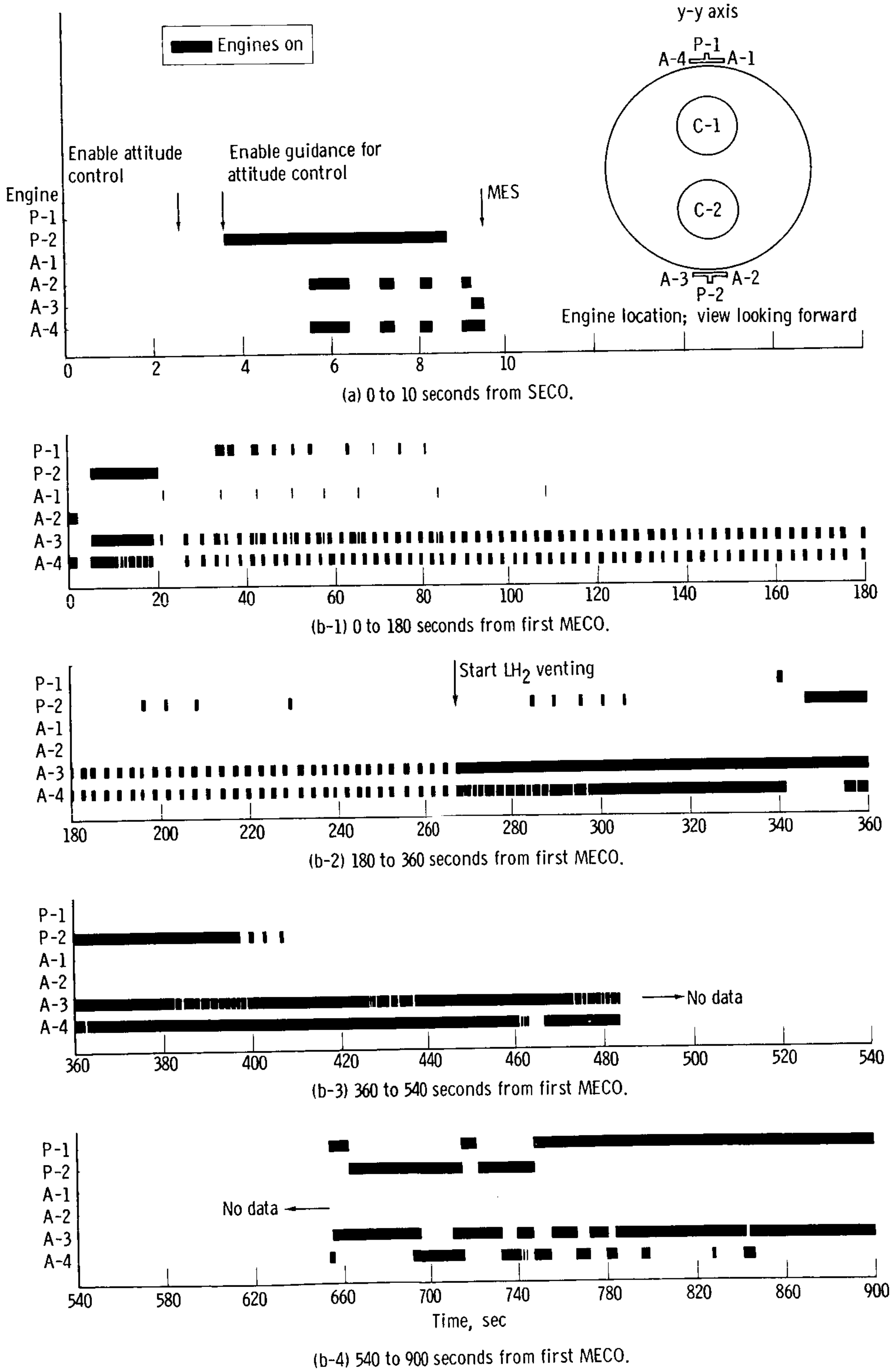

Figure VI-20. - Hydrogen peroxide engine commands.

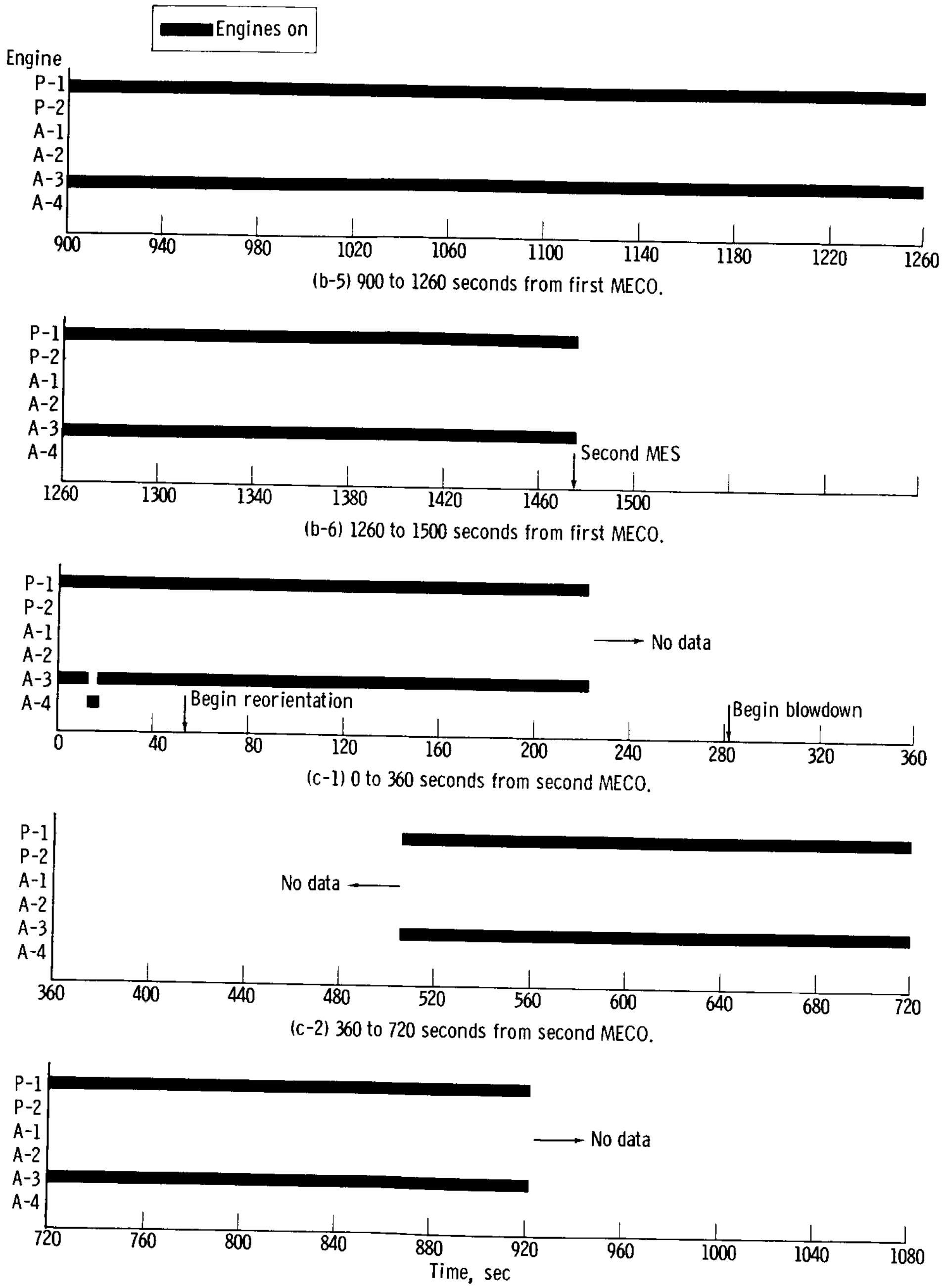

(c-3) 720 to 1080 seconds from second MECO.

Figure VI-20. - Concluded.

VII. CENTAUR PROPELLANT SYSTEMS

SUMMARY

Centaur propellant system performance on the AC-4 flight was nominal with the exception of the coast-phase hydrogen venting and propellant behavior. Large fluid displacements, excited by vehicle transients at MECO, failed to settle out prior to venting. Unsettled propellants at the forward end of the tank resulted in liquid entrainment in the vent flow, with consequent high vent flow rates and impingement forces against the forward bulkhead that caused the vehicle to lose attitude control. The ensuing near liquid depletion, due to venting residual LH_2 overboard, precluded achieving a programed second main engine start and retromaneuver.

Tank pressurization control during flight to maintain structural integrity and support main engine firing was satisfactory. Anomalous, however, was an uncontrolled pressure rise during the LH_2 venting period, from T + 1055 to T + 1366 seconds, resulting from the inability of the limited LH_2 flow rate to relieve the tank pressure fully. Also unusual was a rapid decrease in the hydrogen tank ullage pressure, at the time of second main engine start, caused by spraying LH_2 into the ullage from the boost-pump volute bleed line.

CENTAUR PROPELLANT LOADING

Propellant loading on the AC-4 vehicle to required flight levels was successfully accomplished with 100-percent level sensors and a ΔP propellant level indicating system (PLIS). Total propellants tanked at lift-off were 5080.8 pounds of LH_2 and 24 460 pounds of LOX.

Tanking of LH_2 and LOX propellants on the AC-4 Centaur vehicle was controlled with a liquid head pressure sensing system as shown in figure VII-1. The liquid level indication at any time was proportioned to the liquid head pressure, which was measured as a differential pressure between the sensing ports in the ullage and the bottom of the tank. These sensing lines were purged of cryogenics by bubbling helium through them at the rate of 1.5 scfh. During tanking, the differential pressure of the rising liquid was monitored on the pneumatics panel in the blockhouse as a percentage of the required ΔP for the planned 100-percent flight level.

In addition to the ΔP system, each tank utilized a hot-wire level sensor as a backup to indicate the 100-percent tanking level. Of the two, however, only the LOX 100-percent sensor functioned properly during the launch operation.

A malfunction in the ΔP PLIS in the LOX tank occurred during the quad tanking test and resulted in an overfilling and overpressurizing of the LOX tank to 54 psia. An erroneous reading of the LOX level resulted from a leak in the ullage pressure sensing line at about the 20-percent level. This was corrected by capping the PLIS ullage sensing line and tying into the regular tank ullage pressure measurement line. System operation thereafter was acceptable.

A summary of the propellant loading conditions at lift-off for the AC-4 launch is given in the following table.

Propellant	Ullage pressure, psia	Ullage volume, cu ft	Density, lb/cu ft	Station at lift-off	Volume at lift-off, cu ft	Weight at lift-off, lb
LH_2	20.87	33.94	4.21	184.88	1206.80	5 080.8
LOX	31.10	48.30	68.65	381.39	356.30	24 460

TANK PRESSURIZATION AND CONTROL

The tank pressurization control system operation on the AC-4 flight was essentially as predicted except for an unscheduled rise in fuel tank pressure above the primary vent valve operating range while venting during the coast phase, and a rapid decrease in fuel tank pressure during the attempted engine restart after coast. These anomalies, however, resulted from unpredicted propellant behavior rather than a system malfunction.

Propellant tank pressure control was effected in two ways: by controlled lockup or venting of GH_2 or GO_2 boil-off gases or by metering helium gas into the tank ullage. A schematic arrangement of the pressurization system is shown in figure VII-2.

The hydrogen tank venting was controlled with two pilot-operated relief valves: a primary (number 1) valve, with provisions for latching solenoid control by pulse signal, which regulated between 19.0 and 21.5 psia, and a secondary (number 2) valve, which regulated between 24.8 and 26.8 psia. The valves were connected in parallel between a single ullage standpipe in the tank and the nonpropulsive vent on the exit side. The latching solenoid control on the primary valve, actuated by programer signals, permitted the valve to relieve within the valve operating range when in the relief mode, but disabled the valve and prevented venting when in the locked mode. The secondary valve, however, was always in the relief mode and prevented overpressurizing the tank during the primary valve lockups. The controlled vent periods restricted overboard venting of hydrogen gas to nonhazardous times during the ascent and also provided sufficient tank pressure rise to satisfy structural integrity and/or engine start requirements.

LOX tank venting was accomplished using an almost identical vent valve with provisions for latching solenoid control and a 29.0- to 32.0-psia regulating range. The valve was connected to an ullage standpipe and vent duct and was actuated to the locked, nonventing mode just prior to and during main engine firing.

Step increases in the LH_2 and LOX tank pressures, burp pressurization, to ensure adequate NPSH for boost-pump start were effected by locking the vent valves and metering helium into the tanks from the high-pressure helium storage bottle. Flow was controlled by a pilot-operated solenoid valve, a 0.125-inch-diameter orifice, and a check valve. A separate system was provided for each tank, and the solenoid valves were energized by programer signals to effect a given timed burp.

The respective pressure and temperature profiles for the LOX and LH_2 tanks during the AC-4 flight are shown in figures VII-3 and 4. Prior to initial primary vent valve lockup at T - 7 seconds, the hydrogen tank pressure was steady at 20.8 psi, and the corresponding oxygen tank pressure was 31.6 psia. During lift-off, the number 1 LH_2 vent valve was locked from T - 7 to T + 74 seconds. At T + 60.5 seconds, hydrogen tank pressure had reached 26.2 psia, causing the number 2 vent valve to relieve momentarily. An early venting had been predicted on the basis of a pressure rise rate of 6.0 psi per minute compared with 4.72 psi per minute obtained during flight. The AC-3 quad-tanking-test data had similarly indicated a pressure rise rate of 4.1 psi per minute compared with 3.87 psi per minute during flight. The added improvement between tanking and launch on AC-4 was accomplished by fixing poor seals and thermal shorts around the forward bulkhead.

The overall higher pressure rise rate experienced on AC-4 was attributed to differences in thermal integrity and possibly a reduction in ullage volume. Ullage volume on AC-4 was about 30 cubic feet compared with 40 cubic feet on AC-3.

At T + 74 seconds the number 1 LH_2 valve was pulsed to the relief mode, and the pressure dropped from 26.15 psia to the regulating range of the primary valve. The pressure profile through BECO, BECO lockup and blowdown, and through main engine start was as predicted. The LOX tankage was in a near state of equilibrium and the ullage pressure varied only slightly within the vent valve range.

The LOX and primary LH_2 vent valves were locked, prior to MES at T + 223 seconds, and the tanks pressurized with helium to ensure adequate NPSH for boost-pump start. This burping, as shown in figure VII-3(b), produced a step pressure increase to 34.6 psia in the LOX tank, a ΔP of 3.1 psi, and 21.2 psia in the hydrogen tank for a ΔP of 1.1 psia. During main engine firing the tank pressures then decreased, due to normal fuel depletion, to 26.9 psia on the LOX side and 16.6 psia on the LH_2 side at first MECO.

Following MECO (T + 572.8 sec), the vent valves were enabled at T + 614.4 seconds. Hydrogen tank pressure rose gradually to the primary valve cracking pressure of 20.6 psia at T + 840 seconds. The pressure rise rate during this coast-phase period was 0.90 psi per minute. While venting for the next 215 seconds, to T + 1055 seconds and loss of data, the LH_2 tank pressure varied because of mixed-phase or liquid flow but controlled within the number 1 valve range.

A gap in data coverage existed from T + 1100 to about T + 1235 seconds, and at reacquisition of signal, as shown in figure VII-3(c), the LH_2 tank pressure was 2.0 psia higher and rising steadily, even though the primary valve was in the relief mode. Pressure continued to rise to 24.4 psia at T + 1366 seconds, and then abruptly reversed and relieved to a normal tank pressure of 20.4 psia at T + 1455 seconds. The venting flow data, as discussed in the section HYDROGEN VENTING, indicated liquid hydrogen was being vented during this time period, and the liquid flow rate was of insufficient volume to relieve tank pressure. In addition, the possible formation of ice deposits at the vent exits, due to liquid venting, may have further inhibited adequate venting. The pressure recovery then did not begin until the liquid had been largely depleted and the flow was transitioning back to a gaseous state. Once the tank pressure had recovered and the venting was normal, the primary valve again controlled properly within limits.

In preparation for the attempted second engine start, as shown in figure VII-3(d), the number 1 LH_2 and LOX valves were locked at T + 2005.4 seconds. Simultaneously, both tanks were burped; 4 seconds in the LOX tank and 8 seconds in the LH_2 tank. This burping increased the LOX tank pressure 2.5 psi, from 31.4 to 33.9 psia, and the LH_2 tank pressure 0.8 psi from 20.1 to 20.9 psia. After burping, however, the LH_2 pressure suddenly dropped 7.2 psi during the period T + 2014 to T + 2027 seconds. This pressure decay was attributed to cooling of the ullage gas by LH_2 sprayed forward from the boost-pump volute bleed and the propellant-duct-recirculation lines. Notably, the boost pump started 4 seconds after burp initiation, and the pressure decrease began 4 seconds later.

Calculation of heat-transfer effects due to spraying LH_2 into the hydrogen ullage indicated that, for an initial ullage temperature of 60° to 65° R, vaporization of 15 pounds of LH_2 would produce the observed pressure collapse, assuming all heat extraction was from the ullage. Boost-pump-performance data during this attempted restart period indicated that approximately 30 pounds of LH_2 were sprayed into the tank from the volute bleed. Further discussion of this phenomenon is given in the section CENTAUR PROPELLANT BEHAVIOR.

The hydrogen tank pressures remained depressed through the programed but unachieved second main engine firing. Then at programed second MECO, T + 2102 seconds, the pressure rose steadily as shown in figure VII-3(e) to the cracking pressure of the secondary valve, 26.8 psia at T + 2385. Venting occurred only momentarily, however, as 2 seconds later the programed retromaneuver blowdown began and the pressure blew down through the engines. The pressure rise rate during this interval, for essentially a gas-filled tank, was 2.8 psi per minute compared with a predicted pressure rise rate for this configuration of 2.5 psi per minute. The rapid pressure decay during the blowdown was due to gas flow and, therefore, additional evidence of liquid depletion. Had liquid blown down through the engines, increased boil-off gases would have acted to maintain tank pressure.

LOX tank pressures during the attempted second engine burn operation remained reasonably steady and decreased 1.8 psi. Failure to achieve a second burn and only normal venting during the coast phase resulted in a large LOX residual. Therefore, in contrast to the hydrogen tank, the LOX pressures showed no significant drop during the blowdown portion of the retromaneuver, and the LOX boiloff was sufficient to maintain tank pressures.

A summary of these tank pressure data, pressure rise rates, helium consumption, etc., is given in tables VII-I and II.

HYDROGEN VENTING

The performance of the hydrogen vent system in safely discharging the boiloff gases from the vehicle, during boost-flight phase of the AC-4 flight, was completely successful. However, after the first MECO during the near-zero-gravity coast phase, the system performance was not satisfactory. Unexpected liquid entrainment during this venting period resulted in excessive flow rates beyond the design capability of the nonpropulsive vent and powerful reaction forces that caused the vehicle to lose attitude control.

The hydrogen venting configuration for the AC-4 flight, as shown in figure VII-5, was much the same as on the previous AC-3 flight. Significant changes in the system were the inclusion of a Venturi-type flow-rate meter, a minimum ullage standpipe, and a redesigned nonpropulsive vent intended to cancel out reaction forces when venting under zero-gravity conditions.

The nonpropulsive vent, as shown in figure VII-5, was basically a plenum with internal baffles, with the vent flow discharged laterally from both sides. During initial boost flight, one side was capped and the vent flow was directed out through the 50-inch vent stack. At nose-fairing jettison, the ducting leading to the vent stack and cap were separated, and venting continued in the nonpropulsive mode.

Hydrogen venting during the flight was a controlled sequence and the venting schedule as shown in table VII-I was changed slightly from the AC-3 flight. The initial primary vent-valve lockup period was from T - 7 to T + 74 seconds, and the reenabling of the primary vent valve, 54 seconds after first MECO, was at T + 614.4 seconds.

The venting-flow-rate data during the boost-flight phase are shown in figure VII-6. As noted, the initial primary vent-valve lockup period was from T - 7 to T + 74 seconds, but the secondary vent valve relieved momentarily at T + 60.5 seconds. This venting was negligible and was not unexpected in view of the higher pressure rise rates observed during the AC-4 quad tanking tests. Scheduled blowdown after T + 74 seconds and after BECO lockup were accomplished without incident, and the flow rates were about the same as on AC-3. Maximum indicated flow rate was just under 0.7 pound per second during the first blowdown period. A total of about 72 pounds of hydrogen gas were vented during the boost phase.

Dynamic behavior of the vent valves during venting periods can be assessed only generally. Apparently cycling of the primary vent valve was indicated by the oscillations of the flow rate pressure measurements as the valve operated between its cracking and reseat pressures. Perturbations in Venturi pressure, of the order of 1 to 2 cps, developed just prior to the BECO lockup and continued on through the second blowdown period. Prior to this time the pressures were steady, indicating a smooth modulating rather than cyclic mode of operation. The incipience of this cyclic mode, also experienced on the previous Centaur flights, can be attributed to the reduction in back pressure on the valve. At lower altitudes the increased back pressure tends to stabilize the valve operation.

Coast-phase venting after first MECO was initiated at T + 840 seconds as the tank pressure reached the primary vent valve cracking pressure of 20.6 psia. The presence of residual liquid hydrogen at the forward end of the tank resulted in liquid entrainment producing flow rates greater than predicted. Thrust cancellation in the axis of the vents was satisfactory, but large impingement forces of the expanding jets acting against the forward bulkhead and nearby equipment packages exceeded the capability of the attitude control system and forced the vehicle out of control in the positive yaw direction.

The presence of liquid at the forward end of the tank and possibly in the ullage standpipe is confirmed by the liquid temperature indications of the forward bulkhead skin temperature and ullage temperature measurements. Also, the vent flow temperature probe located downstream of the Venturi and just above the forward bulkhead dropped from -346° to -353° F 4 seconds prior to first venting, and then abruptly to -421° F in less than 1 second when the vent valve cracked. Further discussion of the post-MECO propellant location is contained in the section CENTAUR PROPELLANT BEHAVIOR.

The venting flow rates during this coast phase are shown in figure VII-7. Actual quality of the vent flow due to liquid entrainment cannot be established; but flow rates are shown for both the gas and liquid states based on the measured Venturi pressures. The saturated temperature indications and the pronounced fluctuations in the Venturi pressures, as seen in the flow rate data, were evidence of liquid entrainment and flash-off.

Vehicle tumbling excited by the impingement forces of the high flow rates then forced additional liquid forward, increasing the liquid entrainment in the vent flow. This saturated mixture rapidly absorbed any residual heat in the ducting, resulting in less flash-off and a stabilizing influence in the indicated vent pressure measurements. Venting relief, however, appeared adequate, and tank pressures (fig. VII-8), though somewhat unsteady, were maintained until about T + 1055 seconds. Tank pressure then increased and continued upward until loss of data at about T + 1100 seconds.

Data reacquisition, about 130 seconds later at T + 1230 seconds (fig. VII-8(a)), indicated rising tank pressures and high flow rates. Flow rate pressure measurements were extremely clean, and for a pure gas flow the vent rate would have been 0.50 to 0.60 pound per second. This would have been more than enough to relieve the tank pressure. Therefore, it appears that liquid was being vented (about 3 lb/sec) and that the liquid flow was of insufficient volume to relieve the tank pressure. It should also be noted that, in experimental tests, the expanding of a liquid or liquid-vapor mixture into near-vacuum conditions results in ice formation at the exits. Such a formation of hydrogen ice at the nonpropulsive vent exits, in this instance, would restrict the vent capacity and further inhibit adequate pressure relief, as well as contribute to asymmetric thrust.

At T + 1366 seconds, the tank pressure peaked at 24.2 psia and then relieved to the normal tank pressure range by T + 1455 seconds. A decay in vent flow rate and a warming in the ullage gas temperature was coincident with the pressure recovery as shown in figure VII-8(a). Further evidence of liquid depletion was noted 50 seconds later as the vent gas temperature began to increase. Excursions noted in the flow rate data during this interval were attributed to possible buildup and breakaway of ice deposits at the nozzle exits and transition back from liquid to gas flow.

After the tank pressure recovery, T + 1455 seconds through the vent valve lockup at T + 2006 seconds, venting was again normal and proceeded in an intermittent mode, as shown in figure VII-8(b). This was characteristic of the vent valve cycling between its crack and reseat pressures. Ullage and vent gas temperatures continued to rise also, indicating the venting of a warm ullage gas. Average vent flow rate during this interval was about 0.10 pound per second.

The final venting occurrence during the coast phase was nearly coincident with the start of the retrothrust maneuver. At T + 2386 seconds, the tank pressure reached the cracking pressure of the secondary vent valve, and the engine cooldown valves opened at T + 2387 seconds to start propellant blowdown through the engines. Consequently, hydrogen tank pressure dropped off rapidly, and the closure of the vent valve 10 seconds later terminated the venting. The peak flow rate during this last relief period did not exceed 0.2 pound per second.

The estimated total amount of hydrogen vented overboard during the coast phase, from T + 840 seconds to primary vent valve lockup at T + 2006 seconds, was about 960 pounds. This estimate was obtained as shown in the following table.

Time, sec	Fluid state	Pounds vented
T + 840 to T + 1055	Liquid-vapor	70
T + 1055 to T + 1366	Liquid	705
T + 1366 to T + 1455	Liquid-vapor	130
T + 1455 to T + 2006	Vapor	55
Total		960

At first MECO, the amount of residual LH_2 was about 1084 pounds. If 960 pounds were vented overboard during the coast phase, then only about 124 pounds of LH_2 remained in the tank at the time of attempted second main engine start.

CENTAUR PROPELLANT BEHAVIOR

Propellant behavior and location during boost and Centaur-powered phases of flight were normal. Energy inputs to the tank and transients associated with engine cutoff, however, resulted in the forward displacement of LH_2 in the tank at MECO. Subsequent firing of small ullage settling rockets with a total thrust of 4 pounds for the next 267 seconds of coast failed to settle the propellants prior to venting. This resulted in venting liquid or mixed-phase flow, which, because of high impingement forces, forced the vehicle out of control in yaw.

The AC-4 vehicle was the first Centaur tank to be extensively instrumented to study propellant behavior in a near-zero-gravity environment. The hydrogen tank was instrumented with 41 high-response germanium temperature sensors and seven platinum sensors bonded to the tank skin. The location and orientation of these sensors, shown in figure VII-9, were selected to define propellant location or liquid level near the tank walls.

A typical tank skin temperature profile through the powered and controlled coast phase of flight is shown in figure VII-10. Sensor response to specific flight events as noted was very distinct. During boost, the sensors indicated a gradual cooling as the airborne insulation panel purge rate dropped to zero. A further cooling effect was evident at the time of hydrogen venting. An abrupt increase in temperature was noted simultaneously by all sensors at insulation panel jettison.

The most interesting results of the temperature sensor data, however, were the marked indications of liquid level decrease during Centaur main engine burn. Each sensor, as shown in figure VII-9, indicated an abrupt rise in temperature with the passage of the liquid level (fig. VII-10). Correlating these wet to dry indications made it possible to establish the variation of liquid level with time as shown in figure VII-11. The correlation was excellent, and as shown, the liquid level at MECO was accurately established at station 339. This level resulted in 1084 pounds of residual hydrogen at end of first burn.

The post-MECO propellant behavior, however, was not normal and was characterized by severe disturbances. The skin temperature sensors located in the forward bulkhead area at station 184, and the ullage gas temperature probe at station 162, as shown in figure VII-12, showed an abrupt drop to liquid hydrogen level about 4.5 seconds after MECO. The sudden wetting of the forward bulkhead was attributed to a violent forward motion of the residual LH_2 caused by vehicle transients at engine shutdown. Other major contributors were the discharge from the LH_2 boost-pump volute bypass line, which sprayed liquid forward into the ullage and against the forward bulkhead, and residual liquid slosh, which was greatly amplified under the low-gravity environment. These events are discussed in more detail in section XV. <u>COAST-PHASE PROPELLANT AND VEHICLE BEHAVIOR</u>.

AC-4 instrumentation was not adequate to define propellant behavior completely within the LH_2 tank; however, the initial displacement of the liquid surface appeared to be a wave moving up the positive x- and negative y-axes, continuing over the top and coming down the positive y-axis, as shown in figures VII-13 and 14. Fourteen seconds after MECO, all temperatures indicated wet and remained wet until about 50 seconds prior to venting, at which time a few sensors at the forward section of the tank indicated some drying. It appeared then, that the propellants were either beginning to settle, in response to the ullage rockets, or that some local skin drying was taking place. In spite of these isolated drying indications, the ullage temperature probe and forward bulkhead skin temperatures in the very top of the tank remained wet, indicating the continued presence of liquid.

The presence of this liquid at the forward bulkhead area, and probably in the ullage standpipe at T + 840 seconds, resulted in an abnormal venting. Liquid or mixed-phase flow produced excessive impingement forces causing the vehicle to tumble out of control. This tumbling motion, as well as other possible vehicle responses to the vent impingement forces, caused an unknown liquid distribution in the tank. Nevertheless, some quantity of liquid hydrogen was forced forward as evidenced by the continued venting of liquid fuel overboard until about T + 1366 seconds. Further discussion of this venting phenomenon is presented in the venting section of this report.

It appears that a small amount of LH_2 remained in the aft end of the fuel tank until second MES and beyond. This is evidenced by the sudden wetting of tank skin sensors along the positive x-axis following fuel-boost-pump restart. However, the amount of fuel present was insufficient to sustain normal boost-pump and engine operation; consequently, the second engine burn was not achieved.

The amount of liquid hydrogen present in the fuel tank after second MECO was probably insignificant as evidenced by the fuel tank pressure, which rose steeply after second MECO, following the path of heat input to a pure gas.

TABLE VII-I. - AC-4 FLIGHT TANK PRESSURE DATA

Event	Flight time, sec	Tank pressure, psia				Total ΔP, psia		Pressure rise rate, psi/min	
		LH_2		LOX					
		Initial	Final	Initial	Final	LH_2	LOX	LH_2	LOX
Initial vent valve lockup	-7 to +[a]60.5	20.8	26.1	----	----	5.3	----	4.72	------
BECO lockup	148 to 157.5	20.3	21.5	----	----	1.2	----	7.58	------
Tank burp at MES	0.7-sec burp	20.1	21.2	31.6	34.7	1.1	3.1	----	------
First main engine burn	233.8 to 572.6	20.2	16.6	33.8	26.9	-3.6	-6.9	-.635	-1.22
Coast after first burn	572.6 to [b]840	16.6	20.6	26.9	29.3	4.0	2.4	.9	.539
Tank burp at second MES	8-sec LH_2 burp 4-sec LOX burp	20	20.3	31.4	32.7	.3	1.3	----	------
Second main engine burn	2050 to 2100	13.8	13.6	33.2	32.1	-.2	-1.1	----	------
Coast after second burn	2100 to 2385	13.6	26.9	32.1	32.2	13.3	.1	2.8	------

[a]Programed unlock at T + 74 sec. Number 2 valve relieved at T + 60.5 sec.
[b]First indication of hydrogen venting during coast.

[redacted]

TABLE VII-II. - AC-4 HELIUM CONSUMPTION FOR TANK BURP

Event	Bottle pressure, psia	Bottle temperature, °F	Helium used, lb
Lift-off (T - 0)	3020	65.5	8.3
Prior to first burp	3020	65.5	----
After first burp	2810	49.0	.35
Prior to second burp	2570	44.0	----
After second burp	1457	-31.0	2.2

[redacted]

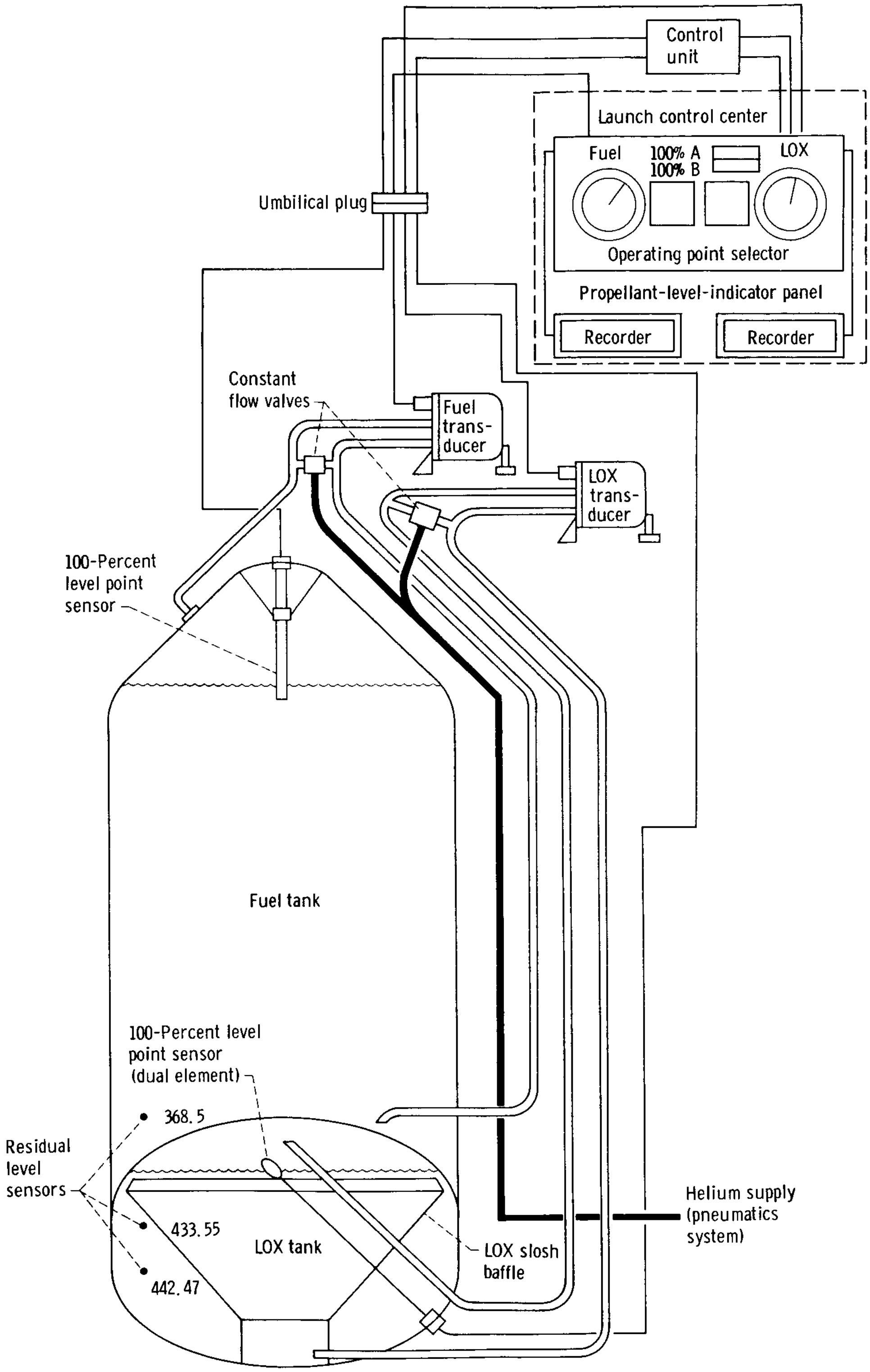

Figure VII-1. - Propellant-level-indicating system.

[redacted]

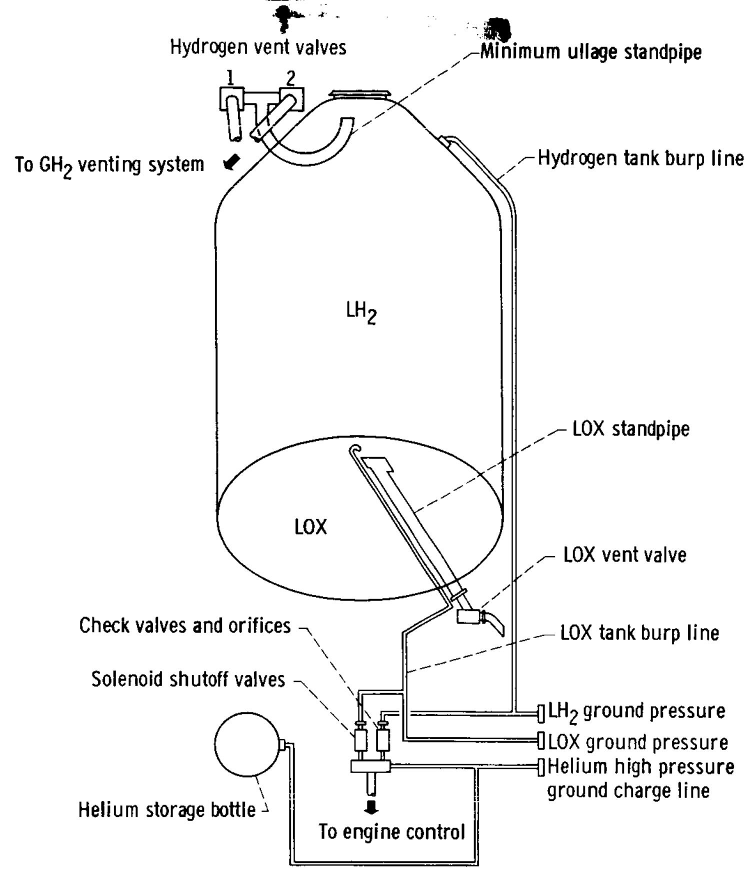

Figure VII-2. - Tank pressurization and control system.

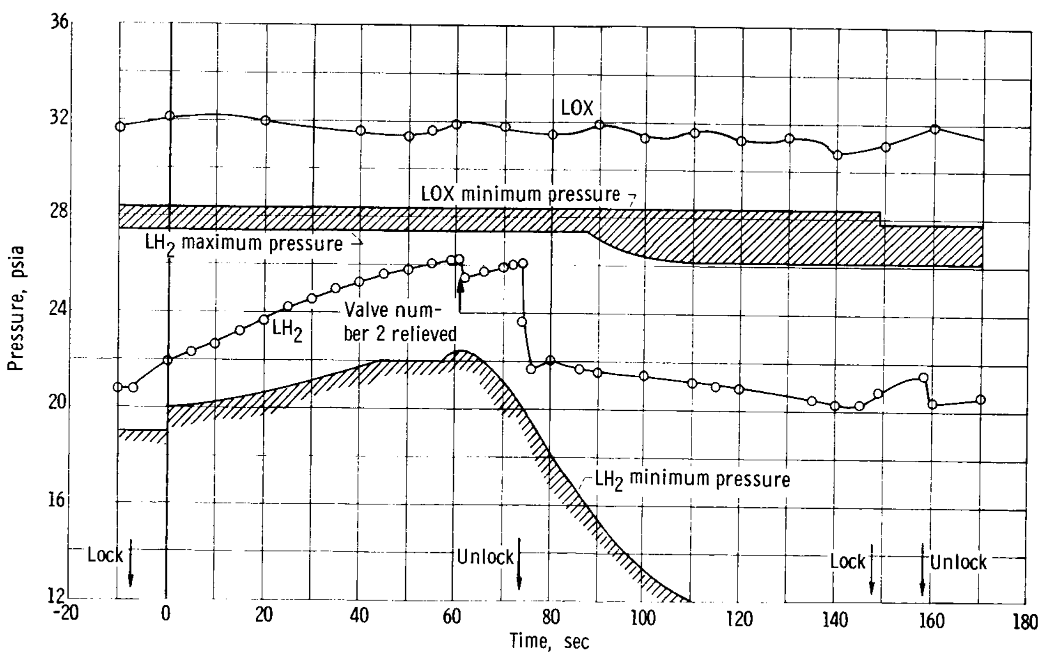

(a) Time, -10 to 170 seconds.

Figure VII-3. - AC-4 LOX and LH_2 tank pressures.

[redacted]

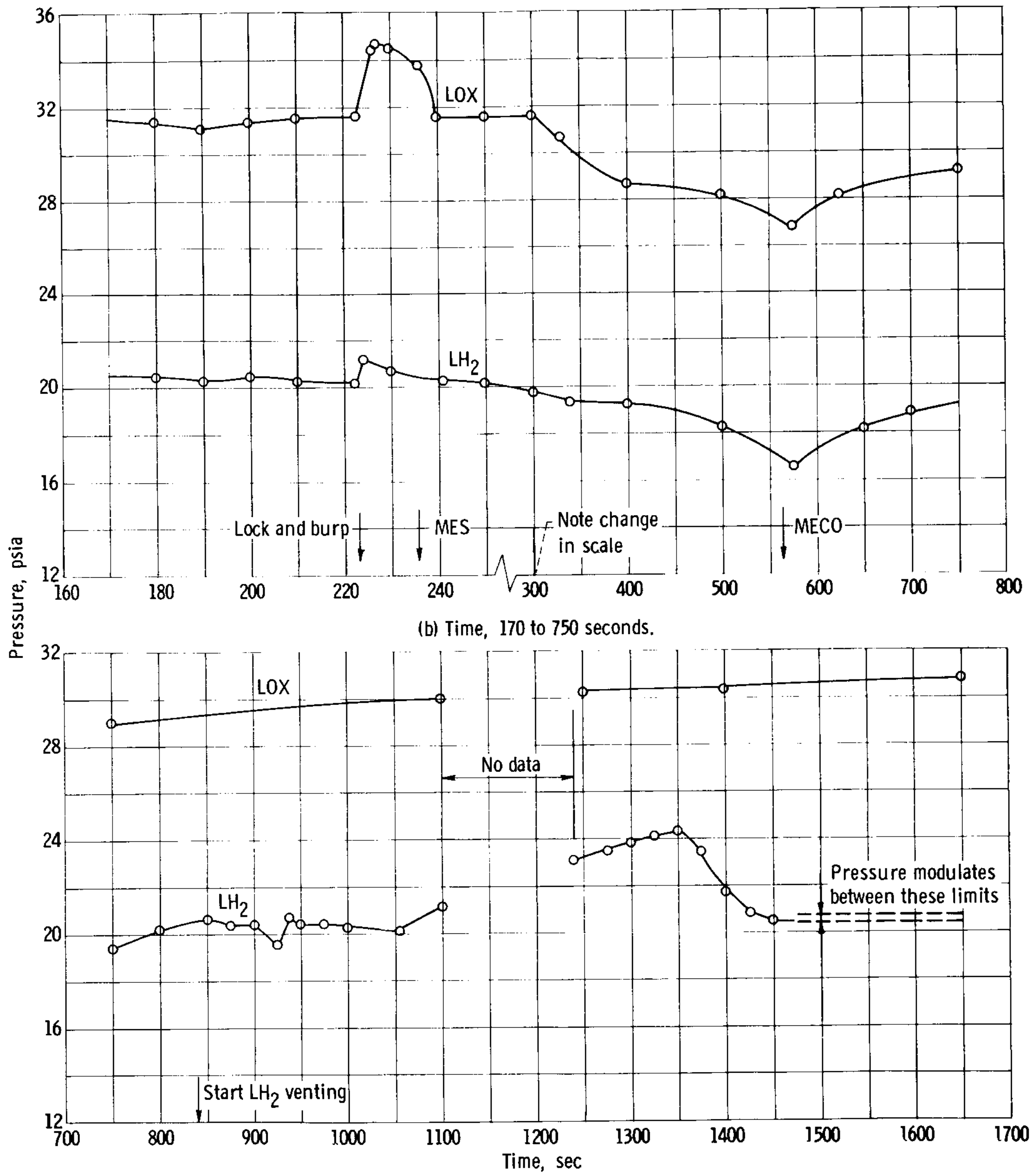

(b) Time, 170 to 750 seconds.

(c) Time, 750 to 1650 seconds.

Figure VII-3. - Continued.

[redacted]

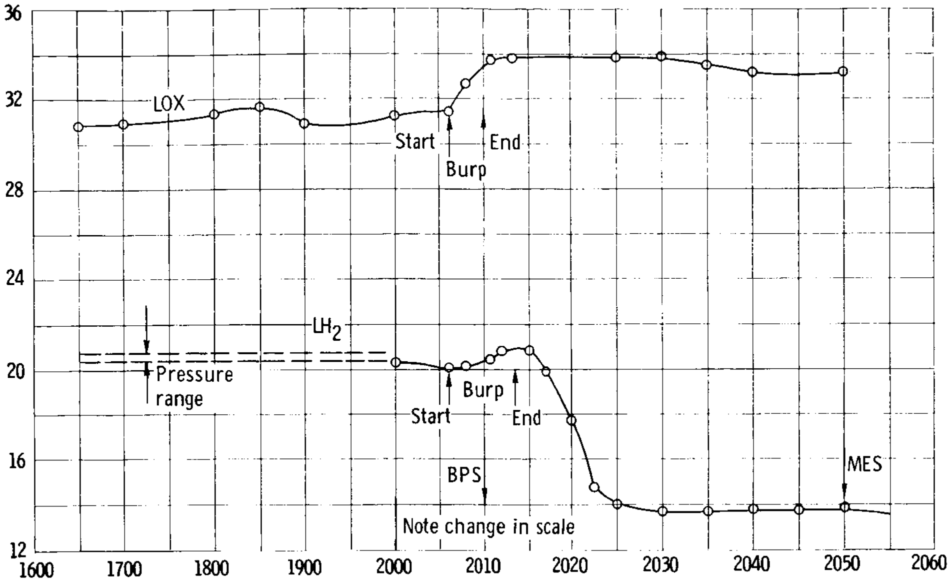

(d) Time, 1650 to 2055 seconds.

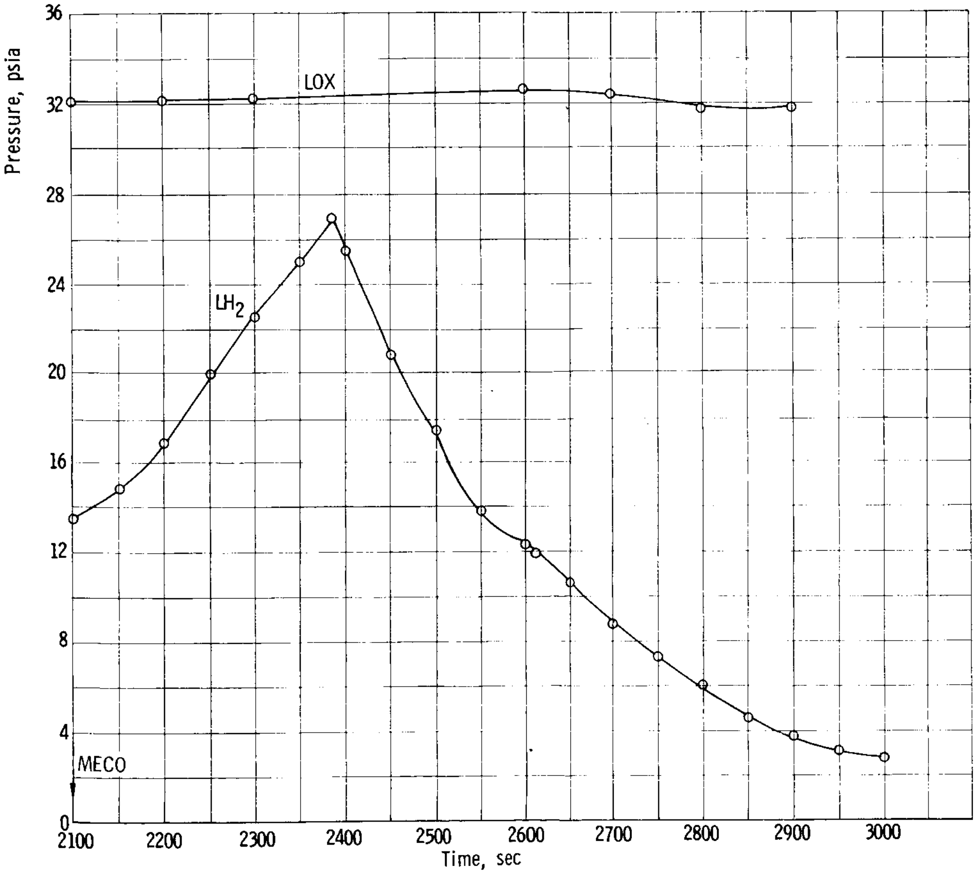

(e) Time, 2100 to 3000 seconds.

Figure VII-3. - Concluded.

[redacted]

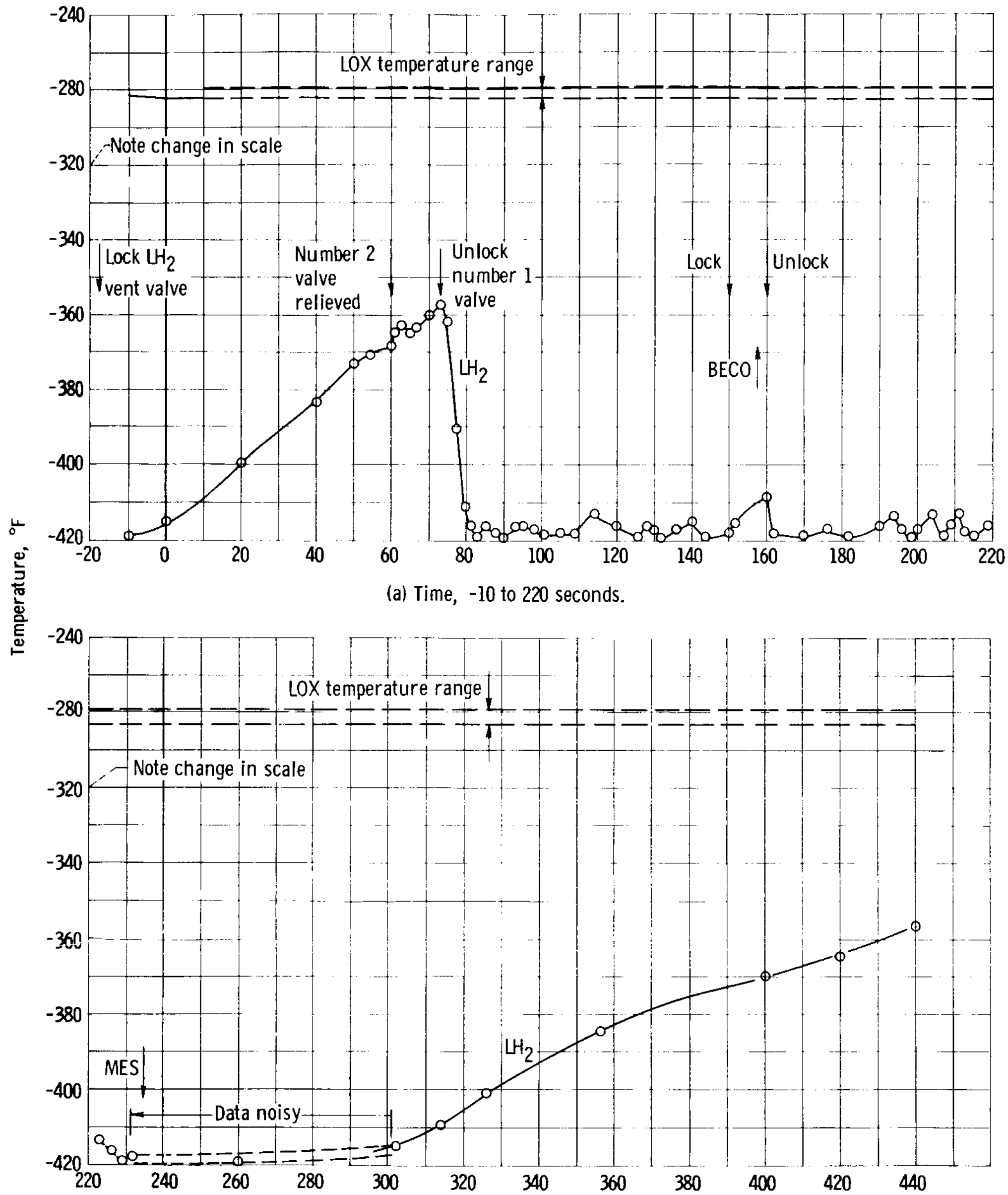

(a) Time, -10 to 220 seconds.

(b) Time, 220 to 440 seconds.

Figure VII-4. - AC-4 LOX and LH_2 ullage temperatures.

[redacted]

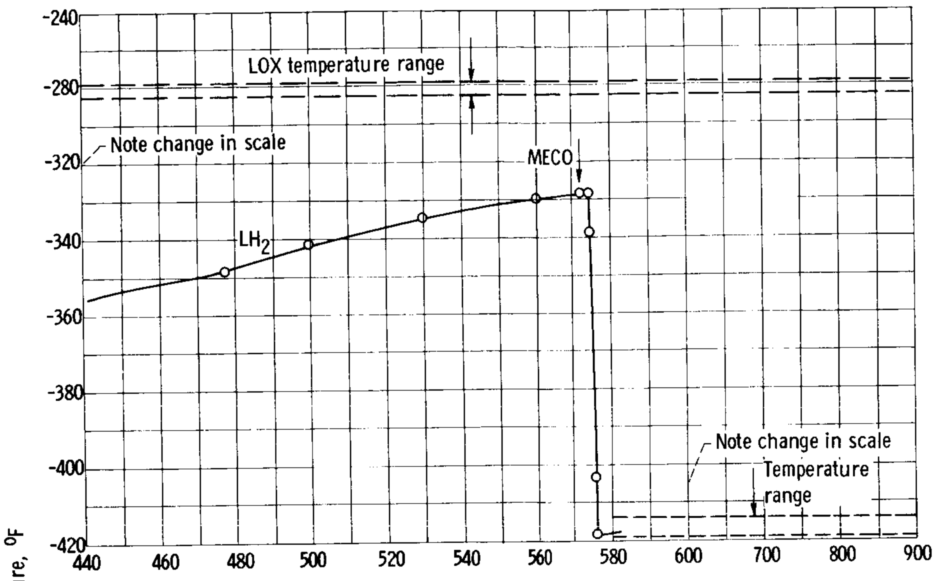

(c) Time, 440 to 900 seconds.

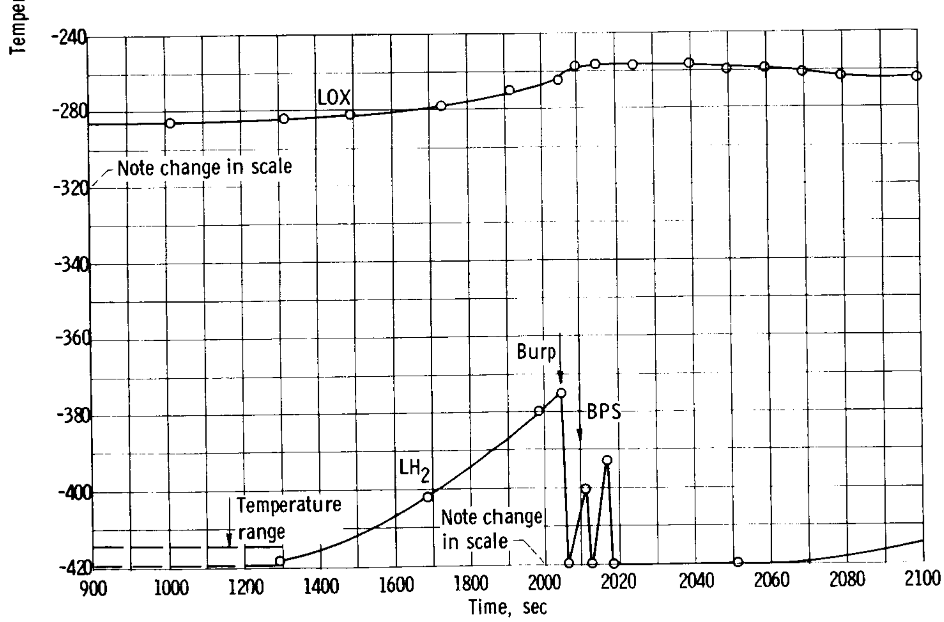

(d) Time, 900 to 2100 seconds.

Figure VII-4. - Continued.

[redacted]

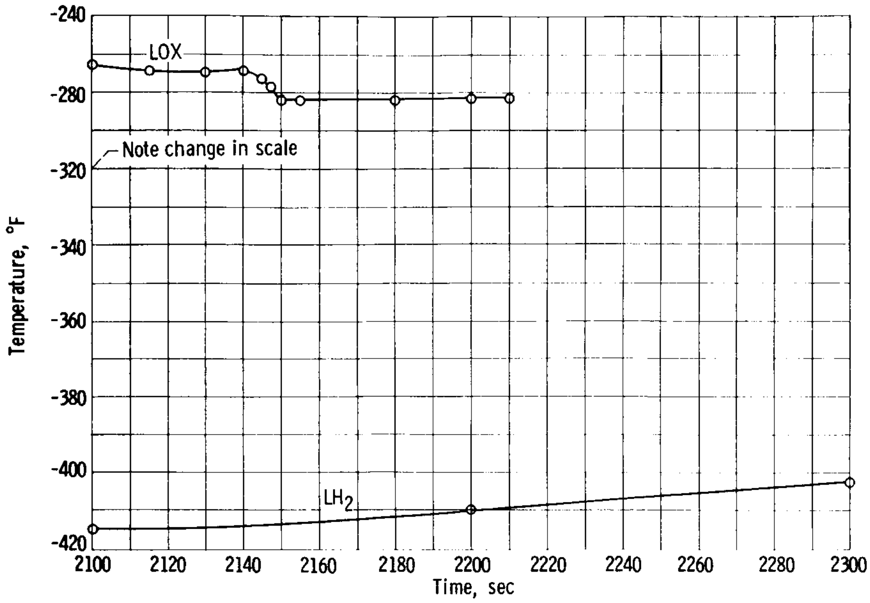

(e) Time, 2100 to 2300 seconds.

Figure VII-4. - Concluded.

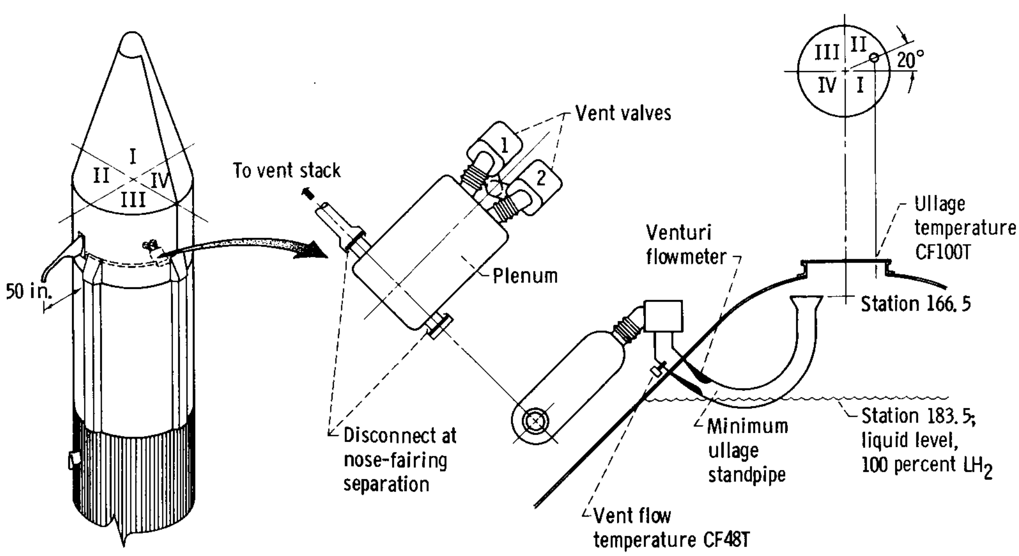

Figure VII-5. - AC-4 vent duct configuration.

[redacted]

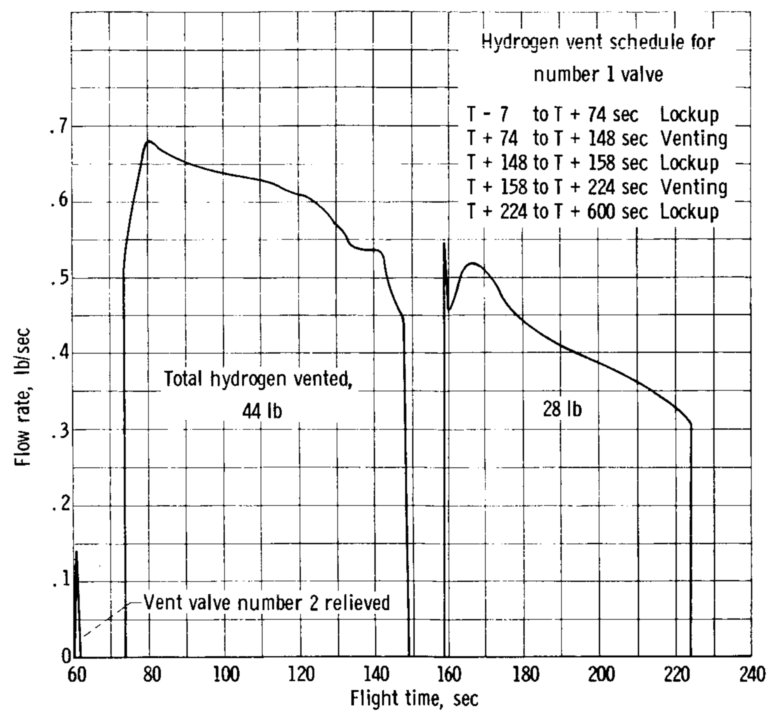

Figure VII-6. - Hydrogen venting flow rate.

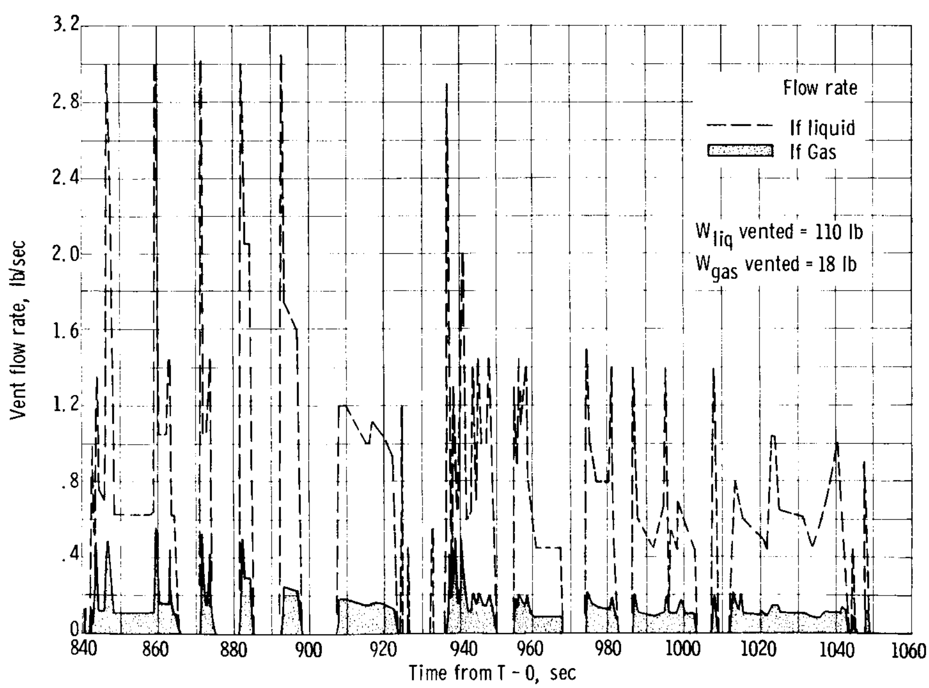

Figure VII-7. - Coast-phase hydrogen venting rates.

[redacted]

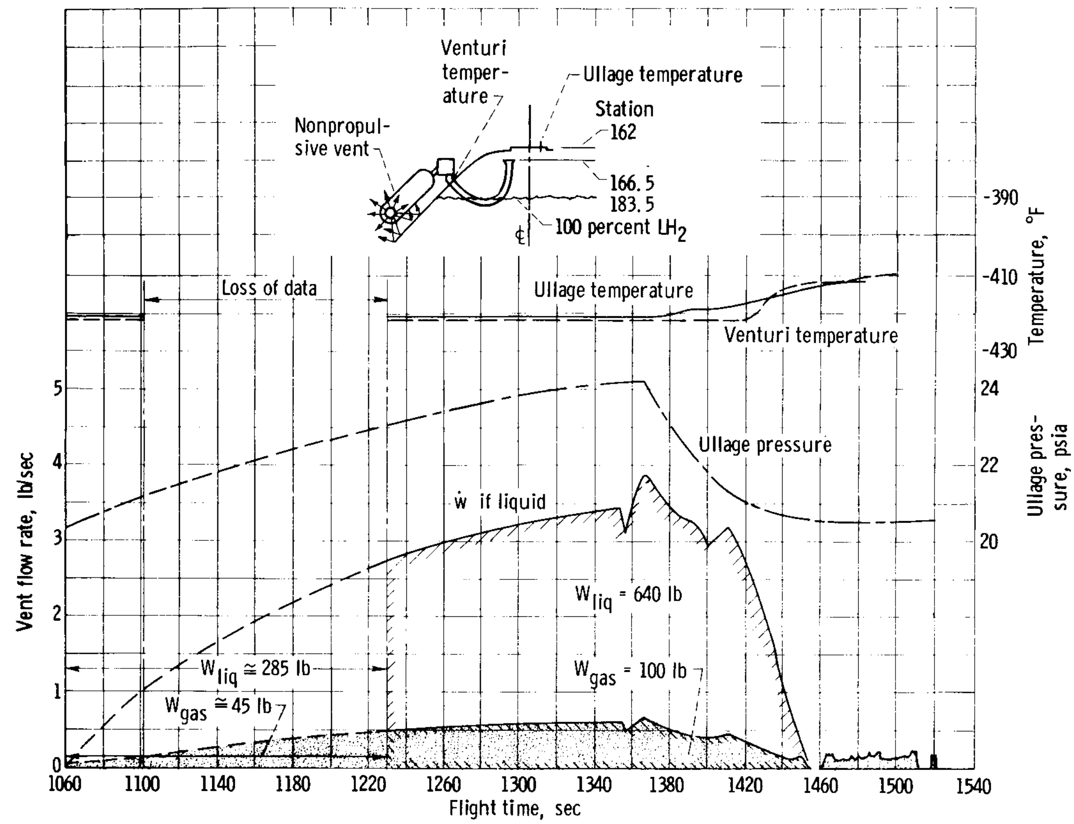

(a) Time, 1060 to 1540 seconds.

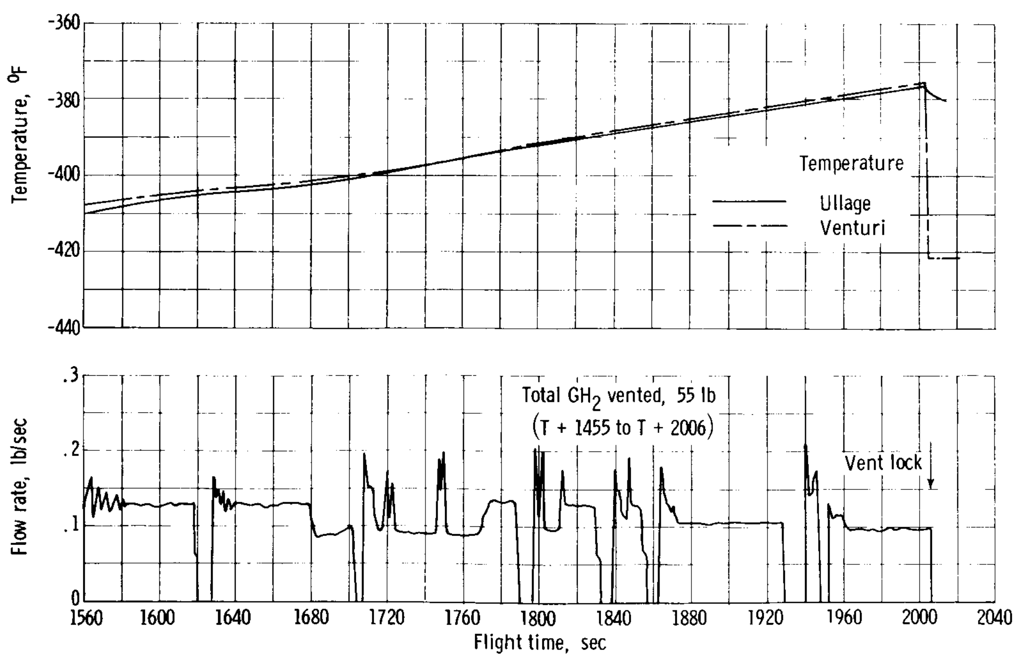

(b) Time, 1560 to 2040 seconds.

Figure VII-8. - Coast-phase hydrogen venting.

[redacted]

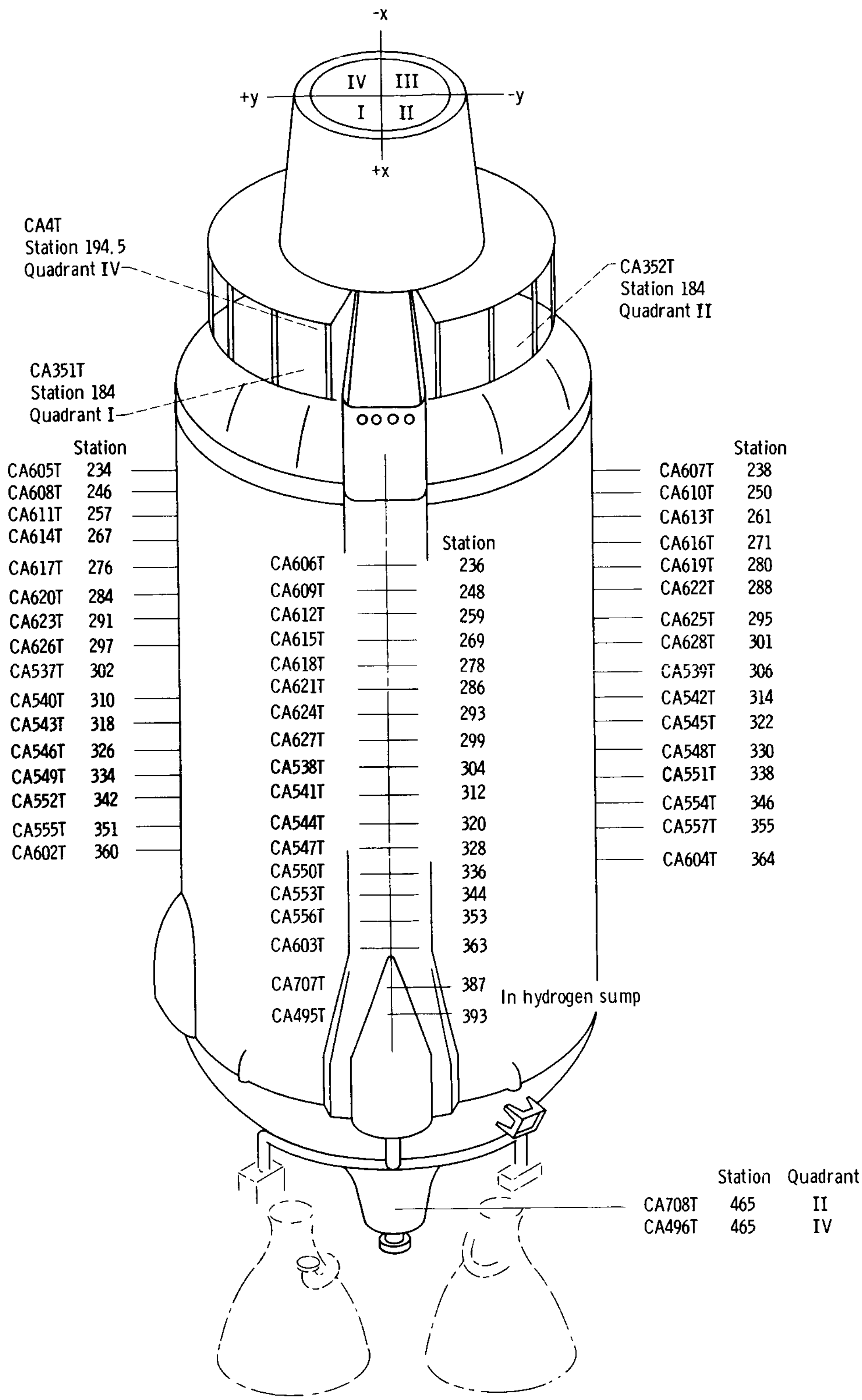

Figure VII-9. - Hydrogen tank skin temperatures.

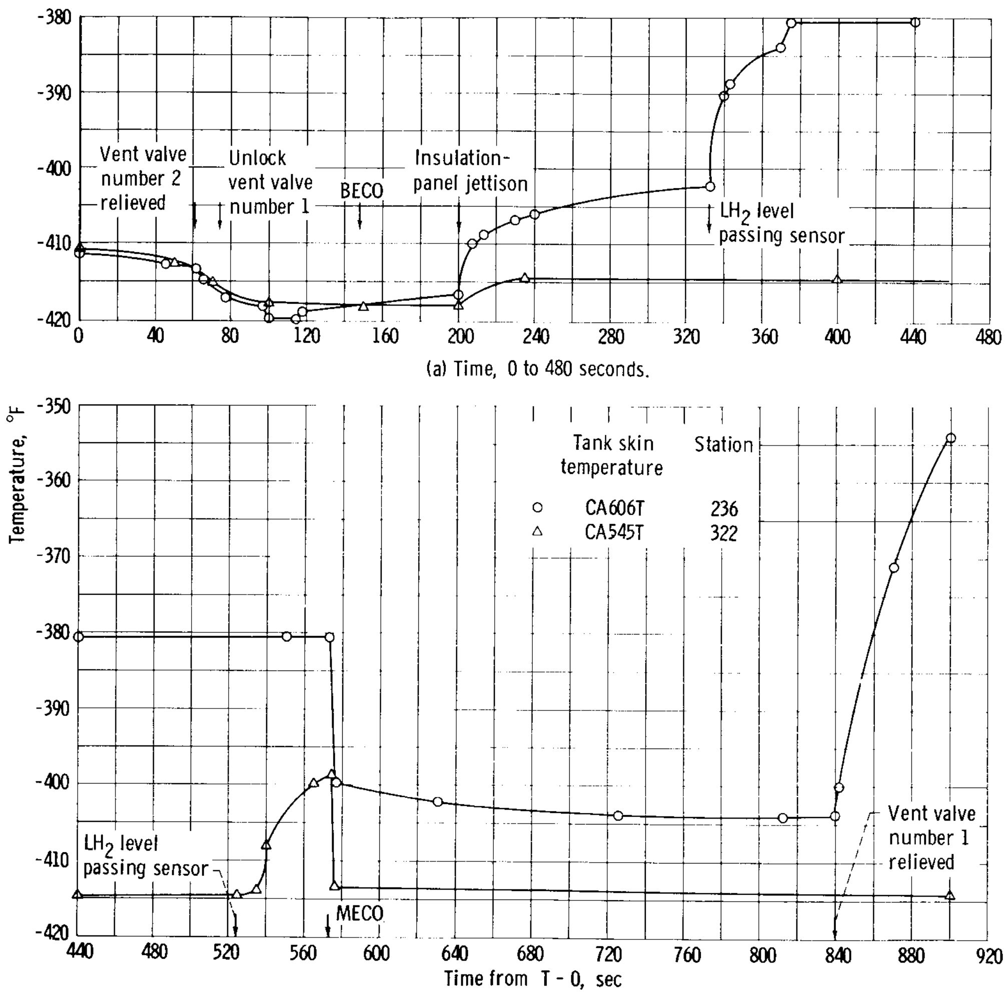

(a) Time, 0 to 480 seconds.

(b) Time, 440 to 920 seconds.

Figure VII-10. - Typical tank skin temperature history.

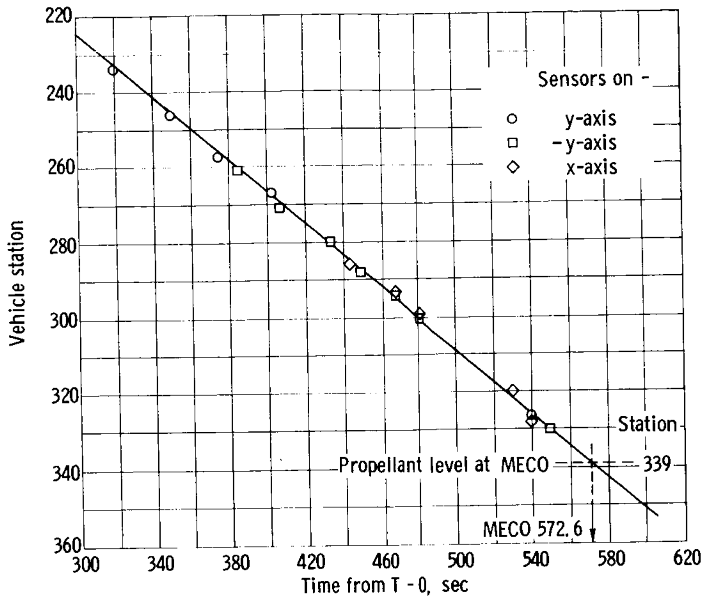

Figure VII-11. - LH_2 liquid level against time. Tank skin temperature data.

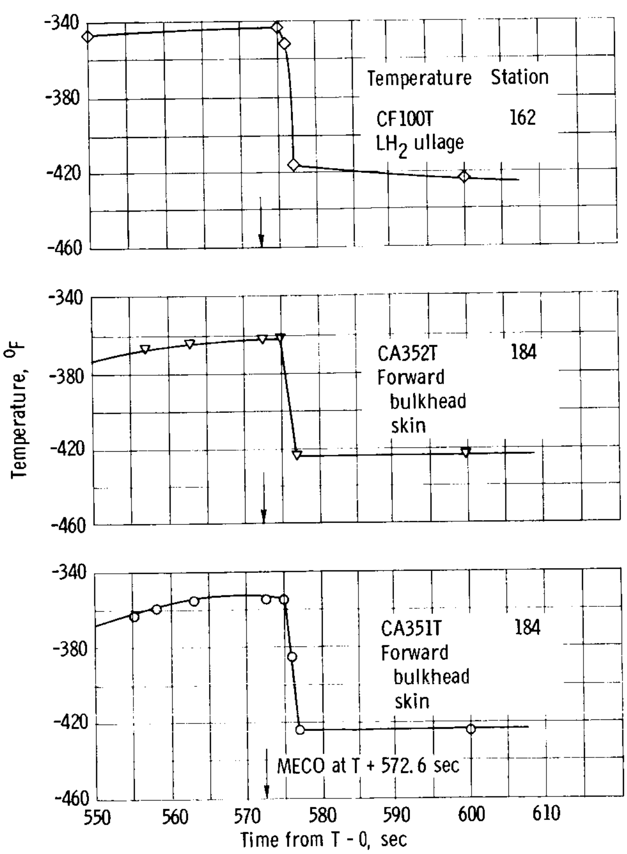

Figure VII-12. - Temperature history near MECO. Forward bulkhead area.

[redacted]

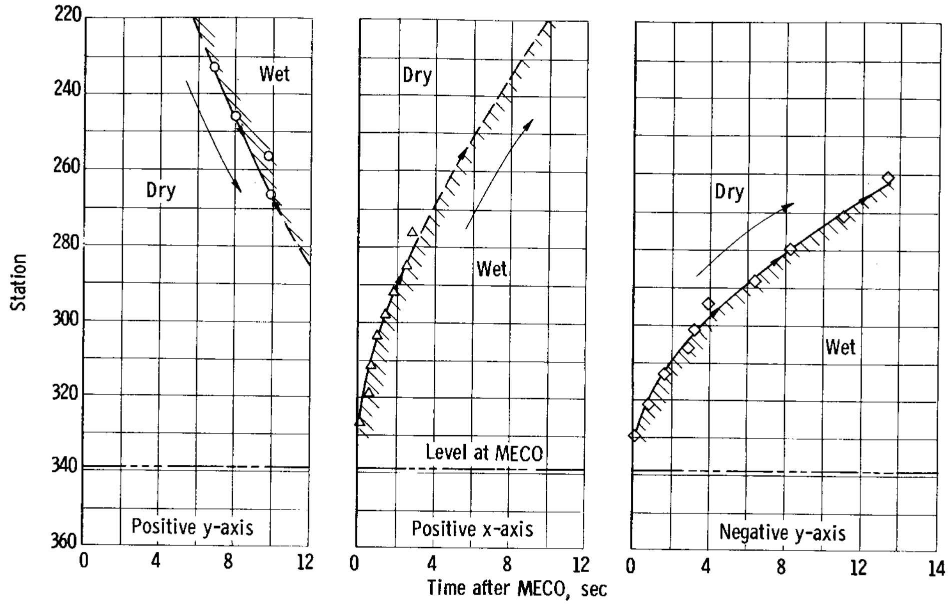

Figure VII-13. - LH_2 tank skin wetting indication at MECO.

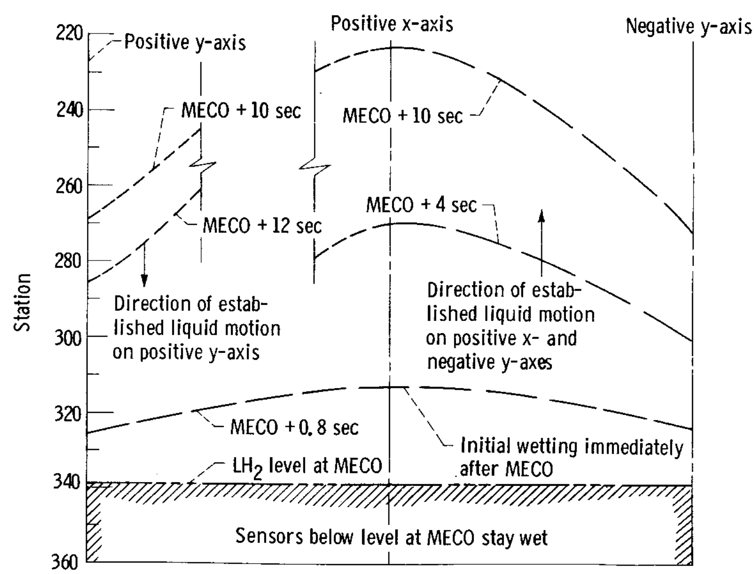

Figure VII-14. - LH_2 profile as indicated by tank skin temperatures. (LH_2 tank skin wetted entirely from MECO + 14 sec to approximately MECO + 210 sec, which is first drying of upper tank sensors.)

[redacted]

VIII. SEPARATION

SUMMARY

The separation systems on the AC-4 flight vehicle effected the jettison of (1) the insulation panels, (2) the nose fairing, and (3) the Atlas booster stage. The successful jettison of the insulation panels and the nose fairings satisfied one of the primary flight objectives, and the operation of the staging system satisfied a secondary objective.

The three systems performed as designed with no anomalies being noted. All four insulation panels jettisoned simultaneously, as indicated by two independent measurements. Subsequent to the AC-3 and prior to the AC-4 flights, tests of the nose-fairing-separation system were conducted at the Lewis Research Center in an effort to determine the cause of, and to effect a remedy for, shocks (measured on the equipment shelf) that were probably responsible for a guidance system malfunction on the AC-3 flight. Inasmuch as these shocks were coincident with nose-fairing jettison, the theory was advanced that this event was their cause. As a result of the test series, extensive modifications were made to the nose fairing and its jettison system, and no unaccounted for shock disturbances were noted on AC-4.

Vehicle staging occurred normally with only a low level of angular motion of the Atlas noted during the separation interval. As a result of the AC-4 flight, the level of confidence in the three separation systems has been increased.

INSULATION-PANEL

Breakwires were located on the insulation-panel-jettison hinges to record panel jettison. It can be concluded from these measurements that all the panels were jettisoned simultaneously at T + 198.47 seconds. This was verified by checking the termination of signals from other panel instrumentation. It was determined from the raw data that the panel instrumentation ceased to function at approximately T + 198.47 seconds, which is a further indication that the panels had separated from the vehicle at that time. It should be noted that the panel instrumentation disconnect (located at station 413) does not come apart until the panels have almost completely separated.

Another check was made by looking at the tank-strain-gage data. These data indicated that a definite increase in tank hoop strain occurred at the time of panel jettison. This would be expected inasmuch as the panels are under tension (circumferentially) and support part of the tank load prior to jettison.

From all these data it can be concluded that the insulation panels had parted simultaneously immediately subsequent to their shaped charge firing at T + 198.47 seconds (BECO discrete + 50.00 sec), which was the planned jettison time.

NOSE FAIRING

Nose-fairing separation was accomplished successfully with none of the indications of malfunction seen in the AC-3 flight. Since the nose-fairing flight-qualification tests run at Lewis included some of the flight transducers, it is possible to make a comparison of flight data with Lewis test data in this report.

Maximum pressure in the middle of the floor of the thrustor bottle cavity during flight jettison was indicated as 9.20 psia compared with 4.9 psia obtained from a similar transducer during the Lewis tests. The value 4.9 psia is somewhat doubtful, however, because an additional transducer located in the same place consistently indicated a pressure of about 8 psia. Pressure on the top of the Surveyor mass model was indicated to be 0.081 psia for the flight and 0.070 psia for the Lewis tests (although a maximum pressure limit has not been definitely established for this region). A value of 0.50 psia was observed during an overpressure test at Lewis with no resultant damage to the Surveyor mast, solar cells, or panels.

Accelerations were measured at the base and at the top of the mass model in the x- and y-directions during flight. The measurements at these locations never exceeded 0.6 g (rms) during the nose-fairing jettison.

During the AC-3 flight, acceleration peaks during nose-fairing separation were indicated to be approximately 15 g's (rms) by an accelerometer located near the equipment shelf. The accelerometer located on the AC-4 A/P gyro package indicated a maximum of 5 g's peak-to-peak at nose-fairing jettison. A plot of these accelerations is shown in figure VIII-1. Strain gages, which measured the nose-fairing vertical loads, were installed on both the Lewis and flight nose-fairing hinges. Figure VIII-2 shows the jettison loads placed on these hinges during flight and during the Lewis test. The maximum measured compressive load of 2600 pounds was well under the hinge load capacity of approximately 8000 pounds. The flight loads in figure VIII-2 were obtained by doubling the indicated load, since only one leg of the two-leg hinge was strain gaged.

Position-indicating transducers measured the angular rotation of the nose fairing about its flight hinge. Figure VIII-3 and 4 shows the angular motion of the fairings, for the flight and for the Lewis test as obtained from these transducers and for the Lewis test as obtained from photographic data. The two methods of obtaining angular rotation during the Lewis flight qualification tests were in close agreement. The angular rate of rotation during flight, as shown by these transducers, was less than that obtained during the Lewis tests possibly due to the weight of an ablative coating added to the flight fairing. Since transducers were located in each quadrant, rotation about the z-axis was also observed. In the quadrant II and III fairing half, data from the flight showed that the quadrant III rate of rotation was slightly more than the quadrant II rate, whereas the Lewis tests showed the opposite to be true. For the quadrant I and IV nosecone half, the quadrant IV rate of rotation was slightly higher than that of the quadrant I rate in both the flight and Lewis tests.

ATLAS-CENTAUR

Inasmuch as the Atlas-Centaur staging sequence had been successfully accomplished twice on previous Atlas-Centaur flights, its successful completion constituted a secondary objective of this flight. As in earlier flights, the separation process was initiated by firing the linear shaped charge thereby severing the interstage adapter at station 413.

The retrorockets were fired at approximately T + 226.86 seconds to decelerate the Atlas; accelerometer and rocket-fairing-cap-breakwire data indicate that all eight rockets ignited.

Information obtained from gyros indicated that the Centaur did not rotate about its center of gravity to an appreciable amount during the separation process (less than 0.2°). Gyro data indicated that the Atlas did not rotate significantly about its pitch axis (which is the more critical axis) but that a rotational component about the yaw axis was experienced that resulted in a yaw of approximately 0.7° at the time the Atlas cleared the Centaur. The path of the forward edge of the interstage adapter resulting from the Atlas angular and z-axis motions is shown in figures VIII-5 and 6.

The flight rotational and translational motion components compared with the predicted values are shown in table VIII-I. It will be noted that the predicted and observed pitch (y-y) motions are both small, whereas the measured yaw (x-x) motion was significantly greater than predicted (7 in. compared with 2 in.). As shown in figure VIII-5, however, the indicated clearance between the engine and the interstage adapter in the plane of the x-x axis was a substantial 33 inches.

TABLE VIII-I. - MAGNITUDES AND DIRECTIONS OF ATLAS COMPONENTS OF MOTION AT FORWARD EDGE OF INTERSTAGE ADAPTER AFTER 9 FEET OF LONGITUDINAL MOTION

Component	Predicted, in.	Observed, in. (see figs. VIII-4, 5)
	Along x-x axis	
Translation	0	--
Rotation about center of gravity	2	7
Total	2	7
	Along y-y axis	
Translation	$-1\frac{1}{4}$	--
Rotation about center of gravity	$-\frac{1}{4}$	-1
Total	$-1\frac{1}{2}$	-1

[redacted]

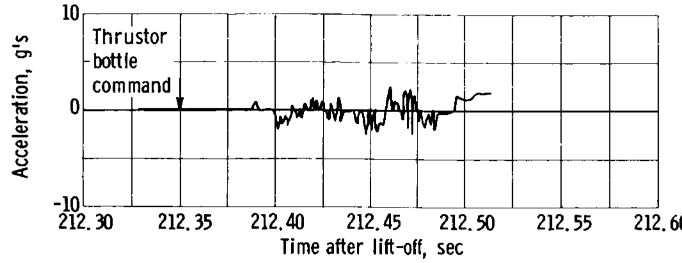

Figure VIII-1. - Equipment platform accelerations of A/P gyro at nose-fairing separation measured along y-axis during AC-3 flight. (Signal attenuated by a factor of 2.62.)

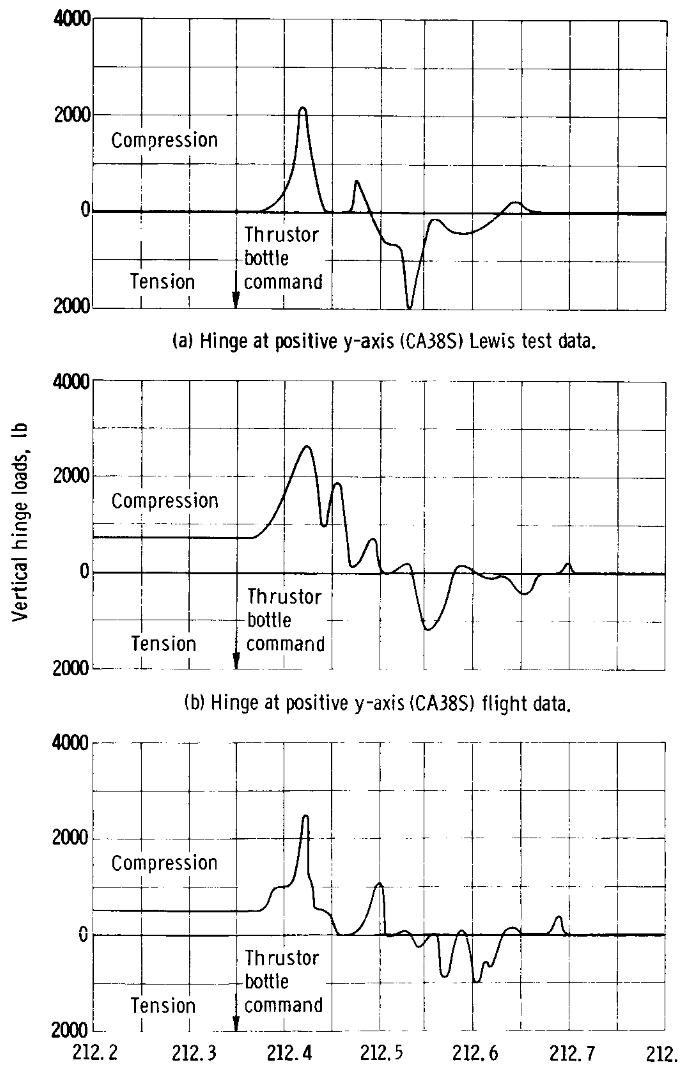

(a) Hinge at positive y-axis (CA38S) Lewis test data.

(b) Hinge at positive y-axis (CA38S) flight data.

(c) Hinge at negative y-axis (CA39S) flight data.

Figure VIII-2. - Vertical hinge loads during nose-fairing separation.

[redacted]

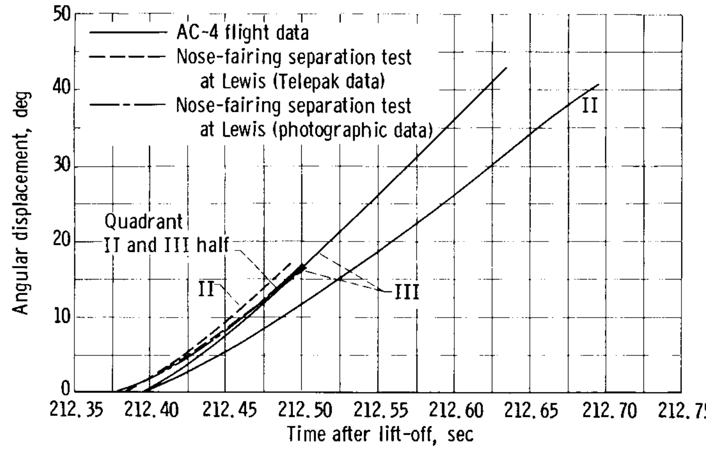

Figure VIII-3. - Quadrants II and III nosecone half angular motion of fairing at separation.

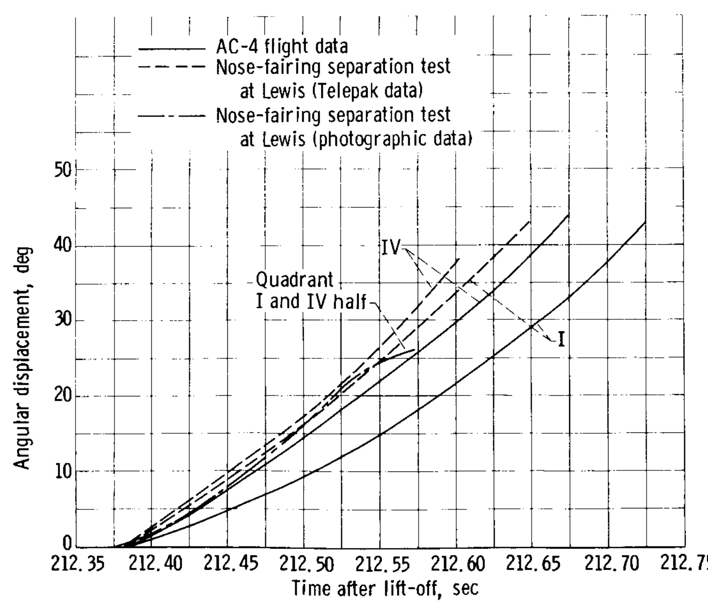

Figure VIII-4. - Quadrants I and IV nosecone half angular motion of fairing at separation.

[redacted]

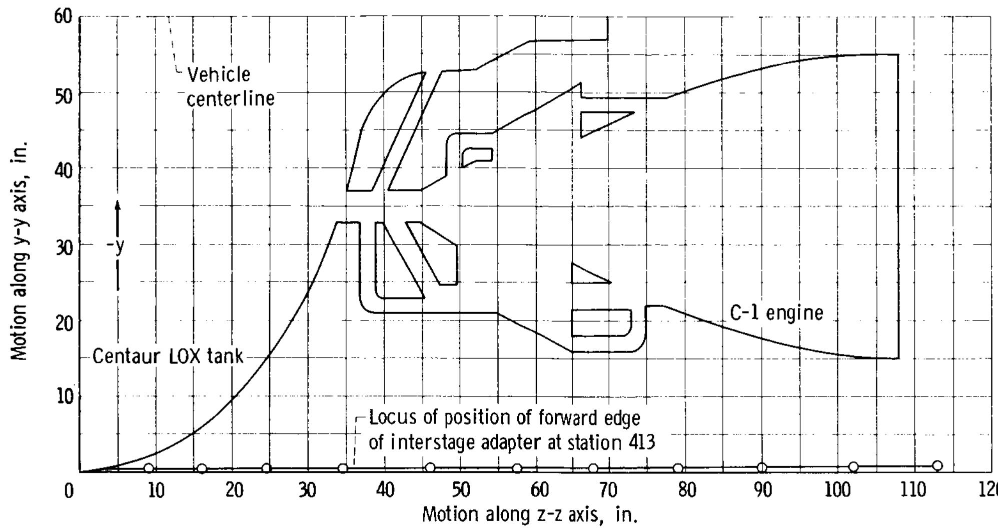

Figure VIII-5. - Motion in y-z plane of station 413 on Atlas with respect to Centaur during staging of AC-4 flight.

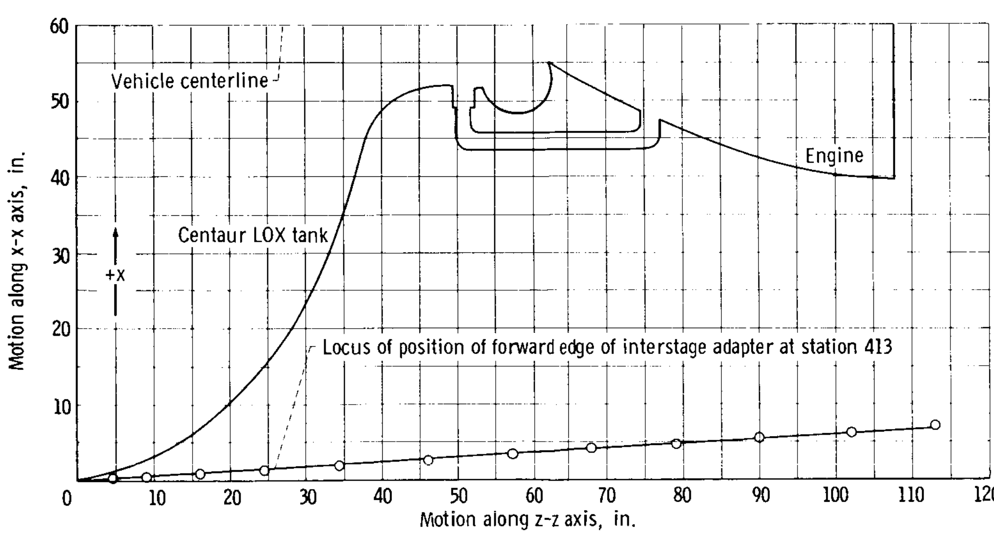

Figure VIII-6. - Motion in x-z plane of station 413 on Atlas with respect to Centaur during staging of AC-4 flight.

[redacted]

[redacted]

IX. ENVIRONMENTAL TEMPERATURES AND PRESSURES

SUMMARY

The exterior environmental temperatures experienced by the AC-4 vehicle were within the design limits and less than the predicted nominal values. The highest temperatures encountered were 585° F on the forwardmost point of the nose-fairing cap, and 976° F on the leading edge of the hydrogen vent stack, 18 inches outboard of the vehicle. Since the AC-4 trajectory would produce aerodynamic heating high enough to reduce the nose-fairing strength to a marginal value at the time of jettison, the nose-fairing and barrel sections were thermally protected with a subliming material (Thermolag T-230). Areas adjacent to protuberances on the insulation panels and interstage adapter were also protected with Thermolag. On the Atlas LOX tank, the maximum measured temperature was 320° F at station 580. At this temperature, the stress capability of the material far exceeds the loads.

The nose-fairing pressure environment was well within predicted values. A peak crushing pressure of 3 psi at T + 60 seconds was measured on the umbilical island. This pressure is below the design value of 5.2 psi. The thrustor bottle compartment pressure showed a peak value of 9.2 psi, which is not considered detrimental to any structure in this area. The insulation panel differential pressure history indicated that, through most of the flight, a crushing pressure is exerted on the panels whose peak value was recorded at 3.04 psi.

NOSE FAIRING

The nose fairing was a phenolic-Fiberglas honeycomb structure designed to withstand aerodynamic loads during the early boost-phase portion of the trajectory and nose-fairing-jettison loads. Preflight analysis of the nominal trajectory indicated temperatures between 500° and 600° F, which were in excess of the bondline strength and would have caused an adhesive failure between the outer skin and honeycomb core. This type of failure was encountered on a recent Agena-Mariner flight that had a similar nose-fairing structure. Also, ground tests have verified this adhesive type of failure on both the Centaur and Mariner nose-fairing structures. Therefore, to reduce these temperatures, a 0.040-inch-thick coating of Thermolag T-230 was applied to the nose-fairing conical and barrel sections. The areas coated are shown in figure IX-1. This coating effectively doubled the outer skin thickness or thermal mass because the Thermolag has a specific heat 25 percent higher than the phenolic.

In figure IX-2 the temperature-time curve is illustrated for various stations on the nose fairing. These temperatures were measured by thermocouples located under the first layer of Fiberglas, which, in turn, was covered by approximately 0.043 inch of Thermolag and phenolic. The sublimation temperature

[redacted]

of the Thermolag is a function of ambient pressure. At 1 millimeter of mercury the theoretical sublimation temperature is approximately 180° F. From the shape of the curves in figure IX-2, sublimation at stations 19 and 125 started at approximately 120 to 130 seconds; however, at station 181 on the barrel section, the Thermolag did not sublime but merely provided enough mass to keep the temperature extremely low. The nose cap, constructed of a phenolic-Fiberglas solid laminate structure 0.20 inch thick, was not coated with Thermolag, and peak temperatures ran just under 600° F, as illustrated in figure IX-3. The inner nose-fairing skin temperatures as well as the Surveyor compartment, remained relatively low throughout flight and showed little or no response to aerodynamic heating. Temperatures remained stable at lift-off values between 60° and 75° F.

The actual pressure environment during flight was less than predicted at all stations. Maximum crushing pressures encountered on the nose fairing occurred during transonic flight. Transducers at station 155 indicated peak crushing pressures of 0.3 psi in quadrant I, 0.44 psi in quadrant II, and 0.49 psi in quadrant III. These values compare with a design crushing pressure of 1.8 psi. At station 180, quadrant IV, a peak crushing pressure of 1.8 psi was recorded at T + 58 seconds; however, the design value in this area is 3.3 psi. The umbilical island showed a crushing pressure of 3 psi at T + 60 seconds, again well below the design value of 5.2 psi.

PROTUBERANCES

The maximum temperature measured on the Centaur vehicle was on the hydrogen vent stack. Measurement CA283T located on the leading edge of the vent stack, 18 inches outboard of the vehicle, indicated a maximum temperature of 978° F at T + 150 seconds, as shown in figure IX-4. Following maximum heating, the stack temperature cooled to 460° F at nose-fairing jettison.

A temperature profile along the quadrant I-II axis, including the umbilical island ramp and boost-pump fairing, is shown in figure IX-5. The umbilical island ramp was protected with a 0.1875-inch-thick layer of cork, and the maximum temperature under the cork was about 125° F. The boost-pump fairing did not have a protective Thermolag coating, and, as shown in figure IX-5, temperatures ran hotter, about 210° to 290° F. These temperatures were below the critical bondline temperatures and in no way impaired the integrity of the Fiberglas structure.

THRUSTOR BOTTLE COMPARTMENT PRESSURE

The thrustor bottle compartment pressure dropped from approximately 14.7 psi at lift-off to flight vacuum at nose-fairing jettison. At jettison, there is a pressure peak of about 9.2 psi due to thrustor bottle pressure. This pressure peak is higher than the pressures of 4.9 psi measured during Lewis Research Center SPC tests of the nose fairing but is not considered detrimental to any structure in this area.

PAYLOAD ADAPTER AND SPACECRAFT TEMPERATURES

All temperatures on the mass model, separation latch points, and payload adapter were within predicted values during the AC-4 flight. Temperatures ranged from 70° F at the top of the payload mast to -130° F at the payload adapter to tank attachment (station 171).

INSULATION PANELS

Locations of the various pressure measurements on the insulation panels are shown in figure IX-6. The external pressure decay history is shown in figure IX-7. At approximately T + 120 seconds, the external pressure reaches a value of zero. Insulation panel differential pressure history during the flight shows that a crushing pressure exists throughout most of the flight. Only in a few cases do the pressure curves become negative, which indicates a bursting pressure acting on the panels. The maximum crushing pressure recorded was 3.04 psi, and the maximum bursting pressure recorded was 0.38 psi. The maximum crushing pressure occurred at T + 70 seconds, immediately after the terminal shock wave passed down the panels. The movement of this shock wave is the cause of the pressure increase at this time. The differential pressure history is shown in figure IX-8. All the differential pressures are well within design limits for the insulation panels and lower than the predicted values.

The insulation panel temperature instrumentation to measure the thermal environment on AC-4 is shown in figure IX-6. The internal panel temperature data shown in figure IX-9 indicate temperatures at time of lift-off between -340° and -370° F. The predicted temperature at lift-off was -360° F, which corresponds very well with actual temperatures. One thermocouple (CA381T) did not fall within this temperature range, reading -260° F at lift-off. A reasonable explanation is that the thermocouple was near the helium purge ring and subject to impingement of warm helium while the vehicle was on the ground.

After lift-off, the temperature readings except for CA381T, gradually increased with time, and at panel jettison were indicating -290° to -330° F. This behavior was as expected because of the heat flux into the panels. The apparent anomaly with CA381T, however, was more a case of coming into equilibrium with the surrounding areas on termination of the helium purge. The airborne purge, activated at T - 16 seconds, provided a peak purge rate of 670 pounds per hour decaying to about 60 pounds per hour in 120 seconds.

The thermocouple locations on the outside of the insulation panels are shown in figure IX-6. These transducers were located directly outside the internal temperature patches and the time history of these measurements are presented in figure IX-10. The maximum temperature recorded by five of the thermocouples ranged from 140° to 175° F. These temperatures are much lower than predicted as shown in figure IX-11. The highest predicted temperature in the basic panel region (cylindrical section) was 420° F, and the highest actual temperature was 175° F read by CA701T located at station 280. The sixth thermocouple read a maximum temperature of only 95° F. This thermocouple was located on the wiring tunnel panel at station 395 in an area that was coated with

Thermolag. The Thermolag increased the mass of the panel, thus the panel was able to absorb more heat without an increase in temperature. These temperatures result in only a small decrease in insulation panel material strength allowables.

Thermocouples CA40T and CA41T read the outside temperatures in the area of the destruct package. These thermocouples were located in a Thermolag-coated area, thus the temperatures realized were much lower than those predicted. The highest temperature read by either of these thermocouples was 88° F as shown in figure IX-12, which is well within design limits.

ATLAS LOX TANK TEMPERATURES

A comparison of predicted and measured values of the Atlas LOX tank skin temperatures at various vehicle stations is shown in table IX-I. The flight data indicate a much less severe thermal environment than the analysis does. The slightly lofted boost phase may account for some margin, but analysis is still very conservative.

TABLE IX-I. - ATLAS LOX TANK SKIN TEMPERATURES

Vehicle station, in.	Peak temperature, °F	
	Predicated maximum for design trajectory with 165K engines	AC-4 measured
574	---	292
575	640	367
580	---	320

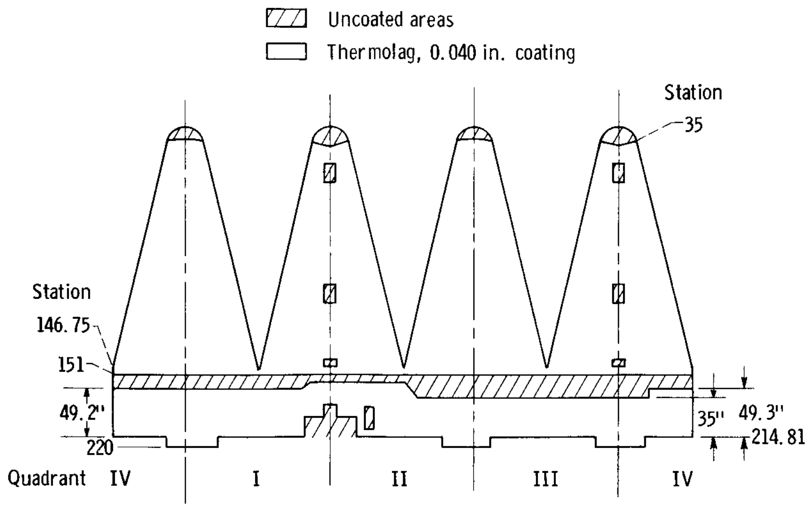

Figure IX-1. - Thermolag coated areas on AC-4 nose fairing.

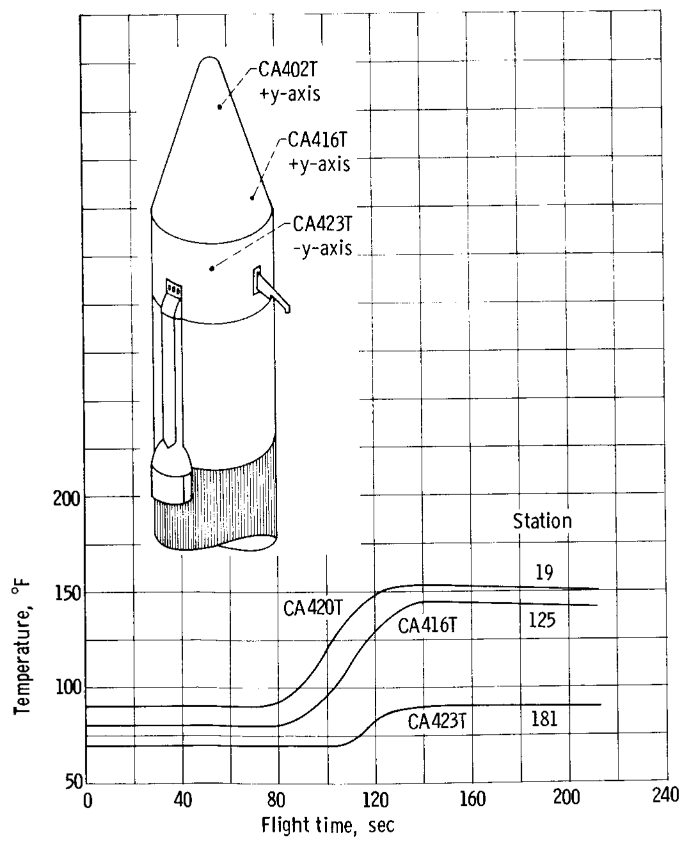

Figure IX-2. - Nose-fairing outside temperatures.

[redacted]

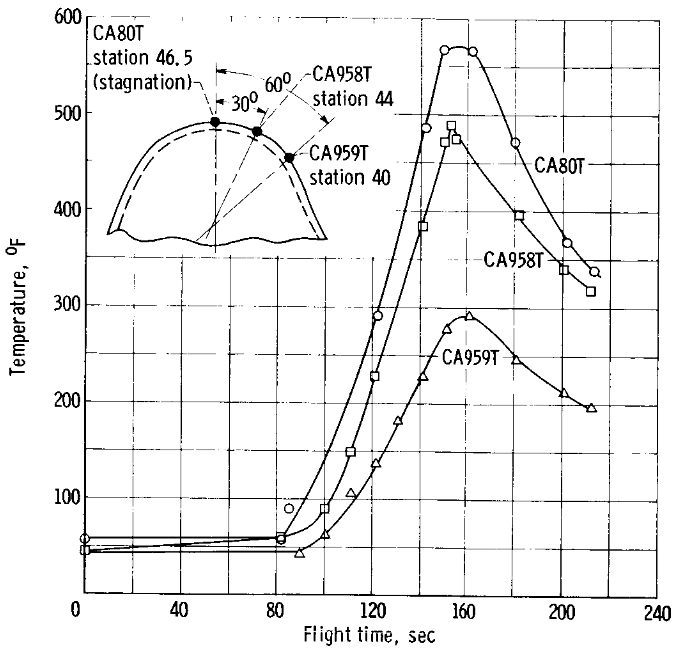

Figure IX-3. - Nose-fairing cap temperatures.

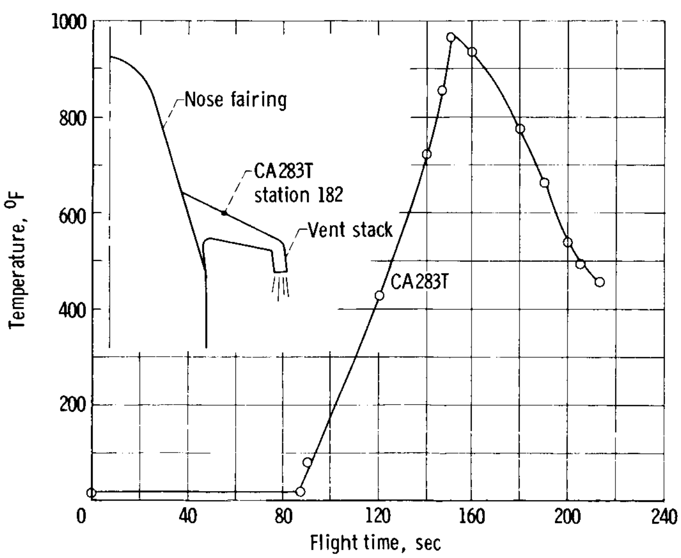

Figure IX-4. - Hydrogen vent stack temperatures.

[redacted]

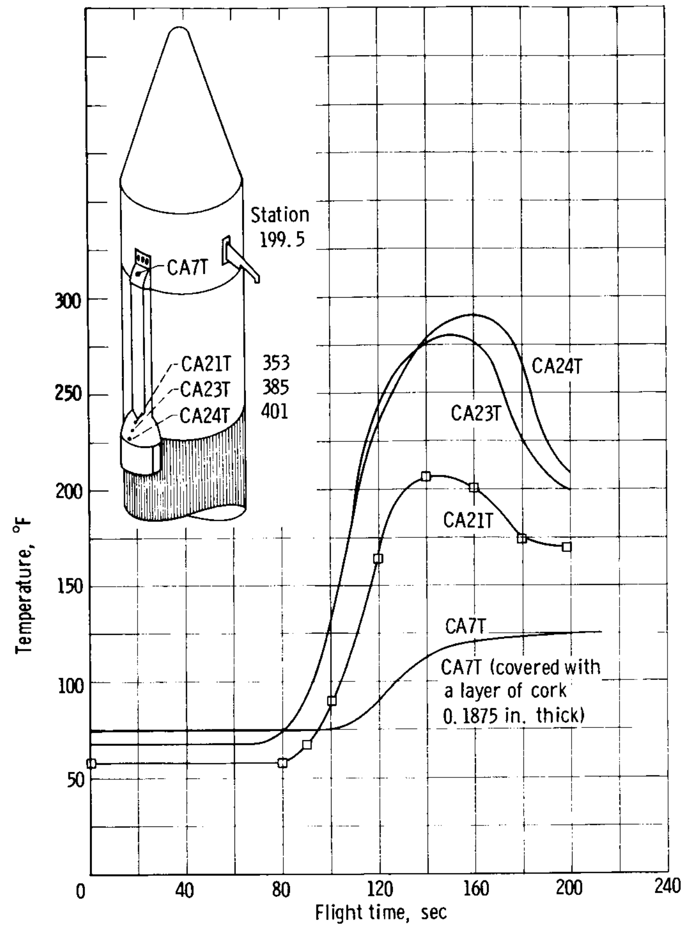

Figure IX-5. - Wiring tunnel and boost-pump-fairing temperatures.

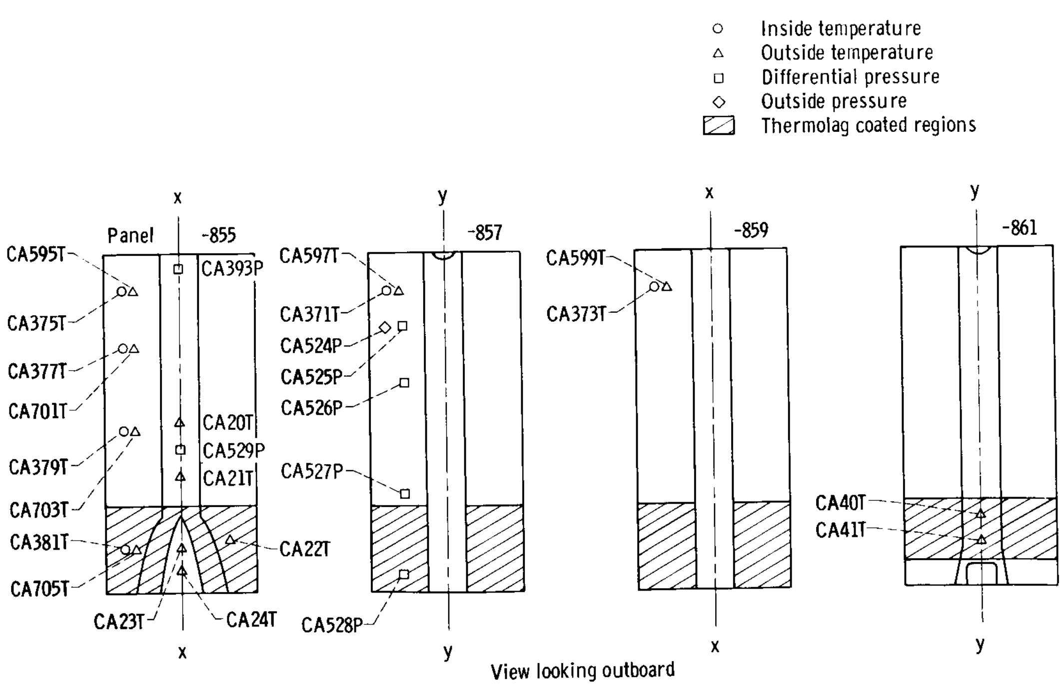

Figure IX-6. - Location of insulation panel instrumentation and Thermolag.

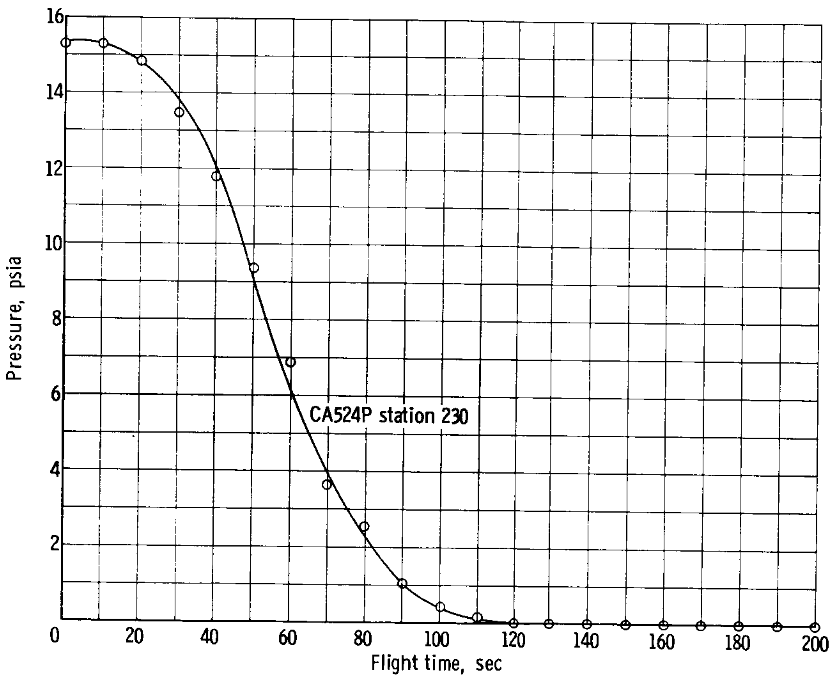

Figure IX-7. - Insulation-panel external pressure.

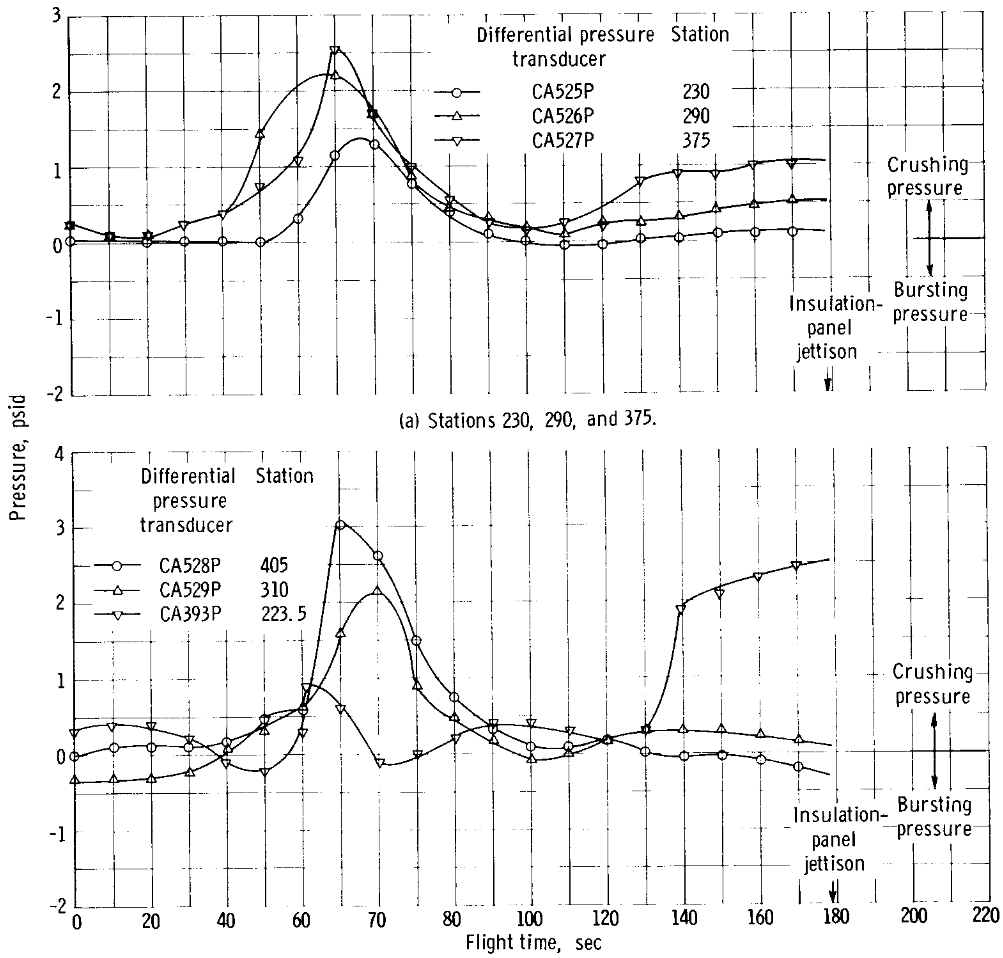

(a) Stations 230, 290, and 375.

(b) Stations 223.5, 310, and 405.

Figure IX-8. - Insulation-panel differential pressure.

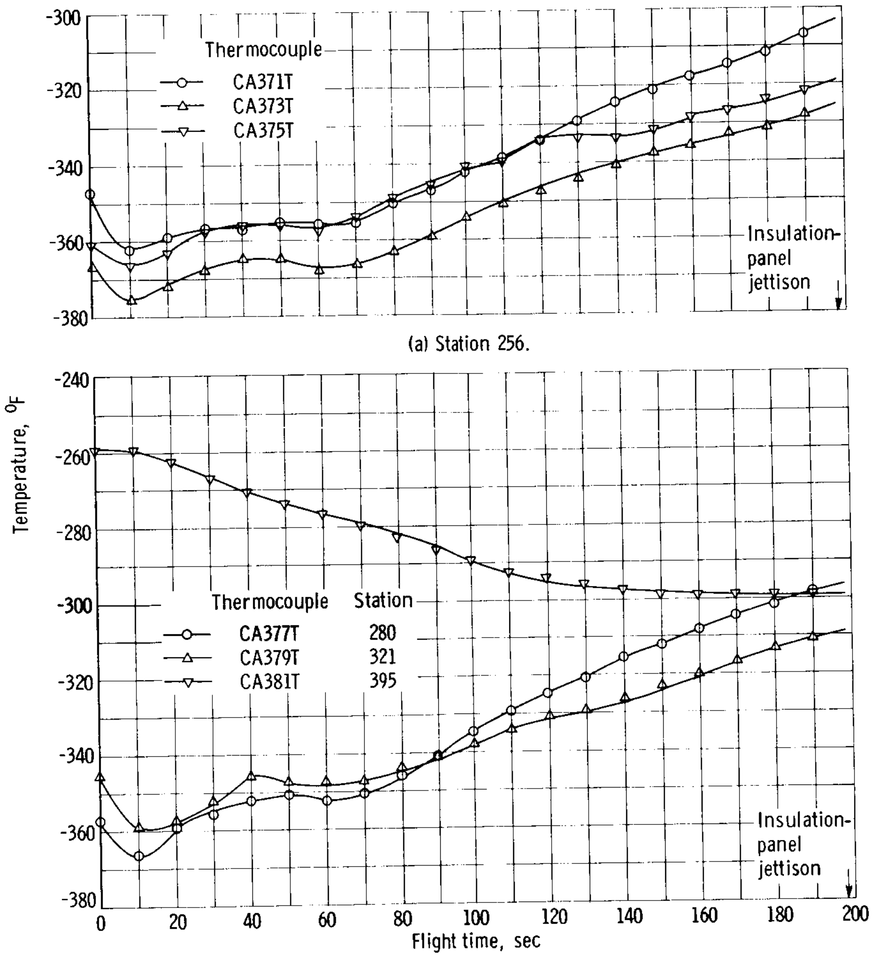

(a) Station 256.

(b) Stations 280, 321, and 395.

Figure IX-9. - Insulation-panel inside temperature.

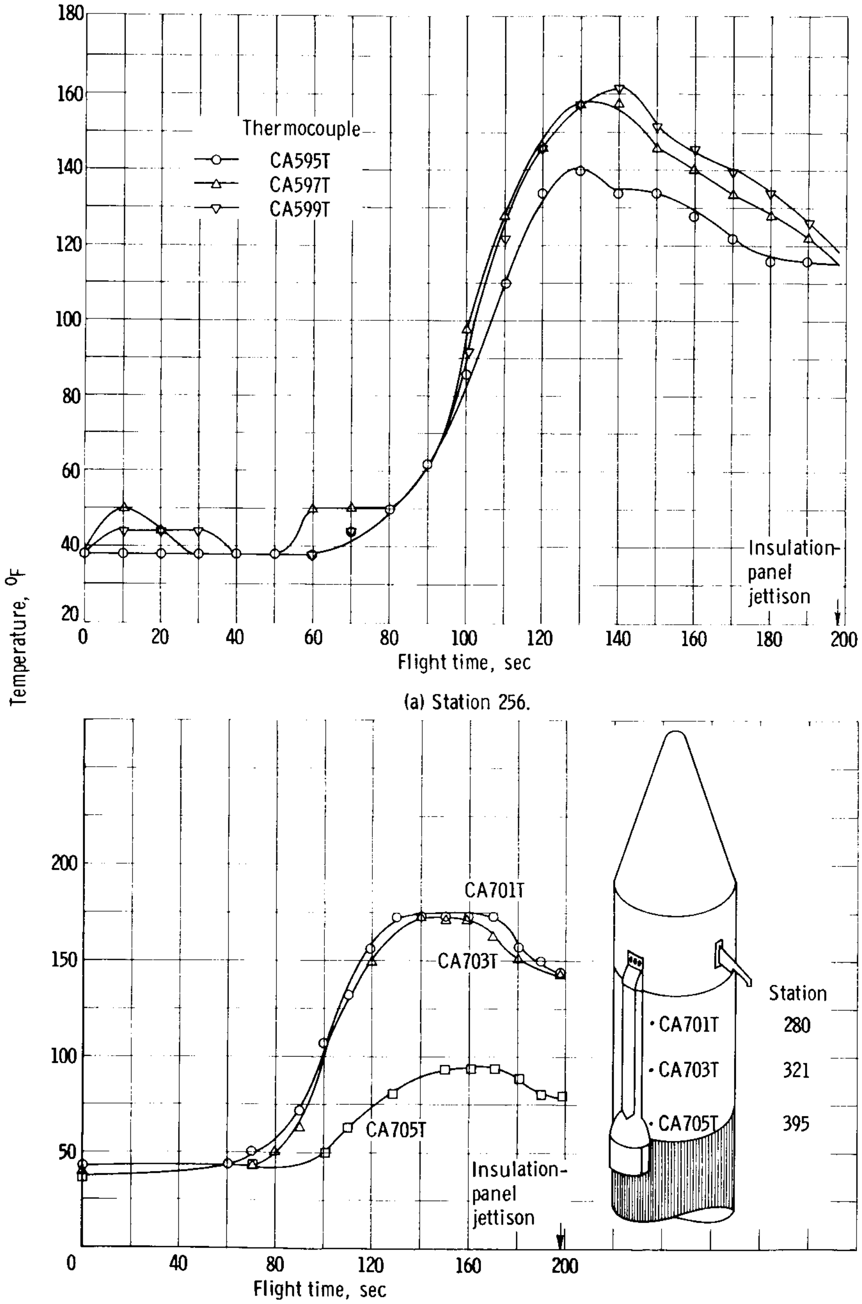

(b) Stations 280, 321, and 395.

Figure IX-10. - Insulation-panel outside temperatures.

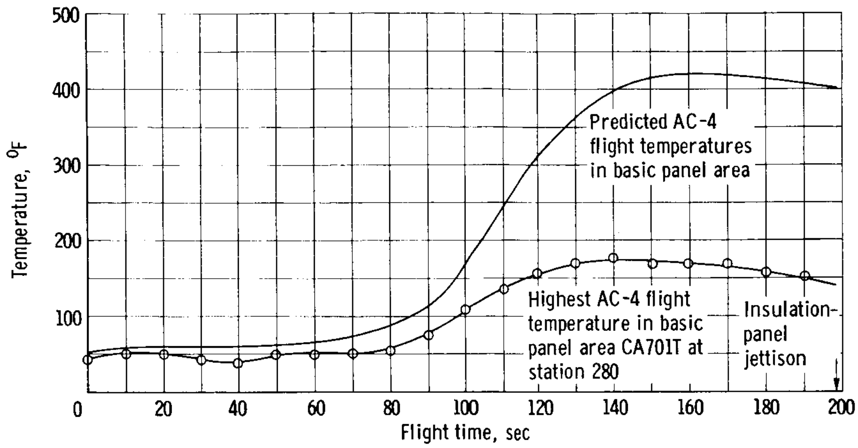

Figure IX-11. - Predicted outside insulation-panel temperature.

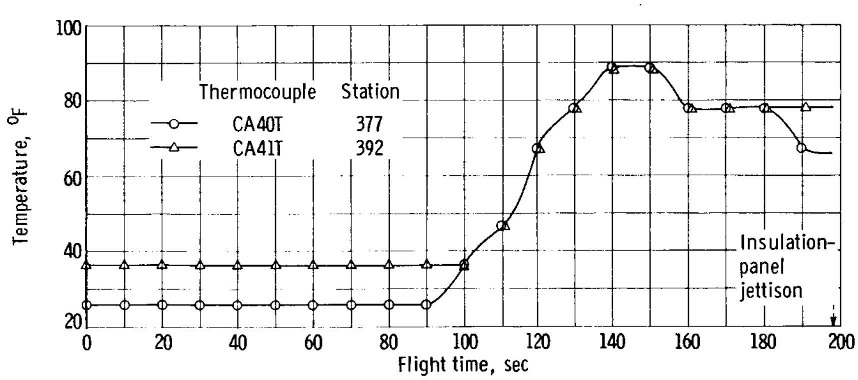

Figure IX-12. - Destruct fairing outside temperature.

X. VEHICLE STRUCTURES

SUMMARY

All mission objectives of structural significance were achieved. Structural integrity of the vehicle was successfully maintained throughout the peak loading periods. Though a few of the measurements were deleted prior to the flight and others were lost during the flight, information received was of acceptable quality and quite valuable in assessing structural performance.

The peak longitudinal load factor experienced during the flight was 5.52 g's at BECO. Aerodynamic drag loads showed a peak of 52 400 pounds at T + 70 seconds. The measured drag load history deviated from the predicted in that the actual drag load appeared to build up and decay somewhat more rapidly than anticipated. Bending loads induced by wind shears and gusts on this flight were quite small. The peak bending moment experienced on this flight occurred at T + 83 seconds: at station 548 it attained a value of 1.43×10^6 inch-pounds.

Intimate contact was maintained throughout the flight between the Centaur LH_2 tank and the insulation panels. Inadvertent overpressurization of the Centaur LOX tank during a preflight tanking test did not appear to have a deleterious effect on vehicle strength. Rework on the nose-fairing hinges apparently achieved their objective, that is, no compression load was transmitted through these hinges during preseparation flight, although some tension loads were reacted by the hinge on the positive y-axis. A positive differential pressure of at least 6.2 psi was maintained across the Atlas intermediate bulkhead during launch, its most critical period. This was very similar though slightly more severe than the AC-3 experience. Interstage adapter skin panels were subjected to sonic and aerodynamic buffeting excitation. A peak response of 30 g's (rms) at launch and 24 g's (rms) at T + 60 seconds was attained. Payload adapter strain measurements indicated that there were adequate structural margins of safety in this area.

Details of structures instrumentation are shown in figures X-1 to 3. Instrumentation performance and failures are discussed in some depth in appendix D.

FLIGHT LOADS

Vehicle Bending Moments

The Atlas-Centaur vehicle is launch restricted by inflight winds, the launch availability being well below 1 for the worst months of the year. Though the winds aloft attain their peak values during the winter months, on the AC-4 launch day, preflight balloon soundings indicated an unusually calm day even though surface winds were marginal. Peak winds through the high dynamic pressure region were all less than 30 knots. Thus, anticipated bending loads were quite small. This was verified by an analysis of loads measured during the flight by strain gage instrumentation on the vehicle.

The bending moment history at the interstage adapter station 548 is shown in figure X-4 about the two principal axes. It is seen that highest value of bending moment attained at this station was only 1.43×10^6 inch-pounds at T + 83 seconds. Although this is not the station of peak load, it is the station where a direct measurement of bending loads was made.

A comparison of actual and predicted loads is shown in figure X-5. The predicted bending loads range is based on T - 0 hour (905 EST) balloon sounding. It is seen that the measured values are approximately in the middle of the predicted range. The trends indicated analytically are confirmed by flight data, although the peak load was predicted at T + 71 seconds and actually occurred at T + 83 seconds. The only explanation that can be offered for this is a slight shift in winds between the balloon sounding and the flight. The relatively large predicted range is due to the use of a 30-foot-per-second (1 - cos) gust criteria. In view of this fact, the agreement between predicted and measured loads may be considered to be very good.

Gust Bending Moments

On this flight, the gust loads encountered were extremely small. The basic data by which gust response is measured are the high-frequency strain measurements at station 548. This high-frequency strain increment is assumed to result from the fine variations in the wind profile that are filtered out by the inherent inertia of the wind sounding instrumentation used. A review of this high-frequency strain response showed a maximum strain increment of 24×10^{-6} inch per inch. This corresponds to a bending moment equivalent to approximately 96 000 inch-pounds. The preflight analytical peak value of bending moment induced by a 30-foot-per-second (1 - cos) gust was 1.27×10^6 inch-pounds. It is apparent that the gust levels were at least an order of magnitude less than the design gust criteria.

Variation of Preflight Wind-Induced Bending Moments

Another factor in the consideration of the wind loads is the inherent time lag between the wind sounding used as the basis for launch decision and the actual launch. An evaluation of the relative changeability of the wind profile during this time becomes quite important. In figure X-6, the analytical bending moment histories are shown at vehicle station 770 on the Atlas LOX tank calculated on the basis of 2215, 0045, 0518, and 0905 EST balloon soundings. It can be seen that, on launch day, the variations in the winds were of a very minor nature. The maximum bending moment changes from 4.04×10^6 to 3.88×10^6 inch-pounds in the last two consecutive soundings, a variation of 4 percent. This compares with a variation of 11 percent recorded for the AC-3 flight. These

[redacted]

data were obtained from unpublished GD/A analyses of simulated flight through the above winds.

LONGITUDINAL LOADS

There are two sources of longitudinal loads on flight vehicles: one is the inertial load resulting from axial acceleration and the other is due to aerodynamic drag forces. Vehicle axial acceleration is known precisely both from onboard accelerometers and from a knowledge of total engine thrust. The inertial loads can then be calculated from known mass distribution. It was of interest to see how well actual aerodynamic drag compared with analysis based on wind tunnel axial force coefficients. The total axial forces are calculated for station 548 from the strain gage data. Subtracting the inertial loads yields the drag forces. Comparison is shown in figure X-7. During the period of peak drag load, the agreement between the two is quite good; however, actual drag buildup and decay are much more rapid than predicted from wind tunnel data. For completeness, total axial load during this period of flight is also shown in figure X-7. From the data it appears that the total impulse resulting from atmospheric drag forces is actually less than that obtained analytically from axial force coefficient data.

ANALYSIS OF INSULATION-PANEL HOOP TENSION LOADS FOR AC-4 FLIGHT

The hoop tension loads in the AC-4 insulation panels were determined by using measured flight temperatures and pressures. The factors that affect the panel hoop tension are (1) panel installation pretension, (2) panel temperature variations, (3) panel delta pressures (crushing and bursting pressures), (4) tank temperature variations, and (5) tank pressure variations. Each of the panel and tank deflections due to these parameters were determined, and a total deflection was obtained. This total deflection indicates that, from T + 0 to panel jettison, an interference pressure existed between the panels and the tank. This interference pressure was converted to panel hoop tension, and a plot of panel hoop load against flight time (fig. X-8) was obtained. The hoop load was determined at approximately the midpoint of the panels, which was station 340.

On installation, the panels were pretensioned to 75 pounds per inch with the tank at standby pressure. During cryotanking, the hoop tension begins to decrease because the tank shrinks more rapidly than the panels. The tank pressure at this time is also increasing, but this increase does not offset the effects of thermal contraction. These factors cause the panel hoop tension to decrease until approximately lift-off. The panel hoop tension at lift-off was calculated to be 11 pounds per inch, which was the minimum hoop tension during the flight. After lift-off, the panel hoop tension increases gradually due to the increase in tank pressure. The deflections due to panel temperature and panel pressure remain somewhat constant. At T + 52 seconds, the panel pretension had recovered to its initial value of 75 pounds per inch. The panel hoop tension increases rapidly to about T + 80 seconds, when it peaks to a maximum. This hoop load is approximately 180 pounds per inch. After the peak is reached, which is only for less than 5 seconds, the hoop load decreases

[redacted]

rapidly. This decrease in hoop load is due primarily to the venting of the LH_2 tank at this time. In addition a decrease in crushing pressure and an increase in panel temperature tends to relieve the hoop tension, which decreases to a value of 42 pounds per inch at about T + 120 seconds. After this point is reached, the hoop load starts to increase due to a lockup of the tank vent and a consequent increase in tank pressure. The hoop tension increases to 64 pounds per inch at T + 140 seconds. At this time, the hoop load again decreases due to a second venting of the tank and increased panel temperatures. The hoop load gradually decreases to 45 pounds per inch at panel jettison.

Another means of analysis was utilized to obtain the panel hoop load. For this method, the increase in tank hoop strain at the time of panel jettison was used. This gives a value of hoop load at only one time, which is just prior to panel jettison. The value of hoop tension at panel jettison obtained by this method was 80 pounds per inch. Although higher than the 45 pounds per inch obtained by the other method, it definitely confirms that the panels and the tank were in contact throughout the flight.

INTERSTAGE ADAPTER PANEL FLUTTER

The interstage adapter configuration for the AC-4 flight was changed from that of the AC-2 and AC-3 adapters by deleting 10 ring stiffeners. This returned the adapter to its initial geometry, that is, the ring spacing used in the quarter section wind tunnel test specimen (ref. 11). The flutter boundary of reference 11 and the longitudinal stiffener load history of figure X-9 were used to obtain an AC-4 flight flutter boundary. A comparison of actual flight flutter parameter and the flutter boundary in figure X-10 indicates that panel flutter was possible only for a few seconds subsequent to the time that the vehicle attained Mach 1 (T + 64 sec). It can be seen that, although the flutter parameter was outside the flutter boundary during most of the flight, the two values are quite close together. The boundary is a function of stiffener load, which in turn is a function of the wind profile bending moments. On the AC-4 flight, the bending loads encountered were very small, as discussed earlier. Therefore, with existing geometry, panel flutter could occur during significant periods of time through the high dynamic pressure flight regime on launch days with a more severe wind environment.

As in the case for the AC-3 flight, accelerometer data indicated skin panel excitation through the first 100 seconds of flight. Pressure fluctuations and panel accelerometer data are illustrated in figures X-11 and 12. In the absence of panel flutter, dynamic response of the skin panels could only be the result of sonic excitation at launch, sonic and aerodynamic buffeting excitation through to Mach 1, and aerodynamic buffeting in the remaining atmospheric phases of flight. As the structural integrity of the adapter was maintained successfully throughout the flight, this level of skin panel excitation is considered within the fatigue capability of the aluminum alloy used.

NOSE-FAIRING HINGE LOADS

Nose-fairing hinges support the two fairings at jettison as each section pivots away from the Centaur tank. Concern was evidenced prior to the flight that the nose-fairing lugs would bottom out on the hinge aft fork and transfer nose-fairing inertial and drag loads into the hinge. To alleviate this possibility, the fork opening was widened, and care was taken to create a gap between the nose-fairing lug and the aft fork of the hinge. (For hinge details see fig. X-13.)

The flight data seem to indicate that this procedure achieved its purpose. No compression was noticed in the hinges until T + 180 seconds, showing that no aft flight loads were felt by the hinges up to T + 180 seconds. There were, however, tension loads in the top y-y axis hinge during the transonic period indicating transfer of fairing bending that was overcoming positive acceleration forces. The flight loads were well within the hinge limit load capacity of 6000 pounds. For a summary of hinge loads during jettison of the fairing see section VIII. SEPARATION.

PAYLOAD ADAPTER LOADS AND STRESSES

The three strain gages mounted on the payload adapter longerons (directly below the separation latch points) indicate compression in the adapter increasing in intensity from launch to BECO. At BECO, there is an abrupt decrease in payload adapter strains. Stress levels do not exceed 10 000 psi in the adapter longerons, indicating that good structural margins of safety exist in this area.

Payload adapter strains at MECO showed an oscillating type of loading (tension to compression reversals) at the separation latch points. Maximum tension and compression levels were approximately 1000 pounds per latch point. There were about four amplitudes at these levels. The loads then decayed rapidly at a frequency of 28 cps. These loads were equivalent to 1.43 g's acceleration of the payload. The normal 1.5 design factor is used to obtain an equivalent test acceleration of 2.15 g's. Previous separation latch DPT procedures called for a 1.4-g load factor limitation at the retromotor simulator. These loads have now been revised, as a result of the AC-4 data, to a 2.15-g limitation on the retromotor simulator (or 3.15 g's including gravity for laboratory test conditions). Separation latches on future vehicles will be qualified to these new loads.

INADVERTENT OVERPRESSURIZATION OF CENTAUR LOX TANK

DURING PREFLIGHT QUAD TANKING TEST

As a result of the overpressurization of the Centaur LOX tank during the first flight control and propellant tanking test on October 27 (see section III. LAUNCH OPERATIONS), there was some concern about the integrity of the structural intermediate bulkhead. Preceding the overpressurization, the fuel and LOX tanks were pressurized to 20.0 and 31.0 psia, respectively. At the time of maximum overpressurization of the LOX tank, the LOX tank ullage pressure had increased to approximately 53 psia. The differential pressure across the intermediate bulkhead including both ullage and fluid head pressure, was 33 psid at the top and 34.4 psid at the tangency point at station 405.6. For structural details of this area see figure X-14. The design limit load allowable for the bulkhead differential pressure is 23.0 psid. The helium leak check and X-ray examination (described in section III) were augmented by an extensive series of specimen tests conducted at GD/A.

The specimens were made up in the configuration of the welds used at the bulkhead top and tangency points, prestressed to levels seen by the tank during factory and cryogenic proof tests, loaded to stress levels experienced by the bulkhead at maximum overpressurization, and then to failure, at various cryogenic temperatures. The specimen tests indicated that a moderate amount of yielding had probably occurred in the annealed weld beads and heat-affected zone of the parent material. The effect of this amount of yielding work-hardened the annealed material considerably (effectively raising the material yield point for subsequent loading) and to be insufficient to affect adversely the fracture toughness of the material at low temperature.

The maximum calculated stresses produced at the top and tangency points of the bulkhead during overpressurization were 106 000 and 130 600 psi, respectively. The stresses required to cause yielding in these areas (for loadings subsequent to the prestressing due to overpressurization) from the specimen tests were about 113 000 psi for the bulkhead top and 180 000 psi for the tangency point weld. The tests also indicated that the prestressing due to overpressurization raised the ultimate allowable stress for subsequent loadings at cryogenic temperature. These ultimate values were well over 200 000 psi. The maximum stresses expected in flight were 75 000 psi at the bulkhead top and 100 000 psi at the tangency point seam weld.

Based on the favorable results of the leak and X-ray examinations and the specimen test results, it was concluded that the structural integrity of the Centaur tank had not been impaired.

ATLAS INTERMEDIATE BULKHEAD DIFFERENTIAL PRESSURE

The measured value of the launch transient minimum differential pressure was 10.2 psi. Had the ullage pressures been at their most adverse (LOX tank, 31 psi; and RP-1 tank, 57 psi), the differential pressure across the bulkhead would have been 6.2 psi. The incremental longitudinal load factor acting on the LOX due to launch release dynamics was calculated to be 0.23 g from differential pressure data. This compares with 0.60 g assumed in the analysis.

The minimum differential pressure measured at T + 99 seconds was 9.0 psi. Again, had the ullage pressures been at their most adverse, the differential pressure across the bulkhead would have been 6.75 psi. At no time either during the flight or during launch release was the bulkhead differential pressure near its critical value of 2 psi for bulkhead reversal.

[redacted]

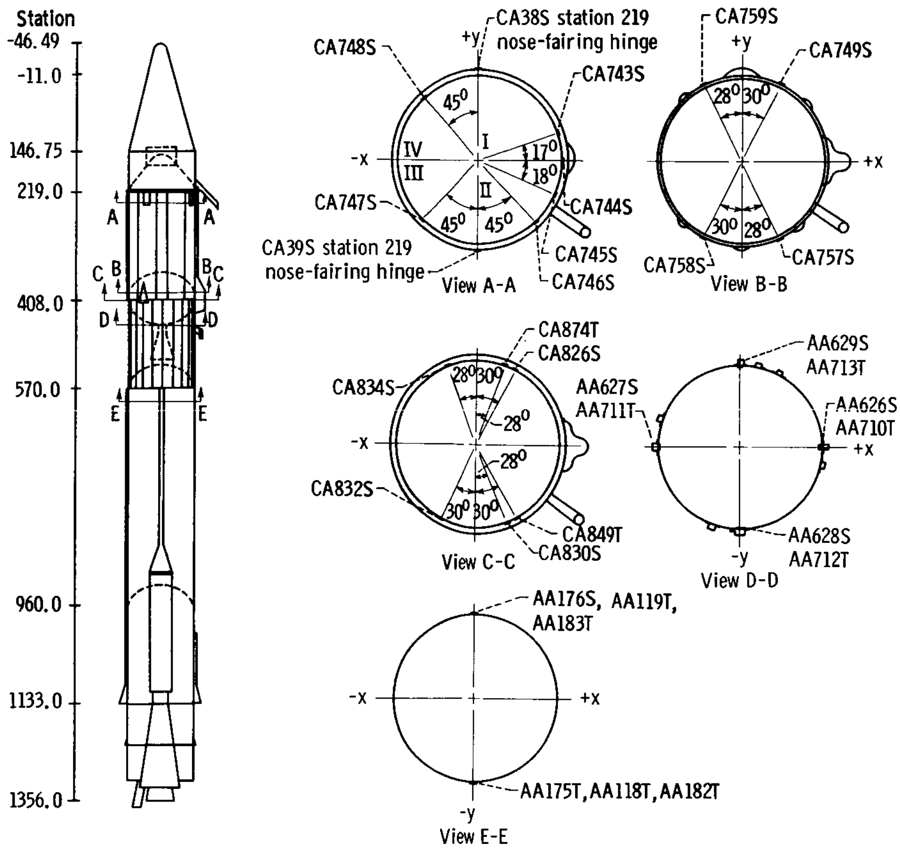

Figure X-1. - AC-4 flight structures instrumentation configuration (ref. 2). (Instrument numbers ending in S are strain gages and in T are thermocouples.)

[redacted]

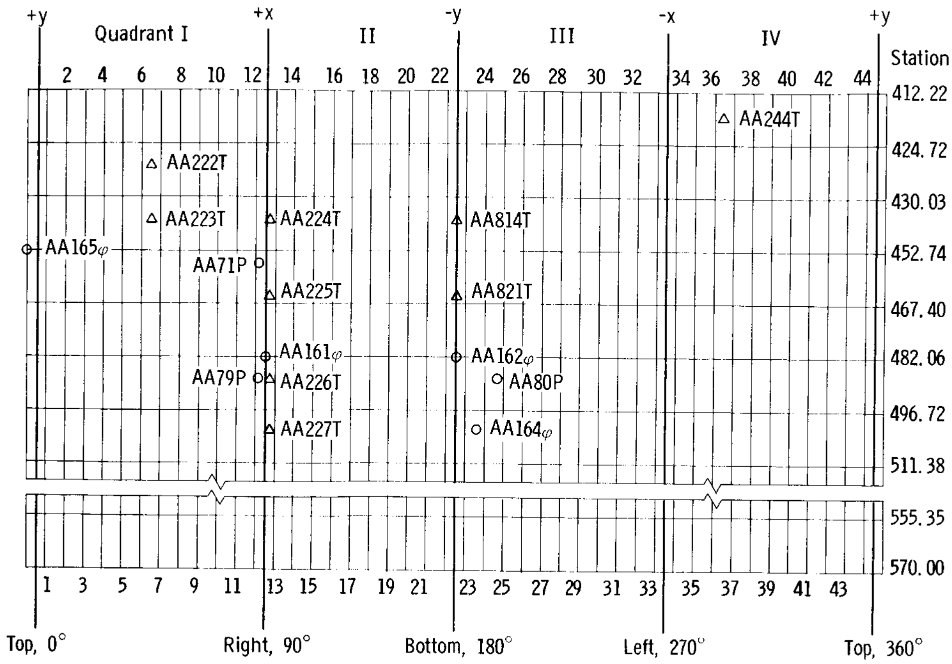

Figure X-2. - AC-4 interstage adapter instrumentation. Flat pattern external surface view.

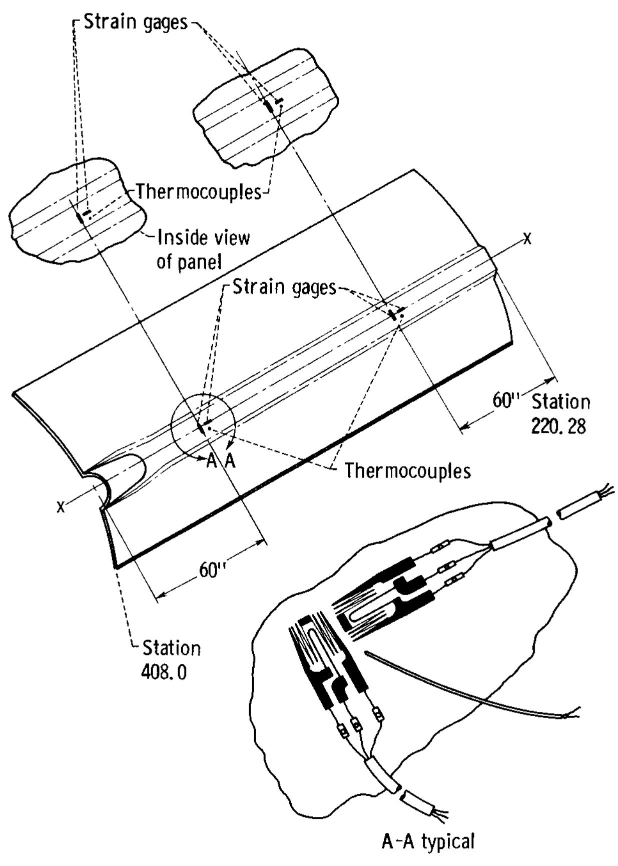

Figure X-3. - Landline insulation panel preload measurement instrumentation (ref. 17).

[redacted]

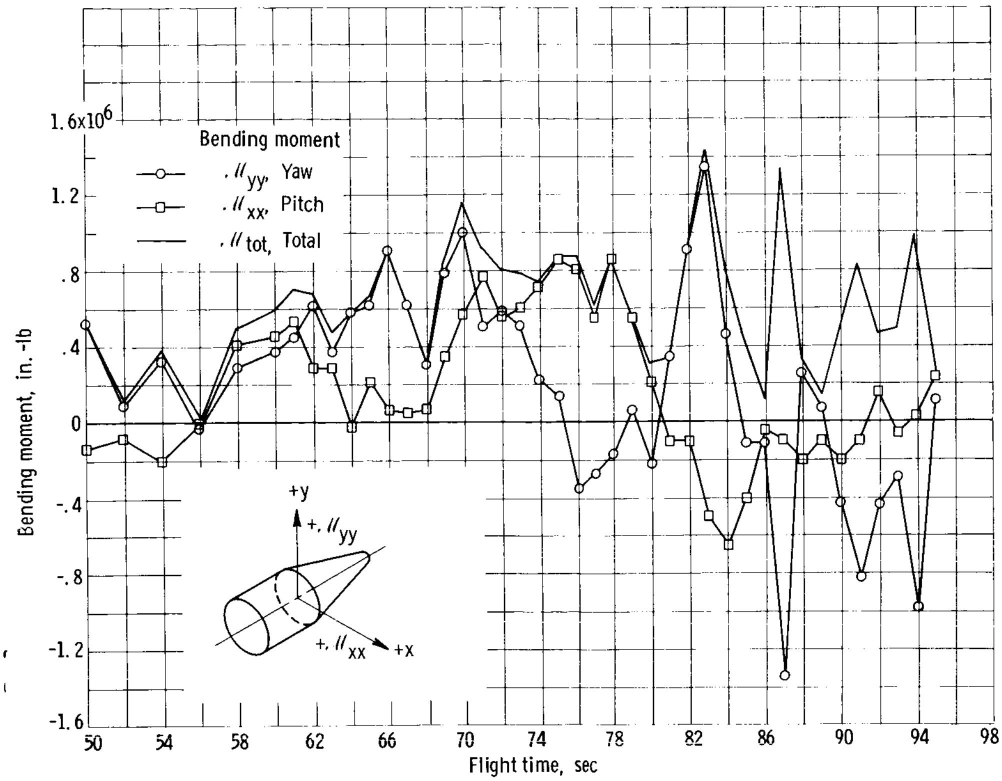

Figure X-4. - AC-4 flight bending moment history at station 548 through high αq region based on strain gage data.

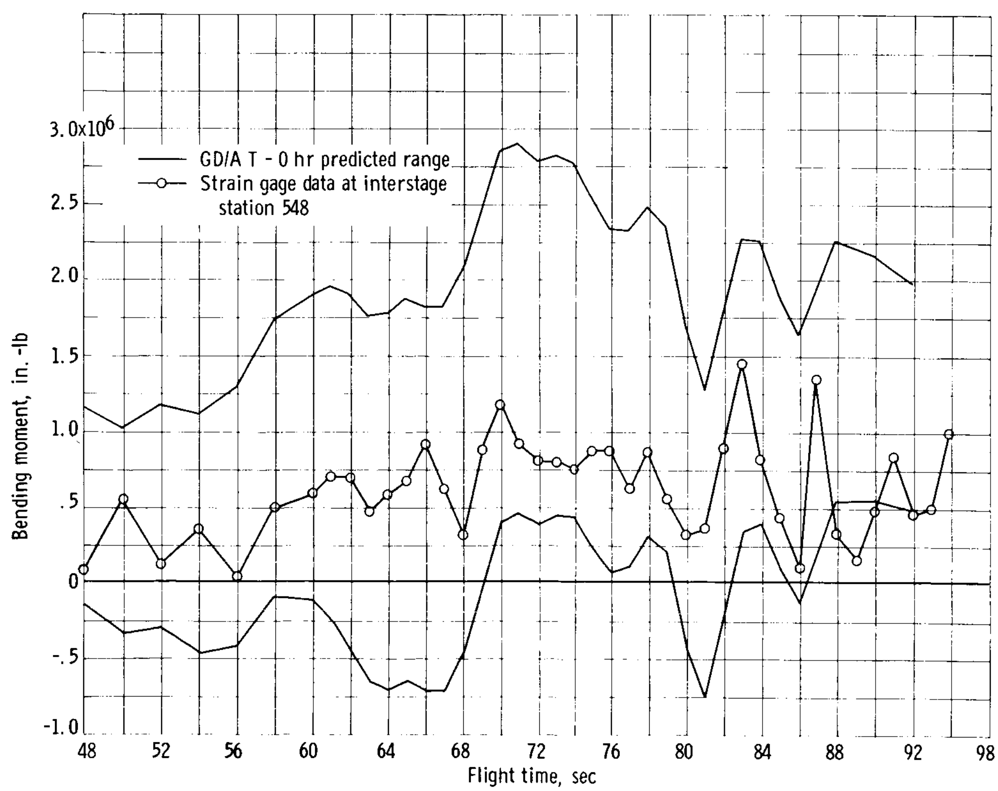

Figure X-5. - Comparison of predicted and measured AC-4 flight bending loads at station 548.

[redacted]

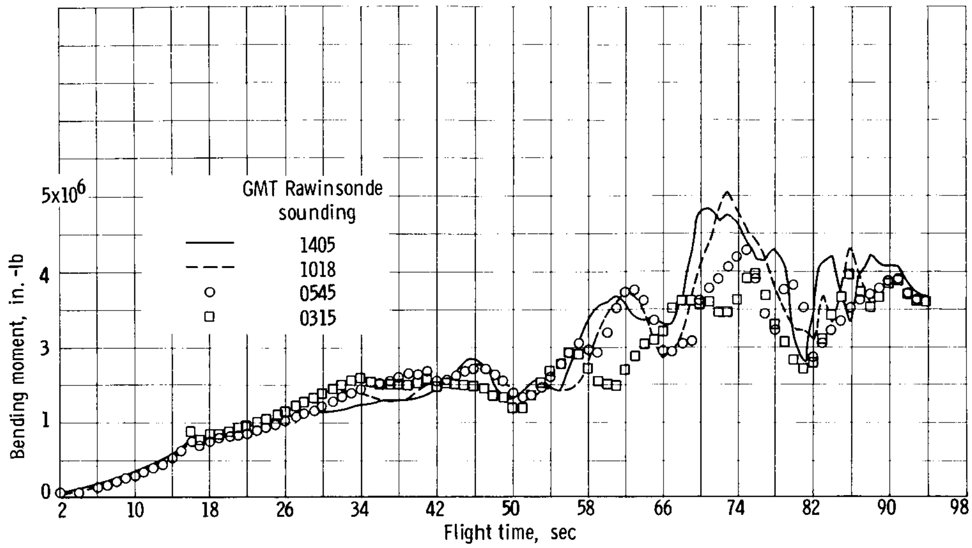

Figure X-6. - Analytical history of AC-4 flight limit bending moments based on four preflight Rawinsonde balloon soundings.

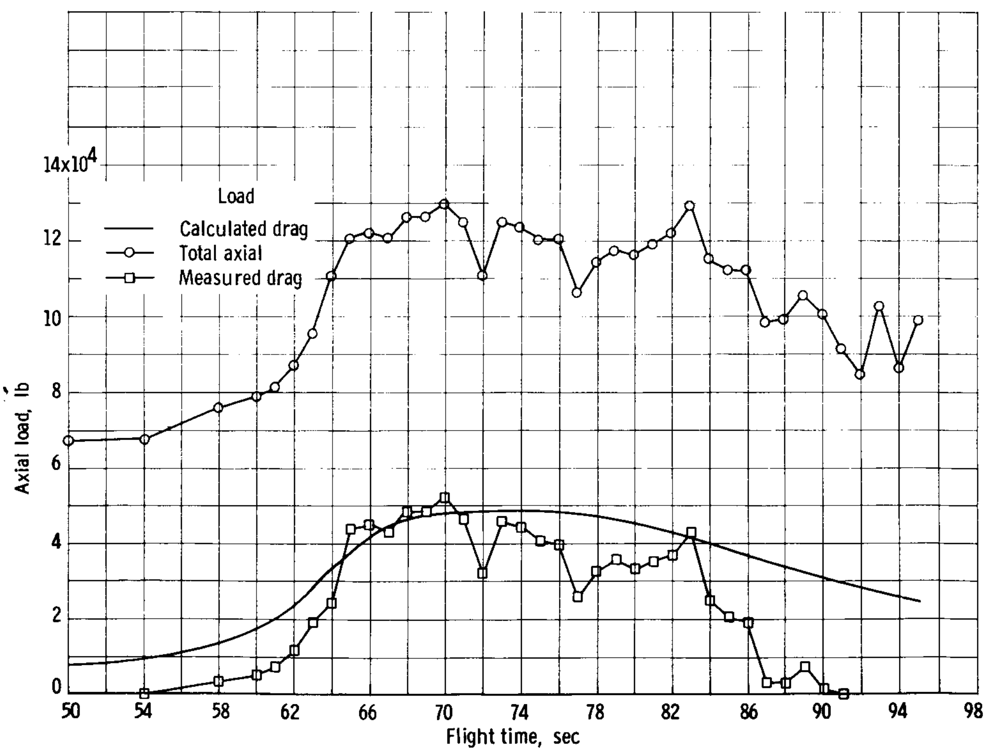

Figure X-7. - History of total axial load and comparison of measured and calculated aerodynamic drag through high q flight regime.

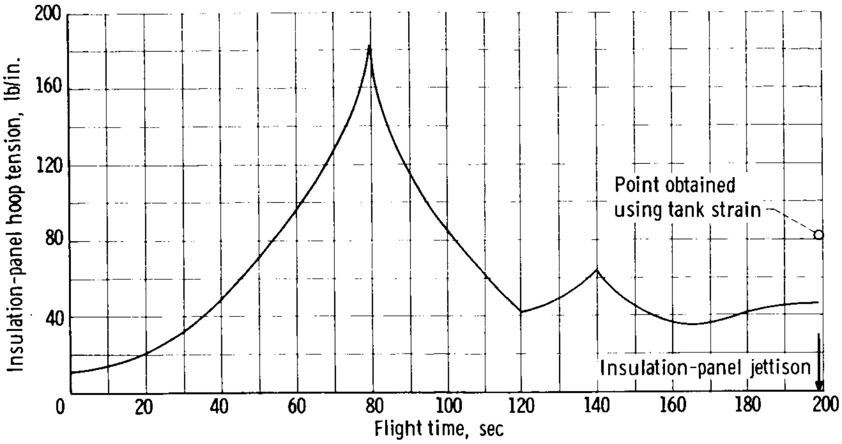

Figure X-8. - Insulation-panel hoop tension against flight time for Centaur AC-4.

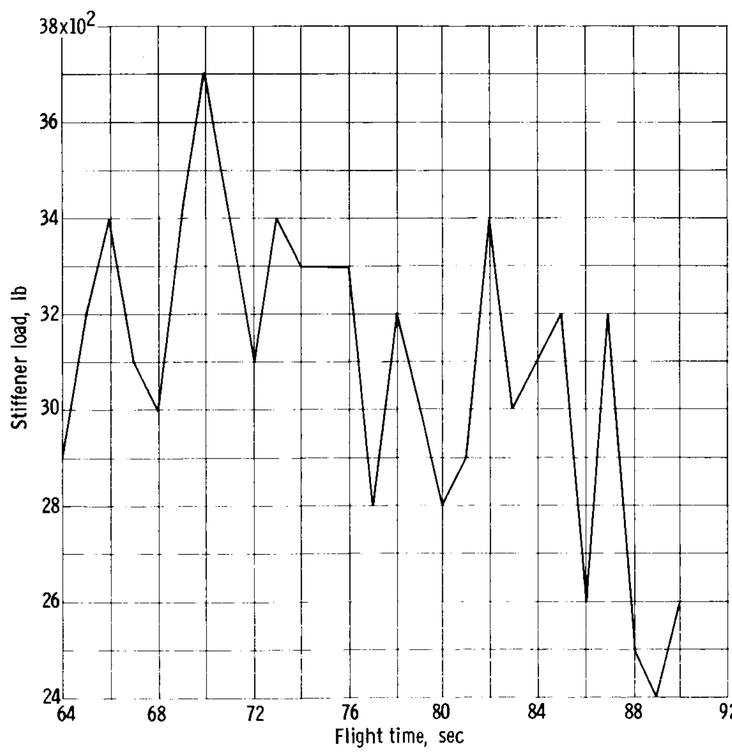

Figure X-9. - Flight history of AC-4 interstage adapter peak compression stiffener load.

[redacted]

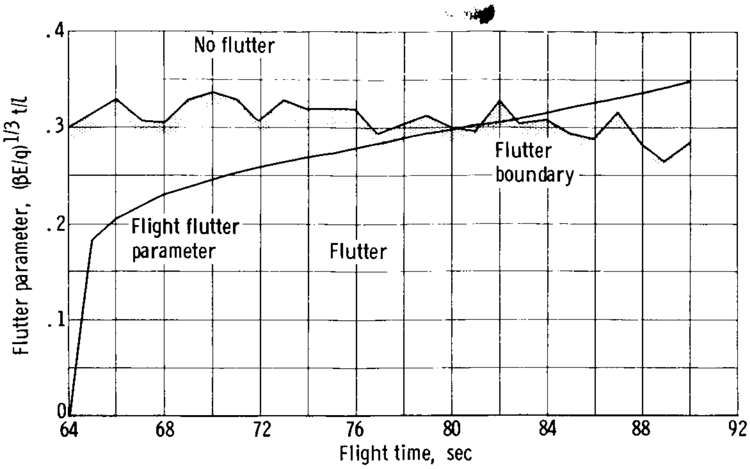

Figure X-10. - Interstage adapter skin panel flutter parameter history on AC-4 flight.

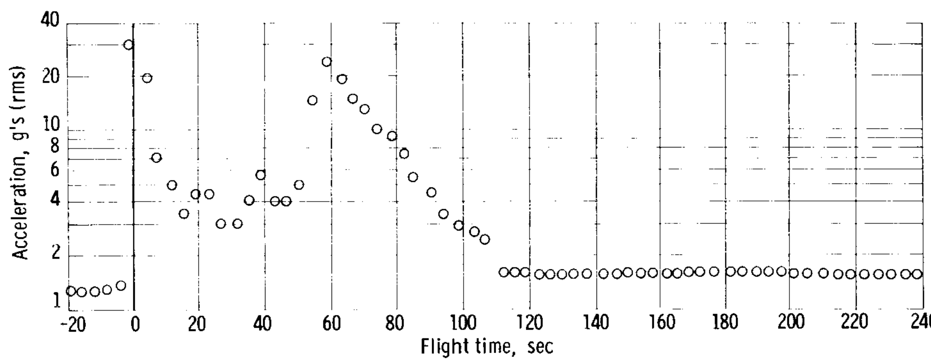

Figure X-11. - Vibration level as recorded by accelerometer AA164φ mounted on skin panel midpoint at station 502 and negative y-axis. Data obtained from reference 2. Analysis band, 20 to 2100 cps; commutated data, one sample every 4 seconds.

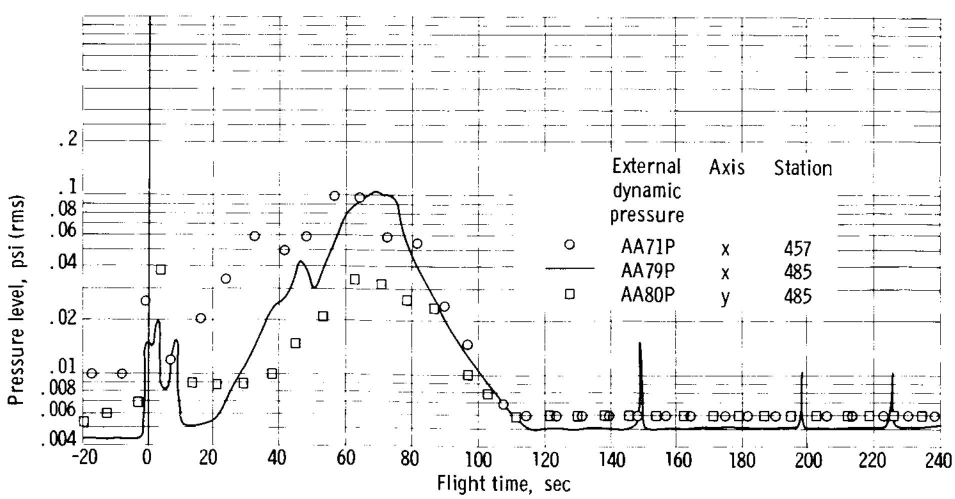

Figure X-12. - Fluctuating pressure level distribution around interstage adapter. AA71P and AA80P commutated data, one sample every 8 seconds (ref. 2).

[redacted]

[redacted]

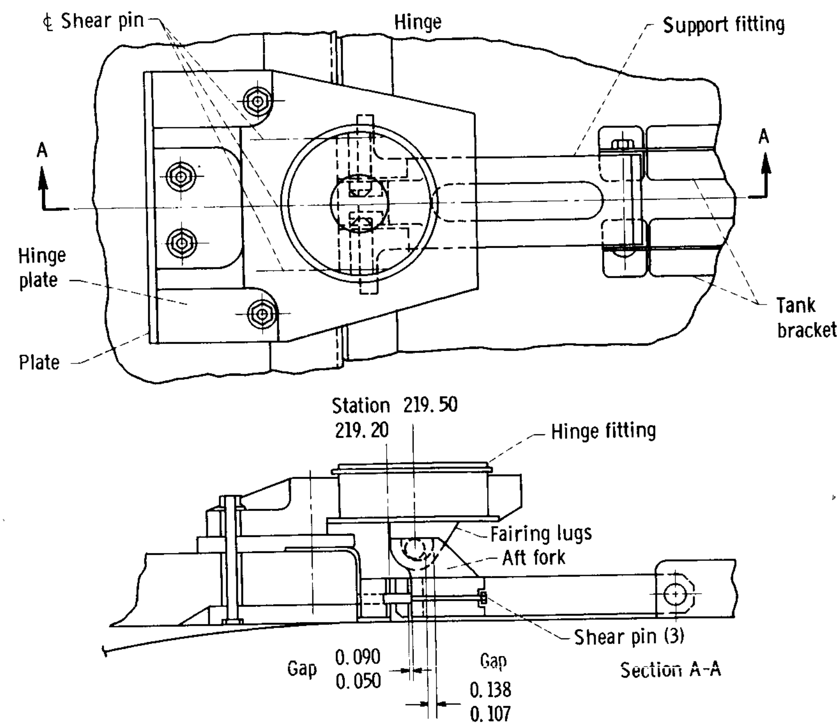

Figure X-13. - Details of nose-fairing-jettison hinge.

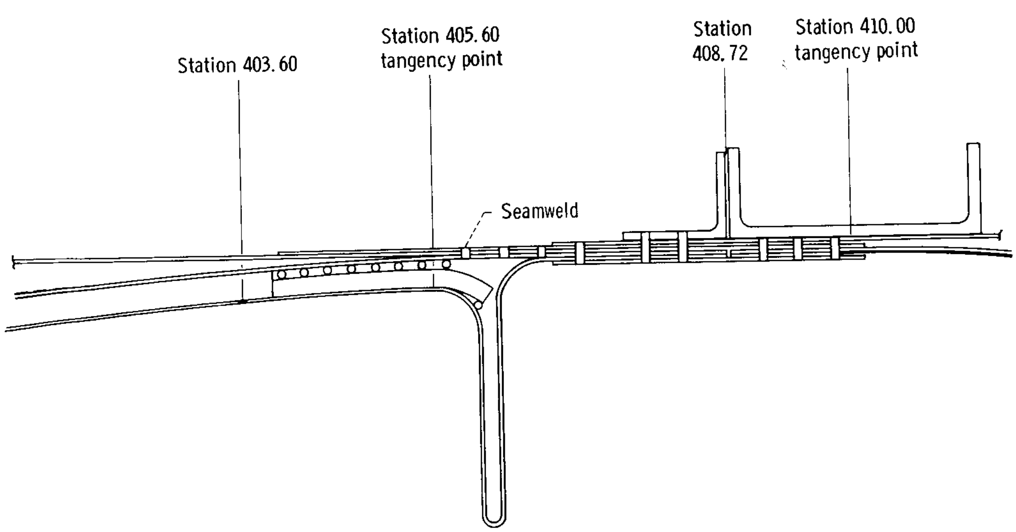

Figure X-14. - Details of station 408 joint of AC-4 vehicle.

[redacted]

[redacted]

XI. VEHICLE MODAL BENDING DYNAMICS AND VIBRATIONS

SUMMARY

During the booster phase of flight from launch to BECO, bending-mode oscillations were quite low in magnitude and, as in the AC-3 flight, this flight was relatively "quiet." Longitudinal and lateral oscillatory motions were similar to those in AC-3 except that second-mode lateral motions were prominent during the early booster phase of flight. Longitudinal frequencies at this time were of the same nominal values. Shortly after lift-off and also during MECO transient a brief-duration excitation occurred in the payload area.

The vibrational environment of the AC-4 flight, as monitored by 23 accelerometers (fig. XI-1), was similar to both AC-2 and AC-3 (table XI-I) and was well within design proof test levels. In general, the largest vibrations occurred either at lift-off or during the transonic region (50 to 80 sec after launch).

MODAL BENDING DYNAMICS

Longitudinal and lateral low-frequency oscillations during the booster phase of flight (launch to BECO) were of low amplitude and were comparable to those experienced on AC-3. Second-mode bending was most prevalent during the first half of booster phase and first-mode bending during the second half.

Three occurrences of longitudinal excitation were evident from the Atlas axial accelerometer (AA165φ), and were similar to excitations encountered on flights AC-2 and AC-3, as shown in figure XI-2. Lift-off perturbations resulting from Atlas LOX pressurization instability occurred at launch and decayed by approximately T + 12 seconds. The oscillatory frequency was 6 cps with a maximum of 0.15 g single amplitude near launch. The duration, frequency, and amplitude compare closely with the values from AC-2 and AC-3. "Pogo" type oscillations occurred several times from mid-booster phase to BECO with the frequency varying from 11.5 to 12 cps and a maximum single amplitude of 0.12 g. AA165φ indicated "pogo" from T + 80 to T + 92, T + 134 to T + 136, and T + 146 seconds to BECO. A 0.1-second-duration engine cutoff transient immediately after BECO was evident from the data that indicated an amplitude of 1.5 g's from zero to peak at a nominal frequency of 90 cps. The Atlas roll-rate gyro measurement (AS52R) showed this excitation at the same frequency.

Lateral modal bending was of very moderate magnitude being less, in general, then that on the AC-3 flight. First and second modal frequencies were of a higher value than those predicted by the GD/A analytical model. A comparison is shown in figure XI-3 including plots of data from Lewis Research Center vibration facility tests on an Atlas-Centaur vehicle. As shown, the flight data

[redacted]

more closely duplicate the vibration facility test frequencies than the predicted frequencies. The first mode is approximately 1/2 cps higher and the second mode $1\frac{1}{2}$ cps higher than the predicted modal frequencies. The lateral accelerometer measurements (CA8φ and CA10φ), the Centaur rate gyro measurements (CS70R, CS71R, CS69R, and CS73R)and, where applicable, the Atlas rate gyro measurements (AS53R and AS54R) indicated approximately the same frequencies at comparable flight times thereby adding confidence to the values.

The amplitudes of first modal bending were obtained by reduction of Centaur rate gyro data. Figures XI-4(a) and (b) show these amplitudes for pitch and yaw, respectively. Predicted mode shapes are shown normalized to the amplitudes measured by the rate gyros located at station 173. The gust design criteria at station 173 for T + 40 and T + 80 seconds are also plotted with the predicted mode shapes normalized to these criteria. Flight amplitudes are seen to be quite low and but a fraction of the design criteria. In figure XI-5, both first and second modal amplitudes from the flight data are shown as well as gust design criteria for several flight times. Second modal amplitudes are seen to be well below the design levels. Figure XI-6 depicts maximum first modal elastic bending amplitudes at station 173 for AC-2, AC-3, and AC-4. The AC-4 amplitudes are generally of smaller value or nonexistent.

At approximately T + 0.5 second, one cycle of 1.1-g (P-P) oscillation (at 6.5 cps) occurred at the forward end of Centaur (station 173), as indicated by the lateral accelerometer pitch plane measurement (CA8φ). The retromotor mass measurement (CY72φ, station 116) indicated a 2.6-g (P-P) excitation in the payload mass area at the same time increment. These amplitudes fit the second mode shape as defined by the Lewis vibration facility test data. To date, no event or disturbance has been uncovered that might have caused this perturbation.

At MECO, as a result of engine shutdown transients, the payload area experienced a longitudinal oscillatory motion with a relatively high negative load. The disturbance started at MECO and lasted for 1/3 second with a frequency of 28.5 cps. Strain gages CA491S (0°), CA492S (120°), and CA493S (240°) gave the best indication of the amplitude of this disturbance and showed negative g values (zero to peak) of approximately 1.5, 1.6, and 1.6, respectively. The longitudinal accelerometers located in the payload area failed to indicate this disturbance because of time sharing. Also, the Centaur axial accelerometer (CM101A) failed to verify it because of the low-frequency response of the transducer.

VIBRATIONS

Maximum Vibrations

The vibration environment of the AC-4 flight, as monitored by 23 accelerometers (fig. XI-1), was similar to both AC-2 and AC-3 (table XI-I) and was well within design proof test levels. In general, the largest vibrations occurred either at launch or during the transonic region (50 to 80 sec after launch).

The largest vibrations (table XI-II) occurred in the interstage adapter during the transonic portion of flight. Measurement of panel radial acceleration (AA164φ) indicated 96.5 g's peak to peak (P-P) after 61.4 seconds of flight. The largest vibration in the propulsion area was measured on the boost-pump fairing, station 407 (CA398φ), at 91.6 seconds, where the peak to peak value was 13.9 g's. The wire tunnel, station 223.5 (CA392φ), indicated the largest vibration in the equipment area, 24.9 g's P-P at 79.5 seconds in the transonic region.

During launch, the payload experienced its maximum vibration (table XI-II). At T + 1.4 seconds, the transducer located at the top of mast sensing in the y-direction (CY75φ) indicated 15.0 g's P-P at a frequency of 6.3 cps. The maximum vibration level of the lower end of the payload was also in the y-direction CY72φ (retromotor mass y) indicated 2.64 g's P-P at a frequency that was approximately the second mode natural frequency: this occurred after 0.47 second of flight.

Vibration Profile

A spectrum analysis (Bruel and Kjaer one-third octave analyzer) was performed on the vibration accelerometer data to determine the frequencies of maximum energy concentration (the analysis frequency ranged from 40 cps to the upper frequency band of the data channel, or 2000 cps, depending on which was lower).

The vibration environment of the interstage adapter was predominately sinusoidal with a maximum energy concentration of 0.2 g^2/cps and a frequency of 50 cps. There were other predominant sinusoids at both 200 and 1000 cps (fig. XI-7). In the propulsion area (fig. XI-7(b)) the largest energy concentration was experienced by the C-2 hydraulic power package y-axis a few seconds after first main engine start of the Centaur (0.0175 g^2/cps at a frequency of 800 cps). In general, the vibration profile in this area was predominately random with sinusoids at only a few discrete frequencies. The Centaur equipment area vibration profile (fig. XI-7(c)) was predominately random with the largest energy concentration (0.13 g^2/cps at 300 to 400 cps) evidenced at maximum q by the wire tunnel at station 223.5 (CA392φ).

[redacted]

TABLE XI-I. - COMPARISON OF AC-3 AND AC-4 MAXIMUM VIBRATIONS

Location	Measurement	AC-3 g's, P-P	Time, sec	Event	AC-4 g's, P-P	Time, sec	Event
Battery mounting x-axis	CA26φ	3.4	216.6 to 217.6	Nose-fairing jettison	5.5	226.6 to 227.6	------------
Near A/P gyro package z-axis	CA27φ	1.2	87.4 to 90.4	Transonic	1.83	211.5 to 212.5	Nose-fairing jettison
Umbilical island accelerometer S/94 Q_1	CA343φ	8.56	54.1 to 55.1	Transonic	5.6	211.4 to 212.4	Nose-fairing jettison
Adapter radial Q_1 and Q_2	AA161φ	42.8	20.6 to 21.6	Lift-off	28.4	151.7 to 152.7	Booster jettison
Panel radial Q_2 and Q_3	AA164φ	34.4	86.8 to 87.6	------------	96.5	61.4 to 62.4	Transonic

[redacted]

[redacted]

TABLE XI-II. - MAXIMUM VIBRATIONS

Location	Measurement	Time, sec	Maximum g's P-P	Frequency band of data channel, cps	Comments
Interstage adapter z-axis	AA165φ	151.8 to 152.8	8.95	0 to 45	56.5 cps
Equipment located on interstage adapter (radial)					
Q_1 and Q_2	AA161φ	151.7 to 152.7	28.9	0 to 220	Booster jettison; high frequency
Q_2 and Q_3	AA162φ	Only visible deflection was at A-C separation		0 to 1200	Short burp, mostly noise
Ring Q_1 and Q_4	AA163φ	Signal level too low		0 to 1200	
Panel radial Q_2 and Q_3	AA164φ	61.4 to 62.4	96.5	0 to 2000	High frequency, transonic region
Propulsion area					
C-1 gimbal mounting	CA31φ	47.6 to 48.6	1.88	0 to 1000	Data channel lost at T = 238.8 sec
C-2 hydraulic power package z-axis	CH101φ	339.1 to 340.1	13.8	0 to 800	
C-1 hydraulic power package y-axis	CH132φ	432.1 to 433.1	7.35	0 to 600	MES + 2 sec
C-2 hydraulic power package y-axis	CH133φ	237.7 to 238.7	9.13	0 to 800	
Boost-pump fairing S407 12R	CA398φ	91.6 to 92.6	13.90	0 to 600	Transonic region
LH_2 duct near y-section	CA601φ	58.4 to 59.4	3.81	0 to 1000	
LOX boost-pump flange	CP556φ	504.8 to 505.8	4.42	0 to 1000	
Equipment area					
Battery mounting x-axis	CA26φ	226.6 to 227.6	5.5	0 to 1000	Nose-fairing jettison, 40 cps
Near A/P gyro package z-axis	CA27φ	211.5 to 212.5	1.83	0 to 1000	Short burp lasted 0.05 sec
Guidance platform y-axis 40°	CA89φ	206.8 to 207.8	1.96	0 to 1000	
Umbilical island accelerometer S194 Q_1	CA343φ	211.4 to 212.4	5.6	0 to 600	
Wire tunnel accelerometer S223.5	CA392φ	79.5 to 80.5	24.9	0 to 600	Transonic region
Payload ring S130/120	CA459φ	198.5 to 199.5	13.48	0 to 220	Excessive cross talk on data channel
LH_2 boil-off valve	CA265φ	91.7 to 92.7	6.28	0 to 600	
Payload					
Retromotor mast x-direction	CY71φ	212.4 to 213.4	1.15	0 to 450	25.0 cps, nose-fairing jettison
Retromotor mast y-direction	CY72φ	.5 to 1.5	2.64	0 to 450	7.7 cps, launch
Top of mast x-direction	CY74φ	92.9 to 93.9	7.5	0 to 45	6.21 cps
Top of mast y-direction	CY75φ	1.5 to 2.5	15.0	0 to 160	6.3 cps, launch

[redacted]

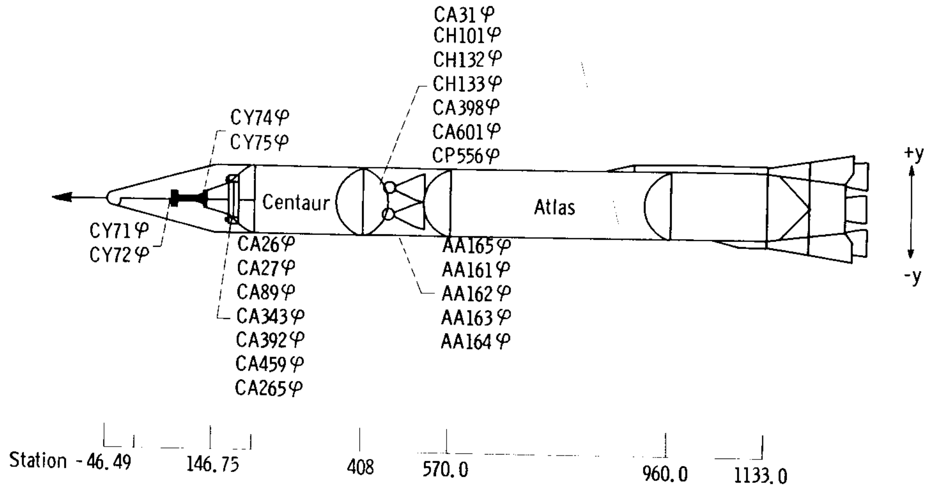

Figure XI-1. - Vibration accelerometer location.

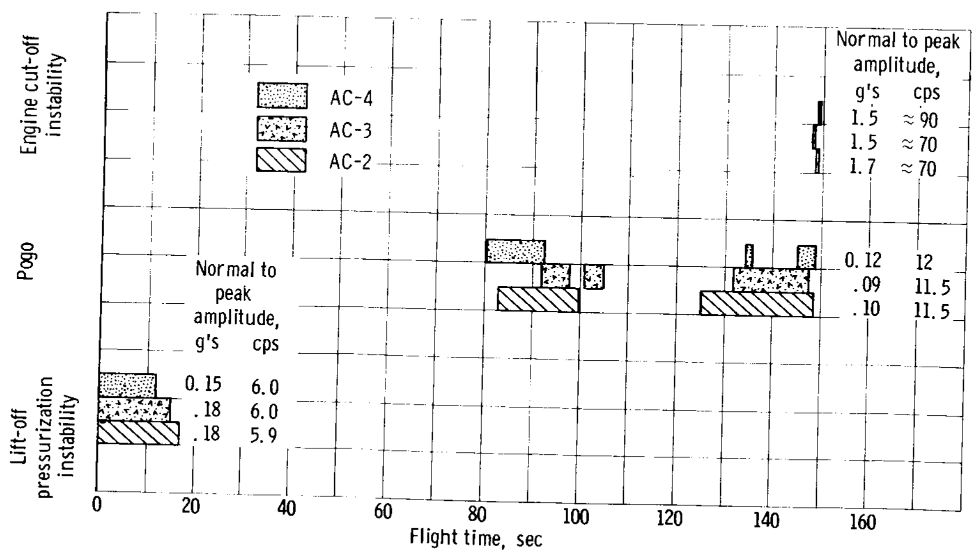

Figure XI-2. - Longitudinal oscillation occurrences, frequencies, and maximum amplitudes.

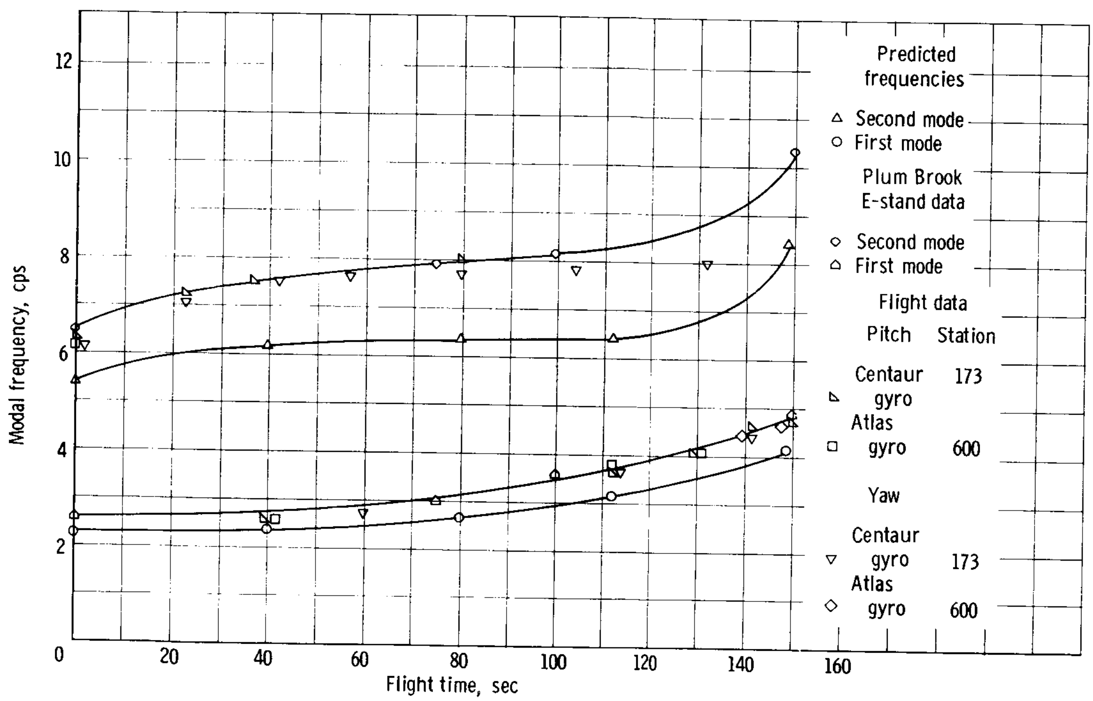

Figure XI-3. - Predicted, experimental, and flight data lateral modal frequencies for AC-4 Atlas-Centaur elastic bending.

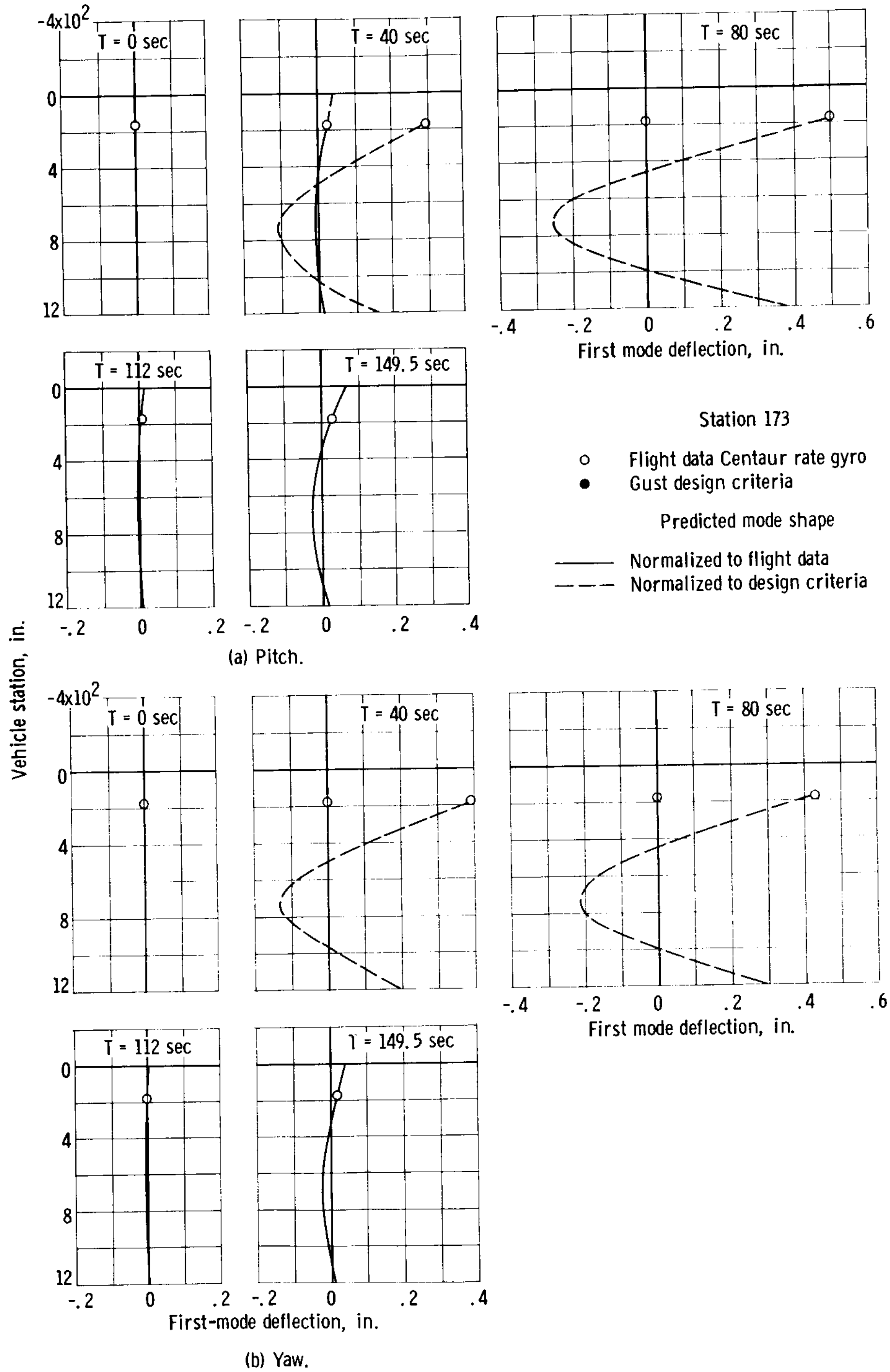

Figure XI-4. - Flight and design wind-gust lateral bending modal amplitudes.

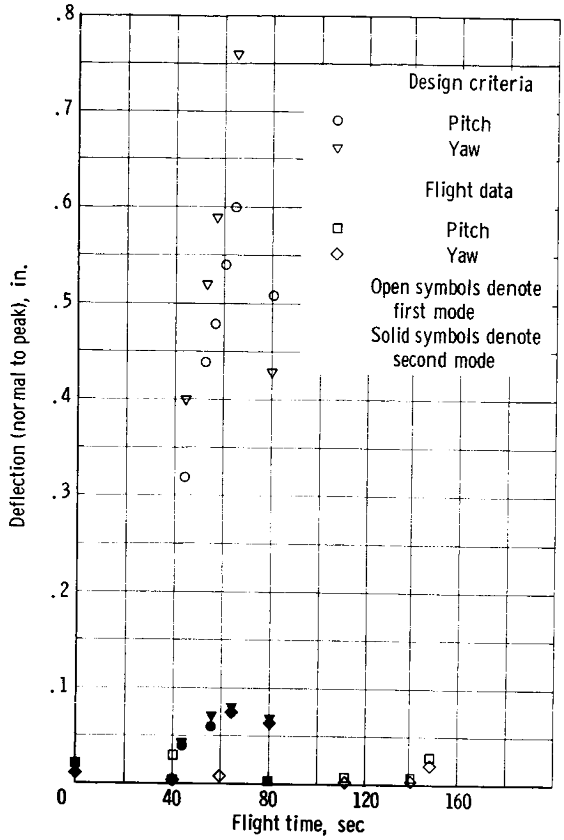

Figure XI-5. - Flight data and design criteria for wind-gust modal amplitudes pitch and yaw planes at station 173.

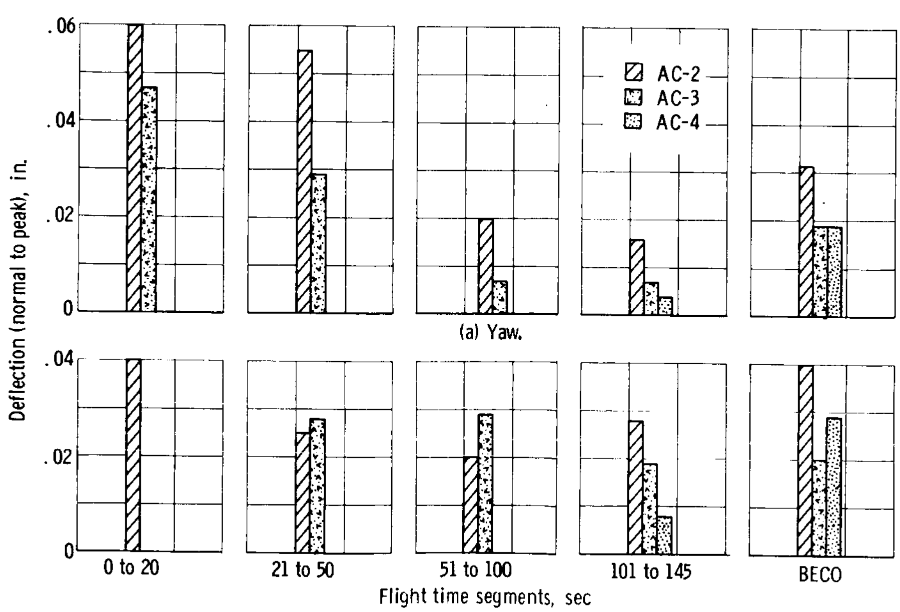

(b) Pitch.

Figure XI-6. - Maximum first modal amplitudes at station 173 for AC-2, AC-3, and AC-4.

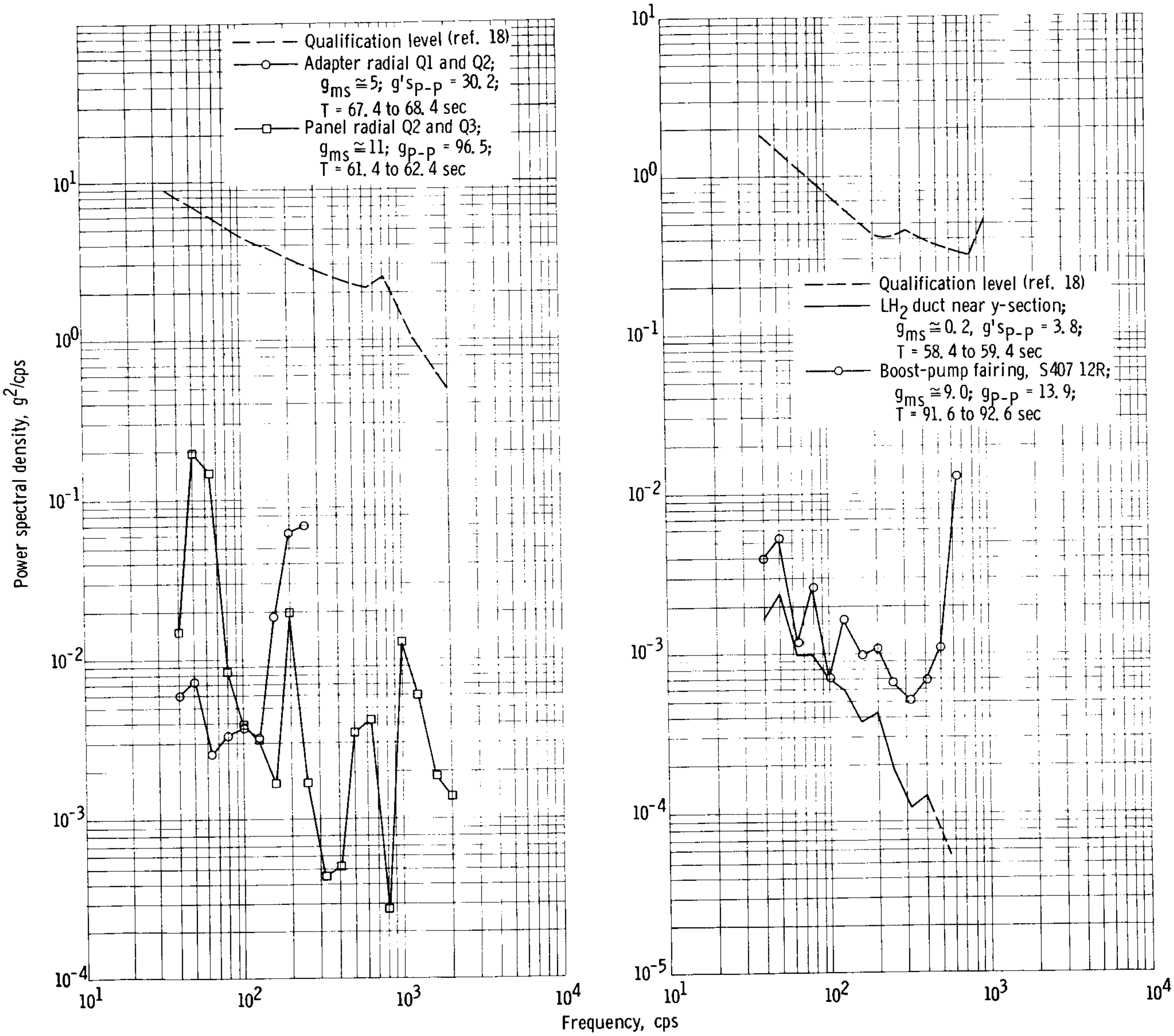

(a) Interstage adapter (radial).

(b-1) Propulsion area.

Figure XI-7. - AC-4 vibration levels.

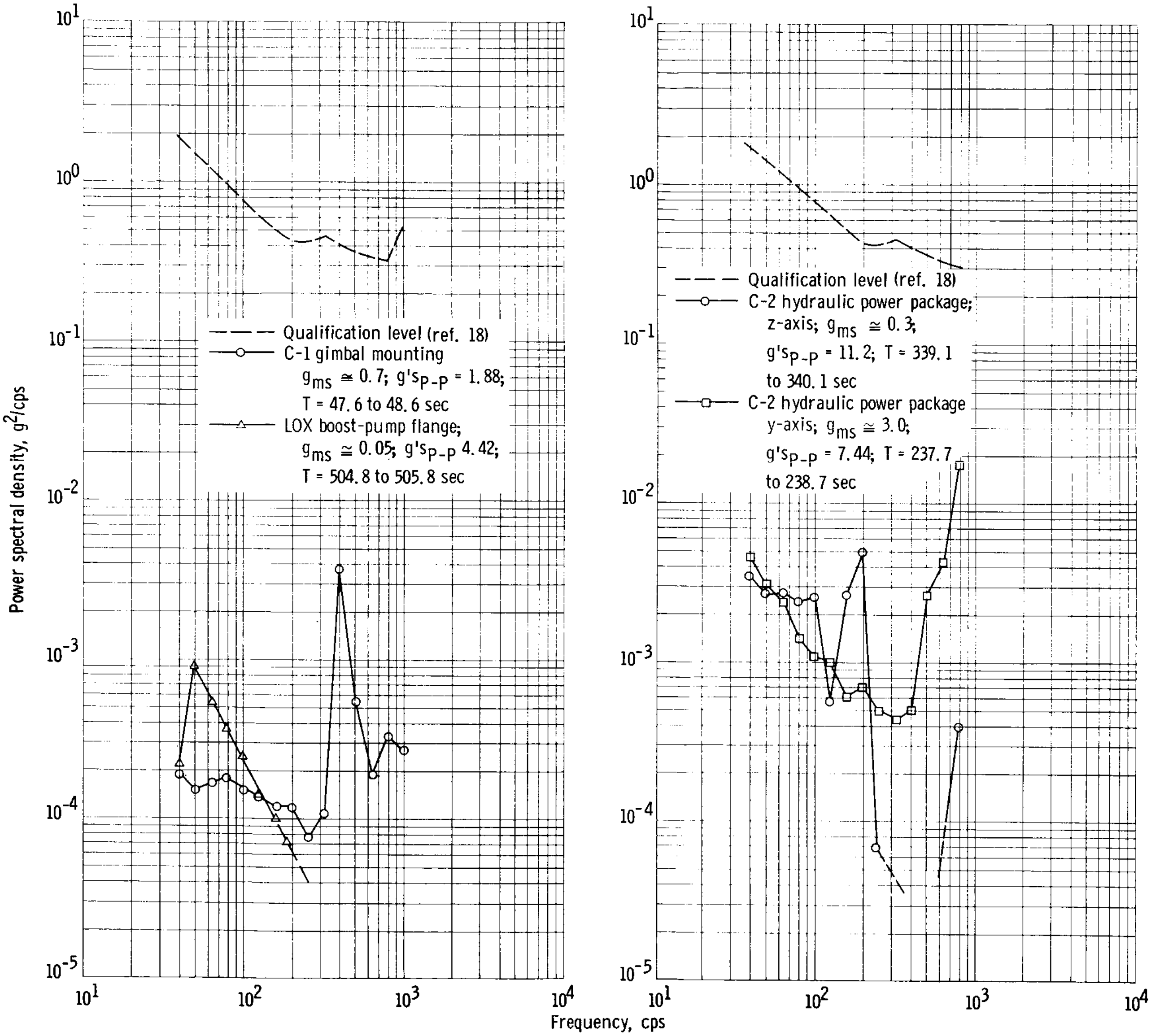

(b-2) Propulsion area.

(b-3) Propulsion area.

Figure XI-7. - Continued.

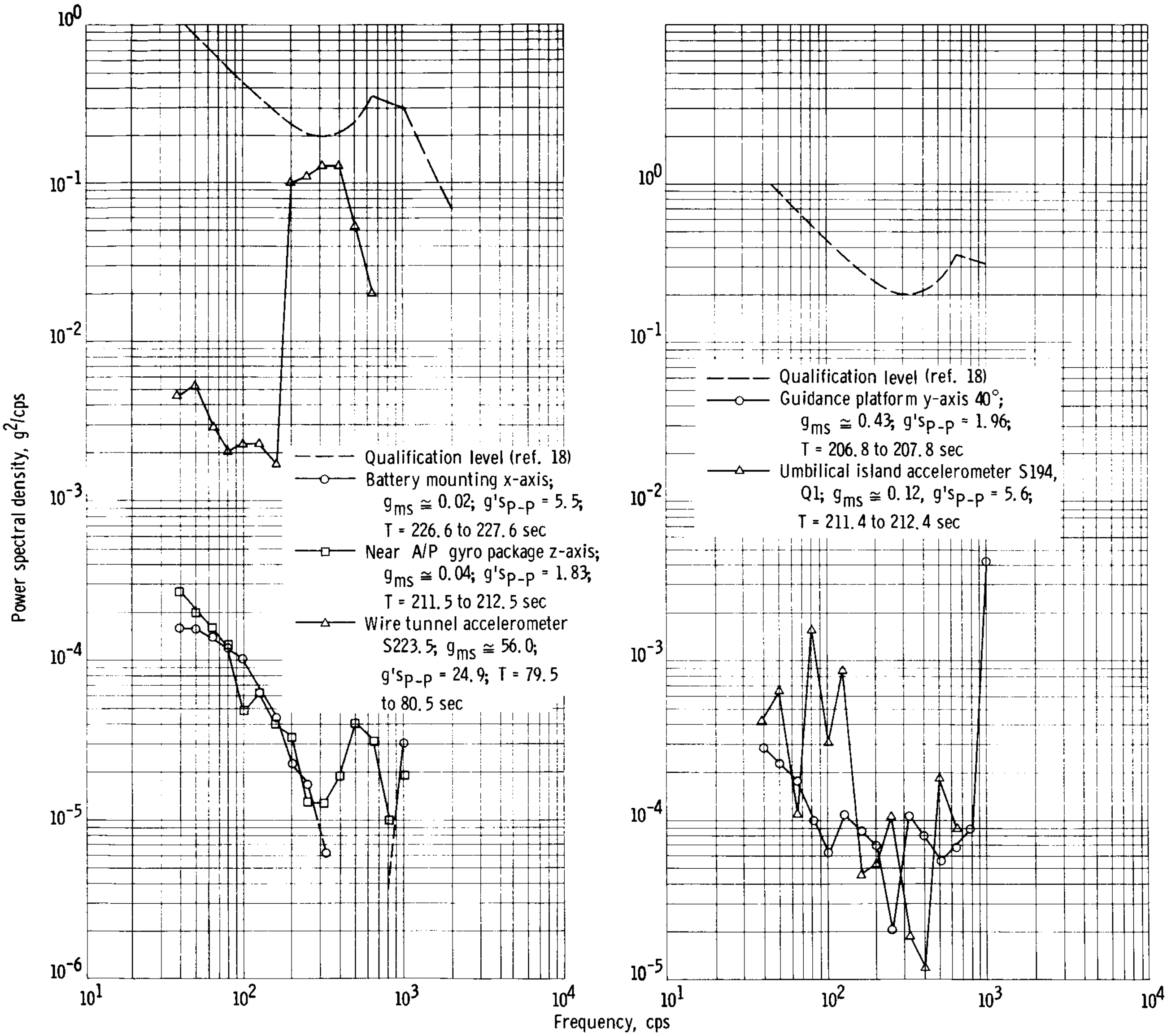

(c-1) Centaur equipment area.

(c-2) Centaur equipment area.

Figure XI-7. - Continued.

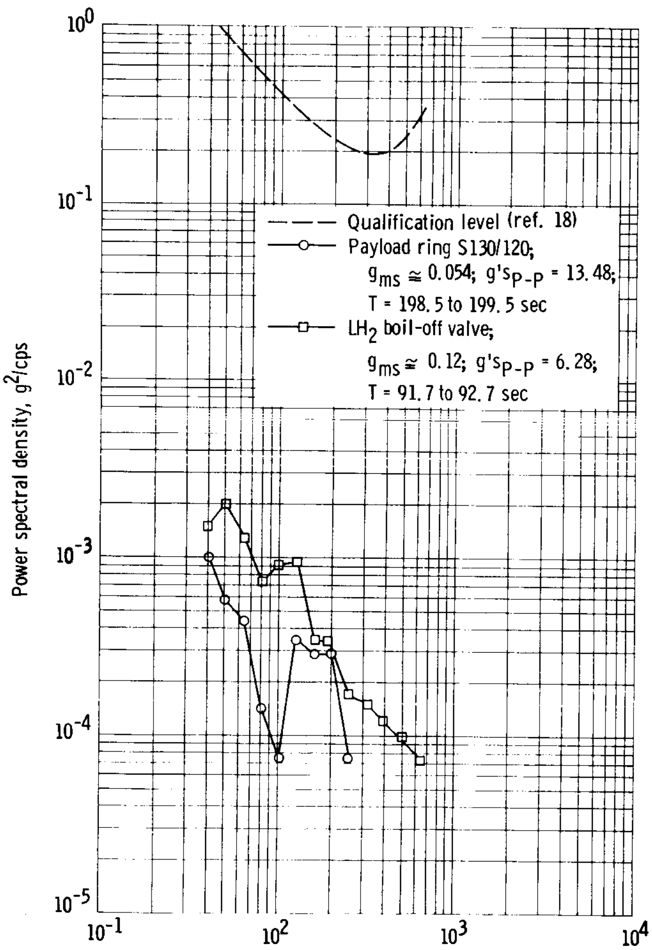

(c-3) Centaur equipment area.

Figure XI-7. - Concluded.

[redacted]

XII. FLIGHT CONTROL SYSTEM

SUMMARY

Analysis of telemetry data indicated that AC-4 control system performance was satisfactory until T + 840 seconds at the start of LH_2 venting during the first coast period. Observed responses during Atlas boost and Centaur first burn followed closely predicted limit cycle frequencies and amplitudes.

ATLAS

At lift-off, a high-frequency vibration near the natural frequency of the second bending mode (35 rad/sec) was observed in both pitch- and yaw-rate gyros. Peak-to-peak amplitudes averaged 0.1 degree per second in both planes and decayed in approximately 2 seconds after lift-off. Similar oscillations were observed on the AC-3 flight.

Following lift-off, the Atlas booster flight was smooth through the entire atmospheric ascent. No transients or oscillations of unusual magnitude were observed from telemetry until BECO when the Atlas roll- and pitch-rate gyros showed a diverging oscillation at the limit cycle frequency of the Atlas LOX sloshing mode. The diverging oscillation started at approximately 7 seconds prior to BECO, reaching peak-to-peak rates of 3.47 degrees per second in roll and 1.18 degrees per second in pitch at a frequency of 1.6 cps as telemetered from the Atlas rate gyros. These oscillations discontinued with the initiation of BECO. Figure XII-1 shows the time history of the vehicle responses at BECO.

Root locus analysis had predicted a stable limit cycle for the Atlas LOX sloshing mode prior to BECO. The engine limit cycle amplitude from analysis is approximately 0.82 degree peak-to-peak. Figure XII-1 shows the booster 1 and 2 engines at a maximum peak-to-peak amplitude of 0.9 and 1.3 degrees, respectively. A similar divergence had occurred on AC-3, although amplitudes were smaller. The coupling into the roll plane, however, had not been predicted by analysis. Figure XII-2 shows a comparison of AC-3 and AC-4 roll rates as measured by the Centaur roll-rate gyros. Prior to BECO, the primary difference in the autopilot configuration is the nominal operating gain (K_a) of 1.0 degree per degree; an increase of approximately 15 percent over the AC-3 position gain of 0.87 degree per degree. Consequently, larger amplitudes were to be expected over AC-3 responses. The following table shows a comparison of autopilot, engine, and sloshing parameters for AC-3 and AC-4.

[redacted]

Parameter	AC-3	AC-4
BECO (discrete), sec	147.8	148.3
Position gain, K_a, deg/deg	.87	1.0
Engine limit cycle amplitude (peak-to-peak), δ, deg	.70	.82
Atlas LOX limit cycle frequency, $\omega_{A\text{-}LOX}$, cps	1.6	1.6

The physical inertial properties of the vehicle show that pitch oscillations have a strong tendency to couple in roll. No diverging oscillations were observed which indicates booster engines gimbaling differentially (the primary source of booster-phase roll control). The booster engines, however, are complemented by a sensitive vernier roll-control moment that effectively reduces roll-limit-cycle amplitudes caused by booster-engine dead zones. Also, roll signals into the booster vernier engines are not led through an integrator-filtered feedback network. As a result, the unsymmetrical autopilot configuration tends to null out small oscillations in roll with the vernier engines.

Attempts to duplicate the diverging oscillations at BECO on the GD/A six-degree-of-freedom analog simulation using nominal control gains and filter failed to show the type of responses observed from telemetered data. It was possible, however, to determine the control gains and filter required to obtain the diverging oscillation: (1) position gain, 115 percent of nominal; (2) rate gain, 126.5 percent of nominal; (3) filter, approximately 85 percent of nominal. Analog runs with these gains showed good correlation with test data, both in amplitude and frequency. Figure XII-3 shows the roll, pitch, and yaw rates that are directly comparable with those of telemetered data.

There appears to be no single cause for the diverging oscillation. Possible sources of gain and filter variations are (1) autopilot tolerances, (2) increased acceleration, which can be interpreted as a direct increase in static gain, (3) increases in the Atlas inverter frequency, and (4) unknown engine gimbal friction that determines engine dead-zone deflections.

Following BECO, telemetry shows small oscillations in rigid-body first-modal bending and Atlas LOX sloshing. Jettison of the insulation panels and the nose fairing excited the first bending mode as observed from the Centaur yaw-rate gyros. Peak-to-peak amplitudes were very small (0.1 deg/sec), thus, no oscillations were observed in pitch. Figure XII-4 shows a plot of predicted and flight test frequencies from lift-off to SECO. The predicted frequencies are limit-cycle frequencies as calculated by time-slice studies using root-locus techniques. Flight test frequencies are those observed from telemetry of yaw- and pitch-rate-gyro outputs.

CENTAUR

The observed ignition transient was the smallest recorded to date (see fig.

[redacted]

XII-5), indicating small differential thrust buildup of the RL-10 engines. Observed rates were 0.38 degree per second yaw, 1.02 degrees per second pitch, and 1.17 degrees per second roll. Centaur powered history was smooth, and no significant oscillations occurred during the remainder of the flight. From the Centaur rate gyros, frequency data were obtained and plotted with predicted frequencies against flight time. Figure XII-4 shows the good correlations between the predicted and flight test data.

The coast phase followed first MECO and was to terminate approximately 1477 seconds later with the initiation of second MES. The coast-phase attitude control system maintains an attitude reference that is alined with the local horizontal and in the plane of the trajectory, but allows roll drift to a threshold.

Telemetry showed that the vehicle was maintaining its attitude as commanded with sporadic corrections in pitch and roll, and a nearly constant 30-percent duty cycle in yaw until T + 840 seconds when venting forces exceeded the capability of the attitude control engines (see fig. VI-20).

Failure of the ullage rocket to settle the propellant and the subsequent venting of liquid and gaseous mixtures of LH_2 coupled with the large buildup of rotational rates and decline of fuel tank pressure, starved the fuel boost pump, aborting the second MES.

Temperature transducers at the forward bulkhead indicated wet immediately following MECO and continued to remain wet for the remainder of controlled coast (see section VII. CENTAUR PROPELLANT SYSTEMS). This indicated that the axial accelerations imparted to the vehicle by the forces of the two ullage rockets were insufficient to settle and maintain the propellants during the controlled coast period.

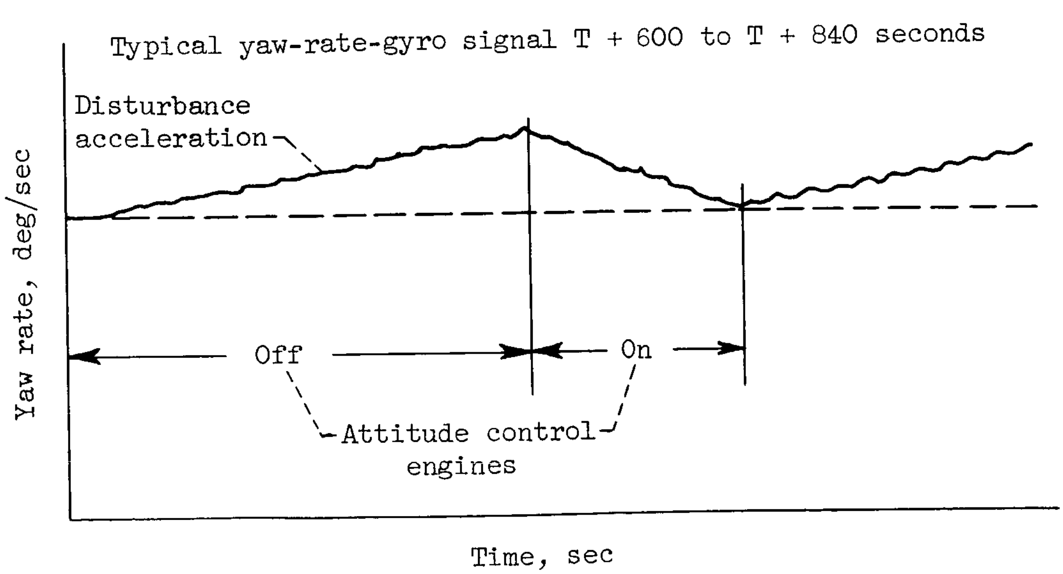

(a)

[redacted]

To obtain some indication as to the behavior of the propellants prior to venting, the yaw-rate-gyro signal was analyzed, since it showed a regular "on-off" pattern of the attitude control engines. The preceding sketch shows the rate-gyro pattern observed from telemetry. The disturbance acceleration, defined as the slope of the curve where the attitude control engines are off, is an indication of the disturbance torques acting on the vehicle. Major sources of these torques are

(1) Ullage jet thrust misalinement

(2) Ullage jet impingement against the main engine bells

(3) Center of gravity offsets caused by propellant motion

Figure XII-6 shows the disturbance accelerations from approximately 100 seconds prior to LH_2 venting. A nearly constant disturbance acceleration is noted averaging 0.012 degree per second squared. This results in disturbance torques of 8.4 to 9.4 foot-pounds depending on the mass moment of inertia. Ullage jet thrust misalinements and impingement can account only for 5 foot-pounds of torque. Lateral center-of-gravity offset from the longitudinal axis is the only major contributing source of torque remaining. In figure XII-7 a curve relates center-of-gravity offset with ullage jet impingement forces. Analysis has shown that impingement forces are of the order of 0.26 pound. From figure XII-7 this results in center-of-gravity offsets averaging 12 inches. This is the center-of-gravity offset in the yaw plane on an axis toward the boost pump.

The relation between center-of-gravity location and mass moment of inertia as calculated from the vehicle dynamics and from the vehicle mass properties is shown in figure XII-8. No physical significance is meant to be given by the curve drawn through the points that relates center of gravity and moment of inertia by mass properties. Actually, several other points could be calculated by assuming other propellant locations that would not fall on a line between an empty vehicle case and a propellant settled and rigid case. The figure does show, however, the center of gravity and mass moment of inertia relation that must have existed to obtain the vehicle dynamics observed from telemetry. Venting force calculations using the range of center-of-gravity location and mass moment of inertia shown in figure XII-8 indicated forces between 8 and 10 pounds were acting on the vehicle.

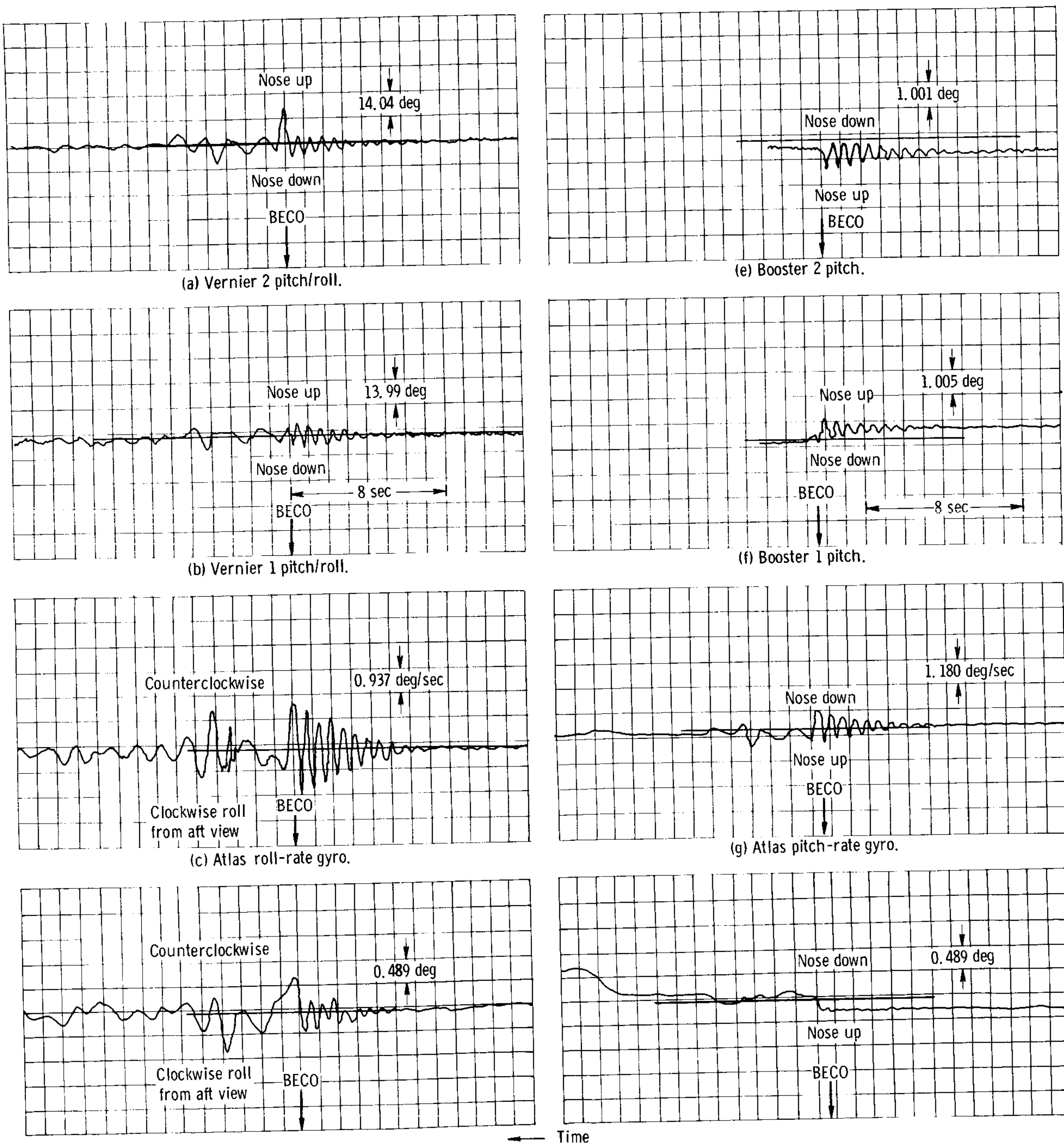

(a) Vernier 2 pitch/roll.

(b) Vernier 1 pitch/roll.

(c) Atlas roll-rate gyro.

(d) Atlas roll-displacement gyro.

(e) Booster 2 pitch.

(f) Booster 1 pitch.

(g) Atlas pitch-rate gyro.

(h) Atlas pitch-displacement gyro.

Figure XII-1. - AC-4 responses at BECO.

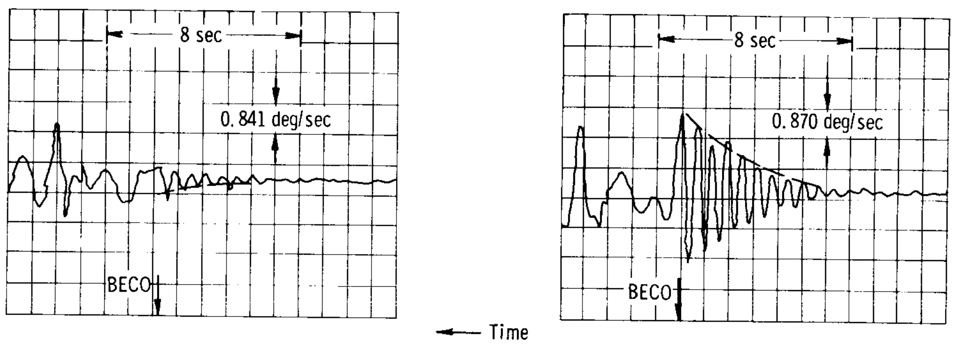

(a) AC-3.

(b) AC-4.

Figure XII-2. - Comparison of AC-3 and AC-4 roll rates at BECO measured by Centaur roll-rate gyro.

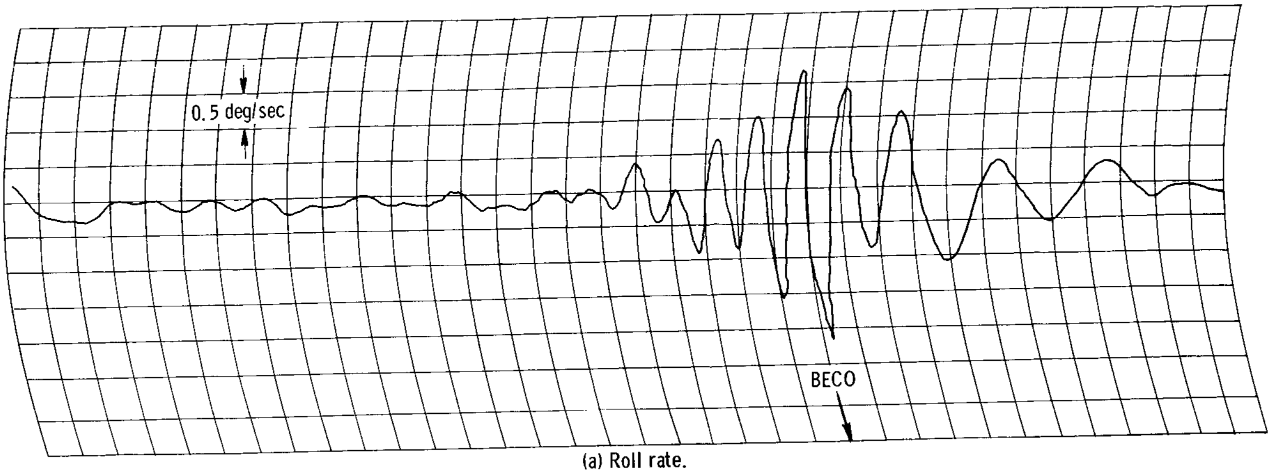

(a) Roll rate.

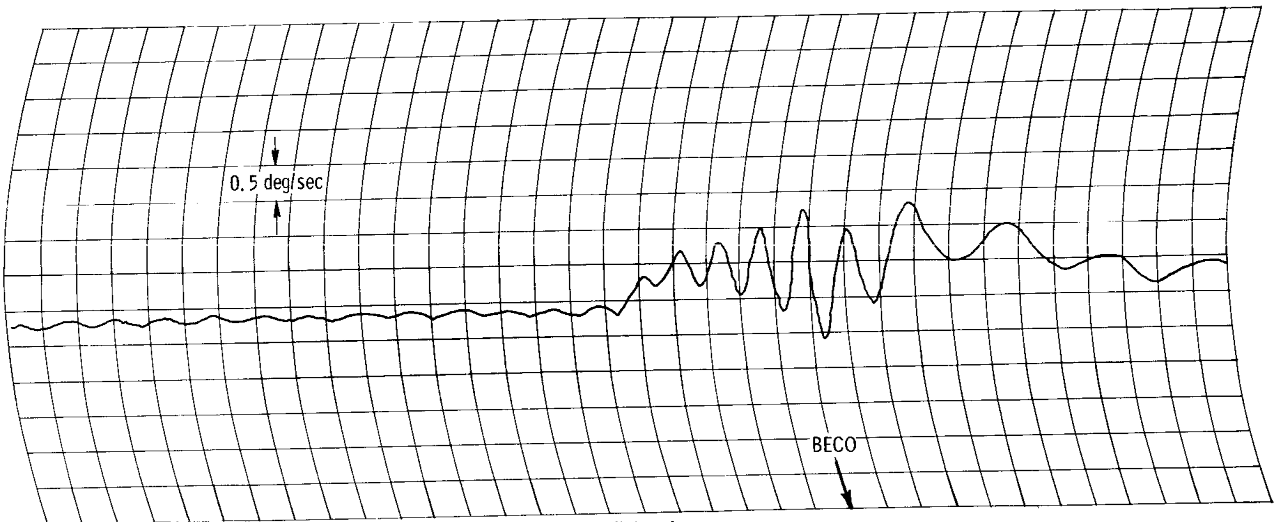

(b) Pitch rate.

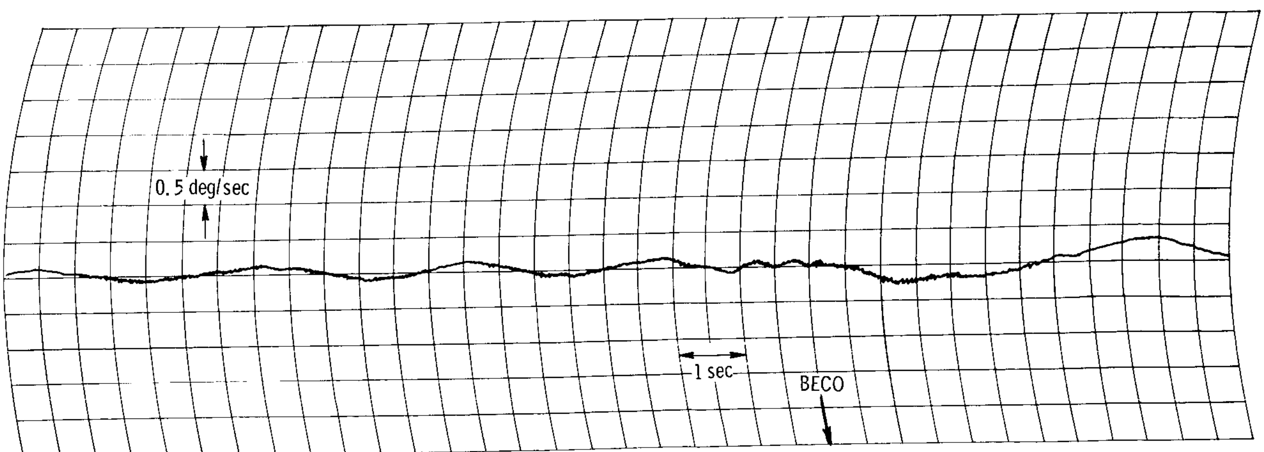

Time, sec →

(c) Yaw rate.

Figure XII-3. - Analog simulation outputs at BECO.

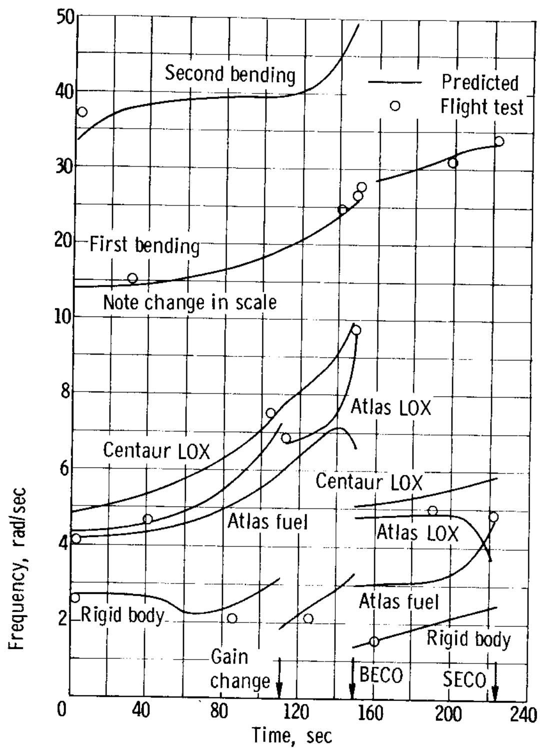

(a) Atlas.

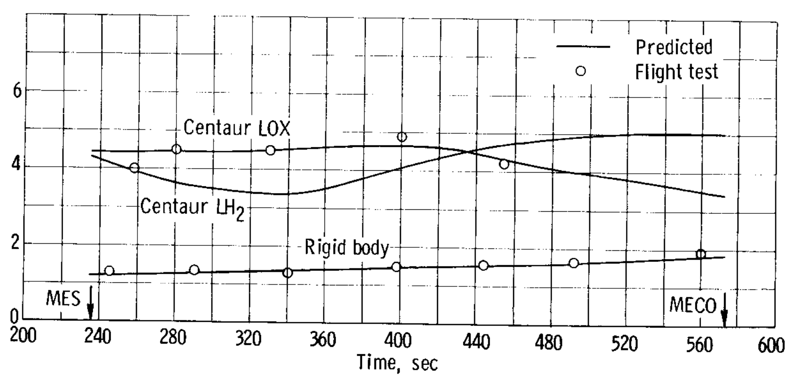

(b) Centaur.

Figure XII-4. - AC-4 Predicted and flight test frequencies during powered flight.

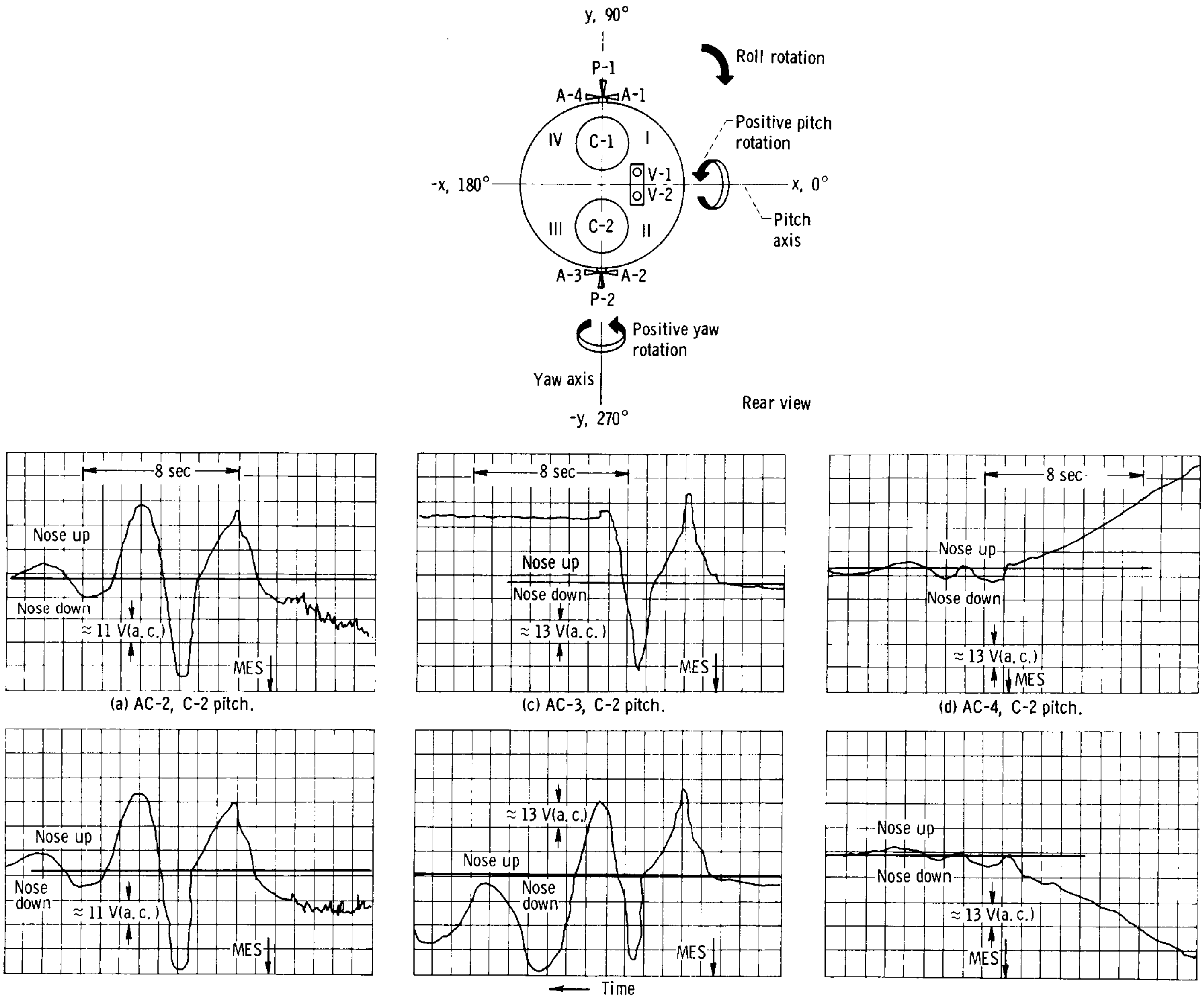

(a) AC-2, C-2 pitch.

(c) AC-3, C-2 pitch.

(d) AC-4, C-2 pitch.

(b) AC-2, C-1 pitch.

(d) AC-3, C-1 pitch.

(f) AC-4, C-1 pitch.

Figure XII-5. - Comparison of Centaur pitch-engine deflections as MES.

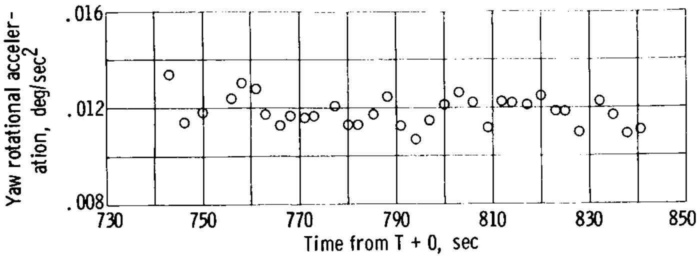

Figure XII-6. - Yaw rotational accelerations as function of time. Accelerations were measured with attitude engines off.

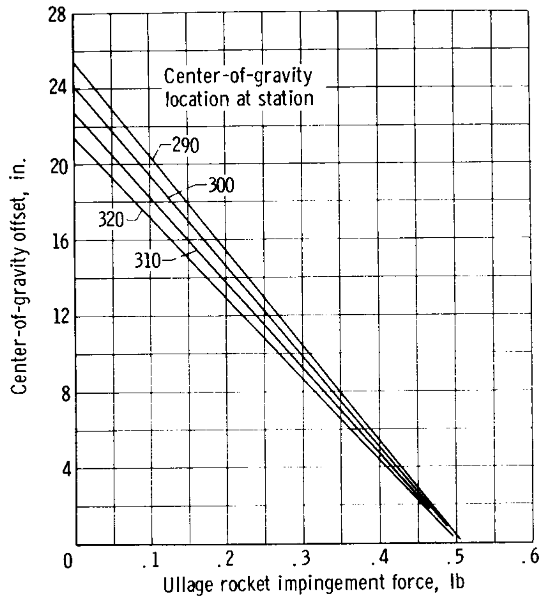

Figure XII-7. - Center-of-gravity offset determination as function of ullage rocket impingement.

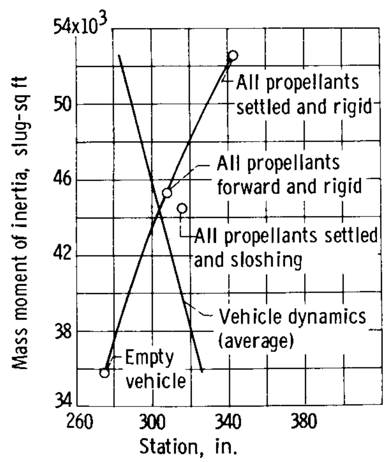

Figure XII-8. - Mass moment of inertia and center-of-gravity determination at time 14:38:00 (midcoast).

XIII. GUIDANCE

SUMMARY

The Centaur inertial guidance system performed satisfactorily throughout the prelaunch countdown and the flight with the velocity errors, shown in the following table, extrapolated to burnout (T + 580 sec).

Axis	Velocity error, ft/sec	Nominal specification value, ft/sec
U	0.5	<12
V	1.0	<23
W	7.0	<12

Figure XIII-1 shows a comparison of guidance minus BET velocity (ref. 19). A block diagram of the Centaur inertial guidance system is shown in figure XIII-2.

A discrepancy existed, however, between telemetered computer digital torquing command for the W-gyro and the analog output of this signal. From analysis of the guidance system velocity comparisons, it is concluded that the telemetered analog data were not a valid indication of the gyro torquing rate.

PERFORMANCE

Prelaunch Countdown

The Centaur inertial guidance system MGS 24 (table XIII-I) was calibrated on F - 1 day to verify parameter stability. Power was applied to the system throughout the night to ensure continued parameter stability (preclude any shut-down transient effects). On F - 0 (launch) day the system was again calibrated. Shifts in the critical gyro and accelerometer loop parameters were well within the specification limits.

The guidance countdown was normal until T - 90 minutes, when a momentary dropout of inverter power occurred during a Centaur power changeover. The guidance computer storage (D and J values) was read out to ensure that there had been no change. To verify that the power interruption had not affected inertial component calibration, the KSC ground computer was used to determine the U- and V-gyro constant torque parameters. These were consistent with previous values. In addition, the W-accelerometer performance stability was indicated by a 10-minute count of acceleration pulses. This also was satisfactory.

Optical azimuth alinement was used for the first time on AC-4. The performance of this system was satisfactory throughout the countdown.

Flight

The guidance system was switched to the "inertial mode" at T - 7.755 seconds. Throughout the early portion of flight, normal response to the rigid body and sloshing frequencies was observed in the gimbal servoloops. The platform (gimbal 4) uncaged at 20° pitch angle (determined by integration of pitch-rate-gyro outputs). The guidance steering loop was closed at BECO + 10 seconds. Resolver chain outputs remained at null through SECO, indicating that the booster was steering to the computed vector. Transients observed on the resolver chain outputs and inputs at T + 224.37 seconds are the results of temporary loss of power to the signal conditioner, which normally occurs when the interstage umbilical is ejected. Since the resolver outputs were near null from MES through MECO, the vehicle continued to follow the computed vector. For computer operation regarding inflight telemetry sequence, discrete issuance, and codeword change times see tables XIII-II to IV.

The only guidance anomaly that occurred during powered flight was a step change in the W-gyro torquing potentiometer voltage (figs. XIII-5) at T + 212.47 seconds. The magnitude of this step change (about 2 percent) is approximately the same as TLM resolution and is believed to be attributable to a malfunction in the W-channel amplifier module in the guidance signal conditioner. The U- and V-gyro torquing traces (figs. XIII-3 and 4) are normal.

Functional Performance

The computer digital steering value minus the telemetered analog value as a function of time is shown in figures XIII-6 to 8. Analysis indicates that this difference was held to zero within instrumentation accuracy. The computer generated missile actual velocity and the missile nominal velocity that was expected to be generated are shown in figures XIII-9 to 11. The guidance computer correctly calculated the missile velocity that closely approximated the nominal expected velocity as a function of time.

Missile position and nominal position are shown in figures XIII-12 to 14. The guidance computer correctly calculated the missile position that closely approximated the nominal expected position as a function of time.

The guidance torque motor inputs shown in figure XIII-15 indicate that nominal performance with no abnormally high transients to the platform existed during the periods of Atlas boost, separation, and Centaur burn. Data recorded after Centaur MECO, during the initial coast, and subsequent vehicle tumbling indicated that the platform was maintaining stability.

Analysis of the resolver chain inputs and outputs (fig. XIII-16) indicates that after BECO (when guidance was admitted for steering) the vehicle followed the steering commands. Nominal transients occurred at BECO, SECO, and MECO.

The guidance system component temperature environment was within the specified range of 30° to 130° F (fig. XIII-17). There was an increase of approximately 25° F in all four units listed from the prelaunch temperatures of 40° to 55° F.

The guidance system platform skin temperature (fig. XIII-18) indicated a normal rise from lift-off to T + 800 seconds, where it appeared to stabilize within 5° for the next 2100 seconds of flight.

CONCLUDING REMARKS

An attempt was made to fit the velocity error curves with the known shapes of several possible sources of system errors. This yielded two solutions, both of which fit the V-error curve extremely well, but varied slightly in the U- and W-fits. Significant portions of inaccurate tracking information contributed largely to the uncertainty between the two solutions. Both solutions contain the identical error sources but differ somewhat in their magnitudes.

	Error source				
	V-gyro constant drift, deg/hr	W-accelerometer misalinement to U, mr	U-accelerometer scale factor, ppm	W-gyro constant drift, deg/hr	V-accelerometer misalinement to W, mr
Inflight shift specifications	0.18	0.75	210	0.36	1.5
Solution:					
1	-0.07	0.16	10	-0.085	-0.24
2	.15	.09	40	.085	.24

From these solutions, it is apparent that both are within the inflight shift specifications.

TABLE XIII-I. - MISSILE GUIDANCE SYSTEM 24

Component	Serial number	Accumulated hours
Platform	G7	1245
Platform Electronics	G8	819
Coupler	G12	556
Computer	007	1997
Signal Conditioner	G8	760

TABLE XIII-II. - AC-4 INFLIGHT TELEMETRY SEQUENCE

Telemetry order	Telemetered parameter		Discrete length (word times)
	Definition	Symbol	
1	Thrust velocity, w-component	v_{tw}	6
2	Time	t_i	8
3	Thrust position, v-component	r_{tv}	8
4	Thrust position, w-component	r_{tw}	8
5	Thrust velocity, u-component	v_{tu}	8
6	Thrust position, u-component	r_{tu}	8
7	Thrust velocity, v-component	v_{tv}	8
8	Inertial position, v-component	r_{mv}	8
9	Inertial position, w-component	r_{mw}	8
10	Codeword	$A_0 \rightarrow A_{24}$	8
11	Inertial position, u-component	r_{mu}	8
12	Inertial velocity, w-component	v_{mw}	8
13	Inertial velocity, v-component	v_{mv}	8
14	Inertial platform torquing rate	ω_{du}	8
15	Inertial platform torquing rate	ω_{dv}	8
16	Inertial platform torquing rate	ω_{dw}	8
17	Square of thrust acceleration[a]	a_{Ti}^2	8
	Energy to be gained[b]	ϵ_i	8
18	Inertial velocity, u-component	v_{mu}	8
19	Steering vector	f_u^*	10
20	Steering vector	f_w^*	10
21	Steering vector	f_v^*	10

[a]Telemetered during booster phase only.

[b]Telemetered during sustainer and Centaur phases only.

TABLE XIII-III. - OUTPUT TIMES AND CRITERIA FOR DISCRETE ISSUANCE

Discrete	Time of output, sec		Criteria	Remarks
	Nominal	Actual		
BECO	150.36	148.807	$At^2 > E_5$ $E_5 = 0.2934\times10^5\ ft^2/sec^4$	Based on time when acceleration is sampled and when test is performed. Discrete would output at 5.51±0.08 g's. Actual was 5.50 g's. Time earlier than nominal due to booster high performance.
MECO	573.41	572.758	To enter cutoff subroutine $\epsilon < E_{13}$ $13 = 0.12\times10^8\ ft^2/sec^4$	Actual was earlier than nominal due to higher than nominal energy gained during booster phase.

[redacted]

TABLE XIII-IV. - MAJOR CODEWORD CHANGE TIMES

Event	Test	Computer		Description
		Actual time of telemetry, sec	Nominal time of telemetry, sec (a)	
Initialize code word	---	1.415	1.415	First computer cycle - initialization performed
First cycle	---	2.545	2.545	First compute cycle of basic equations
Second cycle	---	3.545	3.545	Second compute cycle of basic equations
Enable BECO test	E_4	147.731	148.735	Start performing test for BECO
Booster staging	E_5	157.741	159.744	Pass BECO test
Sustainer guidance	E_6	160.011	162.015	Enter sustainer equations
Sustainer δR altitude correction	E_{10}	165.041	165.805	Complete sustainer altitude control term
Sustainer integral control steering	E_1	185.011	185.775	Enter integral control after stabilize to "f" vector
Centaur guidance	E_{11}	236.469	238.495	Enter Centaur equations
Centaur δR altitude correction	E_{12}	267.618	265.925	Complete Centaur altitude control term
Centaur integral control steering	E_1	280.148	278.454	Enter integral control after stabilize to "f" vector
Rescale vector	E_{19}	561.632	562.465	Rescale "f" vector to facilitate calculation accuracy
Enter cut	E_{13}	579.511	580.345	Enter MECO test
Enter separate test	---	580.491	581.325	Go to E_{15} test
Enter postinjection	E_{15}	584.431	585.265	Based on elapsed time from E_{13} test
Coast phase (attitude reference vector)	---	585.431	586.265	Enter coast-phase rotating attitude control vector

[a]Nominal times from nominal closed-loop interpretive (COFLIC) run.

[redacted]

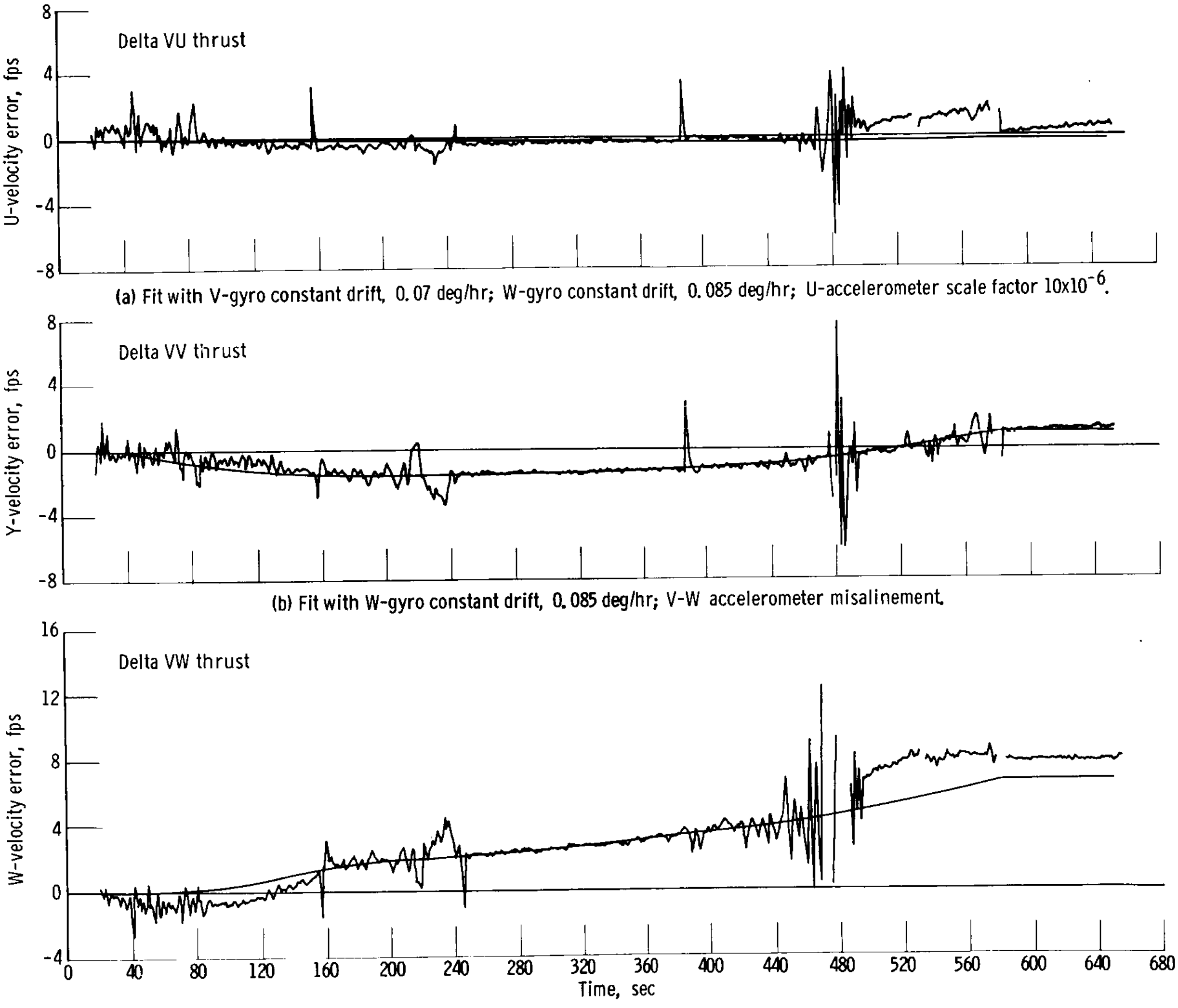

(a) Fit with V-gyro constant drift, 0.07 deg/hr; W-gyro constant drift, 0.085 deg/hr; U-accelerometer scale factor 10×10^{-6}.

(b) Fit with W-gyro constant drift, 0.085 deg/hr; V-W accelerometer misalinement.

(c) Fit with V-gyro constant drift, 0.07 deg/hr; W-U accelerometer misalinement.

Figure XIII-1. - Comparison of guidance minus best estimate of trajectory velocity.

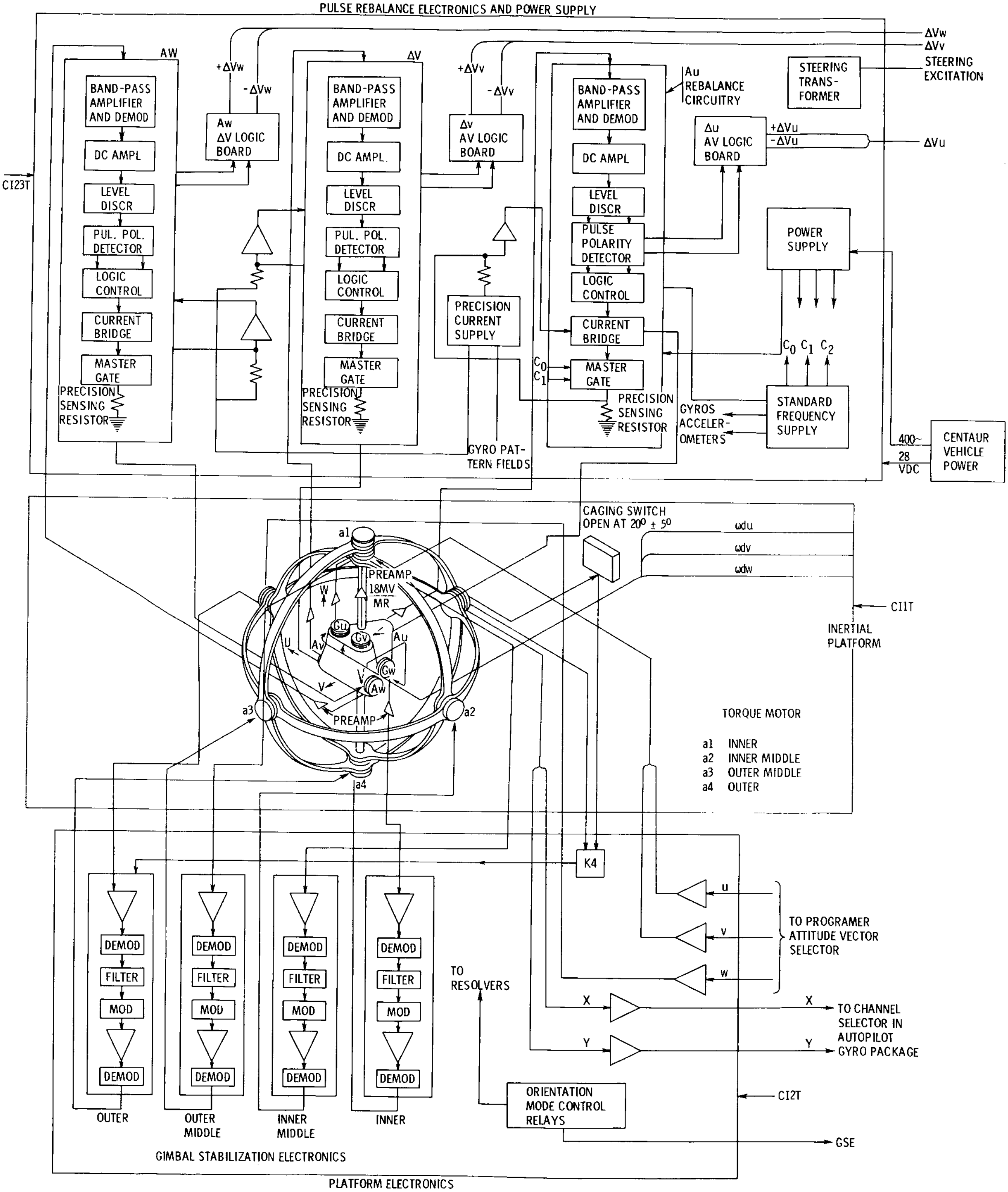

Figure XIII-2. - Centaur

[redacted]

[redacted]

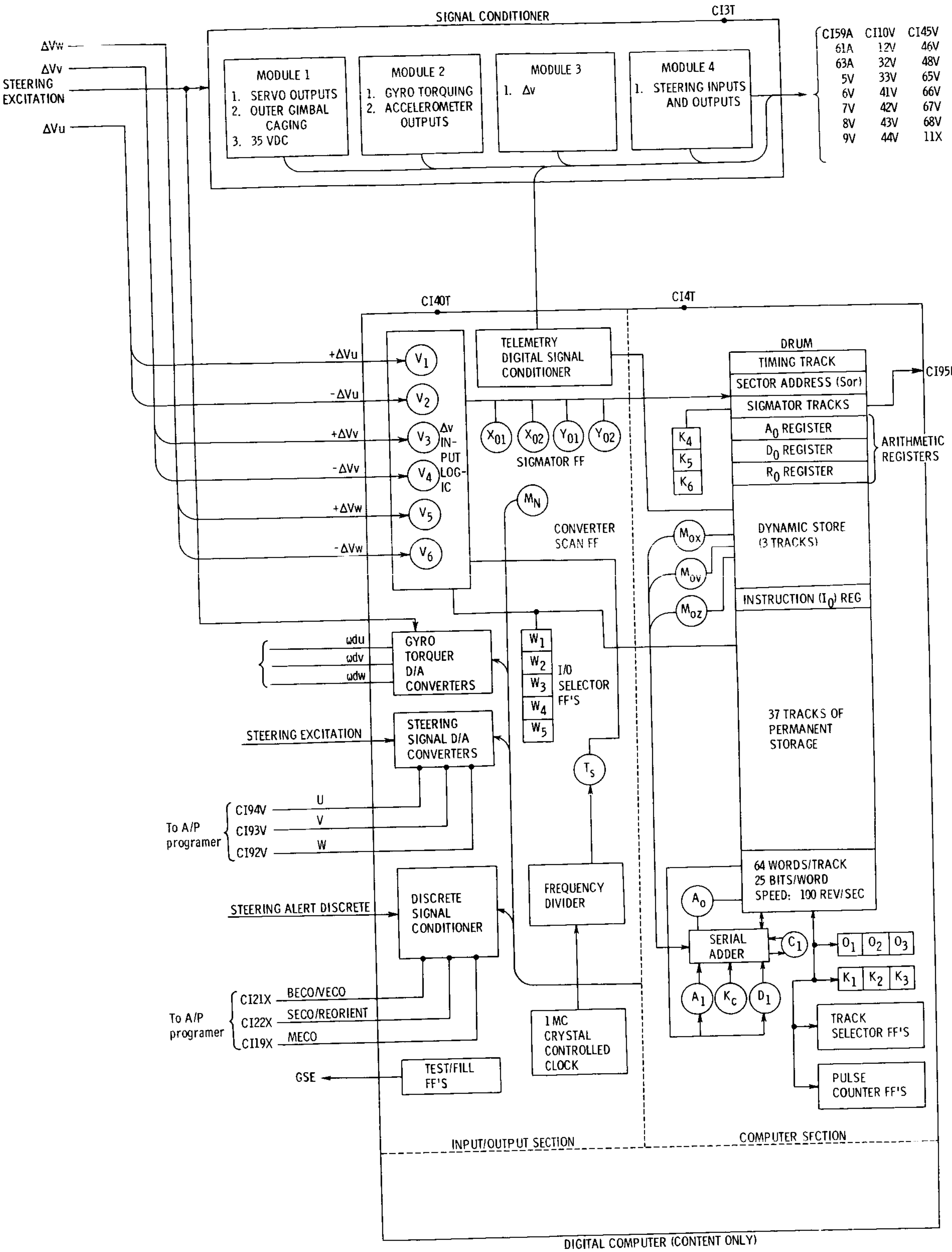

guidance system.

[redacted]

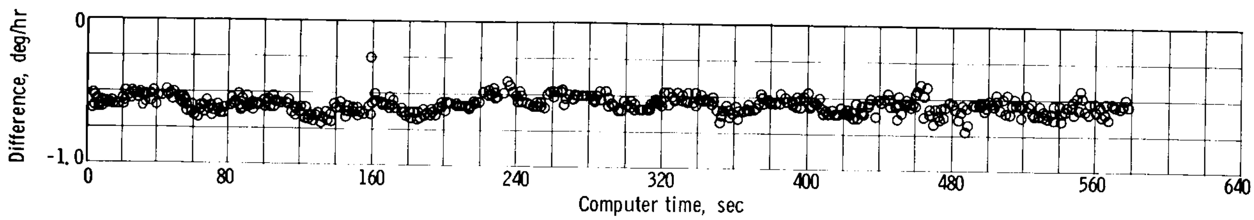

Figure XIII-3. - Computer gyro torquing digital value W_{DU} minus telemetered analog value I 41 V as function of time.

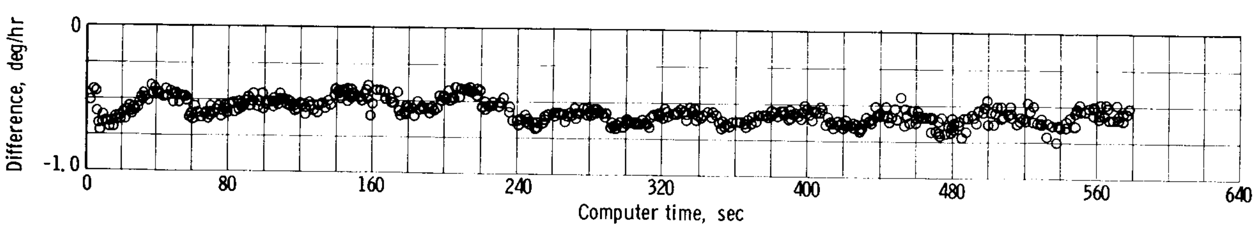

Figure XIII-4. - Computer gyro torquing digital value W_{DV} minus telemetered analog value I 42 V as function of time.

[redacted]

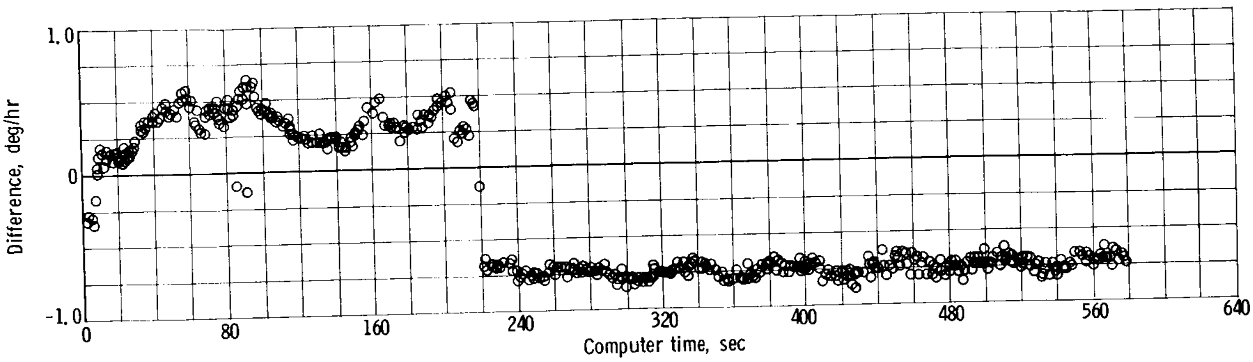

Figure XIII-5. - Computer gyro torquing digital value W_{DW} minus telemetered analog value I 43 V as function of time.

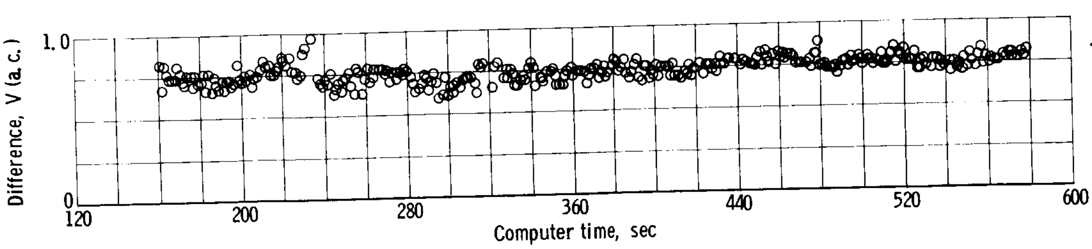

Figure XIII-6. - Computer digital steering value F_{CU} minus telemetered analog steering value I 8 V as function of time.

[redacted]

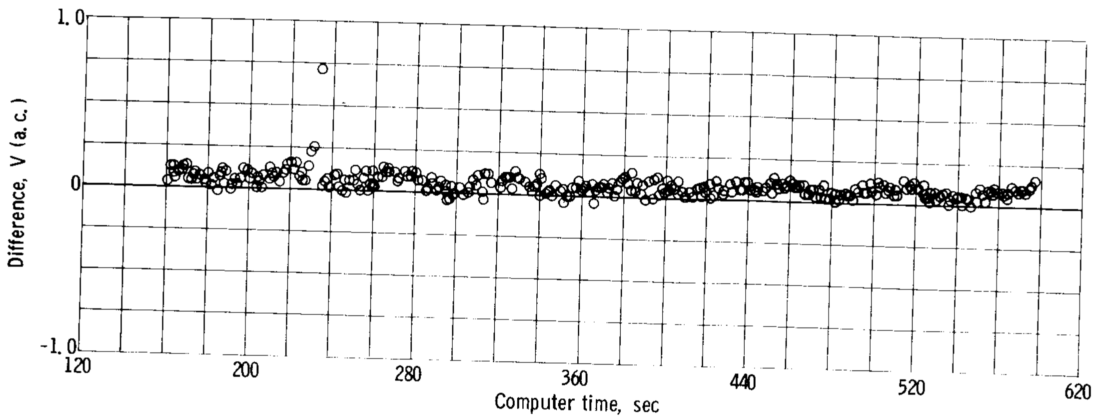

Figure XIII-7. - Computer digital steering value F_{CV} minus telemetered analog steering value I 9 V as function of time.

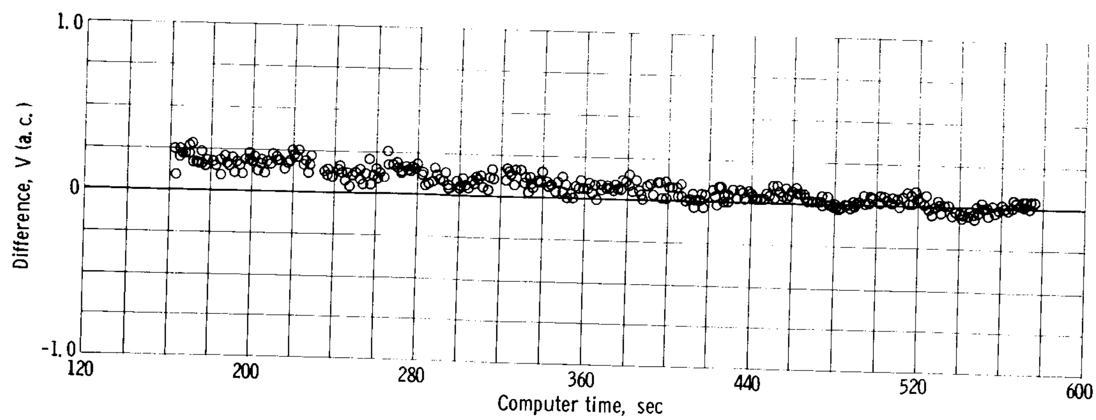

Figure XIII-8. - Computer digital steering value F_{CW} minus telemetered analog steering value I 10 V as function of time.

[redacted]

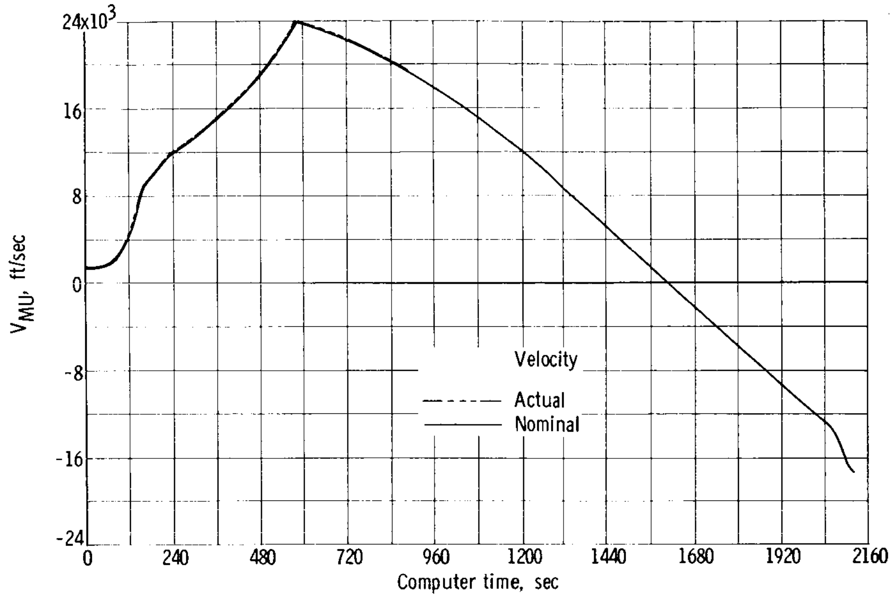

Figure XIII-9. - Missile velocity and nominal velocity as function of time for values of V_{MU}.

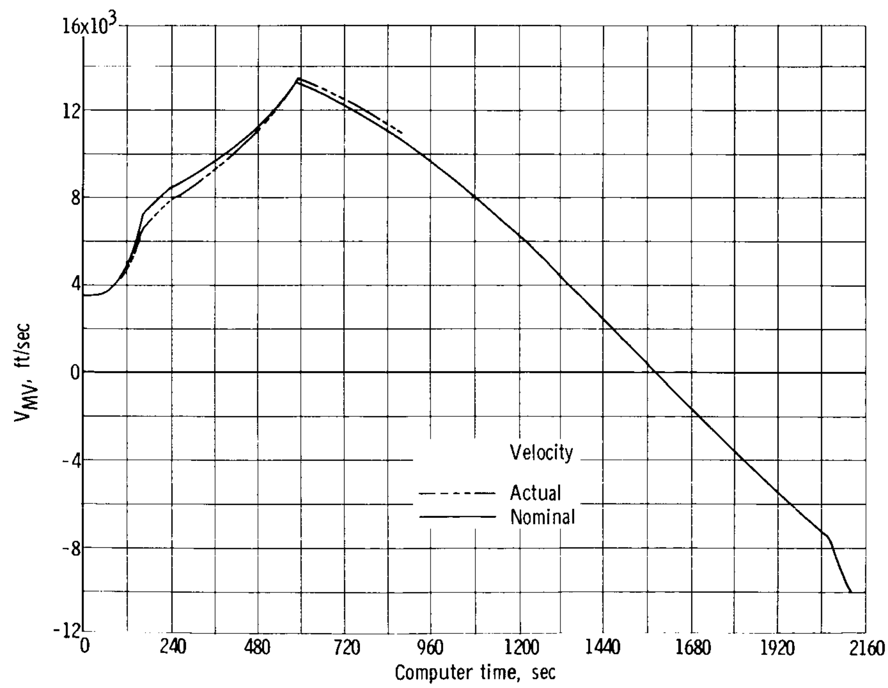

Figure XIII-10. - Missile velocity and nominal velocity as function of time for values of V_{MV}.

[redacted]

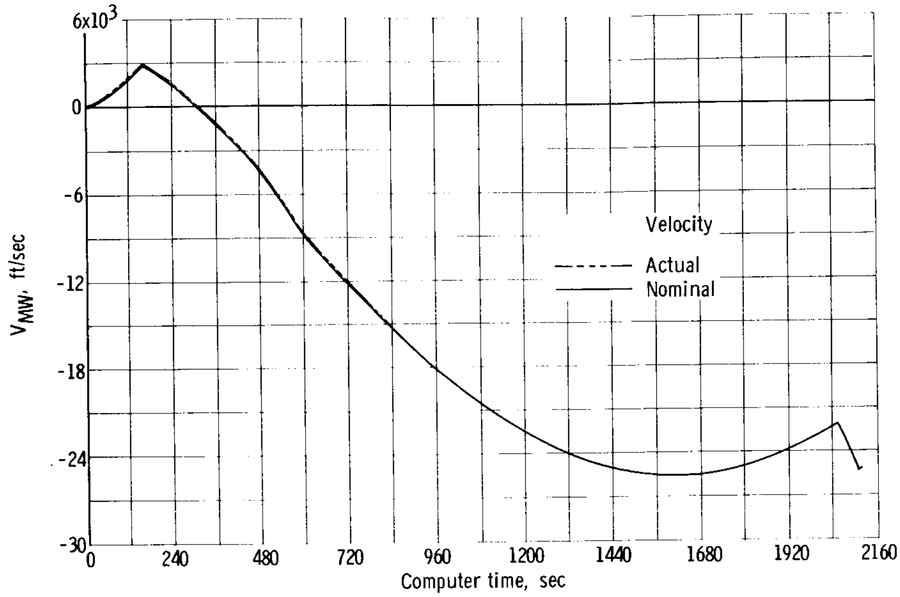

Figure XIII-11. - Missile velocity and nominal velocity as function of time for values of V_{MW}.

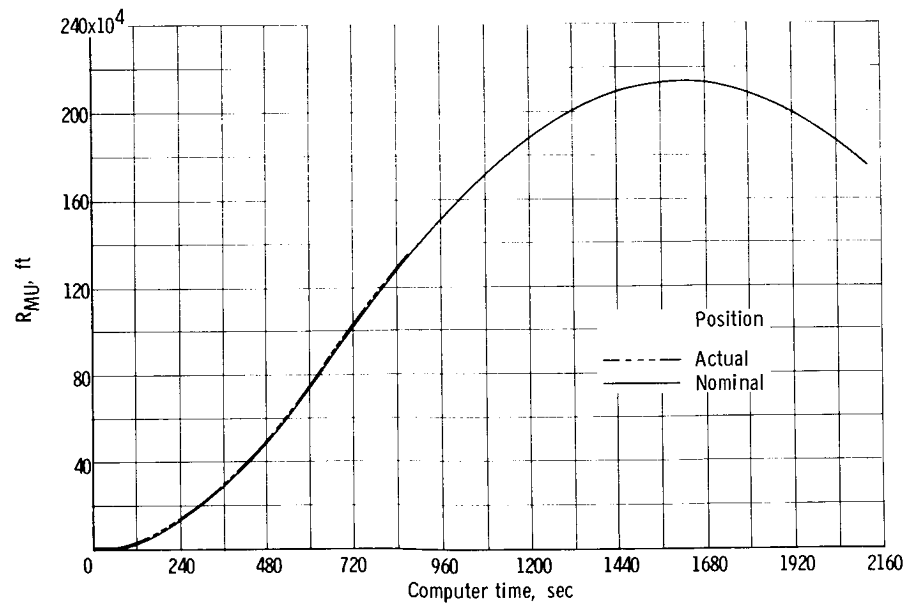

Figure XIII-12. - Missile position and nominal position as function of time for values of R_{MU}.

[redacted]L•

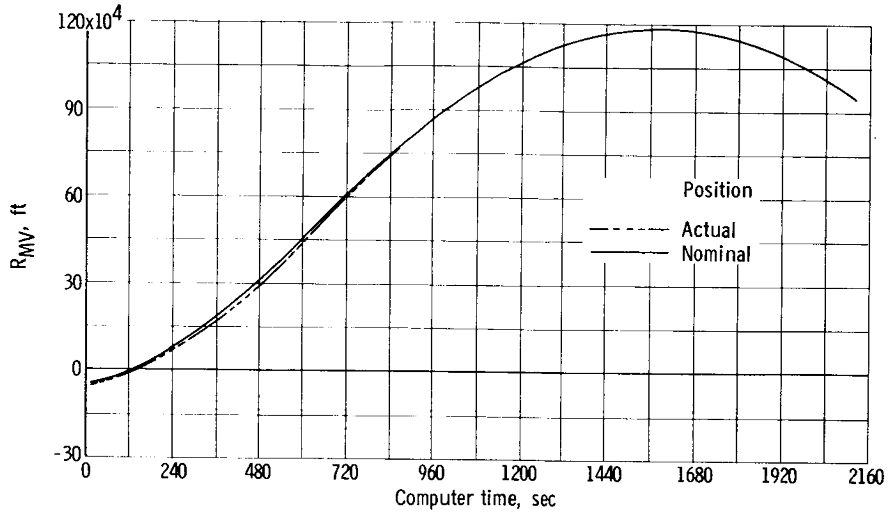

Figure XIII-13. - Missile position and nominal position as function of time for values of R_{MV}.

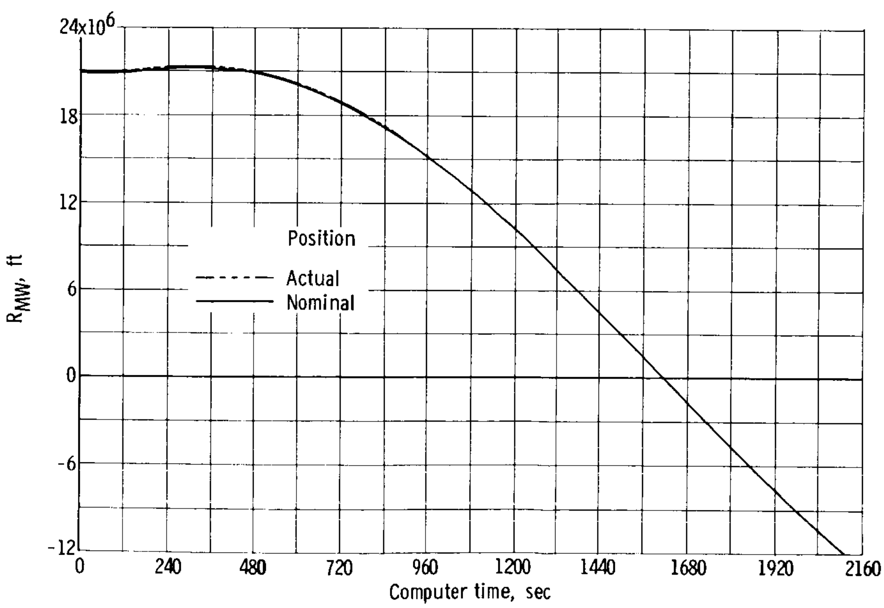

Figure XIII-14. - Missile position and nominal position as function of time for values of R_{MW}.

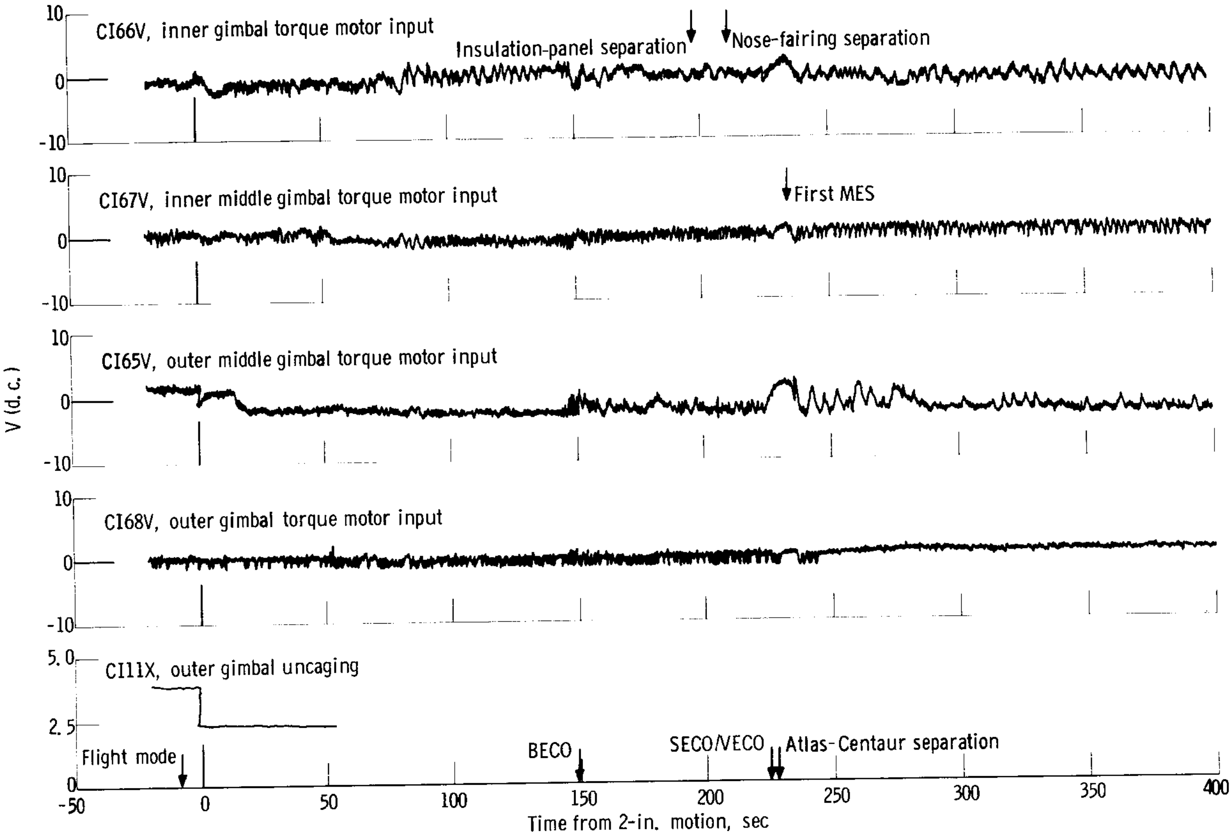

(a) Time, -10 to 400 seconds.

Figure XIII-15. - Centaur guidance system telemetered data.

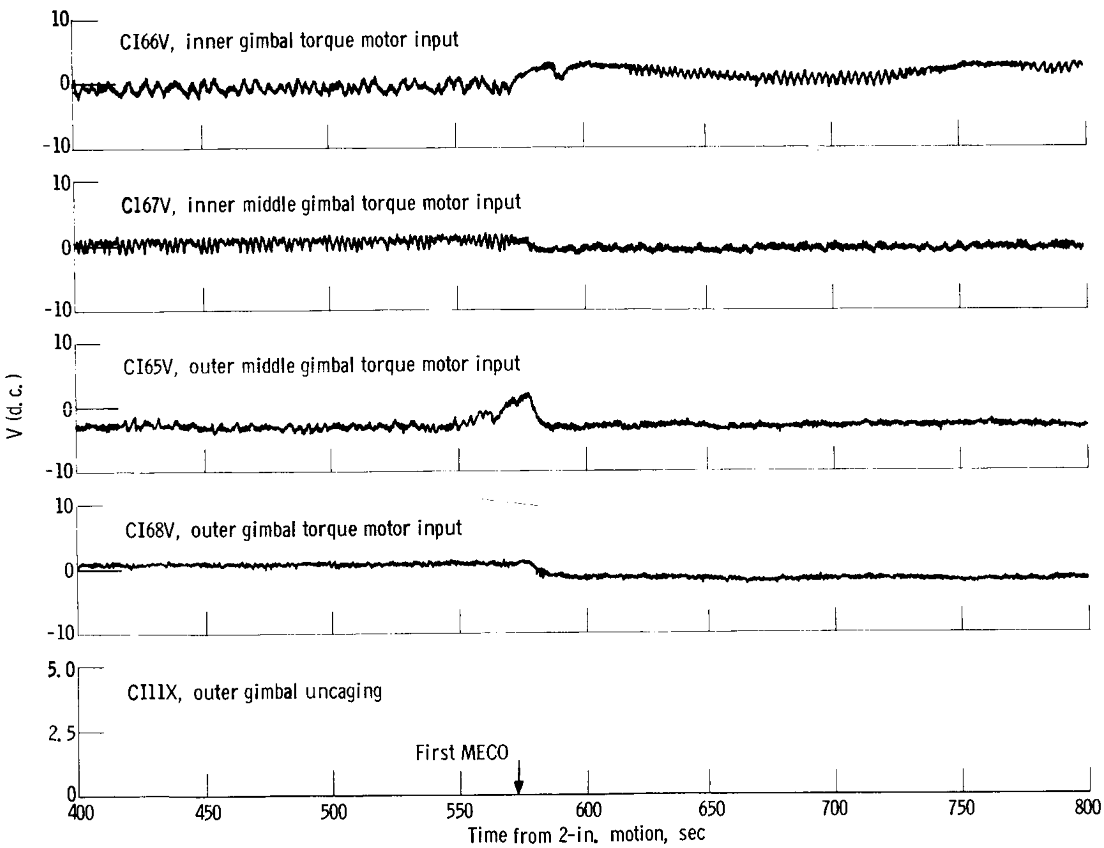

(b) Time, 400 to 800 seconds.

Figure XIII-15. - Concluded.

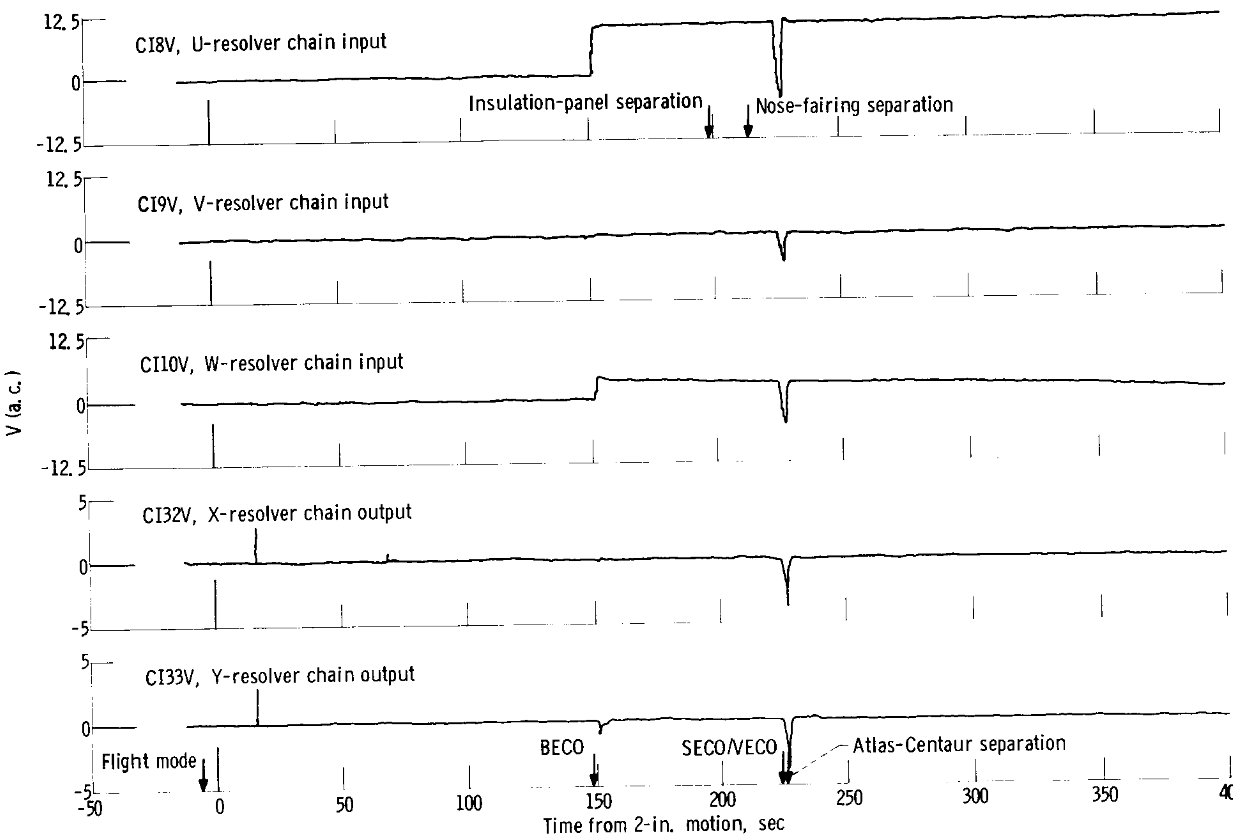

(a) Time, -10 to 400 seconds.

Figure XIII-16. - Centaur guidance system telemetered data.

[redacted]

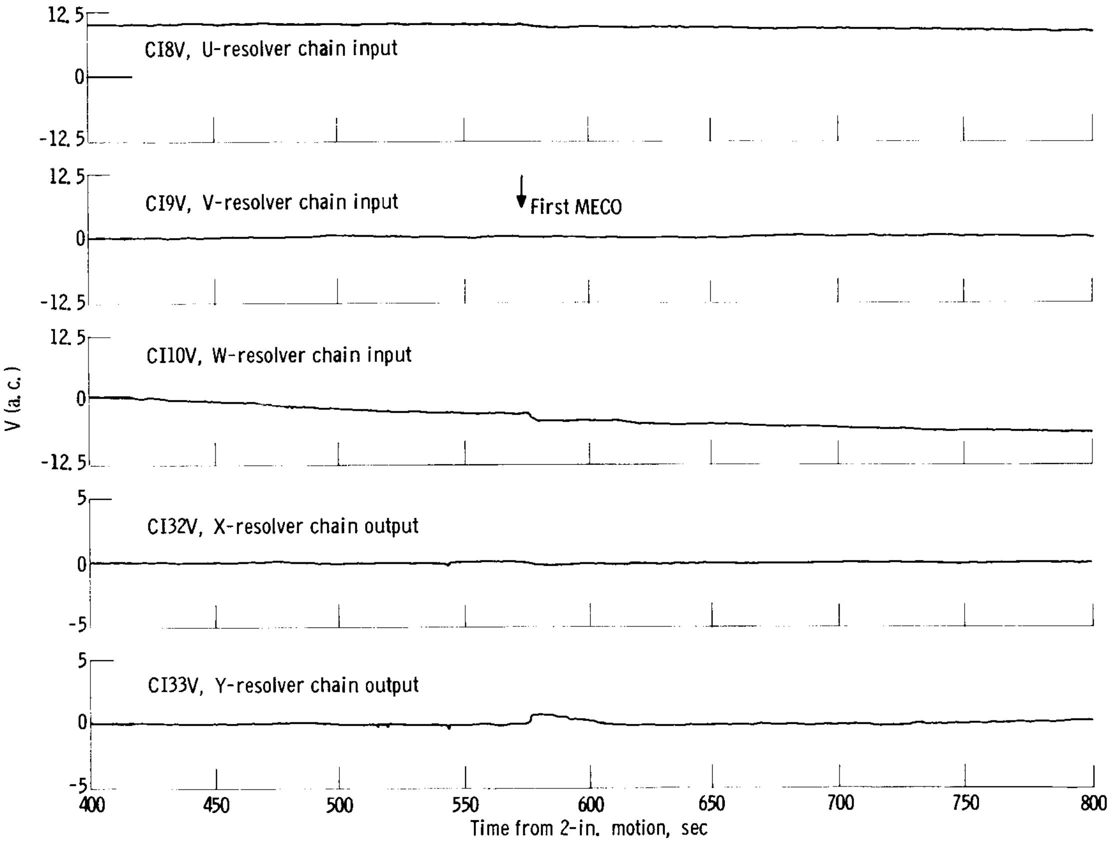

(b) Time, 400 to 800 seconds.

Figure XIII-16. - Concluded.

[redacted]

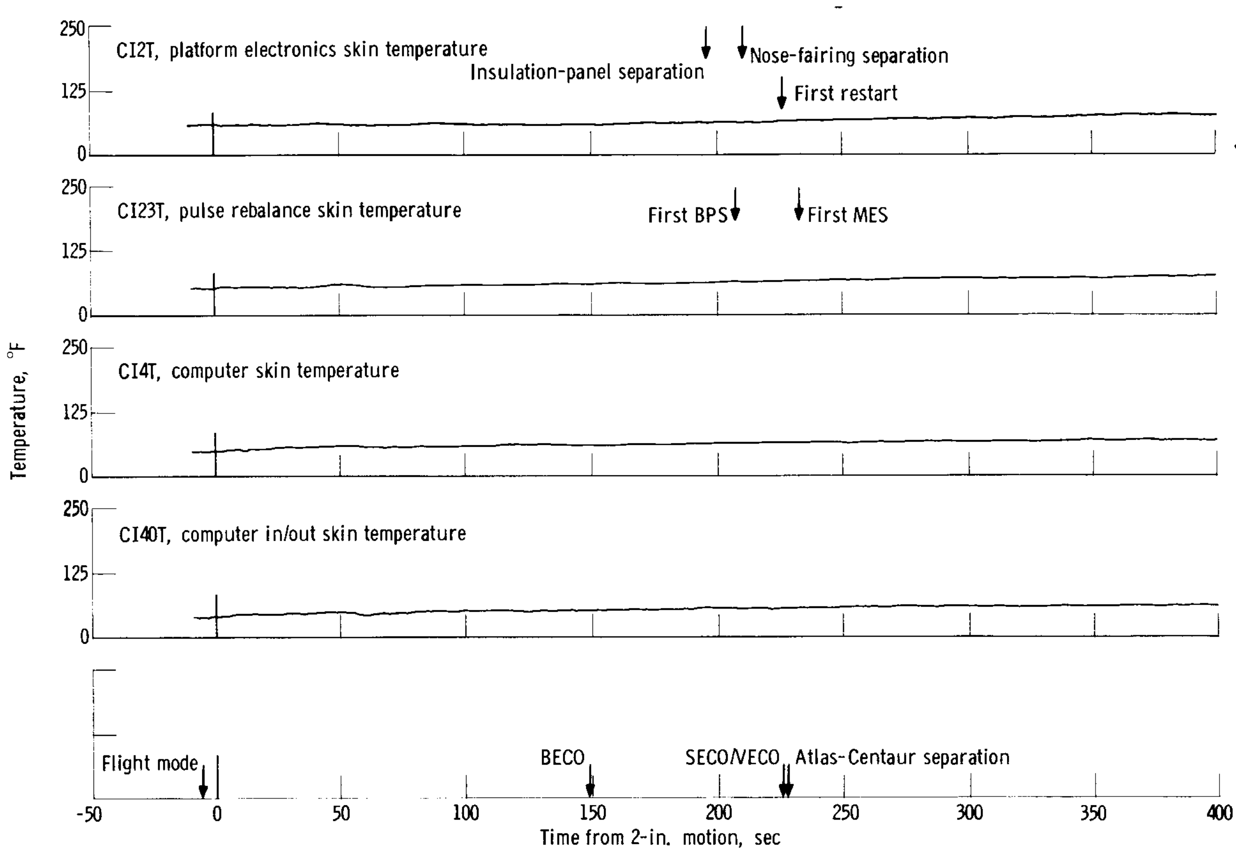

(a) Time, -10 to 400 seconds.

Figure XIII-17. - Centaur guidance system telemetered data.

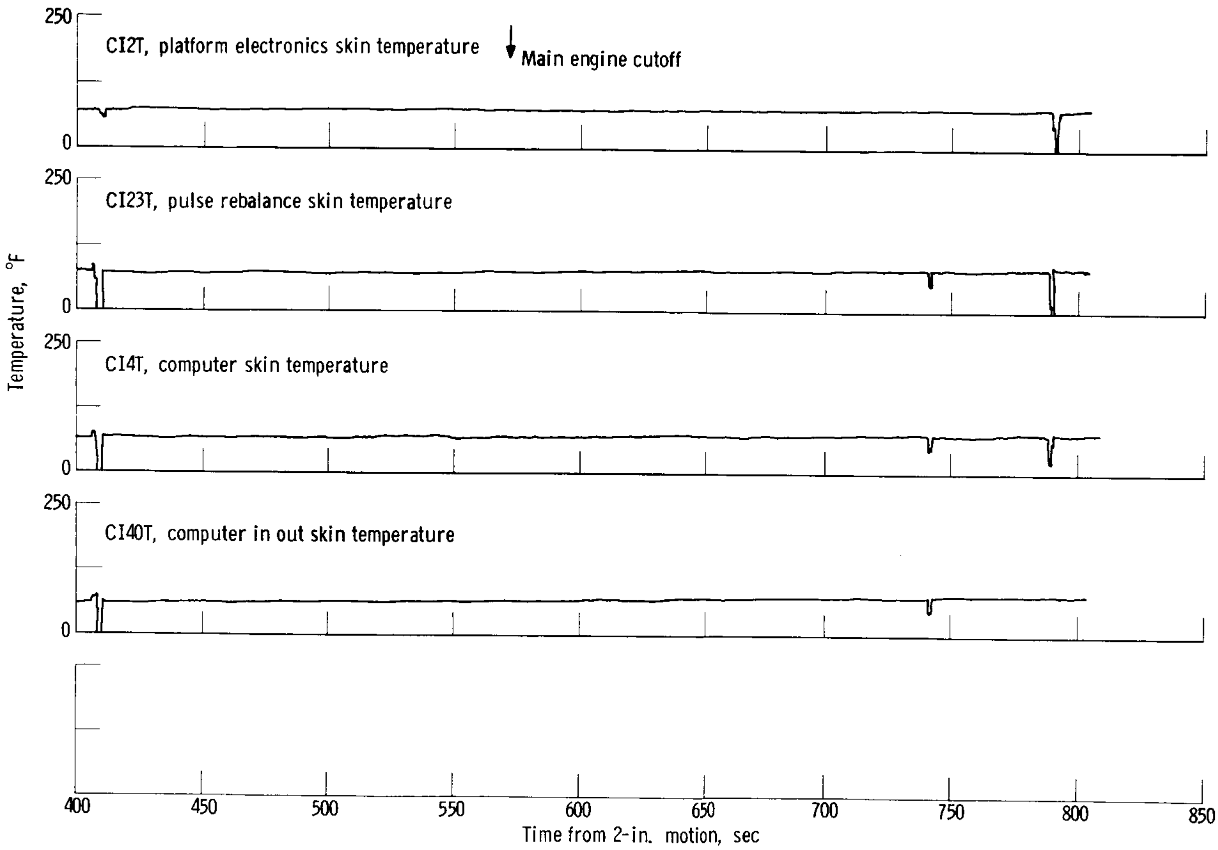

(b) Time, 400 to 810 seconds.

Figure XIII-17. - Concluded.

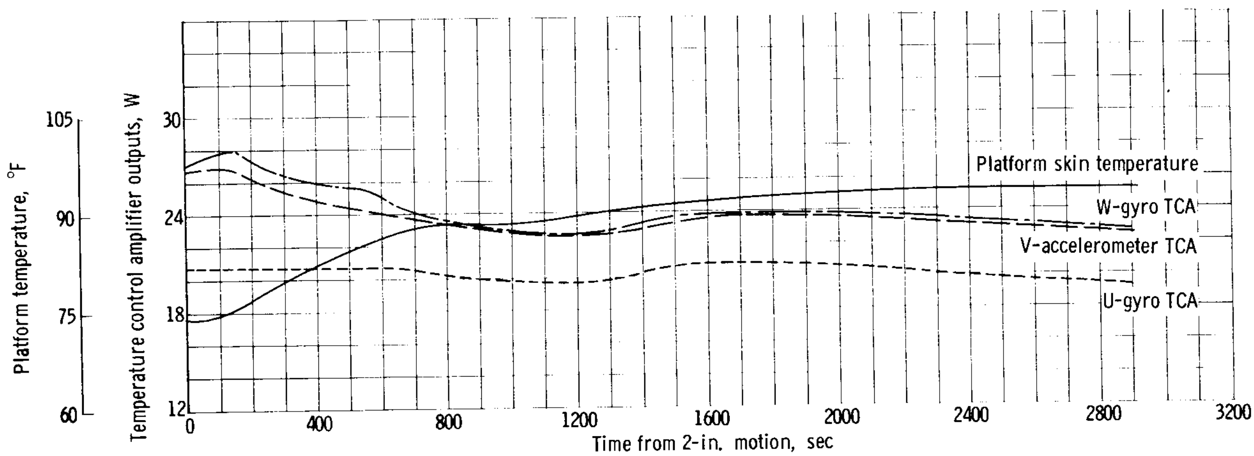

Figure XIII-18. - Platform skin temperature and component temperature control amplifier.

[redacted]

XIV. ELECTRICAL SYSTEMS

SUMMARY

The airborne electrical systems provide onboard electrical power storage, conversion, distribution, and protection, as well as fulfilling the requirements of instrumentation, telemetry, tracking, and range safety command systems. The electrical power system adequately supported the flight, with all red-line measurements within the specified limits and all other measurements at the expected levels. Figure XIV-1 shows the Centaur electrical system. The range safety system experienced no malfunctions during the flight, and performance of the tracking system was nominal.

The operation of the Atlas-Centaur telemetry-instrumentation system was satisfactory. Normal operation was confirmed beyond the first four complete orbits. Generally, data quality was good. Continuous coverage was provided through T + 3480 seconds with the exception of a 100-second period between the range instrumentation ship, Timber Hitch, and Ascension Island. This data void occurred during coast phase after venting, and no significant data loss resulted. To measure Centaur vehicle performance, 455 measurements were telemetered; 97 percent of these yielded valid data. There were 175 Atlas booster measurements. The types of measurements made by the airborne system are shown in table XIV-I.

Several GSE peculiarities were noted during preflight testing: (1) the possibility of losing Atlas programer reset command during transfer from external to internal power, (2) loss of "guidance ready" command on umbilical ejection, (3) ripple problem on 28-volt d-c main-power bus, as well as (4) operator error coupled with equipment failure during tanking operations.

ELECTRICAL

Atlas Main Battery and Inverter

The Atlas battery voltage at lift-off was 29.3 volts d.c. and exhibited a gradual drift upwards to about 30.2 volts at T + 226 seconds, Atlas-Centaur separation. At T + 235 seconds, the voltage jumped to 31 volts, while at T + 320 seconds it returned to 29.3 volts d.c. The inverter voltage output for the three phases remained reasonably constant at 114.8 to 115.1 volts. Phase A voltage displayed a gradual downward drift from 115.1 volts a.c. at lift-off to 114.8 volts a.c. at T + 300 seconds, about 70 seconds after Atlas-Centaur separation. The inverter frequency varied from 402.1 to 402.5 cps throughout the boost and sustainer portions of the flight.

[redacted]

The Atlas inverter was deliberately set at 402 cps to produce a 2-cycle beat with the Centaur inverter. The beat frequency is outside of the lowest resonance of the vehicle and would not interfere with the steering signals fed to Atlas from Centaur guidance on a closed-loop flight.

Staging Disconnect

The staging disconnect actuator temperature dropped from 62° F at lift-off to approximately 8° F at separation, while the receptacle temperature decreased to the same separation temperature from 32.4° F at T - 0. The temperature at staging disconnect is marginal. On future vehicles, red-line temperature at T - 0 will be increased.

Centaur Main Battery and Inverter

During the countdown, a malfunction of the Centaur power changeover switch for 20 milliseconds at T - 90 minutes caused the Centaur inverter to drop out for approximately 180 milliseconds. This, in turn, caused the guidance power failure indicator to illuminate. Fortunately, the information stored in the computer was not affected.

The Centaur battery was 28.4 volts d.c. at lift-off, while at T + 3000 seconds, it appeared to be holding steady at 28.2 volts. At MES (T + 235 sec), the battery voltage dropped to 27.4 volts, recovered to 27.6 volts during thrust, and rose 28.0 volts at MECO (T + 572 sec). The battery internal temperature rose gradually from 106° F at lift-off to 138° F at T + 3000 seconds.

Comparison of the calculated battery-load-current - time profile with the measured current profile reveals close correlation between the sequential events, but with the absolute values of measured current being some 20 percent lower than predicted. Lift-off load current was approximately 44 amperes, while at T + 3000 seconds the same value was being delivered. The Centaur AC-4 load profile is shown in figure XIV-2.

The inverter phase voltages varied less than 0.4 volt throughout the 3000 seconds of telemetry data with an average output of 113.5 volts a.c. The load currents for each phase decreased gradually from lift-off to T + 3000 seconds by a factor of 0.8 to 0.3 ampere dependent on the particular phase. Since the inverter output voltage and frequency, as well as the operation of the equipment supplies by the inverter, were normal, the drift could be attributed to a malfunction in the telemetry circuit. The inverter frequency throughout the flight was essentially constant at 400 cps.

The inverter skin temperature was 78° F at lift-off and rose to a maximum value of 152° F at T + 900 seconds when LH_2 vented and produced a cooldown to 101° F at T + 1620 seconds. The inverter temperature again rose to 167° F at main power cutoff. Two additional points were obtained on the second pass and are shown in figure XIV-3.

TELEMETRY AND INSTRUMENTATION

Telemetry

Ten measurements of Centaur telemetry system parameters were made on AC-4. All yielded valid data, and all remained within the predicted limits except for the RF-4 skin temperature and the C-1 engine forward instrumentation box. No data were lost due to these anomalies. RF-4 temperature decreased from 55° F at T + 840 seconds, when venting occurred, to 20° F at T + 1600 seconds. After T + 1600 seconds, temperature decayed at a slower rate and stabilized at 5° F at T + 3000 seconds. The RF-4 package was mounted on the lower tier close to the vent. The C-1 engine forward-instrumentation-box temperature abruptly went off scale (high) at T + 2750 seconds, approximately 40 seconds after the vehicle entered the Earth's shadow. The C-1 instrumentation-box temperature came back in band at 110° F and decreased linearly to 90° F at T + 2900 seconds (end of Uniform data). Temperature had stabilized at 20° F on the first pass over ETR. Telemetry battery current was 18 amperes as expected after T + 3000 seconds. Multiplexer, thermocouple-reference-junction, C-2 rear-instrumentation-box, and aft-instrumentation-box temperatures were all within expected limits. Telemetry and instrumentation details are given in appendix B.

Centaur Instrumentation

Six measurements yielded no data on AC-4. Two failed during flight, and 20 experienced anomalies such as offset time delays or bonding failure. Eleven measurements were deleted prior to launch. The measurements in the following table, which were inaccessible for repair prior to flight, were deleted prior to launch.

Measurement		Station
CA744S	Tank strain	225
CA757S	Tank strain	402
CA759S	Tank strain	402
CA408T	Outer nose	72
CA856T	Aft bulkhead skin	---
CA866T	Aft bulkhead skin	---
AA176S	Strain	582
AA919T	Temperature	575
AA925T	Temperature	614
CA756T	Tank skin	---
CA537T	Tank skin	302

The following measurements yielded no data during all or portions of the flight.

<u>CA2650 LH$_2$ boil-off valve accelerometer</u>. - This transducer failed to respond during vent-valve operation. Sensor or associated amplifier failure caused this loss of data, since no noise or bias shift was evidenced.

<u>CA310 C-1 gimbal mounting z-axis vibration</u>. - Full-scale noise due to an apparent open circuit appeared during the Centaur burn.

CA451P Nose-fairing differential pressure. - This measurement read zero throughout the flight. An open harness or transducer failure is suspected. Two other nose-fairing differential pressure transducers provided data on AC-4.

CH152T and CH153T C-1 and C-2 hydraulic insulation adapter temperatures. - These temperatures went off scale (low) prior to launch and remained off scale throughout flight. These thermocouples were reworked just prior to flight. Wire reversal is the probable cause of this data loss.

CU12X LOX liquid level at station 433.5. - This measurement erroneously indicated dry from main-engine start until T + 860 seconds then indicated wet.

CM810V Air Force Cambridge Research Laboratories Spectrometer. - The commutator in this device failed prior to launch. After main-engine cutoff, the commutator began operating. Spectrometer data on the LH_2 engine exhaust was not obtained as a result of this failure.

CP29T LH_2 boost-pump-turbine nozzlebox temperature. - Valid data were obtained until T + 610 seconds. At that time, the trace went off scale (low) due to an apparent short circuit.

CP28P LH_2 boost-pump turbine-inlet pressure. - An excessive 10-second time delay occurred in responding to pressure rise due to failure of the potentiometer drive linkage.

CP123T and CP125T C-2 engine fuel and LOX pump temperatures. - These measurements displayed an unexplained delay in response characteristic of a poor thermal bond. Identical measurements on the C-1 engine operated as expected. CP125T required 50 seconds to indicate a 100° F drop in temperature at measurement, while similar measurements on the C-1 engine showed a similar drop in less than 10 seconds. This is not a confirmed instrumentation failure, since several temperature measurements associated with the C-2 engine were high.

CP882T Ullage control unit quadrant I. - This temperature data was offset by 25 percent information bandwidth compared with a similar measurement (CP883T) in quadrant II. Both of these measurements clearly indicated identical temperature rise rates of H_2O_2 propellant settling motors; therefore, little data were lost as a result of this malfunction. Probable failure occurred in the thermocouple compensator.

The measurements in the following table yielded data until insulation-panel jettison. At that time apparent wiring damage caused each to go off scale.

Measurement		Station
CA540T	Tank skin temperature	310
CA758S	Tank strain	402
CA826S	Ring strain	408
CA830S	Ring strain	408
CA832S	Ring strain	408

The temperature measurements in the following table indicated increased temperatures at insulation-panel jettison probably due to varying degrees of bonding failure. It appears that these measurements yielded erroneous data after panel jettison. Forty-three germanium sensors had been bonded to the Centaur tanks to determine liquid position during coast and to provide temperature data. Approximately 25 percent exhibited bonding anomalies.

Measurement		Station
CA543T	Tank skin	318
CA544T	Tank skin	320
CA546T	Tank skin	326
CA547T	Tank skin	328
CA549T	Tank skin	334
CA551T	Tank skin	338
CA707T	LH_2 pump	387
CA495T	LH_2 pump	393
CA600T	Tank skin	248
CA624T	Tank skin	293
CA626T	Tank skin	297

AC-4 RANGE SAFETY SUBSYSTEM

Operation of the Range Safety command subsystem was entirely satisfactory with no anomalies experienced. The system is designed to perform three functions, each on receipt of an appropriate radio command from the UHF command-control system operated by the AFETR under direction of the Range Safety Officer.

The first two functions are termination of thrust and dispersion of the propellants, produced by the MECO and DESTRUCT commands, respectively. Neither of these was required, since the trajectory and performance were well behaved until orbital velocity was achieved.

The last function of the system is to turn itself off on receipt of the DISARM command. This was accomplished at T + 601.4 seconds. A summary of activities relating to the RSC subsystem is shown in the following table.

Event	Planned time, sec	Actual time, sec
Switch from Cape to GBI transmitter	T + 114	T + 115.6
Switch from GBI to San Salvador transmitter	T + 185	T + 185.2
Switch from San Salvador to Grand Turk transmitter	T + 310	T + 309.5
Switch from Grand Turk to Antigua transmitter	T + 520	T + 522.0
Send DISARM command	Within 30 after MECO	MECO + 28.5

From T - 0 until the DISARM command was sent, the minimum signal strength at either receiver was 36.1 microvolts. Since the receivers have a nominal sensitivity of 5 microvolts, there was never less than a 17-decibel gain margin.

ELECTRICAL GROUND SUPPORT EQUIPMENT

Several GSE peculiarities discussed hereinafter occurred during preflight testing, and some latent problems were brought to light:

(1) A safety measure was incorporated in the GSE logic to ensure that the Atlas programer reset command was provided during transfer from external to internal power until the cycle had positively been completed. There was concern that if there were a delay in transfer time of the changeover switch (max. specification time for transfer is 2 sec), the programer reset signal would have been removed for approximately 0.5 second. Any transient caused in the transfer would activate all the programer high-power switches, necessitating action by the test conductor to reset the engine-start logic prior to arming the engine start switch.

(2) A new "guidance ready" circuit was installed to support guidance on the assumption that optical acquisition could not be obtained with gimbal 4 caged. It was discovered during the FACT test that the new circuitry was a function of "guidance caged" and dependent on airborne umbilical 600 P/J 402 being mated. The loss of 600 P 402 at "main engine complete" drops out the "function safe release" ladder resulting in cutoff. Systems testing verified that the circuit was unnecessary, and gimbal 4 was subsequently kept in the caged position by procedural change.

(3) Power supply 3, which is the main source of the 28-volt d-c power backed up with a 10-cell nickel-cadmium battery on the line, was the target for much concern and criticism as the probable cause of excessive ripple appearing on the 28-volt d-c bus. This power supply is a 400A Christie unit similar to that used with the Atlas E series configuration. The specification calls for an output ripple of 0.28 volt (rms) or 0.8 volt P-P. The power supply had a ripple of 1.2 volts P-P. With the battery on the line, the ripple was reduced to 0.6 volt P-P. The measurements established that the power supply was at fault, and the trouble could no longer be attributed to extraneous ground feedback loops inherent in the equipotential grounding scheme employed at the complex. It was clear that the Christie unit (PS-3) had to be replaced to bring the ripple contact within acceptable limits. This was accomplished after the launch.

(4) Operator error in combination with equipment failure resulted in the overtanking condition experienced during the quad tanking test. It is evident that some method must be devised to cut off tanking operations automatically at some predetermined level (90 to 95 percent). A manual override capability could be built in to alert the operator that the most critical phase of the tanking process was rapidly approaching.

[redacted]

TABLE XIV-I. - AC-4 MEASUREMENT SUMMARY

Vehicle system	Measurement type																
	Acceleration	Rotation rate	Current	Deflection	Power	Light intensity	Vibration	Pressure	Frequency	Rate	Strain	Temperature	Voltage	Discrete position	Acoustic	Digital	Total
Atlas																	
Airframe	4	-	-	1	-	1	13	6	-	-	12	29	--	4	-	-	70
C-band beacon	-	-	-	--	-	-	--	--	-	-	--	--	--	--	-	-	---
Range safety command	-	-	-	--	-	-	--	--	-	-	--	--	1	1	-	-	2
Electrical	-	-	-	--	-	-	--	--	1	-	--	1	2	2	-	-	6
Pneumatic	-	-	-	--	-	-	--	7	-	-	--	2	--	--	-	-	9
Hydraulic	-	-	-	--	-	-	--	6	-	-	--	--	--	--	-	-	6
Guidance	-	-	-	--	-	-	--	--	-	-	--	--	--	--	-	-	---
Propulsion	-	3	-	2	-	-	--	19	-	-	--	2	--	7	-	-	33
Flight control	-	-	-	13	-	-	--	--	-	3	--	--	--	7	-	-	23
Telemetry	-	-	-	--	-	-	--	--	-	-	--	1	--	--	-	-	1
Propellant level control	-	-	-	--	-	-	--	2	-	-	--	--	1	--	-	-	3
Azusa	-	-	-	--	-	-	--	--	-	-	--	--	--	--	-	-	---
Payload	-	-	-	--	-	-	--	--	-	-	--	--	--	--	-	-	---
Miscellaneous	1	-	-	1	-	-	--	--	-	-	--	--	--	26	-	-	28
Total	5	3	-	17	-	1	13	40	1	3	12	35	4	47	-	-	181
Centaur																	
Airframe	2	-	-	--	-	-	10	22	-	-	17	150	--	1	-	-	202
C-band beacon	-	-	-	--	-	-	--	--	-	1	--	---	--	--	-	-	1
Range safety command	-	-	-	--	-	-	--	--	-	-	--	---	2	3	-	-	5
Electrical	-	-	4	--	-	-	--	--	1	-	--	5	4	--	-	-	14
Pneumatic	-	-	-	--	-	-	--	9	-	-	--	5	--	2	-	-	16
Hydraulic	-	-	-	--	-	-	3	4	-	-	--	12	--	--	-	-	19
Guidance	3	-	-	--	-	-	--	--	-	-	--	6	19	4	-	1	33
Propulsion	-	4	-	--	-	-	1	20	-	-	--	37	--	16	-	-	78
Flight control	-	-	-	--	-	-	--	--	-	6	--	2	8	26	-	-	42
Telemetry	-	-	1	--	-	-	--	--	-	-	--	10	--	--	-	-	11
Propellant level control	-	-	-	--	-	-	--	--	-	-	--	---	--	2	-	-	2
Azusa	-	-	-	--	2	-	--	--	-	-	--	1	--	--	-	-	3
Payload	-	-	-	--	-	-	4	3	-	-	--	8	--	--	-	-	15
Miscellaneous	3	-	-	5	-	-	--	--	-	-	--	5	1	--	1	-	15
Total	8	4	5	5	2	-	18	58	1	7	17	241	34	54	1	1	456

[redacted]

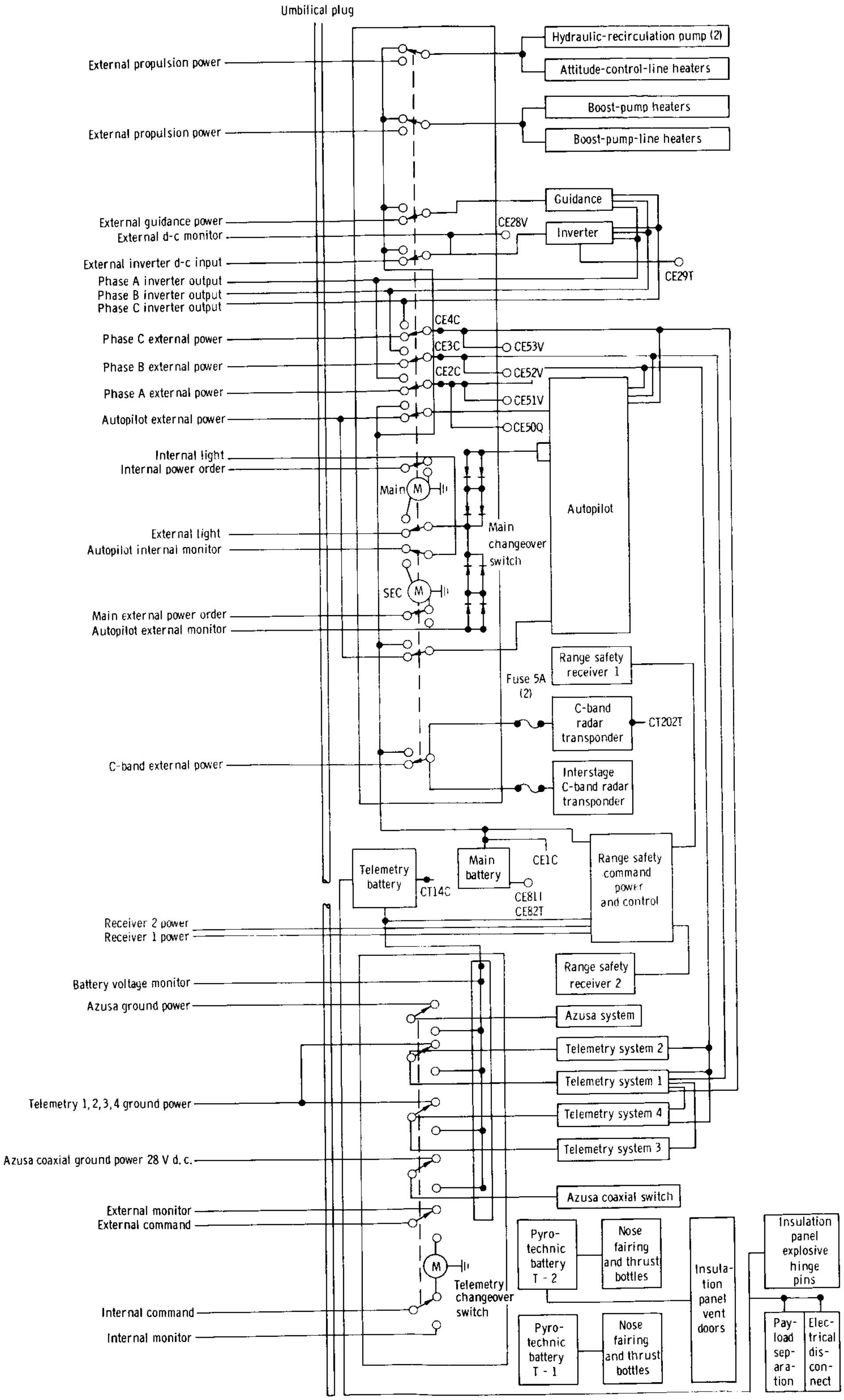

Figure XIV-1. - Centaur electrical system.

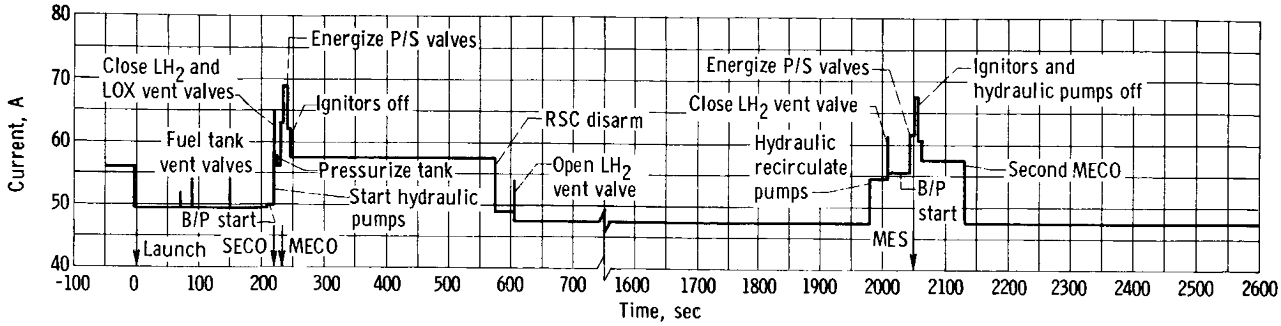

Figure XIV-2. - Centaur AC-4 missile battery current load profile.

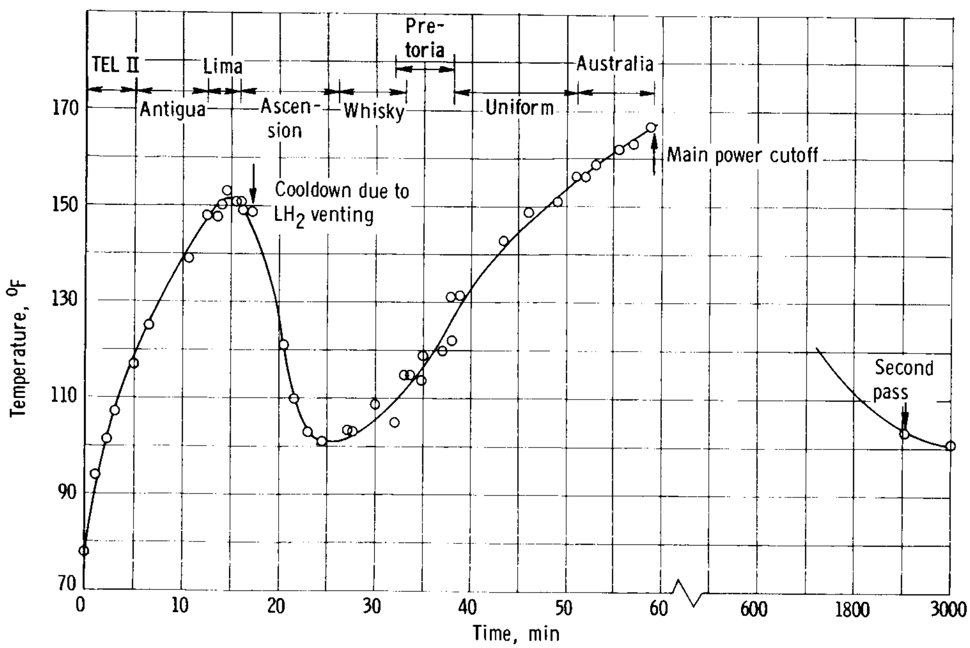

Figure XIV-3. - AC-4 static inverter temperature against flight time.

XV. COAST-PHASE PROPELLANT AND VEHICLE BEHAVIOR

SUMMARY

The AC-4 coast-phase vehicle behavior was not normal, and the programed mission requirements for controlled hydrogen venting, second main engine start, turnaround, and retromaneuver were not accomplished. Failure to accomplish these objectives resulted primarily from an uncontrolled propellant behavior excited by vehicle disturbances at first MECO. The combined effects of engine shutdown transients, vehicle dynamics, and other energy inputs to the propellants, induced a forward displacement and circulation of the liquid residuals within the tank. Viscous damping was insufficient to dissipate propellant energy, and the ullage motor thrust was inadequate to settle the propellants from the disturbed state. Failure to settle the LH_2 at the time of venting resulted in mixed-phase or liquid flow, which, on expanding from the vent exits, produced high impingement forces in excess of the attitude control system capability, and the vehicle tumbled out of control. Continued tumbling and vent depletion of the LH_2 residual prevented accomplishment of the coast-phase mission.

A composite correlation of these post-MECO coast-phase events is presented in the following time sequence: (1) First MECO to start of hydrogen venting, T + 572.8 to T + 840 seconds, (2) first phase hydrogen venting, T + 840 seconds to loss of signal at T + 1100 seconds, (3) second-phase hydrogen venting to second MES prestart, T + 1255 to T + 2006 seconds, and (4) second MES prestart through retromaneuver, T + 2006 to T + 3000 seconds.

FIRST MECO T + 572.8 SECONDS TO START OF HYDROGEN VENTING T + 840 SECONDS

The vehicle at MECO was holding a flight-path angle of approximately -0.02 degree in pitch and was rolled counterclockwise approximately 15 degrees. Rates imparted to the vehicle following the MECO transient were -1.0 degree per second in pitch, 0.2 degree per second in yaw, and -0.5 degree per second in roll. Coincident with MECO, the attitude control and ullage engines were enabled. Attitude control engines A-2 and A-4 (see fig. XV-1) were activated immediately and burned for 1.6 seconds to null the roll rate below the 0.2 degree per second threshold. No other attitude control activity was observed until T + 577.8 seconds, approximately 5 seconds after MECO, when a programed change in the guidance-steering equations commanded an 8-degree pitch error (command nose down) and a 1-degree yaw error (command nose left). This maneuver was designed to give the vehicle an attitude parallel with the local horizontal and in the plane of the trajectory. The attitude control jets P-2, A-3, and A-4 responded to guidance commands immediately, and the desired attitude was achieved in 16 seconds.

Throughout the remainder of the controlled coast (to start LH_2 venting at T + 840 sec), sporadic corrections were observed in pitch and roll, and a nearly constant 30-percent duty cycle was observed in yaw (see fig. VI-20). Attitude control operation was more frequent than expected, and was probably due to

(1) Unpredicted propellant behavior

(2) Ullage engine exhaust impinging on the main engine bells and other components in the thrust section

(3) Misalinement of the ullage thrust vector

The 30-percent duty cycle observed from the yaw rate gyro, is shown in sketch (a). The disturbance accelerations, defined as the slope of the curve where the attitude control engines are off, is an indication of the disturbing torques acting on the vehicle. During the controlled coast period, the disturbance accelerations averaged 0.012 degree per second per second with resulting disturbing torques of 100 to 113 inch-pounds, depending on chosen vehicle mass moment of inertia. Ullage motor misalinement and calculated impingement forces can account for only 60 inch-pounds of torque. The vehicle behavior could be characterized by an offset of the center of gravity from the vehicle longitudinal axis of approximately 12 inches. A center-of-gravity shift attributable to propellant location is not stable, and there were no indications of hardware movement. Therefore, motor misalinement beyond design tolerances and attitude control engine thrusts below nominal could account for the rate responses observed.

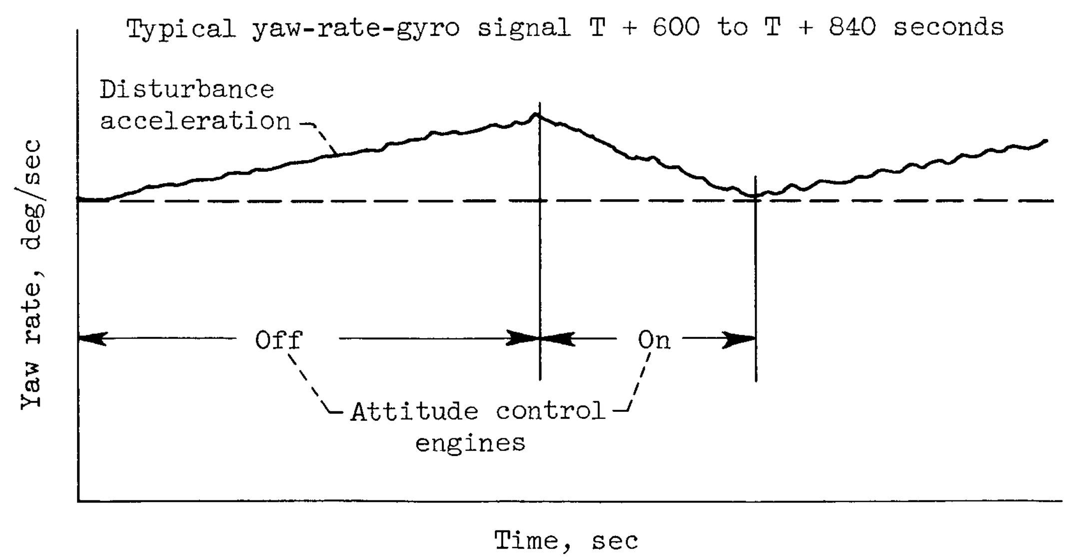

(a)

[redacted]

Termination of Centaur powered flight appeared normal, but immediately on entering the coast phase, the propellant behavior was characterized by a predominant forward movement of LH_2 in the tank. Within 14 seconds following MECO, all instrumented tank surfaces (see fig. VII-9) indicated the presence of LH_2. Forward bulkhead skin temperatures and the LH_2 ullage gas temperature dropped abruptly to LH_2 temperatures within 4.5 seconds after MECO. This effect is shown in figure VII-12. This abnormal behavior of the LH_2 residual has been attributed to the following disturbances, as illustrated in figure XV-2:

(1) Fuel-boost-pump volute bleed spray toward the forward end of the tank during boost-pump coastdown

(2) Hydrogen-duct-recirculation-line spray entering the tank at station 350 on the positive x-axis; this spray is directed across the tank

(3) Residual slosh energy in the fluid at MECO

(4) Springback of the intermediate bulkhead and lower cylindrical section of the tank by thrust termination at MECO

(5) Backflow of mixed-phase hydrogen through the propellant ducting and boost-pump inlet at MECO due to expansion back to tank pressure and temperature of high energy LH_2 between pump and engine inlet valves

The fuel-boost-pump volute bleed-line flow was calculated to be initially about 340 gallons per minute. During pump coastdown, approximately 20 pounds of LH_2 were returned to the tank. Similarly, the hydrogen-duct-recirculation-line return flow was estimated initially at about 50 gallons per minute maximum.

The possible energy inputs to the LH_2 residual from these five disturbing sources have been estimated as shown in the following table.

Source	Energy level, ft-lb
Fuel-boost-pump volute bleed	102
Hydrogen-duct-recirculation line	35
Slosh (10° slosh angle)	35
Bulkhead springback	.126
Backflow from propellant ducts	35

The initial displacement of the LH_2 in the tank by these disturbances, appeared to be a wave moving forward along the positive x-axis and negative y-axis as shown in figure XV-2. The more rapid flow along the positive x-axis was probably quickened by the volute bleed-line discharge, whereas the wetting along the negative y-axis progressed at a slower rate. Generally, this wetting sequence was attributed to spray from the recirculation line hitting the nega-

[redacted]

tive x-axis, dispersing laterally and wetting the negative y-axis in the forward direction. The wave motion then continued over the forward bulkhead and down the positive y-axis as evidenced by the wetting from fore to aft. (There were no sensors on the negative x-axis, so the wetting action on that wall could not be evaluated.)

All temperature sensors remained wet from MECO to until approximately 50 seconds prior to venting. The propellant behavior at this time was uncertain, but there was some evidence of drying toward the forward end of the tank, as sensors on the positive y-axis began drying from the top, as shown in figure XV-3. It may be conjectured that either the ullage motors were beginning to settle the propellants or some local skin drying was occurring (ref. 20).

START OF LH_2 VENTING T + 840 SECONDS TO LOSS OF SIGNAL T + 1100 SECONDS

The LH_2 vent valve was programed in the relief mode at T + 614.4 seconds. Fuel tank pressure at this time was below the valve cracking pressure but by T + 840 seconds had reached the valve cracking pressure. The first indications of hydrogen venting were noted at this time.

The presence of LH_2 at the forward end of the tank, however, resulted in mixed-phase and liquid flow through the vent system. Indicated flow rates were high, and Venturi flow temperature dropped abruptly to LH_2 levels.

Simultaneous with venting was the incipience of an overpowering yaw torque, which exceeded the capabilities of the attitude control system and produced an increasing yaw instability and vehicle spin-up.

A comparison of the predicted vehicle torques due to normal gaseous hydrogen venting with the actual measured results is shown in the following table.

Condition	Vehicle torques, in.-lb		
	Pitch	Yaw	Roll
Inputs due to normal GH_2 venting	0.4	33	2
Attitude control system predicted capability (based on center of gravity at station 343)	228	228	180
Estimated torque inputs from AC-4 flight data (maximum)	500	4500	240

The uncontrollable yaw torque experienced during venting was credited to large lateral impingement forces on the forward bulkhead due to liquid or mixed-phase flow. Calculated lateral forces of 2 to 10 pounds were required to produce the yaw torques noted. The predicted force for pure gaseous venting was only 0.2 pound. Forward bulkhead skin temperatures and the LH_2 ullage temperature, indicating liquid temperatures prior to and during venting, support the evidence of an unknown quantity of LH_2 located in the forward end of the tank. Also, excellent correlation of uncontrolled vehicle rates with vent periods is evident in figure XV-4.

By T + 910 seconds, vehicle roll had increased to ±0.2 degree per second, and yaw had increased to ±0.5 degree per second. At T + 915 seconds, a torquing transient in pitch and roll coupled the yaw steering error into the pitch channel. At this time, the roll rate reversed, and the pitch rate began to increase, reaching ±0.2 degree per second by T + 925 seconds. By T + 1055 seconds, vehicle rates had increased to 2.4 degrees per second in yaw, 0.2 degree per second in pitch, and -1.3 degrees per second in roll.

Hydrogen tank pressure was unsteady but was controlled within limits until about T + 1055 seconds when it began a steady rise. This resulted from a vent flow of increasing liquid quality that was no longer of sufficient volume to relieve tank pressure. The centrifugal force due to the increasing tumbling rates was settling the LH_2 in the forward end of the tank and pure liquid was being vented.

SECOND VENTING PERIOD T + 1225 to T + 2006 SECONDS

Reacquisition of data at T + 1255 seconds, as shown in figure XV-5, indicated that the LH_2 tank pressure, vent flow rates, and vehicle yaw rates were up sharply and increasing steadily. Again the inability of the tank pressure to relieve under high indicated flow rates was further evidence of liquid vent flow, which, in turn, produced an excessive yaw torque to the vehicle.

These rates continued until about T + 1366 seconds when the tank pressure, which had reached 24.2 psia, suddenly started to recover and there was evidence of liquid depletion at the forward end of the tank. Ullage and Venturi gas flow temperature data, shown in figure VII-8(a), show a distinct warming and liquid-to-vapor transition in the character of the vent flow. Complete tank pressure recovery was then accomplished by T + 1455 seconds.

Vehicle motion during this time, obtained from the resolver chain output data, indicated that the vehicle was tumbling predominantly in the yaw plane with a slight nose-high attitude. Yaw rate increased from about 8.5 rpm at T + 1255 seconds to a maximum of about 21 rpm at about T + 1550 seconds. Corresponding pitch and roll rates were not excessive and varied in a random manner. This random nature of the pitch and roll rates is believed to be caused by the buildup and breakaway of solid hydrogen deposits at the vent exit ports. Experimental investigations by the National Bureau of Standards have indicated that solid deposits can build up at vent exits during extended venting of a liquid or a liquid-vapor mixture into a vacuum.

The response of the vehicle to venting was very pronounced as indicated at T + 1350 seconds when depletion of liquid flow rate and transition to gas were coincident with changes in yaw rate (see fig. XV-5). Significantly, however, the vent impingement forces continued to spin-up the vehicle until about

T + 1550 seconds, about 100 seconds after the Venturi flow indicated nominal coast-phase gas flow rate. This lag was attributed to the purging of residual LH_2 in the vent system downstream of the Venturi, and sublimation of possible ice deposits built up on the forward bulkhead.

Once the hydrogen tank pressure and venting were stabilized, the vehicle began to respond to the attitude control system, and the rates started to attenuate slowly by the time of attempted second main engine start. During the total coast-vent period, however, it was estimated that about 960 pounds of LH_2 were vented overboard and only about 120 pounds remained in the tank. Temperature sensors indicated that the forward end of the tank was completely dry; however, tank skin temperature sensors, below station 344 on the positive x-axis, and the boost-pump-inlet temperature remained at liquid level, indicating some slight residual at the bottom of the tank and in the sump.

SECOND ENGINE PRESTART T + 2006 SECONDS TO END OF RETROMANEUVER T + 3000 SECONDS

The prestart sequence for second MES began at approximately T + 2006 seconds, with the vent valve lockup and initiation of tank burp. At this time, however, as shown in figure VII-4(d), the LH_2 tank ullage temperature dropped from approximately -380° to -420° F. Apparently, a small quantity of LH_2 remained in the forward end of the tank and was entrained with the helium pressurizing gas as it blew across the forward bulkhead.

The LH_2 boost-pump start, as shown in figure XV-6, began at about T + 2010 seconds. Boost-pump headrise (ΔP) appeared normal (liquid being pumped) for the first 7 seconds of pump operation. Coincident with a drop in pump-inlet pressures and ullage pressure, the pump headrise became erratic, indicating the occurrence of cavitation or pull-through. By T + 2027 seconds boost-pump headrise had peaked-out at about 25 psid, and ullage pressure had dropped to approximately 14 psia. Within 5 seconds, headrise dropped to 2 psid and boost-pump over-speed trip-out occurred indicating an absence of liquid at the pump inlet.

Liquid hydrogen remaining in the tank by T + 2010 seconds had been reduced drastically because of the liquid venting during coast. This left a considerably large ullage at BPS, with probably a small amount of LH_2 in the aft end of the tank. The decay of the LH_2 ullage pressure at boost-pump start can in all probability be attributed to the cooling of the large ullage by the LH_2 boost-pump volute bleed spray. Calculations of heat-transfer effects show that if all heat to vaporize the sprayed LH_2 is extracted from ullage and the initial ullage temperature is 60° to 65° R, approximately 15 to 17 pounds of LH_2 would be required to produce the pressure drop noted. Calculations based on boost-pump pressure rise, also indicated that the boost pump returned approximately 30 pounds of LH_2 to the tank during this time.

The command for second MES occurred at T + 2049.7 seconds. Insufficient LH_2, as already discussed, was available to sustain boost-pump operation and normal engine start did not occur.

[redacted]

Liquid hydrogen tank pressures remained well below the cracking pressure of vent valve 1 throughout the planned second-engine-burn period. At MECO, LH_2 tank pressure rapidly began to increase at about 2.8 psi per minute. Heat-transfer calculations show that this pressure-rise rate would be associated with a full tank of hydrogen gas. At T + 2385 seconds, the hydrogen tank pressure reached the cracking pressure of the secondary vent valve and relieved momentarily (valve 1 was locked at burp). Two seconds later, the retrothrust signal was commanded, and the engine inlet valves were opened. This allowed the LOX and LH_2 tanks to blow down and should have produced an axial thrust of approximately 30 pounds. Propellant tank pressures should have remained relatively steady during the blowdown, with liquid in the tanks. The absence of residual LH_2, however, resulted in the hydrogen pressure dropping off rather rapidly to 3 psia at T + 3000 seconds. LOX tank pressure, however, remained fairly constant indicating that a quantity of LOX still remained in the tank, and the boil-off was sufficient to maintain pressure. Actual thrust levels produced by the engine blowdown could not be assessed because the data were obscured by the vehicle spinning motion.

Tank pressure recovered gradually on subsequent orbits of the vehicle as they were influenced by solar heating and vehicle position in and out of the Earth's shadow. The vehicle impacted in the South Pacific Ocean after completing 10 orbits.

[redacted]

Engine	Thrust, lb	Function
A-1 A-2 A-3 A-4	1.5 1.5 1.5 1.5	Attitude control
P-1 P-2	3.0 3.0	Attitude control
V-1 V-2	2.0 2.0	Propellant setting

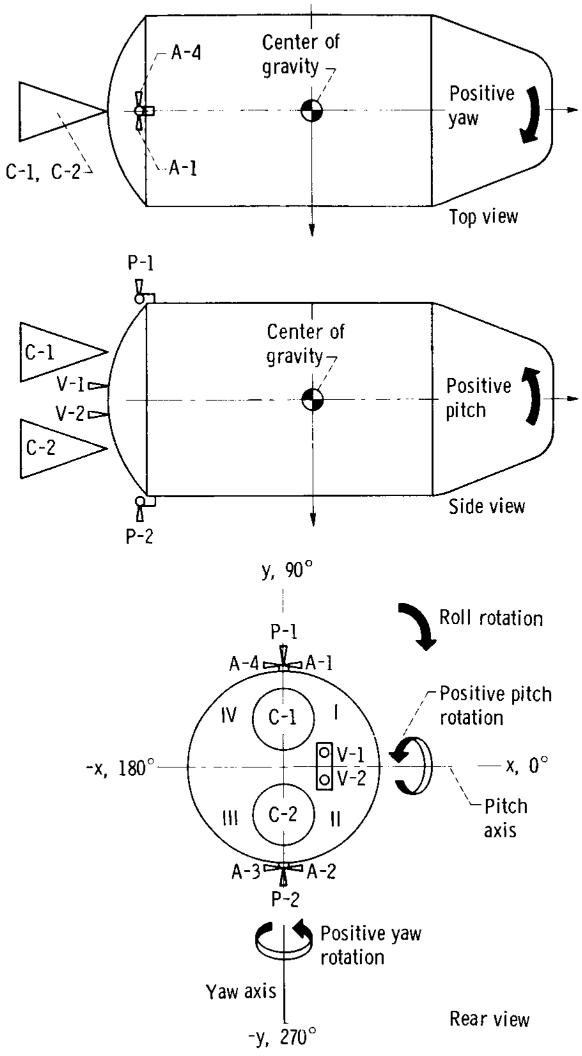

Figure XV-1. - Location of attitude control and propellant settling engines.

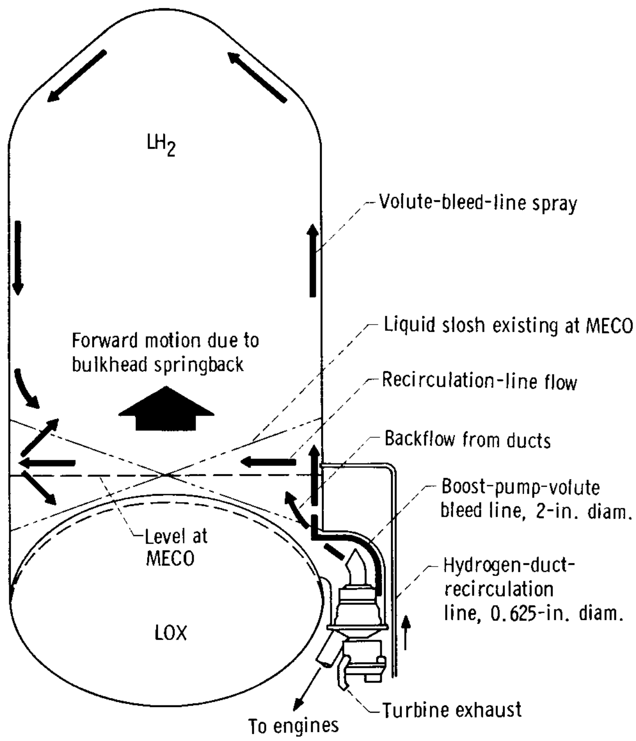

Figure XV-2. - Residual LH_2 motion after MECO.

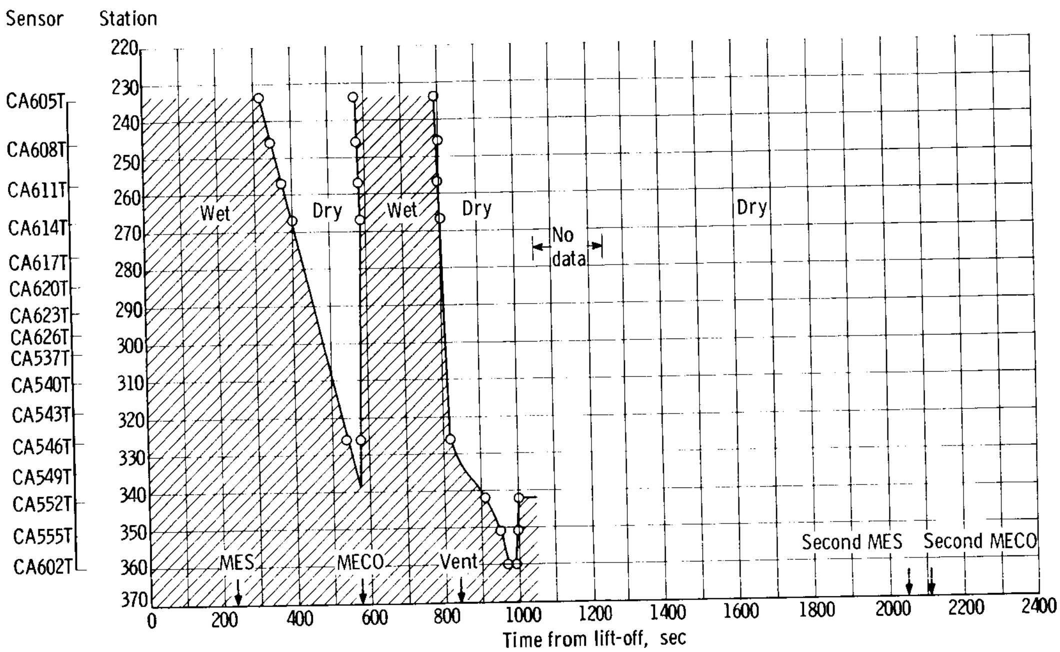

(a) Positive y-axis.

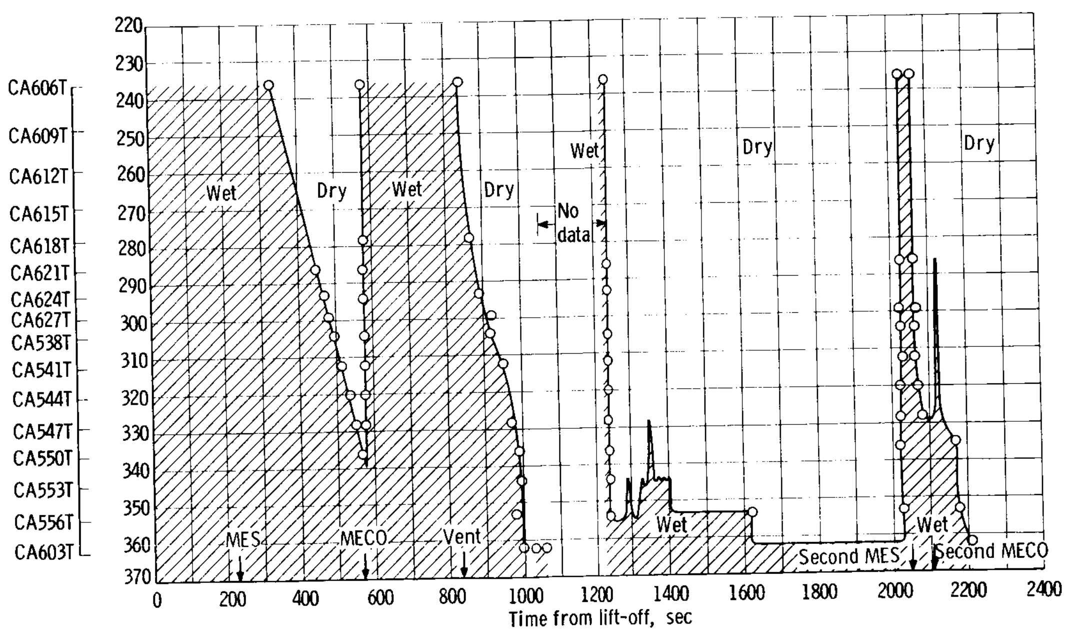

(b) Positive x-axis.

Figure XV-3. - LH_2 tank wall liquid indication.

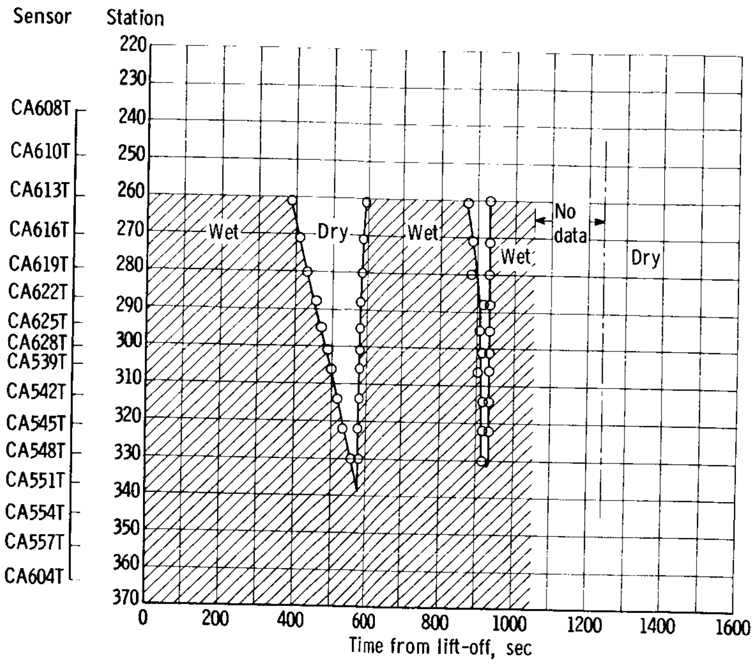

(c) Negative y-axis.

Figure XV-3. - Concluded.

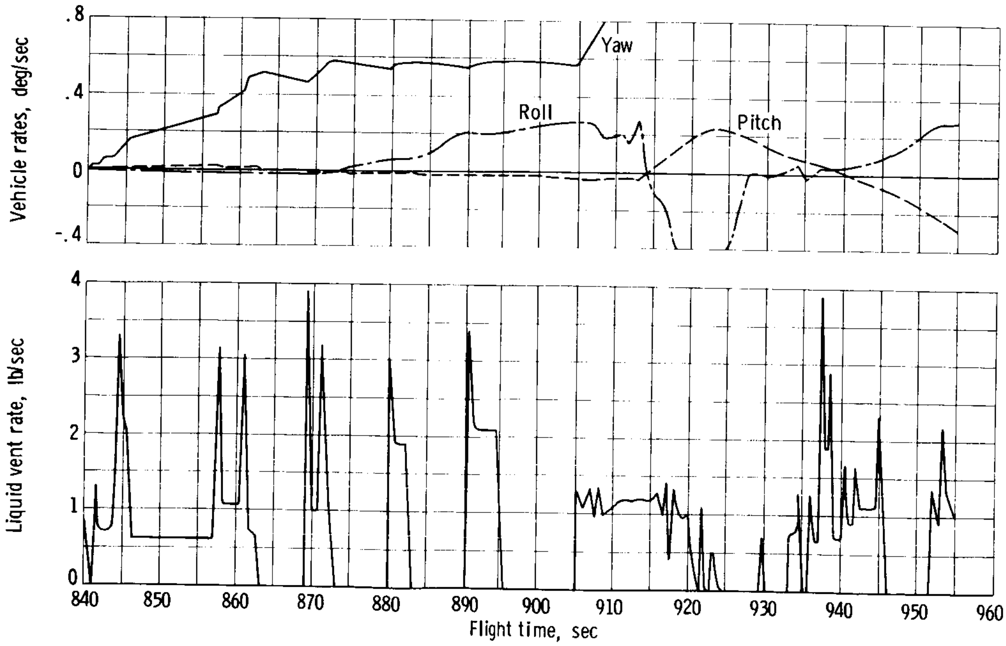

Figure XV-4. - Coast-phase vent and vehicle instability.

[redacted]

[redacted]

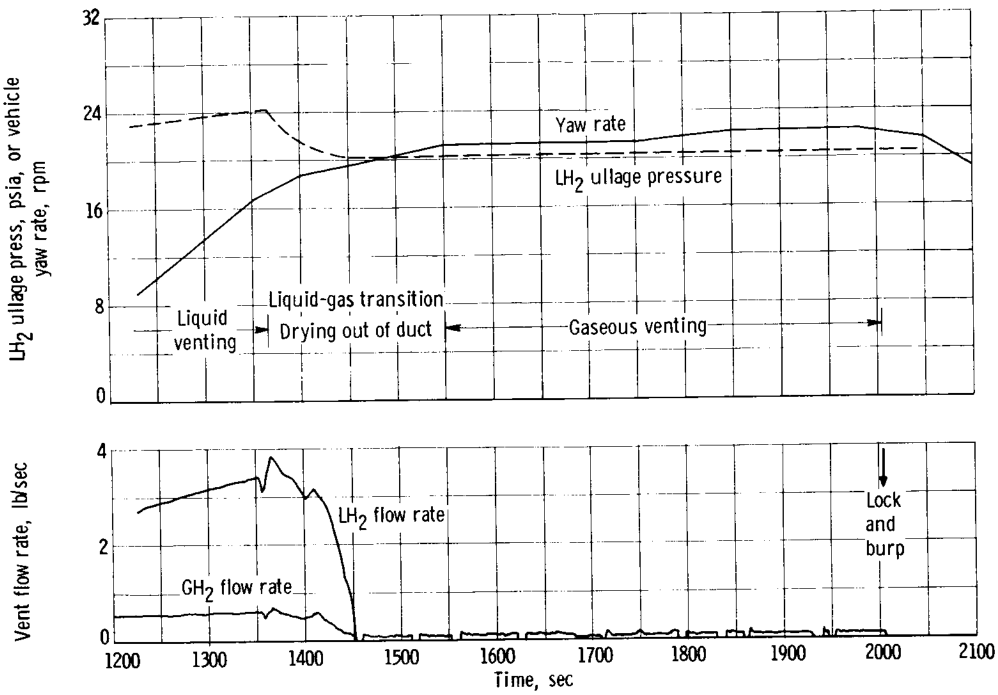

Figure XV-5. - Coast-phase venting and vehicle yaw rate.

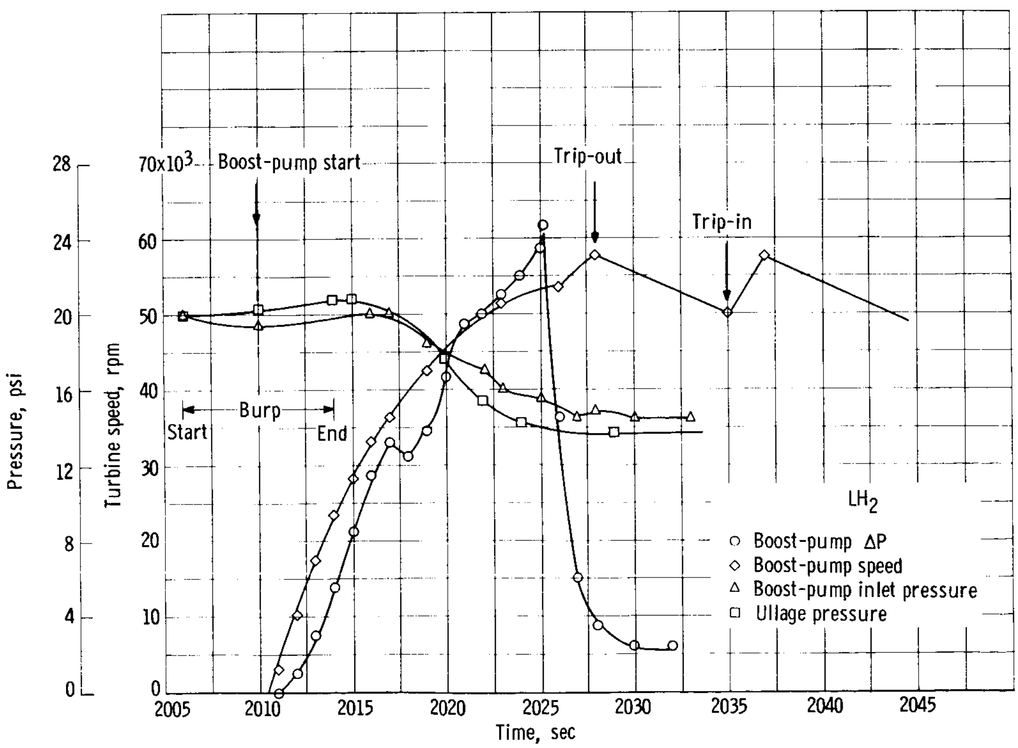

Figure XV-6. - Hydrogen tank pressure and boost-pump performance at second MES.

[redacted]

APPENDIX A

ABBREVIATIONS AND SYMBOLS

ABBREVIATIONS

A/B	automatic tracking of beacon
A-C	Atlas-Centaur
A/C	air conditioning
AFCRL	Air Force Cambridge Research Laboratories
AFETR	Air Force Eastern Test Range
ANT	Antigua
AOS	acquisition of signal
A/P	autopilot
A/S	automatic skin track
a. c.	alternating current
BECO	booster engine cutoff
BET	best estimate of trajectory
BPS	boost pump start
CAPE	Cape Kennedy
CPT	composite readiness test
cps	cycles per second
DEPRO	detailed propulsion simulation of three engines used by Atlas vehicle
DPT	design proof test
d. c.	direct current
EST	Eastern Standard Time
ETR	Eastern Test Range
F-	days prior to launch day

F+	days after launch day
FACT	flight acceptance composite test
GBI	Grand Bahama Island
GD/A	General Dynamics/Astronautics
GH_2	gaseous hydrogen
GLOTRACK	global tracking
GMT	Greenwich Mean Time
GN_2	gaseous nitrogen
GO_2	gaseous oxygen
GSE	guidance support equipment
gal	U.S. gallon
He	helium
H_2O_2	hydrogen peroxide
I/A	interstage adapter
IGS	inertial guidance system
LHe	liquid helium
LH_2	liquid hydrogen
LOX	liquid oxygen
MECO	main engine cutoff
MES	main engine start
NPSH	net pump suction head
NPSP	net pump suction pressure
PAFB	Patrick Air Force Base
PETN	pentaerythritol tetra nitrate
P/L	payload
PLIS	propellant level indicating system

[redacted]

P-P	peak to peak
PU	propellant utilization
ppm	parts per million
psi	pounds per square inch
psia	pounds per square inch absolute
psid	pounds per square inch differential
Q	quadrant
QUAD	quadrant
Q_1, Q_2, Q_3, Q_4	quadrants I, II, III, IV, respectively
RF	radiofrequency
RIS	range instrumentation ship
rms	root mean square
RP-1	rocket propulsion fuel
rpm	revolutions per minute
RSC	range safety command
SANSAL	San Salvador
SECO	sustainer engine cutoff
SPC	Lewis Research Center Space Power Chamber
STL	Space Technology Laboratories
scf	standard cubic feet
scfh	standard cubic feet per hour
T	time of launch
T-	time prior to launch (2-in. motion)
T+	time after launch (2-in. motion)
TCA	temperature control amplifier

[redacted]

TDPU	time delay pickup
TEL	telemetry receiving station
TLM	telemetry
TRW	Thompson Ramo Wooldridge
UHF	ultra high frequency
VECO	vernier engine cutoff
VHF	very high frequency

SYMBOLS

D	drag
E	modulus of elasticity
F	vehicle thrust
g	acceleration due to gravity
$\bar{I}$	specific impulse
k_a	normal operating gain
l	panel length (streamwise)
M	Mach number
$\mathcal{M}$	bending moment
$\mathcal{M}_{tot}$	total bending moment
$\mathcal{M}_{xx}$	pitch plane bending moment
$\mathcal{M}_{yy}$	yaw plane bending moment
q	dynamic pressure
t	skin thickness
W	weight
α	pitch plane angle of attack, deg
β	yaw plane angle of attack, deg

β $\sqrt{M^2 - 1}$

δ cycle amplitude

ω cycle frequency

Subscripts:

gas gas or gaseous

liq liquid

ms mean square

APPENDIX B

TELEMETRY AND INSTRUMENTATION DETAILS

Four VHF telemetry links were carried on the Centaur stage: RF-1, 225.7 megacycles, RF-2, 235.0 megacycles, RF-3, 243.8 megacycles, and RF-4, 251.5 megacycles, all at 4 watts power. Two VHF links were carried on the Atlas booster: RF-1, 229.9 megacycles at 3.5 watts power, and RF-2, 232.4 megacycles at 2.8 watts power. Telemetry coverage from the ETR stations is shown in figure B-1. Continuous coverage was obtained from T - 420 to T + 3030 seconds, with the exception of 91 seconds from T + 1101 to T + 1192. The following ETR stations supported the test:

Station	Location
1	TEL II at Cape Kennedy
3	Grand Bahama Island
7	San Salvador Island
91	Antigua Island
Lima	Timber Hitch, ship located approximately 14.6° N latitude, 42.7° W longitude
12	Ascension Island
Whiskey	Coastal Crusader, ship located approximately 19.0° S latitude, 10.0° E longitude
13	Pretoria
Yankee	Sword Knot, ship located approximately 29.0° S latitude, 53.0° E longitude
Uniform	Twin Falls, ship located approximately 31.0° S latitude, 78.0° E longitude

In addition to coverage by ETR, the four Centaur telemetry links were recorded by the following stations of the Manned Space Flight Network.

Station	Location	Orbits covered	Station	Location	Orbits covered
1	Cape Kennedy	1,2	11	Sword Knot (ship)	1 only
2	Grand Bahama Island	1,2	12	Twin Falls Victory (ship)	1 only
3	Grand Turk Island	1,2	13	Carnarvon	1,2
4	Bermuda	1 only	14	Hawaii	1,2,3,4
5	Antigua	1,2	15	Saint Nicolas	1,2,3,4
6	Timber Hitch (ship)	1 only	16	California	1,2
7	Ascension	1 only	17	Guaymas	1,2,3
8	Coastal Crusader (ship)	1 only	18	White Sands	1 only
9	Pretoria	1 only	19	Texas	1,2
10	Tananarive	1,2,3,4,5	20	Elgin	1 only

The four Centaur links were in operation for a total of 6 hours and 45 minutes. Acquisition was lost on the fifth Earth orbit between Tananarive and Hawaii. Radar and Azusa - GLOTRACK provided additional tracking coverage in addition to the telemetry links (figs. B-2 and 3).

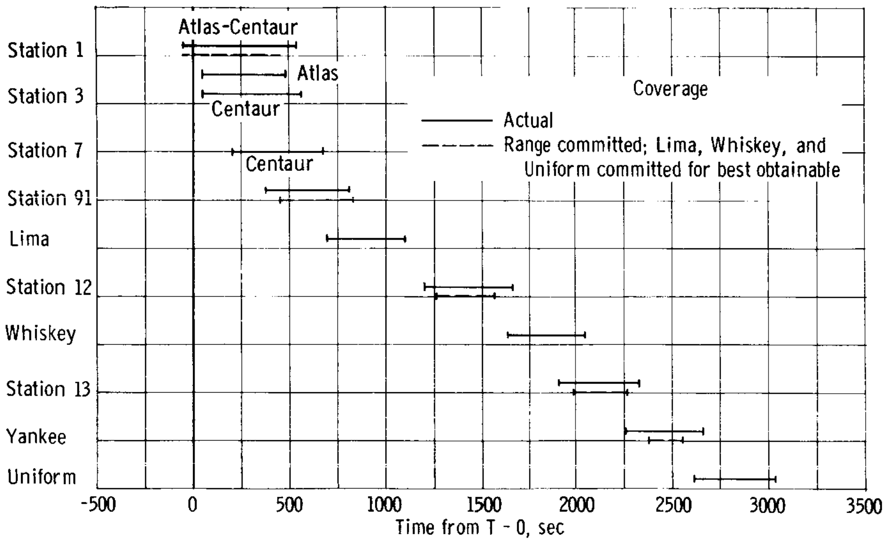

Figure B-1. - Telemetry coverage from Eastern Test Range.

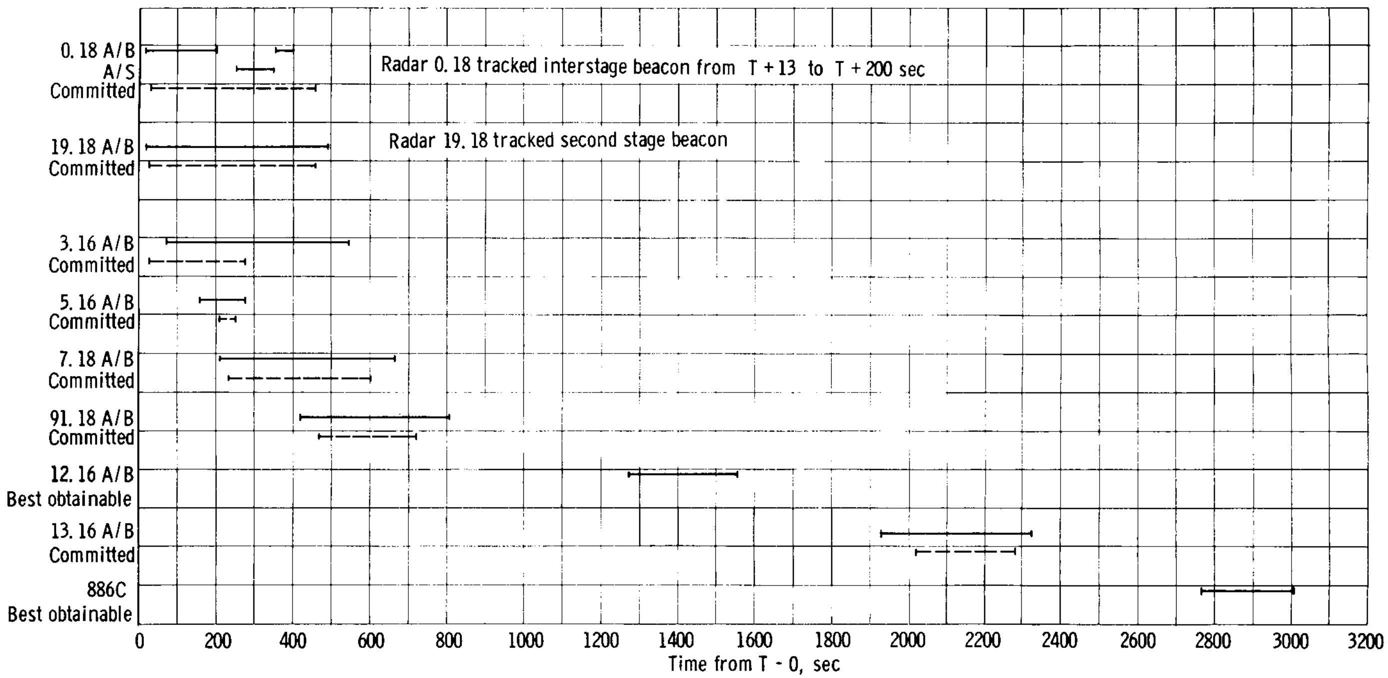

Figure B-2. - Radar coverage intervals.

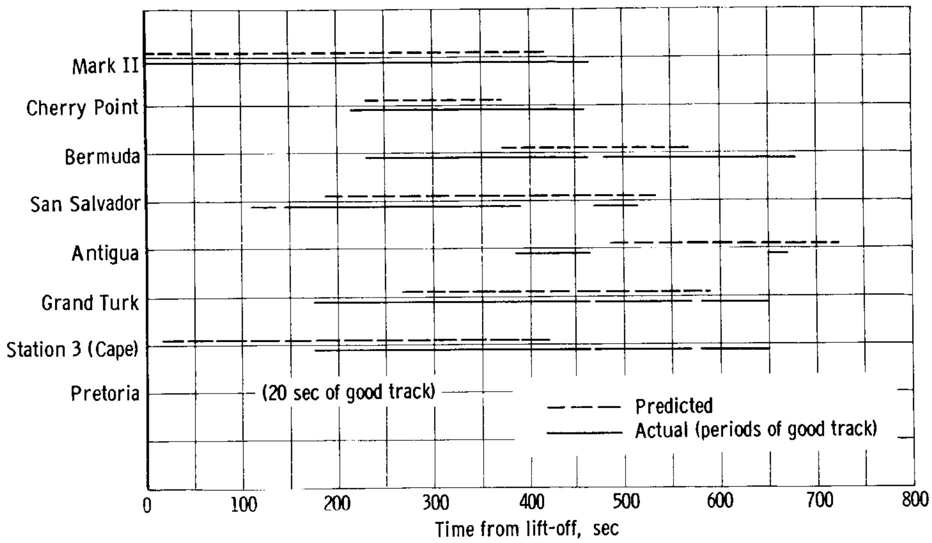

Figure B-3. - Azusa - GLOTRACK coverage.

APPENDIX C

PROPULSION SYSTEM PERFORMANCE TECHNIQUES

The Lewis Venturi technique (LEWP) utilizes three curves based on ground testing to determine Centaur performance. Liquid-hydrogen flow rate is determined from a curve of $\dot{w}_{LH_2}$ as a function of a ratio of fuel Venturi upstream pressure to the square root of fuel turbine inlet temperature. LOX flow is then determined from a curve of mixture ratio as a function of fuel turbine inlet temperature. A curve of the vacuum thrust coefficient as a function of mixture ratio then allows one to determine the propulsion system performance.

The Pratt & Whitney C* Iteration technique (PWAP) determines the fuel flow rate in a manner similar to the LEWP. A value of LOX flow rate is assumed and another value is then calculated utilizing the characteristic exhaust velocity efficiency. Iterations are then used until the value of LOX flow rate assumed is equal to the value calculated. When the values are equal, the ideal specific impulse can be determined from a curve of ideal specific impulse plotted against mixture ratio. Actual specific impulse can then be determined by multiplying the ideal specific impulse times the impulse efficiency for that particular engine. The remainder of the performance values can then easily be determined.

The Pratt & Whitney Regression technique utilizes the engine pump inlet conditions (i.e., pressures and temperatures) and correlates them with a nominal engine performance. The degree to which the engines are off nominal is determined from the engine acceptance data. Combination of these effects determines engine performance.

The DEPRO Program uses the pump inlet conditions, the PU valve setting, and altitude to determine engine performance in a manner similar to the Centaur Regression program.

These four methods are strongly dependent on ground test data.

[redacted]

APPENDIX D

STRUCTURES INSTRUMENTATION

The structural instrumentation consisted of strain gages, pressure and temperature transducers, accelerometers, and angle-of-attack differential pressure transducers. In general, the instrumentation yielded data of acceptable quality. The instrumentation configuration is shown in figures IX-1 and X-1 to 3. Of the strain gages, two at station 402 and one at station 225 were not functional at launch. The necessity of removing the insulation panels to repair these gages rendered this repair impractical. An additional strain gage at station 225 was lost during the flight. All four strain gages at interstage adapter station 548 yielded valid data. One of the two strain gages on the Atlas LOX tank at station 582 was deleted prior to the flight, and the other appeared to drift during the flight. Strain gages on the payload adapter and nose-fairing hinges yielded valid data throughout the flight.

Pressure measurements of prime interest, structurally, were the ullage pressure transducers in each of the four main propellant tanks. In addition, there were pressure surveys of the nose-fairing and insulation panels. Valuable data were obtained from these transducers.

The AC-4 flight trajectory was aerodynamically "hotter" than the AC-3 flight, and there were many thermocouples on the vehicle for temperature survey of critical areas on the vehicle. In general, good coverage was achieved, and valuable data were retrieved.

Accelerometers and high-frequency fluctuating pressure transducers located at various points on the interstage adapter were reading throughout the flight. Reasonable data were obtained, and there were no apparent failures in these transducers. The differential-pressure angle-of-attack transducers appeared to yield valid data. The associated dynamic pressure measurement, however, did not yield usable data. As dynamic pressure can be accurately determined from tracking and atmospheric data, loss of this measurement was of little consequence.

[redacted]

APPENDIX E

SYMBOLS AND DETAILED LISTING OF TRAJECTORY RECONSTRUCTION FOR AC-4 FLIGHT

	DESCRIPTIONS
TIME	elapsed time from lift-off
WEIGHT	total weight of vehicle
TOTAL FLOW	total weight flow
GRND RANGE	ground-range great-circle distance (spherical earth, R_o = 3443.9 n. mi.) from launch pad to vehicle subpoint
THETA I	inertial range angle, measured between launch radius vector and present radius vector
Q*ALPHA	product of ALPHA and dynamic pressure
ALTITUDE	altitude above oblate spheroidal earth
RADIUS	magnitude of radius vector from Earth center to vehicle
VEL E	magnitude of velocity with respect to Earth
VEL R	magnitude of velocity with respect to air
VEL I	magnitude of velocity in inertial system
Q*BETA	product of BETA and dynamic pressure
ALPHA	angle of attack in pitch (XI, ZETA) plane positive for ship above relative velocity vector, V_R
BETA	angle of attack in yaw (XI, ETA) plane positive for ship left of relative velocity vector, V_R
PSI	inertial attitude angle, measure of angle between ship longitudinal axis and inertial u-v plane, positive above plane
PSIDOT	time rate of change of PSI
CROSS RANGE	minimum ground distance from vehicle subpoint to plane formed by launch vertical vector and launch down-range vector
DOWN RANGE	distance from vehicle subpoint to launch site along Great Circle at 100.5° azimuth through launch site
GEOCENT LAT	geocentric latitude, degrees north of equator

LONGITUDE	degrees from Greenwich, positive east
AZI E	azimuth of VEL E, angle between projection of VEL E into azimuth plane (plane perpendicular to radius vector) and north direction, positive clockwise from north
AZI R	azimuth of VEL R
AZI I	azimuth of VEL I
PHI	inertial attitude angle - angle between projection of minus ZETA axis in u-v plane and the u-axis
THRUST FIXED	fixed thrust magnitude - nongimbaled engines thrust
THRUST CONTL	controlled thrust magnitude - gimbaled engines
GAMMA E	flight path angle of VEL E, measured angle between velocity vector and local horizontal, positive above horizontal
GAMMA R	flight path angle of VEL R
GAMMA I	flight path angle of VEL I
EAST WIND	magnitude of wind velocity component from east
AXL FORCE	aerodynamic force along longitudinal axis, XI
SIDE FORCE	aerodynamic force along side axis, ETA
NORM FORCE	aerodynamic force normal to vehicle along ZETA
AXL LD FCTR	instantaneous value of thrust-drag/weight
WIND VEL	magnitude of wind velocity
NORTH WIND	magnitude of wind velocity component from north
ATM PRESS	atmospheric (ambient) pressure
DYNM PRESS	dynamic pressure, $\frac{1}{2} \rho_a V_r^2$
HEAT PARAM	heating parameter, integrated product of air density and relative velocity squared divided by time
MACH NUMBER	Mach number, ratio of VEL R and local speed of sound
RHO-VR CUBED	product of air density and VEL R cubed
TOTAL ISP	instantaneous quotient of total axial thrust by total flow

[redacted]

DETAILED PROPULSION (DEPRO) DESCRIPTIONS

THRUST (I)	total thrust of booster, sustainer or vernier engines, respectively (vernier gimbaled)
THRUST TOT	total thrust of all engines
THRUST CORR (B)	booster thrust correction for nonlinearities of model
THRUST CORR (S)	sustainer thrust correction, due to propellant-utilization-system effects
PC(B)	effective chamber pressure of booster engines
FUEL FLOW (I)	total fuel flow of booster, sustainer or vernier engines, respectively; vernier flow included in sustainer
FUEL FLOW TOT	total fuel flow for all engines
F FLOW CORR (B)	booster fuel flow correction (nonlinear)
F FLOW CORR (S)	sustainer fuel flow correction (PU)
PC(S)	effective chamber pressure of sustainer engine
OXID FLOW (I)	total LOX flow of booster, sustainer or vernier engines, respectively; vernier flow included in sustainer
OXID FLOW TOT	total LOX flow for all engines
O FLOW CORR (B)	booster LOX flow correction (nonlinear)
O FLOW CORR (S)	sustainer LOX flow correction (PU)
PC(V)	effective chamber pressure of vernier engines
FP INLTP (I)	fuel pump inlet pressure, booster or sustainer
FUEL DENSITY	fuel density
OXID DENSITY	LOX density based on telemetry measurements
MIX RATIO (B)	ratio of LOX to fuel-booster
MIX RATIO (S)	ratio of LOX to fuel-sustainer
OP INLTP (I)	LOX pump inlet pressure, booster or sustainer
FUEL WEIGHT	weight of fuel above sustainer pump inlet
OXID WEIGHT	weight of LOX above sustainer pump inlet

[redacted]

AXL LD FCTR	axial load factor, required by propulsion model to calculate effect of headrise on pump inlet conditions
CAP RATIO (PU)	capacitance output from fuel manometer divided by capacitance output from oxidizer manometer; this ratio is calculated from telemetry values of PU valve angle position
OIL WEIGHT (I)	weight of lubrication oil remaining, booster or sustainer
FUEL LEVEL	height of fuel above sustainer pump inlet
OXID LEVEL	height of LOX above sustainer pump inlet
NPSH	net positive suction head of sustainer LOX pump
VALVE ANGLE (PU)	propellant utilization fuel valve angle, value used from telemetry
ATM PRESS	atmosphere (ambient) pressure
VAPOR PRESS	vapor pressure of LOX
FUEL TNK PR (G)	gage pressure of fuel tank (telemetry)
OXID TNK PR (G)	gage pressure of LOX tank (telemetry)
ACS ITER	internal counter

CENTAUR DESCRIPTIONS

THRUST	total Centaur thrust
LH2 FLOW	total LH_2 flow
LO2 FLOW	total LO_2 flow
RATIO	ratio LO_2/LH_2
C-1 THRUST	thrust of C-1 engine
C-1 LH2 FLOW	LH_2 flow for C-1 engine
C-1 LO2 FLOW	LO_2 flow for C-1 engine
C-1 RATIO	ratio LO_2/LH_2 for C-1 engine
C-2 THRUST	thrust of C-2 engine
C-2 LH2 FLOW	LH_2 flow for C-2 engine

C-2 LO2 FLOW	LO_2 flow for C-2 engine
C-2 RATIO	ratio LO_2/LH_2 for C-2 engine
LH2 WEIGHT	weight of LH_2
LO2 WEIGHT	weight of LO_2
C-1 LH2 PRESS	pump inlet pressure for C-1 engine LH_2 (telemetry)
C-2 LH2 PRESS	pump inlet pressure for C-2 engine LH_2 (telemetry)
C-1 ISP	specific impulse of C-1 engine equals C-1 thrust/C-1 flow
C-1 FLOW	total propellant flow for C-1 engine
C-1 LO2 PRESS	pump inlet pressure for C-1 engine LO_2 (telemetry)
C-2 LO2 PRESS	pump inlet pressure for C-2 engine LO_2 (telemetry)
C-2 ISP	specific impulse of C-2 engine equals C-2 thrust/C-2 flow
C-2 FLOW	total propellant flow for C-2 engine
C-1 LH2 TEMP	pump inlet temperature for C-1 engine LH_2 (telemetry)
C-2 LH2 TEMP	pump inlet temperature for C-2 engine LH_2 (telemetry)
C-1 PU VALVE	propellant utilization valve setting (not in use)
C-2 PU VALVE	propellant utilization valve setting (not in use)
C-1 LO2 TEMP	pump inlet temperature for C-1 engine LO_2 (telemetry)
C-2 LO2 TEMP	pump inlet temperature for C-2 engine LO_2 (telemetry)

ORBIT ELEMENTS DESCRIPTIONS

PERIGEE RAD	radius at perigee of instantaneous conic
APOGEE RAD	radius at apogee of instantaneous conic
PERIGEE ALT	perigee altitude (above spherical Earth with radius = 3443.9 n. mi.)
APOGEE ALT	apogee altitude (above spherical Earth with radius = 3443.9 n. mi.)
PERIGEE VEL	velocity at perigee

APOGEE VEL	velocity at apogee
SEMI LAT REC	semilatus rectum
PERIOD	period
SEMI MAJ AXIS	semimajor axis
ENERGY	energy, $v^2/2 - \mu/r$
ECCENTRICITY	orbit eccentricity
INCLINATION	orbital inclination
TRUE ANOMALY	true anomaly
ASCEND NODE	ascending node

[redacted]

Listing

```
0 1  TIME               ALTITUDE           ALPHA              GEOCENT LAT        THRUST FIXED       AXL FORCE          ATM PRESS
P 2  WEIGHT             RADIUS             BETA               LONGITUDE          THRUST CONTL       SIDE FORCE         DYNM PRESS
1 3  TOTAL FLOW         VEL E              PSI                AZI E              GAMMA E            NORM FORCE         HEAT PARAM
  4  GRND RANGE         VEL R              PSIDOT             AZI R              GAMMA R            AXL LD FCTR        MACH NUMBER
  5  THETA I            VEL I              CROSS RANGE        AZI I              GAMMA I            WIND VEL           RHO-VR CUBED
  6  Q*ALPHA TOT        ALT                DOWN RANGE         PHI                EAST WIND          NORTH WIND         TOTAL ISP

0 1  SEC                FT                 DEG                DEG                LBS                LBS                PSI
P 2  LBS                FT                 DEG                DEG                LBS                LBS                LBS/FT SQD
1 3  LBS/SEC            FT/SEC             DEG                DEG                DEG                LBS                FT*LBS/FT SQD
  4  N. MI.             FT/SEC             DEG/SEC            DEG                DEG
  5  DEG                FT/SEC             N.MI.              DEG                DEG                FT/SEC             LBS/SEC CUBED
  6  DEG-PSF            N.MI               N.MI.              DEG                FT/SEC             FT/SEC             SEC

D 1  THRUST (B)         FUEL FLOW (B)      OXID FLOW (B)      FP INLTP (B)       OP INLTP (B)       OIL WEIGHT (B)     ATM PRESS
E 2  THRUST (S)         FUEL FLOW (S)      OXID FLOW (S)      FP INLTP (S)       OP INLTP (S)       OIL WEIGHT (S)     VAPOR PRESS
P 3  THRUST (V)         FUEL FLOW (V)      OXID FLOW (V)      FUEL DENSITY       FUEL WEIGHT        FUEL LEVEL         FUEL TNK PR (G)
R 4  THRUST TOT         FUEL FLOW TOT      OXID FLOW TOT      OXID DENSITY       OXID WEIGHT        OXID LEVEL         OXID TNK PR (G)
0 5  THRUST CORR (B)    F FLOW CORR (B)    O FLOW CORR (B)    MIX RATIO (B)      AXL LD FCTR        NPSH               ACS ITER
  6  THRUST CORR (S)    F FLOW CORR (S)    O FLOW CORR (S)    MIX RATIO (S)      CAP RATIO (PU)     VALVE ANGLE (PU)
  7  PC(B)              PC(S)              PC(V)

D 1  LBS                LBS/SEC            LBS/SEC            PSI                PSI                LBS                PSI
E 2  LBS                LBS/SEC            LBS/SFC            PSI                PSI                LBS                PSI
P 3  LBS                LBS/SEC            LBS/SEC            LBS/CUBIC FT       LBS                INCHES             PSI
R 4  LBS                LBS/SEC            LBS/SEC            LBS/CUBIC FT       LBS                INCHES             PSI
0 5  LBS                LBS/SEC            LBS/SEC                                                  FEET
  6  LBS                LBS/SEC            LBS/SEC                                                  DEG
  7  PSIA               PSIA               PSIA

0 1  THRUST XI          DEL XI-ETA         CG XI              CP NORM            AERO MOM XI        INERTIA XI         INERTIA XI-ETA
P 2  THRUST ETA         DEL XI-ZETA        CG ETA             CP SIDE            AERO MOM ETA       INERTIA ETA        INERTIA ETA-ZETA
5 3  THRUST ZETA                           CG ZETA                               AERO MOM ZETA      INERTIA ZETA       INERTIA XI*ZETA

0 1  LBS                DEG                INCHES             INCHES             FT-LBS             SLUG-FT SQD        SLUG-FT SQD
P 2  LBS                DEG                INCHES             INCHES             FT-LBS             SLUG-FT SQD        SLUG-FT SQD
5 3  LBS                                   INCHES                                FT-LBS             SLUG-FT SQD        SLUG-FT SQD

0*1  0                 -91.250000          90.061818          28.310592          56915.743         -52.123972          14.826744
P 2  302958.09          0.2090977E 08      90.261275         -80.537986          306155.89          357.99565          0.7187242
1 3  1502.2778          0.4925779E-04      89.958259          93.055058         -1.3868513          279.99281          0
  4  0.4200749E-04      24.830520          0                  118.32658         -0.9536743E-06      1.1982455          0.2192946E-01
  5  0.7002325E-06      1342.3866          0.4100833E-04      89.999999          0.9536743E-06      24.830523          1148.3735
  6  64.641945         -0.1501782E-01      0.9107653E-05     -0                  21.857250         -11.781998          241.58075

D 1  306155.89          381.26722          844.22995          71.661651          58.596910          166.00000          14.826744
E 2  55205.240          95.715529          179.74974          71.675674          64.274861          53.000000          27.166583
P 3  1710.5033          0                  0                  50.350000          75673.645          939.21946          58.673256
R 4  363071.63          476.98275          1023.9797          69.089998          171829.45          553.51569          29.973255
0 5 -55.678170          0.3168766E-01      0.7102200E-01      2.2142736          1.1982456          77.342275          5.0000000
  6 -1201.7500          11.362500         -10.005000          1.8779579          0.4543835          17.050000
  7  545.94617          675.46138          308.03659

0 1  363070.31          0.9279586E-01      798.06546          295.29673          0                  0                  0
P 2  588.02676          0.1075579          0.5000727          624.75014         -140475.43          0                  0
5 3  681.57074                             0.3901455                             61843.021          0                  0
```

[redacted]

[redacted]

O*1	4.0000000	-37.500000	43.251799	28.310595	57973.454	-120.33050	14.799522
P 2	296950.82	0.2090982E 08	11.753529	-80.537987	306270.54	116.61164	1.7112475
1 3	1502.0187	27.645402	89.958259	35.723422	88.905410	321.61862	127.12028
4	0.1453601E-03	38.336825	0	117.37070	46.136042	1.2262042	0.3386900E-01
5	0.1471308E-01	1342.3664	-0.8717471E-04	89.981698	1.1798458	27.037348	4221.4733
6	75.183669	-0.6171706E-02	-0.1163197E-03	-0.1407989E-01	23.899750	-12.641998	242.50297
O 1	306270.54	381.23307	844.39242	71.601823	58.728700	161.75200	14.799522
E 2	56262.492	77.564855	197.51294	71.648840	64.431741	52.400000	27.195572
P 3	1710.9615	0	0	50.350000	73817.622	944.27941	58.620477
R 4	364243.99	458.79793	1041.9053	69.085999	167683.47	563.57880	29.920477
O 5	-55.039693	0.3132678E-01	0.7020308E-01	2.2148981	1.2262043	77.613531	92.000000
6	-187.50000	-6.7875000	7.7687500	2.5464231	0.4332724	-5.7500000	
7	545.98455	684.07923	308.11824				
O 1	364242.68	0.7765813E-01	800.50975	296.77995	0	0	0
P 2	493.69120	0.1167417	0.5027886	624.74997	-161303.63	0	0
5 3	742.15551		0.3955773		20012.038	0	0
O*1	4.0000000	-37.500000	43.251799	28.310595	57973.454	-120.33050	14.799522
P 2	296950.82	0.2090982E 08	11.753529	-80.537987	306270.54	116.61164	1.7112475
1 3	1502.0187	27.645402	89.958259	35.723422	88.905410	321.61862	127.12028
4	0.1453601E-03	38.336825	0	117.37070	46.136042	1.2262042	0.3386900E-01
5	0.1471308E-01	1342.3664	-0.8717471E-04	89.981698	1.1798458	27.037348	4221.4733
6	75.183669	-0.6171706E-02	-0.1163197E-03	-0.1407989E-01	23.899750	-12.641998	242.50297
O 1	306270.54	381.23307	844.39242	71.601823	58.728700	161.75200	14.799522
E 2	56262.492	77.564855	197.51294	71.648840	64.431741	52.400000	27.195572
P 3	1710.9615	0	0	50.350000	73817.622	944.27941	58.620477
R 4	364243.99	458.79793	1041.9053	69.085999	167683.47	563.57880	29.920477
O 5	-55.039693	0.3132678E-01	0.7020308E-01	2.2148981	1.2262043	77.613531	93.000000
6	-187.50000	-6.7875000	7.7687500	2.5464231	0.4332724	-5.7500000	
7	545.98455	684.07923	308.11824				
O 1	364242.68	0.7765813E-01	800.50975	296.77995	0	0	0
P 2	493.69120	0.1167417	0.5027886	624.74997	-161303.63	0	0
5 3	742.15551		0.3955773		20012.038	0	0
O*1	9.9999995	268.25000	26.180427	28.310607	58397.476	-521.33038	14.644578
P 2	287943.00	0.2091012E 08	6.2403026	-80.538001	306813.29	301.93003	8.2445369
1 3	1501.2416	75.487277	89.958259	47.078975	88.613931	939.65301	1853.0061
4	0.1221043E-02	84.431787	0	115.48315	63.354804	1.2665183	0.7473296E-01
5	0.3677118E-01	1343.1943	-0.7016430E-03	89.946897	3.2207670	39.610443	44792.542
6	220.39307	0.4414827E-01	-0.9993261E-03	1.8398001	35.518250	-17.533997	243.27247
O 1	306813.29	381.13428	844.65602	71.378935	58.911666	155.38000	14.644578
E 2	56683.774	84.729915	189.40604	71.473526	64.650872	51.500000	27.238899
P 3	1713.7015	0	0	50.350000	71036.073	954.75837	58.655320
R 4	365210.76	465.86419	1034.0621	69.079999	161465.09	577.35162	29.955321
O 5	-53.745587	0.3059533E-01	0.6854325E-01	2.2161639	1.2665184	77.986742	159.00000
6	-10.500000	0.3850000	-0.2800000	2.2354093	0.4389206	0.3500000	
7	546.03465	685.51493	308.60649				
O 1	365206.43	0.9115318E-01	804.17495	297.03846	0	0	0
P 2	581.01583	0.2387279	0.5068611	624.74998	-473134.56	0	0
5 3	1521.6733		0.4037221		51843.890	0	0

[redacted]

[redacted]

0*1	12.000000	436.50000	23.281729	28.310615	58539.169	-724.76434	14.559156
P 2	284940.61	0.2091029E 08	5.8114239	-80.538012	307085.63	407.55024	11.931165
1 3	1501.1115	93.195109	89.958259	50.312367	88.427876	1210.3853	3747.5206
4	0.1936244E-02	101.78689	0	115.60937	66.240683	1.2805956	0.9015506E-01
5	0.4411875E-01	1343.6864	-0.1049426E-02	89.930244	3.9756012	43.494069	78146.536
6	284.59703	0.7183866E-01	-0.1627198E-02	2.4577603	38.948916	-19.357580	243.56937

D 1	307085.63	381.10081	844.64622	71.267525	58.898641	153.25600	14.559156
E 2	56823.944	84.538621	189.51052	71.378728	64.650476	51.200000	27.253345
P 3	1715.2257	0	0	50.350000	70104.423	957.60506	58.640843
R 4	365624.79	465.63943	1034.1567	69.077999	159396.98	581.93417	29.920844
0 5	-53.572914	0.3049773E-01	0.6832178E-01	2.2163328	1.2805957	77.958060	181.00000
6	-5.4000000	0.1980000	-0.1440000	2.2417035	0.4387632	0.1800000	
7	546.02013	685.52077	308.87811				

0 1	365618.47	0.9868998E-01	805.39658	297.26066	0	0	0
P 2	629.76568	0.2924176	0.5082184	624.74997	-610123.11	0	0
5 3	1866.0049		0.4064369		70250.822	0	0

0*1	12.000000	436.50000	23.281729	28.310615	58539.169	-724.76434	14.559155
P 2	284940.61	0.2091029E 08	5.8114239	-80.538012	307085.63	407.55024	11.931165
1 3	1501.1115	93.195109	89.958259	50.312367	88.427876	1210.3853	3747.5206
4	0.1936244E-02	101.78689	0	115.60937	66.240683	1.2805956	0.9016506E-01
5	0.4411875E-01	1343.6864	-0.1049426E-02	89.930244	3.9756012	43.494069	78146.536
6	284.59703	0.7183866E-01	-0.1627198E-02	2.4577603	38.948916	-19.357580	243.56937

D 1	307085.63	381.10081	844.64622	71.267525	58.898641	153.25600	14.559155
E 2	56823.944	84.538621	189.51052	71.378728	64.650476	51.200000	27.253345
P 3	1715.2257	0	0	50.350000	70104.423	957.60506	58.640843
R 4	365624.79	465.63943	1034.1567	69.077999	159396.98	581.93417	29.920844
0 5	-53.572914	0.3049773E-01	0.6832178E-01	2.2163328	1.2805957	77.958060	182.00000
6	-5.4000000	0.1980000	-0.1440000	2.2417035	0.4387632	0.1800000	
7	546.02013	685.52077	308.87811				

0 1	365618.47	0.9868998E-01	805.39653	297.26066	0	0	0
P 2	629.76568	0.2924176	0.5082184	624.74997	-610123.11	0	0
5 3	1866.0049		0.4064369		70250.822	0	0

0*1	15.000000	757.75000	17.794609	28.310632	58796.840	-1067.5041	14.395144
P 2	280437.42	0.2091061E 08	4.9992250	-80.538034	307616.54	550.12414	18.665817
1 3	1501.0472	121.51217	89.958259	53.339885	88.165822	1451.2663	8988.4994
4	0.3504751E-02	127.91413	0	117.49613	71.707113	1.3027411	0.1134188
5	0.5513243E-01	1344.8170	-0.1716735E-02	89.900731	5.1814213	43.993009	153638.69
6	343.46268	0.1247096	-0.3055513E-02	2.4472004	38.734750	-20.856746	244.10517

D 1	307616.54	381.04728	844.65148	71.104920	58.897232	150.07000	14.395144
E 2	57078.679	83.425383	190.60765	71.242257	64.668935	50.750000	27.275013
P 3	1718.1613	0	0	50.350000	68709.209	961.81791	58.654855
R 4	366413.37	464.47266	1035.2591	69.074999	156292.94	588.74579	29.904855
0 5	-53.240484	0.3030984E-01	0.6789540E-01	2.2166579	1.3027411	77.954756	223.00000
6	-11.800000	-0.9080000	1.0080000	2.2847680	0.4378187	-0.8400000	
7	546.00555	685.41220	309.40121				

0 1	366404.86	0.1090532	807.18505	297.95220	0	0	0
P 2	697.39294	0.3406690	0.5109870	624.74998	-731339.82	0	0
5 3	2178.5941		0.4109870		95086.976	0	0

[redacted]

[redacted]

0*1	15.000000	757.75000	17.794609	28.310632	58796.840	-1067.5041	14.395144
P 2	280437.42	0.2091061E 08	4.9992250	-80.538034	307616.54	550.12414	18.665817
1 3	1501.0472	121.51217	89.958259	53.339885	88.165822	1451.2663	8988.4994
4	0.3504751E-02	127.91413	0.4580341	117.49613	71.707113	1.3027411	0.1134188
5	0.5513243E-01	1344.8170	-0.1716735E-02	89.900731	5.1814213	43.993009	153638.69
6	343.46268	0.1247096	-0.3055518E-02	2.4472004	38.734750	-20.856746	244.10517
D 1	307616.54	381.04728	844.65148	71.104920	58.897232	150.07000	14.395144
E 2	57078.679	83.425383	190.60765	71.242257	64.668935	50.750000	27.275013
P 3	1718.1613	0	0	50.350000	68709.209	961.81791	58.654855
R 4	366413.37	464.47266	1035.2591	69.074999	156292.94	588.74579	29.904856
O 5	-53.240484	0.3030984E-01	0.6789540E-01	2.2166579	1.3027411	77.954756	224.00000
6	-11.800000	-0.9080000	1.0080000	2.2847680	0.4378187	-0.8400000	
7	546.00555	685.41220	309.40121				
O 1	366404.86	0.1090532	807.18505	297.95220	0	0	0
P 2	697.39294	0.3406690	0.5109870	624.74998	-731339.82	0	0
5 3	2178.5941		0.4109870		95086.976	0	0
0*1	19.999999	1493.0000	11.021464	28.310669	59392.158	-1821.2031	14.023922
P 2	272932.63	0.2091135E 08	4.3305321	-80.538079	308833.38	916.81052	35.793216
1 3	1500.8699	173.56931	87.668088	24.103556	88.968763	1732.7652	29592.251
4	0.6747345E-02	178.72519	0.4580341	120.10998	76.166508	1.3424285	0.1591239
5	0.7348515E-01	1352.3936	-0.3381899E-02	89.878240	7.3726120	45.305088	411643.75
6	422.48086	0.2457162	-0.5838644E-02	2.4296005	38.244584	-24.287913	245.34141
D 1	308833.38	380.94954	844.69909	70.841620	58.932411	144.76000	14.023922
E 2	57667.327	82.799020	191.10685	71.025792	64.739722	50.000000	27.311123
P 3	1724.8316	0	0	50.350000	66389.713	968.78267	58.776076
R 4	368225.54	463.74855	1035.8059	69.069999	151114.23	600.11153	29.976077
O 5	-52.531207	0.2990894E-01	0.6698568E-01	2.2173516	1.3424286	78.032696	260.00000
6	-18.500000	-1.5200000	1.6200000	2.3080811	0.4373465	-1.3500000	
7	545.99594	685.26928	310.58982				
O 1	368213.76	0.1362907	809.65372	298.99172	0	0	0
P 2	875.87979	0.3969024	0.5241533	624.74998	-870106.02	0	0
5 3	2550.7508		0.4241533		159406.53	0	0
0*1	29.999999	3825.2500	4.2883117	28.310714	61188.325	-3782.3665	12.901624
P 2	257928.94	0.2091368E 08	3.0184122	-80.537758	312423.99	1745.6391	96.746240
1 3	1499.9183	298.73544	83.087747	91.378385	84.624528	1844.7195	186353.73
4	0.1404133E-01	303.40326	0.4580341	117.44130	78.604037	1.4337883	0.2727490
5	0.1105509	1402.5142	-0.9712383E-02	90.026930	12.243291	36.937368	1888814.8
6	506.71994	0.6295552	0.1014046E-01	2.3944007	25.225064	-26.982685	249.08844
D 1	312423.99	380.60309	844.49197	69.737778	58.664560	134.14000	12.901624
E 2	59443.329	82.181011	191.32688	70.029760	64.553849	48.500000	27.383354
P 3	1744.9970	0	0	50.350000	61754.564	982.70925	58.798375
R 4	373612.32	462.78410	1035.8188	69.059998	140758.84	622.83595	29.998375
O 5	-51.024062	0.2905708E-01	0.6505260E-01	2.2188258	1.4337887	77.505813	375.00000
6	-26.999999	-2.0849999	2.2199999	2.3281154	0.4368835	-1.8500000	
7	545.83118	684.80629	314.18318				
O 1	373597.88	0.1967434	814.61137	299.33569	0	0	0
P 2	1282.8727	0.4163947	0.5506188	624.74998	-910667.55	0	0
5 3	2715.1546		0.4504951		304088.98	0	0

[redacted]

[redacted]

0*1	40.000000	7535.5000	2.3700181	28.310558	63789.566	-6249.9016	11.276605
P 2	242939.32	0.2091739E 08	1.5049480	-80.535942	317514.68	1835.3280	197.11028
1 3	1498.0679	459.92755	78.507405	97.388825	77.901855	2108.9241	745146.88
4	0.1080743	462.92812	0.4580341	108.59989	76.276603	1.5437464	0.4154234
5	0.1489340	1507.1960	-0.2131230E-01	90.488482	17.360147	24.290934	5871619.1
6	553.19878	1.2401838	0.1059524	2.3592010	8.4751793	-22.764463	254.53068
D 1	317514.68	380.24195	843.55384	68.285407	58.026546	123.52000	11.276605
E 2	62015.483	81.405094	191.55163	68.707150	64.014110	47.000000	27.600006
P 3	1774.0838	0	0	50.350000	57130.913	996.12325	58.923394
R 4	381304.24	461.64704	1035.1055	69.030000	130406.03	645.49397	29.923394
0 5	-51.391922	0.2926500E-01	0.6552442E-01	2.2184660	1.5437466	75.961623	507.00000
6	-43.499999	-2.7899999	2.9849999	2.3530669	0.4363280	-2.4500000	
7	545.42609	684.14113	319.36630				
0 1	381286.61	0.2025848	820.77150	299.39999	0	0	0
P 2	1348.1480	0.4600625	0.5848417	624.74998	-1015596.7	0	0
5 3	3061.6466		0.4778734		304441.60	0	0
0*1	40.000000	7535.5000	2.3700181	28.310558	63789.566	-6249.9016	11.276605
P 2	242939.32	0.2091739E 08	1.5049480	-80.535942	317514.68	1835.3280	197.11028
1 3	1498.0679	459.92755	78.507405	97.388825	77.901855	2108.9241	745146.88
4	0.1080743	462.92812	0.6717834	108.59989	76.276603	1.5437464	0.4154234
5	0.1489340	1507.1960	-0.2131230E-01	90.488482	17.360147	24.290934	5871619.1
6	553.19878	1.2401838	0.1059524	2.3592010	8.4751793	-22.764463	254.53068
D 1	317514.68	380.24195	843.55384	68.285407	58.026546	123.52000	11.276605
E 2	62015.483	81.405094	191.55163	68.707150	64.014110	47.000000	27.600006
P 3	1774.0838	0	0	50.350000	57130.913	996.12325	58.923394
R 4	381304.24	461.64704	1035.1055	69.030000	130406.03	645.49397	29.923394
0 5	-51.391922	0.2926500E-01	0.6552442E-01	2.2184660	1.5437466	75.961623	508.00000
6	-43.499999	-2.7899999	2.9849999	2.3530669	0.4363280	-2.4500000	
7	545.42609	684.14113	319.36630				
0 1	381286.61	0.2025848	820.77150	299.39999	0	0	0
P 2	1348.1480	0.4600625	0.5848417	624.74998	-1015596.7	0	0
5 3	3061.6466		0.4778734		304441.60	0	0
0*1	49.999998	12916.000	0.8286906	28.309949	67025.025	-9045.9813	9.2472309
P 2	227969.32	0.2092277E 08	0.9240515	-80.531251	323891.57	2072.1832	347.29575
1 3	1495.9190	668.12285	71.789573	99.179718	70.774240	1381.9841	2282444.5
4	0.3581852	666.44640	0.6717834	105.33828	71.191902	1.6750548	0.6103987
5	0.1898485	1683.5341	-0.3939043E-01	91.274687	22.007256	24.285179	0.1489360E 08
6	431.03320	2.1257002	0.3560140	2.3240013	-10.040831	-22.112251	261.32202
D 1	323891.57	379.77134	842.45608	66.510092	57.132447	112.90000	9.2472309
E 2	65214.472	80.094302	192.28195	67.086787	63.237597	45.500000	27.744461
P 3	1810.5543	0	0	50.350000	52525.047	1010.4941	59.152768
R 4	390916.59	459.86563	1034.7380	69.009998	120055.04	668.19077	29.752769
0 5	-51.536568	0.2934676E-01	0.6570994E-01	2.2183245	1.6750548	74.061898	800.00000
6	-79.473675	-4.0058681	4.3815786	2.4006945	0.4353679	-3.4868419	
7	544.95016	683.19815	325.86513				
0 1	390907.09	0.2145541	825.69719	296.66641	0	0	0
P 2	1463.8270	0.2935046	0.6256340	625.43877	-574864.16	0	0
5 3	2002.4865		0.5083100		320915.74	0	0

[redacted]

O*1	59.999997	20226.000	1.3225116	28.308486	70739.124	-18679.539	6.9745440
P 2	213025.07	0.2093008E 08	0.3827191E-01	-80.521665	330930.80	479.53903	535.32472
1 3	1492.5649	932.94903	65.071740	100.56728	63.455890	3756.3768	5797752.9
4	0.8723183	928.25915	0.6717834	102.73352	64.041382	1.7977396	0.8726106
5	0.2350814	1943.6679	-0.6329869E-01	92.468677	25.429375	19.541017	0.3197581E 08
6	708.26931	3.3287715	0.8700620	2.2888016	-13.683061	-13.950814	269.11387
D 1	330930.80	379.19362	840.86374	64.112674	55.925782	102.28000	6.9745440
E 2	68887.925	83.308965	187.88321	64.834147	62.140236	44.000000	28.033355
P 3	1851.2001	0	0	50.350000	47919.599	1024.3243	59.125454
R 4	401669.93	462.50258	1028.7469	68.969997	109729.39	690.79144	29.925455
O 5	-52.374466	0.2982035E-01	0.6678464E-01	2.2175050	1.7977395	71.210540	1022.0000
6	-8.0909345	-0.6854561	0.7854561	2.2552580	0.4379904	-0.6545467	
7	544.25997	682.91572	333.10799				
O 1	401643.13	0.9762930E-01	829.52714	386.37066	0	0	0
P 2	684.38154	0.5926777	0.6716293	654.64023	-1371853.5	0	0
5 3	4154.8161		0.5409052		-7997.9437	0	0
O*1	65.000000	24659.250	0.6696322	28.307270	72496.036	-32391.430	5.8348175
P 2	205568.63	0.2093452E 08	0.2829517	-80.514377	334226.47	1808.3201	611.83848
1 3	1489.9971	1082.7681	61.712821	101.06771	60.055338	2650.0490	8678805.2
4	1.2643000	1069.0294	0.6717834	103.29803	61.359449	1.8208857	1.0199397
5	0.2599015	2098.8562	-0.7548978E-01	93.131499	26.552545	35.465801	0.4208831E 03
6	444.77514	4.0583906	1.2620950	2.2712017	-31.996873	-15.297816	272.96866
D 1	334226.47	378.97412	838.93757	62.601769	54.600945	96.970001	5.8348175
E 2	70624.618	85.400609	185.36942	63.350556	60.835356	43.250000	28.286125
P 3	1871.4182	0	0	50.350000	45601.885	1031.2956	59.015181
R 4	406722.51	464.37473	1024.3070	68.934999	104597.25	701.99692	30.115182
O 5	-56.257729	0.3201524E-01	0.7176535E-01	2.2137068	1.8208854	67.992882	1155.0000
6	-60.999998	1.4675000	-1.2800000	2.1705866	0.4398465	1.3500000	
7	543.55334	681.87643	336.71074				
O 1	406708.42	0.1555473	829.91215	374.36318	0	0	0
P 2	1104.1399	0.4032915	0.6947294	612.68954	-868620.36	0	0
5 3	2862.7722		0.5537385		139326.16	0	0
O*1	65.000000	24659.250	0.6696322	28.307270	72496.036	-32391.430	5.8348175
P 2	205568.63	0.2093452E 08	0.2829517	-80.514377	334226.47	1808.3201	611.83848
1 3	1489.9971	1082.7681	61.712821	101.06771	60.055338	2650.0490	8678805.2
4	1.2643000	1069.0294	0.6412477	103.29803	61.359449	1.8208857	1.0199397
5	0.2599015	2098.8562	-0.7548978E-01	93.131499	26.552545	35.465801	0.4208831E 03
6	444.77514	4.0583906	1.2620950	2.2712017	-31.996873	-15.297816	272.96866
D 1	334226.47	378.97412	838.93757	62.601769	54.600945	96.970001	5.8348175
E 2	70624.618	85.400609	185.36942	63.350556	60.835356	43.250000	28.286125
P 3	1871.4182	0	0	50.350000	45601.885	1031.2956	59.015181
R 4	406722.51	464.37473	1024.3070	68.934999	104597.25	701.99692	30.115182
O 5	-56.257729	0.3201524E-01	0.7176535E-01	2.2137068	1.8208854	67.992882	1156.0000
6	-60.999998	1.4675000	-1.2800000	2.1705866	0.4398465	1.3500000	
7	543.55334	681.87643	336.71074				
O 1	406708.42	0.1555473	829.91215	374.36318	0	0	0
P 2	1104.1399	0.4032915	0.6947294	612.68954	-868620.36	0	0
5 3	2862.7722		0.5537385		139326.16	0	0

[redacted]

O*1	69.999996	29596.000	0.8697970	28.305666	74230.742	-41385.802	4.7441748
P 2	198124.99	0.2093946E 08	0.2358479	-80.505077	337483.65	2116.8574	685.40145
1 3	1487.9584	1241.2789	58.506585	101.34195	56.693182	3576.9651	0.1238179E 08
4	1.7651998	1223.5391	0.6412477	103.21399	57.979597	1.8689813	1.1971868
5	0.2865051	2268.4364	-0.8801034E-01	93.763981	27.213959	40.308939	0.5396323E 08
6	617.68095	4.8708751	1.7630460	2.2536018	-37.055498	-15.865074	276.69750
D 1	337483.65	378.70686	837.64489	61.188753	53.730165	91.660006	4.7441748
E 2	72339.981	85.343819	184.94748	61.994297	60.006895	42.500000	28.538902
P 3	1890.7611	0	0	50.350000	43280.731	1038.2677	58.855825
R 4	411714.39	464.05068	1022.5924	68.899999	99481.336	713.14706	30.255825
O 5	-58.294268	0.3316632E-01	0.7438383E-01	2.2118556	1.8689814	65.767648	1308.0000
6	-60.999998	1.4675000	-1.2800000	2.1670870	0.4398465	1.3500000	
7	543.03621	681.33678	340.15755				
O 1	411677.70	0.1216707	830.29649	265.65390	0	0	0
P 2	874.22144	0.6817381	0.7177898	561.69803	-1636580.2	0	0
5 3	4898.6088		0.5665499		38195.354	0	0
O*1	80.000000	41033.500	0.6903574	28.301034	77413.656	-34822.122	2.8133107
P 2	183246.69	0.2095090E 08	-0.3797455	-80.479381	344003.41	-862.49350	771.95485
1 3	1487.9153	1620.1213	52.094105	102.09391	50.795722	3328.5351	0.2286274E 08
4	3.1518018	1597.4577	0.6412477	102.26410	51.803165	2.1095972	1.6498971
5	0.3460088	2670.1455	-0.1110163	95.156054	28.045465	36.702237	0.7935172E 08
6	608.21620	6.7532455	3.1499045	2.2184021	-36.650099	1.9555965	283.22651
D 1	344003.41	378.11174	839.06724	59.668069	55.430228	81.040001	2.8133107
E 2	75488.897	83.803981	185.61699	60.757558	61.919800	41.000000	29.333340
P 3	1924.7590	0	0	50.350000	38649.645	1052.1890	59.086689
R 4	421417.06	461.91572	1024.6842	68.790000	89247.282	735.43829	31.286689
O 5	-50.745189	0.2889945E-01	0.6469492E-01	2.2190986	2.1095971	68.214134	1528.0000
6	-0.1000000	-0.1000000E-01	0.1200000E-01	2.2148946	0.4385872	-0.1000000E-01	
7	543.27912	681.33479	346.21579				
O 1	421398.84	-0.9100669E-01	830.87466	274.18125	0	0	0
P 2	-669.33634	0.4725775	0.7700264	506.97086	-1073269.8	0	0
5 3	3475.7905		0.5966843		-579589.29	0	0
O*1	80.000000	41033.500	0.6903574	28.301034	77413.656	-34822.122	2.8133107
P 2	183246.69	0.2095090E 08	-0.3797455	-80.479381	344003.41	-862.49350	771.95485
1 3	1487.9153	1620.1213	52.094105	102.09391	50.795722	3328.5351	0.2286274E 08
4	3.1518018	1597.4577	0.7939258	102.26410	51.803165	2.1095972	1.6498971
5	0.3460088	2670.1455	-0.1110163	95.156054	28.045465	36.702237	0.7935172E 08
6	608.21620	6.7532455	3.1499045	2.2184021	-36.650099	1.9555965	283.22651
D 1	344003.41	378.11174	839.06724	59.668069	55.430228	81.040001	2.8133107
E 2	75488.897	83.803981	185.61699	60.757558	61.919800	41.000000	29.333340
P 3	1924.7590	0	0	50.350000	38649.645	1052.1890	59.086689
R 4	421417.06	461.91572	1024.6842	68.790000	89247.282	735.43829	31.286689
O 5	-50.745189	0.2889945E-01	0.6469492E-01	2.2190986	2.1095971	68.214134	1529.0000
6	-0.1000000	-0.1000000E-01	0.1200000E-01	2.2148946	0.4385872	-0.1000000E-01	
7	543.27912	681.33479	346.21579				
O 1	421398.84	-0.9100669E-01	830.87466	274.18125	0	0	0
P 2	-669.33634	0.4725775	0.7700264	506.97086	-1073269.8	0	0
5 3	3475.7905		0.5966843		-579589.29	0	0

[redacted]

0*1	90.000000	54698.250	-0.8520983	28.293855	79637.714	-21987.650	1.4142577
P 2	168368.80	0.2096457E 08	-0.6719105	-80.441363	348531.74	-2290.2536	684.96169
1 3	1487.7361	2110.2679	44.154847	102.50356	44.457444	-3038.4288	0.3633913E 08
4	5.2076035	2073.1199	0.7939258	102.02355	45.473759	2.4122614	2.1919901
5	0.4164844	3197.9629	-0.1265310	96.509973	27.526933	53.076978	0.9137466E 08
6	743.23931	9.0021741	5.2060651	2.1832023	-49.676750	18.691869	287.79933

D 1	348531.74	378.12993	839.14131	58.773434	58.073499	70.420001	1.4142577
E 2	77690.068	81.027721	188.12175	60.220091	64.824745	39.500000	31.500008
P 3	1547.6455	0	0	50.350000	34042.073	1066.0439	59.385742
R 4	428169.45	459.15765	1027.2631	68.490000	78990.112	757.35611	32.185742
0 5	-50.654039	0.2884793E-01	0.6457801E-01	2.2191878	2.4122612	70.065151	1908.0000
6	-43.499999	-2.7899999	2.9849999	2.3216962	0.4363280	-2.4500000	
7	543.15416	680.64883	350.29404				

0 1	428137.20	-0.3092160	829.19966	322.19272	0	0	0
P 2	-2310.6090	-0.5539807	0.8875080	484.12490	1873457.9	0	0
5 3	-4139.6968		0.6745048		-1264477.1	0	0

0*1	90.000000	54698.250	-0.8520983	28.293855	79637.714	-21987.650	1.4142577
P 2	168368.80	0.2096457E 08	-0.6719105	-80.441363	348531.74	-2290.2536	684.96169
1 3	1487.7361	2110.2679	44.154847	102.50356	44.457444	-3038.4288	0.3633913E 08
4	5.2076035	2073.1199	0.6717834	102.02355	45.473759	2.4122614	2.1919901
5	0.4164844	3197.9629	-0.1265310	96.509973	27.526933	53.076978	0.9137466E 08
6	743.23931	9.0021741	5.2060651	2.1832023	-49.676750	18.691869	287.79933

D 1	348531.74	378.12993	839.14131	58.773434	58.073499	70.420001	1.4142577
E 2	77690.068	81.027721	188.12175	60.220091	64.824745	39.500000	31.500008
P 3	1947.6455	0	0	50.350000	34042.073	1066.0439	59.385742
R 4	428169.45	459.15765	1027.2631	68.490000	78990.112	757.35611	32.185742
0 5	-50.654039	0.2884793E-01	0.6457801E-01	2.2191878	2.4122612	70.065151	1909.0000
6	-43.499999	-2.7899999	2.9849999	2.3216962	0.4363280	-2.4500000	
7	543.15416	680.64883	350.29404				

0 1	428137.20	-0.3092160	829.19966	322.19272	0	0	0
P 2	-2310.6090	-0.5539807	0.8875080	484.12490	1873457.9	0	0
5 3	-4139.6968		0.6745048		-1264477.1	0	0

0*1	100.00000	70580.250	-0.5556004	28.283057	80865.251	-11416.961	0.5346842
P 2	153493.01	0.2098046E 08	-0.6979802	-80.386648	351335.90	-2018.8036	512.98037
1 3	1489.1397	2727.1106	37.437013	103.02946	38.612250	-1484.9691	0.5069225E 08
4	8.1726446	2731.0943	0.6717834	102.19375	38.545538	2.7413473	2.8316612
5	0.5018900	3853.6712	-0.1227248	97.867004	26.207062	24.287597	0.9015140E 08
6	457.61961	11.616015	8.1717217	2.1480026	10.119540	22.079000	290.23545

D 1	351335.90	377.94489	840.81482	58.120339	60.999231	59.800001	0.5346842
E 2	78905.197	79.836284	189.22837	59.955343	68.036460	38.000000	33.016682
P 3	1960.0542	0	0	50.350000	29453.100	1079.8448	59.465315
R 4	432201.14	457.78117	1030.0432	68.279999	68716.455	779.70808	32.865315
0 5	-45.016289	0.2566138E-01	0.5734698E-01	2.2247021	2.7413473	73.855420	2172.0000
6	-78.857141	-3.9921427	4.3599998	2.3702051	0.4353822	-3.4714285	
7	543.51651	680.16964	352.50519				

0 1	432194.63	-0.1594777	825.25034	315.31662	0	0	0
P 2	-1202.9784	-0.2343154	0.9862411	463.82040	1000701.4	0	0
5 3	-1767.5024		0.7337446		-891499.55	0	0

[redacted]

O*1	1	100.00000	70580.250	-0.5556004	28.283057	80865.251	-11416.961	0.6346842
P	2	153493.01	0.2098046E 08	-0.6979802	-80.386648	351335.90	-2018.8036	512.98037
1	3	1489.1397	2727.1106	37.437013	103.02946	38.612250	-1484.9691	0.5069225E 08
	4	8.1726446	2731.0943	0.4885697	102.19375	38.545538	2.7413473	2.8315512
	5	0.5018900	3853.6712	-0.1227248	97.867004	26.207062	24.287597	0.9015140E 08
	6	457.61961	11.616015	8.1717217	2.1480026	10.119540	22.079000	290.23545
D	1	351335.90	377.94489	840.81482	58.120339	60.999231	59.800001	0.5346842
E	2	78905.197	79.836284	189.22837	59.955343	68.036460	38.000000	33.016682
P	3	1960.0542	0	0	50.350000	29453.100	1079.8448	59.465315
R	4	432201.14	457.78117	1030.0432	68.279999	68716.455	779.70808	32.865315
O	5	-45.016289	0.2566138E-01	0.5734698E-01	2.2247021	2.7413473	73.855420	2173.0000
	6	-78.857141	-3.9921427	4.3599998	2.3702051	0.4353822	-3.4714285	
	7	543.51651	680.16964	352.50519				
O	1	432194.63	-0.1594777	825.25034	315.31662	0	0	0
P	2	-1202.9784	-0.2343154	0.9862411	463.82040	1000701.4	0	0
5	3	-1767.5024		0.7337446		-891499.55	0	0
O*1	1	110.00000	88722.250	-0.6677500	28.267772	81434.479	-4713.9736	0.2699209
P	2	138583.96	0.2099862E 08	-0.1128960	-80.311104	353287.86	0.7108415	332.54023
1	3	1492.7641	3478.7132	32.551316	103.21711	33.713823	-1249.8362	0.6348791E 08
	4	12.272095	3463.6443	0.4885697	103.05526	33.880319	3.1028434	3.4960174
	5	0.6059966	4639.5280	-0.9774676E-01	98.875751	24.593163	18.349653	0.7411509E 08
	6	225.20445	14.601804	12.271736	2.1128029	-18.299922	1.3500363	291.21972
D	1	353287.86	377.23973	845.08425	57.593959	63.779559	49.180001	0.2699209
E	2	79467.816	79.051517	190.07322	59.855556	71.138180	36.500000	33.016682
P	3	1966.6623	0	0	50.350000	24880.414	1093.5986	59.430079
R	4	434722.34	456.29125	1035.1575	68.279999	58393.239	802.72301	33.030078
O	5	-29.194497	0.1671863E-01	0.3705381E-01	2.2401783	3.1028428	80.396833	2340.0000
	6	-106.59091	-4.7647726	5.3010226	2.4044221	0.4347707	-4.1318181	
	7	544.67011	679.89487	353.68273				
O	1	434718.30	0.1739746	820.13996	341.64596	0	0	0
P	2	1319.9956	-0.1384666	1.1009337	469.25294	766412.53	0	0
5	3	-1050.5850		0.8160003		38657.504	0	0
O*1	1	110.00000	88722.250	-0.6677500	28.267772	81434.658	-4713.9736	0.2699209
P	2	138539.96	0.2099862E 08	-0.1128960	-80.311104	353292.03	0.7108415	332.54023
1	3	1492.7843	3478.7132	32.551316	103.21711	33.713823	-1249.8362	0.6348791E 08
	4	12.272095	3463.6443	0.3664273	103.05526	33.880319	3.1038603	3.4960174
	5	0.6059966	4639.5280	-0.9774676E-01	98.875751	24.593163	18.349653	0.7411509E 08
	6	225.20445	14.601804	12.271736	2.1128029	-18.299922	1.3500363	291.21870
D	1	353292.03	377.23784	845.10574	57.596694	63.794951	49.180001	0.2699209
E	2	79467.996	79.051617	190.07368	59.859489	71.154475	36.500000	33.016582
P	3	1966.6628	0	0	50.350000	24880.414	1093.5986	59.430079
R	4	434726.69	456.28946	1035.1794	68.279999	58393.239	802.72301	33.030078
O	5	-29.124764	0.1667921E-01	0.3696437E-01	2.2402464	3.1038594	80.431199	2343.0000
	6	-106.59091	-4.7647726	5.3010226	2.4044249	0.4347707	-4.1318181	
	7	544.67653	679.89640	353.68282				
O	1	434722.65	0.1740215	820.12219	341.64596	0	0	0
P	2	1320.3643	-0.1384070	1.1013090	469.25294	766390.32	0	0
5	3	-1050.1429		0.8162966		39657.492	0	0

[redacted]

[redacted]

0*1	120.00000	109207.25	-0.4378799	28.247236	81654.948	-1070.1007	0.1092069
P 2	123590.84	0.2101913E 08	-0.2358494E-01	-80.210564	354638.55	99.005574	200.54255
1 3	1496.9388	4375.5861	28.887043	103.34116	29.793303	-477.80268	0.7350326E 08
4	17.731789	4333.4073	0.3664273	103.27714	30.113120	3.5214573	4.2682311
5	0.7326180	5563.8074	-0.5728540E-01	99.677181	23.001746	50.000000	0.5592050E 08
6	87.940829	17.973202	17.731789	2.0776031	-50.000000	-0.6146729E-05	291.45713
D 1	354638.55	376.55452	849.68577	57.238475	66.816482	38.560001	0.1092069
E 2	79685.353	77.778068	191.60512	59.994070	74.547277	35.000000	33.016682
P 3	1969.5965	0	0	50.350000	20331.356	1107.2858	59.513869
R 4	436293.50	454.33258	1041.2909	68.279999	48006.333	825.89512	33.113869
0 5	-12.534775	0.7302264E-02	0.1568591E-01	2.2564747	3.5214573	87.586494	2492.0000
6	-157.49999	-6.0374998	6.8537497	2.4634852	0.4338280	-5.1499999	
7	545.93295	679.51556	354.20558				
0 1	436289.97	0.2040015	813.26584	399.63927	0	0	0
P 2	1553.4162	0.3822378E-01	1.2318842	489.62283	285753.44	0	0
5 3	291.06253		0.9209701		81941.374	0	0
0*1	120.00000	109207.25	-0.4378799	28.247236	81654.948	-1070.1007	0.1092069
P 2	123590.84	0.2101913E 08	-0.2358494E-01	-80.210564	354638.55	98.005574	200.54255
1 3	1496.9388	4375.5861	28.887043	103.34116	29.793303	-477.80268	0.7350326E 08
4	17.731789	4333.4073	0.2748205	103.27714	30.113120	3.5214573	4.2682311
5	0.7326180	5563.8074	-0.5728540E-01	99.677181	23.001746	50.000000	0.5592050E 08
6	87.940829	17.973202	17.731789	2.0776031	-50.000000	-0.6146729E-05	291.45713
D 1	354638.55	376.55452	849.68577	57.238475	66.816482	38.560001	0.1092069
E 2	79685.353	77.778068	191.60512	59.994070	74.547277	35.000000	33.016682
P 3	1969.5965	0	0	50.350000	20331.356	1107.2858	59.513869
R 4	436293.50	454.33258	1041.2909	68.279999	48006.333	825.89512	33.113869
0 5	-12.534775	0.7302264E-02	0.1568591E-01	2.2564747	3.5214573	87.586494	2493.0000
6	-157.49999	-6.0374998	6.8537497	2.4634852	0.4338280	-5.1499999	
7	545.93295	679.51556	354.20558				
0 1	436289.97	0.2040015	813.26584	399.63927	0	0	0
P 2	1553.4162	0.3822378E-01	1.2318842	489.62283	285753.44	0	0
5 3	291.06253		0.9209701		81941.374	0	0
0*1	129.99999	132258.50	0.8930459E-01	28.220484	81770.872	533.98109	0.4216569E-01
P 2	108601.76	0.2104221E 08	-0.6666394E-01	-80.080714	355659.11	6.8838766	109.37508
1 3	1500.8307	5437.7825	26.138839	103.47478	26.758312	103.61506	0.8074728E 08
4	24.788024	5394.3765	0.2748205	103.35423	26.991016	4.0327043	5.0728183
5	0.8857253	6646.7392	0.1329292E-02	100.35031	21.613111	50.000000	0.3796598E 08
6	12.189009	21.766950	24.788075	2.0424034	-50.000000	-0.6146729E-05	291.45857
D 1	355659.11	375.84272	854.28989	56.752328	69.801626	27.940008	0.4216569E-01
E 2	79800.045	77.779273	191.60344	60.111234	77.986951	33.500001	33.016682
P 3	1970.8278	0	0	50.350000	15791.596	1120.9448	59.528657
R 4	437429.98	453.62199	1045.8933	68.279999	37570.165	849.17874	32.603667
0 5	-3.6526708	0.2130725E-02	0.4565838E-02	2.2729983	4.0327039	94.840639	2562.0000
6	-157.49999	-6.0374998	6.8537498	2.4634254	0.4338280	-5.1499999	
7	547.16272	679.56108	354.42500				
0 1	437424.80	0.2026249	795.37833	426.57224	0	0	0
P 2	1546.9468	0.1485073	1.4041345	497.79610	47.749803	0	0
5 3	1133.7817		1.0799703		30288.350	0	0

[redacted]

0*1	140.00000	158247.50	-0.1992650E-01	28.186333	81822.671	1031.2807	0.1580340E-01
P 2	93570.172	0.2106823E 08	-0.9996233E-01	-79.916583	356719.83	-14.756943	57.644249
1 3	1505.8091	6700.6573	23.390633	103.62526	24.363752	11.611543	0.8555732E 08
4	33.714275	6656.3811	0.2748205	103.45821	24.536463	4.6977350	6.0155095
5	1.0698979	7925.7161	0.8379098E-01	100.93670	20.411779	50.000000	0.2469046E 08
6	5.8756263	26.044189	33.714275	2.0072037	-50.000000	-0.6146729E-05	291.23379
D 1	356719.83	375.04189	860.04984	56.149330	73.514133	17.320002	0.1580340E-01
E 2	79851.343	77.783188	191.61881	60.293024	82.290712	32.000000	33.016682
P 3	1971.3288	0	0	50.350000	11259.351	1134.6135	59.513362
R 4	438542.50	452.82507	1051.6686	68.279999	27083.978	872.58160	31.838363
O 5	-13.633965	0.7706154E-01	0.1778343E-01	2.2932101	4.6977348	103.91711	2607.0000
6	-157.49999	-6.0374998	6.8537497	2.4634990	0.4338280	-5.1499999	
7	548.66037	679.63173	354.51426				
O 1	438536.60	0.2141314	769.43607	437.48228	0	0	0
P 2	1638.9493	0.1609007	1.6305326	501.64040	13751.181	0	0
5 3	1231.5226		1.2741894		10291.609	0	0
0*1	140.00000	158247.50	-0.1992650E-01	28.186333	81822.671	1031.2807	0.1580340E-01
P 2	93570.172	0.2106823E 08	-0.9996233E-01	-79.916583	356719.83	-14.756943	57.644249
1 3	1505.8091	6700.6573	23.390633	103.62526	24.363752	11.611543	0.8555732E 08
4	33.714275	6656.3811	0.2748205	103.45821	24.536463	4.6977350	6.0155095
5	1.0698979	7925.7161	0.8379098E-01	100.93670	20.411779	50.000000	0.2469046E 08
6	5.8756263	26.044189	33.714275	2.0072037	-50.000000	-0.6146729E-05	291.23379
D 1	356719.83	375.04189	860.04984	56.149330	73.514133	17.320002	0.1580340E-01
E 2	79851.343	77.783188	191.61881	60.293024	82.290712	32.000000	33.016682
P 3	1971.3288	0	0	50.350000	11259.351	1134.6135	59.513362
R 4	438542.50	452.82507	1051.6686	68.279999	27083.978	872.58160	31.838363
O 5	-13.633965	0.7706154E-01	0.1778343E-01	2.2932101	4.6977348	103.91711	2608.0000
6	-157.49999	-6.0374998	6.8537497	2.4634990	0.4338280	-5.1499999	
7	548.66037	679.63173	354.51426				
O 1	438536.60	0.2141314	769.43607	437.48228	0	0	0
P 2	1638.9493	0.1609007	1.6305326	501.64040	13751.181	0	0
5 3	1231.5226		1.2741894		10291.609	0	0
0*1	149.05584	184705.75	-0.4705574	28.147742	81843.204	1264.5319	0.5018093E-02
P 2	79904.858	0.2109473E 08	-0.1269054	-79.733068	358220.61	-17.139401	33.366055
1 3	1513.1687	8069.2665	20.901903	103.77544	22.563909	-88.926805	0.8846808E 08
4	43.703655	8024.3966	0.2748205	103.57187	22.697099	5.5230891	7.4163924
5	1.2683678	9306.4119	0.1847304	101.41685	19.433031	50.000000	0.1722869E 08
6	16.261555	30.398657	43.703450	1.9753274	-50.000000	-0.6146729E-05	290.82269
D 1	358220.61	373.67719	868.76296	55.271109	79.131143	7.7027016	0.5018093E-02
E 2	79871.685	77.785325	191.62790	60.388786	88.641526	30.641624	33.015369
P 3	1971.5197	0	0	50.350000	7163.6774	1147.5535	59.493392
R 4	440063.81	451.46252	1060.3909	68.280180	17526.250	893.27975	31.763888
O 5	-34.446796	0.2507103E-01	0.4430849E-01	2.3249023	5.5230892	117.31320	2693.0000
6	-157.49999	-6.0374998	6.8537497	2.4635482	0.4338280	-5.1499999	
7	550.91876	679.66901	354.54828				
O 1	440057.13	0.2286831	740.15326	448.42193	0	0	0
P 2	1756.3974	0.1696552	1.8745561	505.65907	34477.148	0	0
5 3	1303.0312		1.4755088		3838.6157	0	0

[redacted]

0*1	149.05584	184705.75	-0.4705574	28.147742	360191.21	1264.5319	0.5018093E-02
P 2	79904.858	0.2109473E 08	-0.1269054	-79.733068	79871.653	-17.139401	33.366055
1 3	1513.1642	8069.2665	20.901903	103.77544	22.563909	-88.926805	0.8846808E 08
4	43.703655	8024.3966	0	103.57187	22.697099	5.5227861	7.4163924
5	1.2683678	9306.4119	0.1847304	101.41685	19.433031	50.000000	0.1722869E 08
6	16.261555	30.398657	43.703450	1.9753274	-50.000000	-0.6146729E-05	290.82294
D 1	358219.69	373.67779	868.75792	55.270772	79.127643	7.7027016	0.5018093E-02
E 2	79871.653	77.785308	191.62782	60.388091	97.407758	30.641624	33.015369
P 3	1971.5196	0	0	50.350000	7163.6774	1147.5535	59.493982
R 4	440062.86	451.46310	1060.3857	68.280180	17526.250	893.27975	31.763898
O 5	-34.438088	0.2515085E-01	0.4429761E-01	2.3248851	5.5227865	135.80081	2696.0000
6	-157.49999	-6.0374998	6.8537497	2.4635477	0.4336280	-5.1499999	
7	550.91734	679.66875	354.54826				
O 1	440032.91	0.2286831	740.15326	448.42193	0	0	0
P 2	1756.3012	0.1696546	1.8745561	505.65907	34477.148	0	0
5 3	1302.9554		1.4755088		3838.6157	0	0
0*1	149.99999	187625.75	-0.2764130	28.143264	13612.846	1203.1118	0.5384901E-02
P 2	79313.594	0.2109765E 08	-0.1251571	-79.711897	79417.032	-15.464102	30.565829
1 3	269.29727	8118.1299	20.901903	103.79217	22.394104	-44.601477	0.8871203E 08
4	44.856730	8073.2072	0	103.58623	22.525537	1.1880910	7.5163715
5	1.2909151	9356.6324	0.1968750	101.44190	19.301978	50.000000	0.1593074E 08
6	9.3048419	30.879227	44.856473	1.9753274	-50.000000	-0.6146729E-05	345.45422
D 1	11642.525	0	0	50.407029	29.161057	7.7027016	0.5384901E-02
E 2	79417.032	77.531720	190.45015	50.409069	43.587395	30.500001	32.993263
P 3	1970.3214	0	0	50.350000	6989.1457	1148.1445	59.494615
R 4	93029.878	77.531720	190.45015	68.283241	17110.760	894.61491	31.980327
O 5	-490.79613	0.2786617	0.6314033	2.0916437	1.1880910	22.341572	2923.0000
6	-157.49999	-6.0374998	6.8537497	2.4564159	0.4338280	-5.1499999	
7	17.931699	675.79183	354.33476				
O 1	93028.657	0.2266018	720.40624	448.60540	0	0	0
P 2	367.92541	0.1486231	1.9022760	505.83515	19942.397	0	0
5 3	241.31337		1.4895469		3903.6534	0	0
0*1	151.30000	191628.25	-0.1255973E-01	28.137058	1970.3279	1097.3092	0.4611575E-02
P 2	78963.551	0.2110166E 08	-0.1222565	-79.682599	79403.033	-13.147727	27.002455
1 3	269.24896	8148.0249	20.901903	103.81536	22.163256	4.9502233	0.8901489E 08
4	46.452502	8103.0314	0	103.60657	22.292912	1.0444025	7.5216103
5	1.3221001	9388.4357	0.2138473	101.46834	19.111325	50.000000	0.1407945E 08
6	3.3186022	31.537954	46.452142	1.9753274	-50.000000	-0.6146729E-05	302.22348
D 1	0	0	0	50.238569	27.773162	7.7027016	0.4611575E-02
E 2	79403.033	77.522367	190.41120	50.071045	42.071803	30.305000	32.962811
P 3	1970.3279	0	0	50.350000	6888.3624	1148.4858	59.495388
R 4	81373.360	77.522367	190.41120	68.287457	16863.209	895.38715	32.278244
O 5	-528.61873	0.3001996	0.6802575	2.0856026	1.0444022	19.208430	2970.0000
6	-157.49999	-6.0374998	6.8537498	2.4562098	0.4338280	-5.1499999	
7	0.2336633E-01	675.66199	354.33592				
O 1	81372.421	0.2199531	697.07005	448.67400	0	0	0
P 2	312.38266	0.1593350	1.9295016	506.00267	5633.6074	0	0
5 3	226.29076		1.5012150		3846.9761	0	0

[redacted]

[redacted]

O*1		151.30000	191628.25	-0.1255973E-01	28.137058	1970.3279	1097.3092	0.4611575E-02
P	2	78963.551	0.2110166E 08	-0.1222565	-79.682599	79403.033	-13.147727	27.002455
1	3	269.24896	8148.0249	20.901903	103.81536	22.163256	4.9502233	0.8901489E 08
	4	46.452502	8103.0314	0	103.60657	22.292912	1.0444025	7.5216103
	5	1.3221001	9388.4357	0.2138473	101.46834	19.111325	50.000000	0.1407945E 08
	6	3.3186022	31.537954	46.452142	1.9753274	-50.000000	-0.6146729E-05	302.22348
D	1	0	0	0	50.238569	27.773162	7.7027016	0.4611575E-02
E	2	79403.033	77.522367	190.41120	50.071045	42.071803	30.305000	32.962811
P	3	1970.3279	0	0	50.350000	6888.3624	1148.4858	59.495388
R	4	81373.360	77.522367	190.41120	68.287457	16863.209	895.38715	32.278244
O	5	-528.61873	0.3001996	0.6802575	2.0856026	1.0444022	19.208430	2971.0000
	6	-157.49999	-6.0374998	6.8537498	2.4562098	0.4338280	-5.1499999	
	7	0.2336633E-01	675.66199	354.33592				
O	1	81372.421	0.2199531	697.07005	448.67400	0	0	0
P	2	312.38266	0.1593350	1.9295016	506.00267	5633.6074	0	0
5	3	226.29076		1.5012150		3846.9761	0	0
O*1		151.75000	193007.75	0.7824319E-01	28.134901	1970.3441	1062.0010	0.4358450E-02
P	2	78842.389	0.2110304E 08	-0.1212398	-79.672424	79403.446	-12.415247	25.824279
1	3	269.24889	8157.8180	20.901903	103.82339	22.083894	18.885533	0.8911125E 08
	4	47.006732	8112.8002	0	103.61363	22.212951	1.0455651	7.5580840
	5	1.3329259	9398.8824	0.2197926	101.47736	19.045573	50.000000	0.1348137E 08
	6	3.7263175	31.764990	47.006424	1.9753274	-50.000000	-0.6146729E-05	302.22515
D	1	0	0	0	50.236234	27.881701	7.7027016	0.4368450E-02
E	2	79403.446	77.522073	190.41142	50.070082	42.181395	30.237500	32.952274
P	3	1970.3441	0	0	50.350000	6853.4774	1148.6041	59.495631
R	4	81373.790	77.522073	190.41142	68.288917	16777.524	895.57893	32.381345
O	5	-524.80187	0.2980261	0.6753274	2.0862122	1.0455649	19.461333	2995.0000
	6	-157.49999	-6.0374998	6.8537498	2.4562220	0.4338280	-5.1499999	
	7	0.2336633E-01	675.66213	440.95364				
O	1	81372.853	0.2175393	688.99257	447.68573	0	0	0
P	2	308.95607	0.1622096	1.9389253	506.05781	1999.1639	0	0
5	3	230.37459		1.5052537		3810.4373	0	0
O*1		151.75000	193007.75	0.7824319E-01	28.134901	1580.4751	-573.69926	0.4368450E-02
P	2	71485.389	0.2110304E 08	-0.1212398	-79.672424	79411.667	-8.4074649	25.824279
1	3	268.10931	8157.8180	20.901903	103.82339	22.083894	16.883302	0.8911125E 08
	4	47.006732	8112.8002	0	103.61363	22.212951	1.1249572	7.5580840
	5	1.3329259	9398.8824	0.2197926	101.47736	19.045573	50.000000	0.1348137E 08
	6	3.7263175	31.764990	47.006424	1.9753274	-50.000000	-0.6146729E-05	302.08527
D	1	0	0	0	50.236234	27.881701	0	0.4358450E-02
E	2	79411.667	77.526636	190.43267	50.250048	43.162871	30.237500	32.952274
P	3	1580.4751	0	0	50.350000	6853.4774	1148.6041	59.495631
R	4	80992.142	77.526636	190.43267	68.288917	16777.524	895.57893	32.381345
O	5	-524.80187	0.2980261	0.6753274	2.0862122	1.1249570	21.530959	2998.0000
	6	-157.49999	-6.0374998	6.8537498	2.4563515	0.4338280	-5.1499999	
	7	0.2336633E-01	675.73208	354.34277				
O	1	80991.701	0.1077078	685.15142	377.42604	0	0	0
P	2	152.25294	0.1524770	0.9468465	381.36371	886.19702	0	0
5	3	215.53776		1.4130084		3527.5332	0	0

[redacted]

[redacted]

O*1	158.81000	214282.75	1.4652908	28.100375	1580.6483	-277.30685	0.1798798E-02
P 2	69592.538	0.2112435E 08	-0.1024029	-79.510405	79410.574	-2.8235095	12.482584
1 3	268.09106	8335.9824	20.901903	103.95343	20.878559	101.25299	0.9017782E 08
4	55.836372	8290.6099	0	103.72820	20.998214	1.1597981	8.2971859
5	1.5050356	9586.7036	0.3177368	101.62606	18.052752	50.000000	6659260.9
6	18.335188	35.266405	55.835654	1.9753274	-50.000000	-0.6146729E-05	302.10340
D 1	0	0	0	50.236234	27.881701	0	0.1798798E-02
E 2	79410.574	77.518960	190.42211	50.113199	43.969929	29.178500	32.785896
P 3	1580.6483	0	0	50.350000	6306.1553	1150.5112	59.346822
R 4	80991.222	77.518960	190.42211	68.311815	15433.055	898.58863	32.898200
O 5	-524.80187	0.2980261	0.6753274	2.0862122	1.1597981	23.573620	3082.0000
6	-157.49999	-6.0374998	6.8537498	2.4564585	0.4338280	-5.1499999	
7	0.2336633E-01	675.68713	354.38125				
O 1	80990.600	0.1073279	677.45459	371.82270	0	0	0
P 2	151.71382	0.1943243	0.9753533	381.30720	-28006.494	0	0
5 3	274.68869		1.4671713		2103.4736	0	0
O*1	158.81000	214282.75	1.1981814	28.100375	1580.6483	-277.30685	0.1798798E-02
P 2	69592.538	0.2112435E 08	0.5327420	-79.510405	79410.574	36.285066	12.482584
1 3	268.09106	8335.9824	20.635636	103.95343	20.878559	83.080465	0.9017782E 08
4	55.836372	8290.6099	0	103.72820	20.998214	1.1597980	8.2971859
5	1.5050356	9586.7036	0.3177368	101.62606	18.052752	50.000000	6659260.9
6	16.367363	35.266405	55.835654	2.6486984	-50.000000	-0.6146729E-05	302.10340
D 1	0	0	0	50.236234	27.881701	0	0.1798798E-02
E 2	79410.574	77.518960	190.42211	50.113199	43.969929	29.178500	32.786896
P 3	1580.6483	0	0	50.350000	6306.1553	1150.5112	59.346822
R 4	80991.222	77.518960	190.42211	68.311815	15433.055	898.58863	32.898200
O 5	-524.80187	0.2980261	0.6753274	2.0862122	1.1597981	23.573620	3083.0000
6	-157.49999	-6.0374998	6.8537498	2.4564585	0.4338280	-5.1499999	
7	0.2336633E-01	675.68713	354.38125				
O 1	80990.594	0.1225938	677.45459	376.23000	0	0	0
P 2	173.29300	0.1864893	0.9753533	382.59822	-22086.230	0	0
5 3	263.61335		1.4671713		13638.531	0	0
O*1	159.99999	217802.50	1.3746806	28.094428	1580.6638	-243.76140	0.1537202E-02
P 2	69273.523	0.2112788E 08	0.5333821	-79.482645	79404.954	31.929894	10.972582
1 3	268.07184	8367.2146	20.583413	103.97162	20.680842	83.574674	0.9029359E 08
4	57.349891	8321.7852	0	103.74376	20.798962	1.1655424	8.4150895
5	1.5344703	9619.4963	0.3350794	101.64795	17.889779	50.000000	5875710.4
6	16.178606	35.845681	57.349173	2.6488561	-50.000000	-0.6146729E-05	302.10415
D 1	0	0	0	50.236234	27.881701	0	0.1537202E-02
E 2	79404.954	77.514809	190.40704	49.977225	44.016915	29.000001	32.759118
P 3	1580.6638	0	0	50.350000	6213.9108	1150.8399	59.209574
R 4	80985.617	77.514809	190.40704	68.315675	15206.463	899.09542	32.898462
O 5	-524.80187	0.2980261	0.6753274	2.0862122	1.1655423	23.730090	3099.0000
6	-157.49999	-6.0374998	6.8537498	2.4563956	0.4338280	-5.1499999	
7	0.2336633E-01	675.63567	354.38469				
O 1	80984.988	0.1205922	676.15739	373.31776	0	0	0
P 2	170.45184	0.1878602	0.9801578	382.60014	-22725.679	0	0
5 3	265.53281		1.4762998		11957.295	0	0

[redacted]

O*1	169.99999	246649.50	2.7529483	28.043012	1580.7784	-75.478751	0.3695946E-03
P 2	66593.615	0.2115678E 08	0.5392712	-79.244063	79355.785	9.9842153	3.3975716
1 3	267.90975	8643.0317	20.102925	104.12710	19.086982	52.163042	0.9084595E 08
4	70.365746	8597.1663	0	103.87731	19.192788	1.2142382	9.5497339
5	1.7868125	9907.4792	0.4873810	101.83398	16.574944	50.000000	1879572.1
6	9.5305626	40.593287	70.364310	2.6504139	-50.000000	-0.6146729E-05	302.10384
D 1	0	0	0	50.236234	27.881701	0	0.3695946E-03
E 2	79355.785	77.479803	190.27995	48.829025	44.407897	27.500001	32.524792
P 3	1580.7784	0	0	50.350000	5438.9376	1153.6623	58.055185
R 4	80936.563	77.479803	190.27995	68.348106	13303.028	903.35185	32.899629
O 5	-524.80187	0.2980261	0.6753274	2.0862122	1.2142382	25.036058	3135.0000
6	-157.49999	-6.0374998	6.8537498	2.4558651	0.4338280	-5.1499999	
7	0.2336633E-01	675.20112	354.41016				
O 1	80935.988	0.1116352	665.26017	360.74115	0	0	0
P 2	157.69605	0.1822762	1.0205178	382.61781	-15084.510	0	0
S 3	257.48407		1.5529839		3622.0903	0	0
O*1	179.99999	274247.75	3.9424991	27.988900	1580.8796	-17.806902	0.7209965E-04
P 2	63915.332	0.2118443E 08	0.5449746	-78.995712	79304.815	2.3777199	0.8015531
1 3	267.74668	8942.5808	19.544057	104.28662	17.611515	18.165810	0.9100815E 08
4	83.929268	8896.3472	0	104.01508	17.706063	1.2652262	10.501935
5	2.0483302	10217.641	0.6518120	102.02320	15.355356	50.000000	458858.79
6	3.1899824	45.135375	83.927063	2.6520259	-50.000000	-0.6146729E-05	302.09784
D 1	0	0	0	50.236234	27.881701	0	0.7209965E-04
E 2	79304.815	77.444610	190.15208	47.672464	44.810116	26.000001	32.290558
P 3	1580.8796	0	0	50.350000	4664.3154	1156.6209	56.899927
R 4	80885.694	77.444610	190.15208	68.380539	11400.867	907.60085	32.899927
O 5	-524.80187	0.2980261	0.6753274	2.0862122	1.2652262	26.364466	3162.0000
6	-157.49999	-6.0374998	6.8537498	2.4553300	0.4338280	-5.1499999	
7	0.2336633E-01	674.76331	354.43263				
O 1	80885.162	0.1099732	654.10233	371.30999	0	0	0
P 2	155.25079	0.1734369	1.0605136	382.63492	-4948.3862	0	0
S 3	244.84372		1.6276082		834.23920	0	0
O*1	189.99999	300676.75	4.9386584	27.931936	1580.9866	-3.7831866	0.1435445E-04
P 2	61238.611	0.2121092E 08	0.5496583	-78.737155	79257.753	0.5090433	0.1702949
1 3	267.59718	9266.1385	18.898726	104.44985	16.251478	5.0563046	0.9104475E 08
4	98.066250	9219.5968	0	104.15677	16.335812	1.3199912	10.848688
5	2.3194357	10550.435	0.8290176	102.21540	14.228374	50.000000	101029.60
6	0.8461702	49.485029	98.063172	2.6534010	-50.000000	-0.6146729E-05	302.09115
D 1	0	0	0	50.236234	27.881701	0	0.1435445E-04
E 2	79257.753	77.411808	190.03537	46.610012	45.239849	24.500001	32.056320
P 3	1580.9866	0	0	50.350000	3890.0331	1159.8397	55.849985
R 4	80838.739	77.411808	190.03537	68.412971	9499.9286	911.84270	32.899984
O 5	-524.80187	0.2980261	0.6753274	2.0862122	1.3199911	27.749534	3188.0000
6	-157.49999	-6.0374998	6.8537498	2.4548629	0.4338280	-5.1499999	
7	0.2336633E-01	674.36208	354.45640				
O 1	80838.209	0.1109386	642.70148	386.78386	0	0	0
P 2	156.52272	0.1726844	1.1001687	382.64897	-1253.8930	0	0
S 3	243.63993		1.7003093		172.48243	0	0

[redacted]

O*1	198.47000	322209.25	5.6269637	27.881320	1581.0754	-1.0386490	0.4267130E-05
P 2	58972.604	0.2123250E 08	0.5525478	-78.509823	79217.269	0.1404120	0.4575335E-01
1 3	267.46880	9559.5005	18.276983	104.59104	15.186842	1.6312848	0.9105216E 08
4	110.50941	9512.7386	0	104.27987	15.263309	1.3700728	10.425771
5	2.5568924	10850.669	0.9896462	102.38063	13.343877	50.000000	28518.927
6	0.2643286	53.028822	110.50552	2.6542673	-50.000000	-0.6146729E-05	302.08512
D 1	0	0	0	50.236234	27.881701	0	0.4267130E-05
E 2	79217.269	77.383716	189.93509	45.697868	45.632602	23.229500	31.857929
P 3	1581.0754	0	0	50.350000	3234.4732	1162.8437	54.960645
R 4	80798.344	77.383716	189.93509	68.440441	7890.7510	915.42920	32.899995
O 5	-524.80187	0.2980261	0.6753274	2.0862122	1.3700728	28.982175	3212.0000
6	-157.49995	-6.0374998	6.8537497	2.4544581	0.4338280	-5.1499999	
7	0.2336633E-01	674.01749	354.47614				
O 1	80797.801	0.1122569	633.04996	397.62467	0	0	0
P 2	158.30348	0.1748183	1.1337392	382.65764	-373.03530	0	0
5 3	246.52743		1.7618552		46.168501	0	0

O*1	198.47000	322209.25	5.6269637	27.881320	1581.0811	-1.0386490	0.4267130E-05
P 2	57666.403	0.2123250E 08	0.5525478	-78.509823	79219.897	0.1404120	0.4575335E-01
1 3	267.47705	9559.5005	18.276983	104.59104	15.186842	1.6312848	0.9105216E 08
4	110.50941	9512.7386	0	104.27987	15.263309	1.4011518	10.425771
5	2.5568924	10850.669	0.9896462	102.38063	13.343877	50.000000	28518.927
6	0.2643286	53.028822	110.50552	2.6542673	-50.000000	-0.6146729E-05	302.08564
D 1	0	0	0	50.236234	27.881701	0	0.4267130E-05
E 2	79219.897	77.385176	189.94188	45.755423	45.992431	23.229500	31.857929
P 3	1581.0811	0	0	50.350000	3234.4732	1162.8437	54.960645
R 4	80800.979	77.385176	189.94188	68.440441	7890.7510	915.42920	32.899995
O 5	-524.80187	0.2980261	0.6753274	2.0862122	1.4011518	29.739263	3215.0000
6	-157.49999	-6.0374998	6.8537497	2.4544996	0.4338280	-5.1499999	
7	0.2336633E-01	674.03986	354.47741				
O 1	80800.426	0.1130843	627.48653	397.62467	0	0	0
P 2	159.47549	0.1766209	1.1530903	382.65764	-363.95974	0	0
5 3	249.07752		1.7973322		45.387327	0	0

O*1	199.99999	326020.00	5.7300640	27.871938	1581.0970	-0.8428299	0.3502060E-05
P 2	57257.184	0.2123632E 08	0.5528225	-78.467915	79212.487	0.1139905	0.3793982E-01
1 3	267.45356	9615.9636	18.151951	104.61674	15.003765	1.3541590	0.9105278E 08
4	112.80469	9569.1658	0	104.30230	15.078878	1.4110401	10.366923
5	2.6005800	10908.282	1.0196961	102.41089	13.191851	50.000000	23361.083
6	0.2183879	53.655991	112.80059	2.6543753	-50.000000	-0.6146729E-05	302.08453
D 1	0	0	0	50.236234	27.881701	0	0.3502060E-05
E 2	79212.487	77.380047	189.92352	45.588547	46.070784	23.000001	31.822085
P 3	1581.0970	0	0	50.350000	3116.0784	1163.4405	54.799996
R 4	80793.584	77.380047	189.92352	68.445404	7600.1555	916.07719	32.899995
O 5	-524.80187	0.2980261	0.6753274	2.0862122	1.4110401	29.977358	3231.0000
6	-157.49999	-6.0374998	6.8537498	2.4544249	0.4338280	-5.1499999	
7	0.2336633E-01	673.97679	354.48093				
O 1	80793.028	0.1133300	625.74355	399.24850	0	0	0
P 2	159.80738	0.1771020	1.1591528	382.65847	-297.77570	0	0
5 3	249.73315		1.8084469		36.643980	0	0

[redacted]

[redacted]

O*1	209.99999	350380.75	6.2810651	27.808677	1581.2112	-0.2484720	0.1093610E-05
P 2	54583.333	0.2126075E 08	0.5536286	-78.187296	79169.040	0.3364906E-01	0.1118462E-01
1 3	267.31571	10000.673	17.266645	104.78709	13.867694	0.4530170	0.9105486E 08
4	128.18510	9953.6653	0	104.45141	13.934506	1.4793786	10.072775
5	2.8924314	11299.932	1.2244045	102.61073	12.246757	50.000000	7153.7346
6	0.7051939E-01	57.665255	128.17982	2.6547566	-50.000000	-0.6146729E-05	302.07821

D 1	0	0	0	50.236234	27.881701	0	0.1093610E-05
E 2	79169.040	77.349304	189.81641	44.607235	46.588388	21.500001	31.587852
P 3	1581.2112	0	0	50.350000	2342.4308	1167.6998	53.976922
R 4	80750.251	77.349304	189.81641	68.477837	5701.4518	920.72733	32.899998
O 5	-524.80187	0.2980261	0.6753274	2.0862122	1.4793786	31.544178	3284.0000
6	-157.49999	-6.0374998	6.8537498	2.4540157	0.4338280	-5.1499999	
7	0.2336633E-01	673.60709	354.50630				

O 1	80749.663	0.1165029	605.26170	410.03476	0	0	0
P 2	164.19337	0.1822191	1.2335937	382.66088	-85.807148	0	0
S 3	256.81089		1.9285677		10.124287	0	0

O*1	212.38000	356044.75	6.3803362	27.793115	1581.2378	-0.1747360	0.8629974E-06
P 2	53947.159	0.2126643E 08	0.5535569	-78.118752	79158.443	0.2366069E-01	0.7865500E-02
1 3	267.28.10	10096.349	17.037514	104.82825	13.612264	0.3261872	0.9105509E 08
4	131.94477	10049.298	0	104.48755	13.677234	1.4966295	9.5088532
5	2.9635440	11397.123	1.2752739	102.65884	12.033834	50.000000	5086.2425
6	0.5036996E-01	58.597430	131.93918	2.6547570	-50.000000	-0.6146729E-05	302.07665

D 1	0	0	0	50.236234	27.881701	0	0.8629974E-06
E 2	79158.443	77.341846	189.79026	44.368091	46.709158	21.143000	31.532108
P 3	1581.2378	0	0	50.350000	2158.3477	1168.8225	53.657229
R 4	80739.681	77.341846	189.79026	68.485555	5249.7181	922.00127	32.899998
O 5	-524.80187	0.2980261	0.6753274	2.0862122	1.4966295	31.911768	3292.0000
6	-157.49999	-6.0374998	6.8537498	2.4539142	0.4338280	-5.1499999	
7	0.2336633E-01	673.51692	354.51222				

O 1	80739.085	0.1172382	600.34129	412.34281	0	0	0
P 2	165.20790	0.1834230	1.2514861	382.66067	-59.470364	0	0
S 3	258.47371		1.9573943		7.0027996	0	0

O*1	212.38000	356044.75	6.3803362	27.793115	1581.2477	-0.1747360	0.8629974E-06
P 2	51895.559	0.2126643E 08	0.5535569	-78.118752	79162.984	0.2366069E-01	0.7865500E-02
1 3	267.29636	10096.349	17.037514	104.82825	13.612264	0.3261872	0.9105509E 08
4	131.94477	10049.298	0	104.48755	13.677234	1.5558833	9.5088532
5	2.9635440	11397.123	1.2752739	102.65884	12.033834	50.000000	5086.2426
6	0.5036996E-01	58.597430	131.93918	2.6547570	-50.000000	-0.6146729E-05	302.07756

D 1	0	0	0	50.236234	27.881701	0	0.8629974E-06
E 2	79162.984	77.344366	189.80199	44.467499	47.379804	21.143000	31.532109
P 3	1581.2477	0	0	50.350000	2158.3477	1168.8225	53.657229
R 4	80744.231	77.344366	189.80199	68.485555	5249.7181	922.00127	32.899998
O 5	-524.80187	0.2980261	0.6753274	2.0862122	1.5558832	33.321890	3295.0000
6	-157.49999	-6.0374998	6.8537498	2.4539860	0.4338280	-5.1499999	
7	0.2336633E-01	673.55556	354.51441				

O 1	80743.609	0.1195416	584.47345	412.34281	0	0	0
P 2	168.46322	0.1872669	1.3091874	382.66067	-54.294480	0	0
S 3	263.90526		2.0503575		6.6273555	0	0

[redacted]

O*1	219.99999	373873.75	6.5531623	27.741881	1581.3300	-0.7402432E-01	0.4819165E-06
P 2	49859.185	0.2128431E 08	0.5513231	-77.894444	79127.674	0.9987276E-02	0.3332103E-02
1 3	267.18440	10428.786	16.201107	104.96087	12.840951	0.1438762	0.9105549E 08
4	144.25651	10381.609	0	104.60405	12.900310	1.6187246	8.2821482
5	3.1958002	11734.037	1.4439840	102.81577	11.392188	50.000000	2225.9537
6	0.2191161E-01	61.531705	144.25005	2.6543081	-50.000000	-0.6146729E-05	302.07229
D 1	0	0	0	50.236234	27.881701	0	0.4819165E-06
E 2	79127.674	77.319717	189.71468	43.671519	47.783988	20.000001	31.353622
P 3	1581.3300	0	0	50.350000	1569.0775	1173.0209	52.953845
R 4	80709.003	77.319717	189.71468	68.510268	3803.7578	926.80141	32.899998
O 5	-524.80187	0.2980261	0.6753274	2.0862122	1.6187246	34.534568	3320.0000
6	-157.49999	-6.0374998	6.8537498	2.4536391	0.4338280	-5.1499999	
7	0.2336633E-01	673.25511	354.53269				
O 1	80708.362	0.1215584	566.03841	416.36102	0	0	0
P 2	171.23067	0.1899704	1.3704381	382.65396	-20.750300	0	0
5 3	267.59831		2.1415065		2.6162211	0	0
O*1	224.25000	383629.00	6.5893821	27.712337	1581.3731	-0.5163454E-01	0.3751541E-06
P 2	48723.789	0.2129409E 08	0.5495964	-77.766000	79106.739	0.6946939E-02	0.2324257E-02
1 3	267.11806	10622.346	15.694752	105.03606	12.434006	0.1011999	0.9105561E 08
4	151.31202	10575.108	0	104.67031	12.490442	1.6560168	7.8398361
5	3.3284844	11929.902	1.5419794	102.90442	11.052932	50.000000	1581.6271
6	0.1536767E-01	63.137213	151.30495	2.6538625	-50.000000	-0.6146729E-05	302.06910
D 1	0	0	0	50.236234	27.881701	0	0.3751541E-06
E 2	79106.739	77.305283	189.66278	43.200425	47.976960	19.362500	31.254070
P 3	1581.3731	0	0	50.350000	1240.4983	1175.8558	52.561537
R 4	80688.112	77.305283	189.66278	68.524053	2997.5777	930.19415	32.899999
O 5	-524.80187	0.2980261	0.6753274	2.0862122	1.6560168	35.142348	3329.0000
6	-157.49999	-6.0374998	6.8537498	2.4534259	0.4338280	-5.1499999	
7	0.2336633E-01	673.07700	354.54228				
O 1	80687.466	0.1225351	554.01657	417.20313	0	0	0
P 2	172.56186	0.1908532	1.4071715	382.64878	-13.298141	0	0
5 3	268.77234		2.1915975		1.7378443	0	0

[redacted]

O 1	TIME	ALTITUDE	ALPHA	GEOCENT LAT	THRUST FIXED	AXL FORCE	ATM PRESS
P 2	WEIGHT	RADIUS	BETA	LONGITUDE	THRUST CONTL	SIDE FORCE	DYNM PRESS
1 3	TOTAL FLOW	VEL E	PSI	AZI E	GAMMA E	NORM FORCE	HEAT PARAM
4	GRND RANGE	VEL R	PSIDOT	AZI R	GAMMA R	AXL LD FCTR	MACH NUMBER
5	THETA I	VEL I	CROSS RANGE	AZI I	GAMMA I	WIND VEL	RHO-VR CUBED
6	Q*ALPHA TOT	ALT	DOWN RANGE	PHI	EAST WIND	NORTH WIND	TOTAL ISP
O 1	SEC	FT	DEG	DEG	LBS	LBS	PSI
P 2	LBS	FT	DEG	DEG	LBS	LBS	LBS/FT SQD
1 3	LBS/SEC	FT/SEC	DEG	DEG	DEG	LBS	FT*LBS/FT SQD
4	N. MI.	FT/SEC	DEG/SEC	DEG	DEG		
5	DEG	FT/SEC	N.MI.	DEG	DEG	FT/SEC	LBS/SEC CUBED
6	DEG-PSF	N.MI	N.MI.	DEG	FT/SEC	FT/SEC	SEC
O 1	PERIGEE RAD	PERIGEE ALT	PERIGEE VEL	SEMI LAT REC	SEMI MAJ AXIS	ECCENTRICITY	TRUE ANOMALY
4 2	APOGEE RAD	APOGEE ALT	APOGEE VEL	PERIOD	ENERGY	INCLINATION	ASCEND NODE
O 1	NM	NM	FT/SEC	NM	NM		DEG
4 2	NM	NM	FT/SEC	MIN	FT**2/SEC**2	DEG	DEG
O*1	224.25000	383629.00	6.5893821	27.712337	80688.113	-0.5163454E-01	0.3751541E-06
P 2	48723.789	0.2129409E 08	0.5495964	-77.766000	0	0.6946939E-02	0.2324257E-02
1 3	267.11806	10622.346	15.694752	105.03606	12.434006	0.1011999	0.9105561E 08
4	151.31202	10575.108	0	104.67031	12.490442	1.6560301	7.8398361
5	3.3284844	11929.902	1.5419794	102.90442	11.052932	50.000000	1581.6271
6	0.1536767E-01	63.137213	151.30495	2.6538625	-50.000000	-0.6146729E-05	302.06910
O 1	405.19958	-3038.7339	101267.35	726.78672	1963.6635	0.7936512	177.07420
4 2	3522.1274	78.193848	11650.199	36.376448	-0.5898924E 09	30.352316	156.94243
O*1	224.8360C	384963.00	6.6753512	27.708209	4194.6910	-0.4919473E-01	0.3635055E-06
P 2	48684.186	0.2129543E 08	0.5487771	-77.748108	0	0.6609856E-02	0.2214433E-02
1 3	0.1500000	10630.902	15.694752	105.04769	12.366856	0.9833254E-01	0.9105562E 08
4	152.29516	10583.654	0	104.68084	12.422944	0.8616025E-01	7.7740168
5	3.3469507	11938.827	1.5556711	102.91521	10.994076	50.000000	1508.1105
6	0.1483109E-01	63.356761	152.28798	2.6517998	-50.000000	-0.6146729E-05	27964.607
O 1	406.11311	-3037.8204	101141.73	728.25743	1964.1564	0.7932379	177.08295
4 2	3522.1997	78.266144	11661.742	36.390146	-0.5897443E 09	30.352838	165.94000
O*1	224.8360C	384963.00	6.6753512	27.708209	4194.6910	-0.4919473E-01	0.3635055E-06
P 2	48684.186	0.2129543E 08	0.5487771	-77.748108	0	0.6609856E-02	0.2214433E-02
1 3	0.1500000	10630.902	15.694752	105.04769	12.366856	0.9833254E-01	0.9105562E 08
4	152.29516	10583.654	0	104.68084	12.422944	0.8616025E-01	7.7740168
5	3.3469507	11938.827	1.5556711	102.91521	10.994076	50.000000	1508.1105
6	0.1483109E-01	63.356761	152.28798	2.6517998	-50.000000	-0.6146729E-05	27964.607
O 1	406.11311	-3037.8204	101141.73	728.25743	1964.1564	0.7932379	177.08295
4 2	3522.1997	78.266144	11661.742	36.390146	-0.5897443E 09	30.352838	165.94000
O*1	225.43600	386320.00	6.7705284	27.703979	2624.4268	-0.4677483E-01	0.3522351E-06
P 2	48684.096	0.2129679E 08	0.5485377	-77.729787	0	0.6282262E-02	0.2105504E-02
1 3	0.1500000	10628.290	15.694752	105.06010	12.290920	0.9552980E-01	0.9105564E 08
4	153.30198	10581.031	0	104.69220	12.346681	0.5390631E-01	7.7007223
5	3.3658617	11936.627	1.5698243	102.92515	10.926112	50.000000	1433.5708

[redacted]

[redacted]

6	0.1430122E-01	63.580095	153.29480	2.6496878	-50.000000	-0.6146729E-05	17496.179
0 1	406.21216	-3037.7214	101128.13	728.41684	1964.2098	0.7931931	177.10083
4 2	3522.2074	78.273834	11662.992	36.391629	-0.5897283E 09	30.352935	166.93955
0*1	225.43600	386320.00	6.7937682	27.703979	2624.4268	-0.4677482E-01	0.3522351E-06
P 2	48684.096	0.2129679E 08	0.5531541	-77.729787	0	0.6329569E-02	0.2105504E-02
1 3	0.1500000	10628.290	15.717998	105.06010	12.290920	0.9602954E-01	0.9105564E 08
4	153.30198	10581.031	0	104.69220	12.346681	0.5390631E-01	7.7007222
5	3.3658617	11936.627	1.5698243	102.92515	10.926112	50.000000	1433.5707
6	0.1435076E-01	63.580095	153.29480	2.6543013	-50.000000	-0.6146729E-05	17496.179
0 1	406.21216	-3037.7214	101128.13	728.41684	1964.2098	0.7931931	177.10083
4 2	3522.2074	78.273834	11662.992	36.391629	-0.5897283E 09	30.352935	166.93955
0*1	226.65000	389040.50	7.0541269	27.695410	1772.1571	-0.4238138E-01	0.3312478E-06
P 2	48683.914	0.2129952E 08	0.5575332	-77.692724	0	0.5775707E-02	0.1907739E-02
1 3	0.1500000	10621.874	15.784914	105.08526	12.136397	0.9215604E-01	0.9105567E 08
4	155.33902	10574.593	0	104.71524	12.191496	0.3640042E-01	7.5587977
5	3.4041227	11931.043	1.5985922	102.94511	10.787706	50.000000	1298.1285
6	0.1349856E-C1	64.027831	155.33158	2.6547633	-50.000000	-0.6146729E-05	11814.380
0 1	406.32396	-3037.6096	101112.79	728.59677	1964.2699	0.7931425	177.13795
4 2	3522.2158	78.282227	11664.405	36.393300	-0.5897103E 09	30.353085	165.93886
0*1	226.65000	389040.50	7.0541269	27.695410	1772.1589	-0.4238138E-01	0.3312478E-06
P 2	36243.000	0.2129952E 08	0.5575332	-77.692724	0	0.5775707E-02	0.1907739E-02
1 3	0.1500000	10621.874	15.784914	105.08526	12.136397	0.9215604E-01	0.9105567E 08
4	155.33902	10574.593	0	104.71524	12.191496	0.4889541E-01	7.5587977
5	3.4041227	11931.043	1.5985922	102.94511	10.787706	50.000000	1298.1285
6	0.1349856E-C1	64.027831	155.33158	2.6547633	-50.000000	-0.6146729E-05	11814.392
0 1	406.32396	-3037.6096	101112.79	728.59677	1964.2699	0.7931425	177.13795
4 2	3522.2158	78.282227	11664.405	36.393300	-0.5897103E 09	30.353085	165.93886

$$ SEPARATION

[redacted]

[redacted]

0 1	TIME	ALTITUDE	ALPHA	GEOCENT LAT	THRUST FIXED	AXL FORCE	ATM PRESS
P 2	WEIGHT	RADIUS	BETA	LONGITUDE	THRUST CONTL	SIDE FORCE	DYNM PRESS
1 3	TOTAL FLOW	VEL E	PSI	AZI E	GAMMA E	NORM FORCE	HEAT PARAM
4	GRND RANGE	VEL R	PSIDOT	AZI R	GAMMA R	AXL LD FCTR	MACH NUMBER
5	THETA I	VEL I	CROSS RANGE	AZI I	GAMMA I	WIND VEL	RHO-VR CUBED
6	Q*ALPHA TOT	ALT	DOWN RANGE	PHI	EAST WIND	NORTH WIND	TOTAL ISP
0 1	SEC	FT	DEG	DEG	LBS	LBS	PSI
P 2	LBS	FT	DEG	DEG	LBS	LBS	LBS/FT SQD
1 3	LBS/SEC	FT/SEC	DEG	DEG	DEG	LBS	FT'LBS/FT SQD
4	N. MI.	FT/SEC	DEG/SEC	DEG	DEG		
5	DEG	FT/SEC	N.MI.	DEG	DEG	FT/SEC	LBS/SEC CUBED
6	DEG-PSF	N.MI	N.MI.	DEG	FT/SEC	FT/SEC	SEC
0 1	PERIGEE RAD	PERIGEE ALT	PERIGEE VEL	SEMI LAT REC	SEMI MAJ AXIS	ECCENTRICITY	TRUE ANOMALY
4 2	APOGEE RAD	APOGEE ALT	APOGEE VEL	PERIOD	ENERGY	INCLINATION	ASCEND NODE
0 1	NM	NM	FT/SEC	NM	NM		DEG
4 2	NM	NM	FT/SEC	MIN	FT**2/SEC**2	DEG	DEG
0*1	226.65000	389040.50	7.0541269	27.695410	8.7199999	-0.1497575	0.3312478E-06
P 2	36243.000	0.2129952E 08	0.5575332	-77.692724	0	0	0.1907739E-02
1 3	4.8000000	10621.874	15.784914	105.08526	12.136397	0	0.9105567E 08
4	155.33902	10574.593	0	104.71524	12.191496	0.2364661E-03	7.5587977
5	3.4041227	11931.043	1.5985922	102.94511	10.787706	50.000000	1298.1285
6	0.1349856E-C1	64.027831	155.33158	2.6547633	-50.000000	-0.6146729E-05	1.8166667
0 1	406.32396	-3037.6096	101112.79	728.59677	1964.2699	0.7931425	177.13795
4 2	3522.2158	78.282227	11664.405	36.393300	-0.5897103E 09	30.353085	165.93896
0*1	227.96000	391935.25	7.2641584	27.686152	8.7199999	-0.1353003	0.3110198E-06
P 2	36236.712	0.2130243E 08	0.5617750	-77.652748	0	0	0.1723571E-02
1 3	4.8000000	10613.446	15.784914	105.11246	11.968357	0	0.9105569E 08
4	157.53655	10566.139	0	104.74016	12.022741	0.2369061E-03	7.4146435
5	3.445401C	11923.506	1.6297189	102.96648	10.637064	50.000000	1171.8727
6	0.1255688E-01	64.504246	157.52896	2.6547633	-50.000000	-0.6146729E-05	1.8166667
0 1	406.32560	-3037.6079	101112.57	728.59939	1964.2706	0.7931417	177.17926
4 2	3522.2155	78.281952	11664.427	36.393318	-0.5897101E 09	30.353183	165.93840
0*1	227.96000	391935.25	7.2641584	27.686152	8.7199999	-0.1353003	0.3110198E-06
P 2	36236.712	0.2130243E 08	0.5617750	-77.652748	0	0	0.1723571E-02
1 3	4.8000000	10613.446	15.784914	105.11246	11.968357	0	0.9105569E 08
4	157.53655	10566.139	0	104.74016	12.022741	0.2369061E-03	7.4146435
5	3.4454010	11923.506	1.6297189	102.96648	10.637064	50.000000	1171.8727
6	0.1255688E-01	64.504246	157.52896	2.6547633	-50.000000	-0.6146729E-05	1.8166667
0 1	406.32560	-3037.6079	101112.57	728.59939	1964.2706	0.7931417	177.17926
4 2	3522.2155	78.281952	11664.427	36.393318	-0.5897101E 09	30.353183	165.93840
0*1	230.00000	396359.75	7.5917206	27.671710	8.7199999	-0.1166480	0.2836838E-06
P 2	36226.920	0.2130687E 08	0.5684011	-77.590535	0	0	0.1485962E-02
1 3	4.8000000	10600.557	15.784914	105.15477	11.706170	0	0.9105572E 08
4	160.95737	10553.214	0	104.77892	11.759435	0.2374850E-03	7.2085905
5	3.5096611	11911.982	1.6787935	102.99973	10.402130	50.000000	1009.0846

[redacted]

[redacted]

6	0.1131185E-01	65.232425	160.94958	2.6547633	-50.000000	-0.6146729E-05	1.8166667
0 1	406.32816	-3037.6054	101112.22	728.60349	1964.2716	0.7931405	177.24357
4 2	3522.2151	78.281525	11664.461	36.393348	-0.5897098E 09	30.353336	166.93770
0*1	230.00000	396359.75	7.5917206	27.671710	8.7199999	-0.1166480	0.2836838E-06
P 2	36226.920	0.2130687E 08	0.5684011	-77.590535	0	0	0.1485962E-02
1 3	4.8000000	10600.557	15.784914	105.15477	11.706170	0	0.9105572E 08
4	160.95737	10553.214	0	104.77892	11.759435	0.2374850E-03	7.2086905
5	3.5096611	11911.982	1.6787935	102.99973	10.402130	50.000000	1009.0845
6	0.1131185E-01	65.232425	160.94958	2.6547633	-50.000000	-0.6146729E-05	1.8166667
0 1	406.32816	-3037.6054	101112.22	728.60349	1964.2716	0.7931405	177.24357
4 2	3522.2151	78.281525	11664.461	36.393348	-0.5897098E 09	30.353336	166.93770
0*1	230.00000	396359.75	7.5917206	27.671710	8.7199999	-0.1166480	0.2836838E-06
P 2	36226.920	0.2130687E 08	0.5684011	-77.590535	0	0	0.1485962E-02
1 3	4.8000000	10600.557	15.784914	105.15477	11.706170	0	0.9105572E 08
4	160.95737	10553.214	0	104.77892	11.759435	0.2374850E-03	7.2086905
5	3.5096611	11911.982	1.6787935	102.99973	10.402130	50.000000	1009.0846
6	0.1131185E-01	65.232425	160.94958	2.6547633	-50.000000	-0.6146729E-05	1.8165667
0 1	406.32816	-3037.6054	101112.22	728.60349	1964.2716	0.7931405	177.24357
4 2	3522.2151	78.281525	11664.461	36.393348	-0.5897098E 09	30.353336	166.93770
0*1	235.20395	407182.00	8.4299508	27.634729	8.7199999	-0.8364068E-01	0.2308788E-06
P 2	36201.941	0.2131773E 08	0.5854180	-77.432047	0	0	0.1065486E-02
1 3	4.8000000	10568.986	15.784914	105.26242	11.034625	0	0.9105579E 08
4	169.67681	10521.552	0	104.87754	11.085003	0.2385607E-03	6.7663062
5	3.6734704	11883.765	1.8064799	103.08437	9.8009672	50.000000	721.37776
6	0.9003012E-02	67.013538	169.66809	2.6547633	-50.000000	-0.6146729E-05	1.8165667
0 1	406.33471	-3037.5988	101111.32	728.61401	1964.2744	0.7931375	177.40751
4 2	3522.2141	78.280579	11664.548	36.393426	-0.5897089E 09	30.353729	166.93589
0*1	235.20395	407182.00	8.4299508	27.634729	0	0.3099368E-01	0.2308788E-06
P 2	36201.941	0.2131773E 08	0.5854180	-77.432047	0	0.4413846E-02	0.1065486E-02
1 3	0	10568.986	15.784914	105.26242	11.034625	0.7861779E-01	0.9105579E 08
4	169.67681	10521.552	0	104.87754	11.085003	0.8561330E-06	6.7663062
5	3.6734704	11883.765	1.8064799	103.08437	9.8009672	50.000000	721.37776
6	0.9003012E-02	67.013538	169.66809	2.6547633	-50.000000	-0.6146729E-05	1.8166667
0 1	406.33471	-3037.5988	101111.32	728.61401	1964.2744	0.7931375	177.40751
4 2	3522.2141	78.280579	11664.548	36.393426	-0.5897089E 09	30.353729	165.93589
0*1	236.75395	410280.75	8.6625988	27.623670	31341.984	0.2712080E-01	0.2186029E-06
P 2	36145.664	0.2132084E 08	0.5892965	-77.384869	0	0.4093102E-02	0.9793392E-03
1 3	72.615962	10581.289	15.784914	105.29341	10.851653	0.7557479E-01	0.9105581E 08
4	172.27366	10533.832	0	104.90570	10.901141	0.8671029	6.6666601
5	3.7222593	11896.953	1.8451960	103.11165	9.6393986	50.000000	663.82648
6	0.8502640E-02	67.523527	172.26479	2.6547633	-50.000000	-0.6146729E-05	0.1200838
0 1	407.91199	-3036.0215	100895.55	731.15109	1965.1179	0.7924237	177.44029
4 2	3522.3238	78.390259	11684.475	36.416870	-0.5894558E 09	30.354679	165.93155

[redacted]

[redacted]

O 1	TIME	ALTITUDE	ALPHA	GEOCENT LAT	THRUST FIXED	AXL FORCE	ATM PRESS
P 2	WEIGHT	RADIUS	BETA	LONGITUDE	THRUST CONTI	SIDE FORCE	DYNM PRESS
I 3	TOTAL FLOW	VEL E	PSI	AZI E	GAMMA E	NORM FORCE	HEAT PARAM
4	GRND RANGE	VEL R	PSIDOT	AZI R	GAMMA R	AXL LD FCTR	MACH NUMBER
5	THETA I	VEL I	CROSS RANGE	AZI I	GAMMA I	WIND VEL	RHO-VR CUBED
6	Q*ALPHA TOT	ALT	DOWN RANGE	PHI	EAST WIND	NORTH WIND	TOTAL ISP
O 1	SEC	FT	DEG	DEG	LBS	LBS	PSI
P 2	LBS	FT	DEG	DEG	LBS	LBS	LBS/FT SQD
I 3	LBS/SEC	FT/SEC	DEG	DEG	DEG	LBS	FT'LBS/FT SQD
4	N. MI.	FT/SEC	DEG/SEC	DEG	DEG		
5	DEG	FT/SEC	N.MI.	DEG	DEG	FT/SEC	LBS/SEC CUBED
6	DEG-PSF	N.MI	N.MI.	DEG	FT/SEC	FT/SEC	SEC
O 1	PERIGEE RAD	PERIGEE ALT	PERIGEE VEL	SEMI LAT REC	SEMI MAJ AXIS	ECCENTRICITY	TRUE ANOMALY
4 2	APOGEE RAD	APOGEE ALT	APOGEE VEL	PERIOD	ENERGY	INCLINATION	ASCEND NODE
O 1	NM	NM	FT/SEC	NM	NM		DEG
4 2	NM	NM	FT/SEC	MIN	FT**2/SEC**2	DEG	DEG
C 1	THRUST	C-1 THRUST	C-2 THRUST	LH2 WEIGHT	C-1 ISP	C-2 ISP	C-1 PU VALVE
E 2	LH2 FLOW	C-1 LH2 FLOW	C-2 LH2 FLOW	LO2 WEIGHT	C-1 FLOW	C-2 FLOW	C-2 PU VALVE
N 3	LO2 FLOW	C-1 LO2 FLOW	C-2LO2 FLOW	C-1 LH2 PRESS	C-1 LO2 PRESS	C-1 LH2 TEMP	C-1 LO2 TEMP
T 4	RATIO	C-1 RATIO	C-2 RATIO	C-2 LH2 PRESS	C-2 LO2 PRESS	C-2 LH2 TEMP	C-2 LO2 TEMP
C 1	LBS	LBS	LBS	LBS	SEC	SEC	DEG
E 2	LBS/SEC	LBS/SEC	LBS/SEC	LBS LBS/SEC	LBS/SEC	DEG	
N 3	LBS/SEC	LBS/SEC	LBS/SEC	PSI	PSI	DEG R	DEG R
T 4.				PSI	PSI	DEG R	DEG R
O*1	236.75395	410280.75	8.6625988	27.623670	30551.359	-0.7687813E-01	0.2185029E-05
P 2	36145.664	0.2132084E 08	0.5892965	-77.384869	0	0	0.9793392E-03
I 3	70.917899	10581.289	15.784914	105.29341	10.851653	0	0.9105531E 08
4	172.27366	10533.832	0	104.90570	10.901141	0.8452268	6.5555571
5	3.7222593	11896.953	1.8451960	103.11165	9.6393986	50.000000	663.82648
6	0.8502640E-02	67.523527	172.26479	2.6547633	-50.000000	-0.6146729E-05	430.79899
O 1	407.91199	-3036.0215	100895.55	731.15109	1965.1179	0.7924237	177.44029
4 2	3522.3238	78.390259	11684.475	36.416870	-0.5894558E 09	30.354679	166.93155
C 1	30551.359	15319.711	15231.648	4983.8120	431.95137	430.65209	-0
E 2	11.560988	5.7450033	5.8159851	24357.911	35.446099	35.368801	-0
N 3	55.253911	29.701096	29.552816	36.396900	67.590700	-420.30818	-281.64915
T 4	5.1253327	5.1699005	5.0813087	39.208487	66.467526	-420.39999	-281.44914
O*1	237.90000	412545.25	8.8215104	27.615460	30507.387	-0.7261839E-01	0.2102753E-06
P 2	36064.466	0.2132311E 08	0.5913053	-77.349907	0	0	0.9250751E-03
I 3	70.783407	10605.497	15.784914	105.31563	10.729560	0	0.9105582E 08
4	174.19850	10558.024	0	104.92572	10.778380	0.8459106	6.5063881
5	3.7584106	11921.749	1.8740665	103.13330	9.5331697	50.000000	628.48466
6	0.8178300E-02	67.896215	174.18942	2.6547633	-50.000000	-0.6146729E-05	430.99631
O 1	410.19428	-3033.7392	100585.51	734.81866	1966.3377	0.7913917	177.45329
4 2	3522.4812	78.547638	11713.221	36.450784	-0.5890901E 09	30.355963	165.92569
C 1	30507.387	15290.186	15217.201	4970.5459	432.29579	430.70580	-0

[redacted]

[redacted]

E 2	11.590382	5.7726928	5.8176888	24290.097	35.349560	35.330849	-0
N 3	59.090026	29.576867	29.513160	35.029031	63.487094	-420.34515	-281.87096
T 4	5.0981951	5.1235823	5.0730042	36.990321	64.064515	-420.39999	-281.67096
0*1	237.90000	412545.25	9.7936896	27.615460	30507.387	-0.7261839E-01	0.2102753E-06
P 2	36064.466	0.2132311E 08	0.5465929	-77.349907	0	0	0.9250751E-03
1 3	70.783407	10605.497	16.757038	105.31563	10.729560	0	0.9105582E 08
4	174.19850	10558.024	0	104.92572	10.778380	0.8459106	6.5063882
5	3.7584106	11921.749	1.8740665	103.13330	9.5331697	50.000000	628.48468
6	0.9073456E-02	67.896215	174.18942	2.6087403	-50.000000	-0.6146729E-05	430.99631
0 1	410.19428	-3033.7392	100585.51	734.81866	1966.3377	0.7913917	177.45329
4 2	3522.4812	78.547638	11713.221	36.450784	-0.5890901E 09	30.355963	166.92569
C 1	30507.387	15290.186	15217.201	4970.5459	432.29579	430.70580	-0
E 2	11.590382	5.7726928	5.8176888	24290.097	35.349560	35.330849	-0
N 3	59.090026	29.576867	29.513160	35.029031	63.487094	-420.34515	-281.87096
T 4	5.0981951	5.1235823	5.0730042	36.990321	64.064515	-420.39999	-281.67096
0*1	240.00000	416643.50	10.007098	27.600332	30437.817	-0.6573430E-01	0.1964323E-06
P 2	35916.062	0.2132722E 08	0.5513247	-77.285626	0	0	0.8373796E-03
1 3	70.560358	10649.932	16.686384	105.35666	10.513131	0	0.9105584E 08
4	177.73833	10602.434	0	104.96275	10.560770	0.8474691	6.5031601
5	3.8248692	11967.217	1.9275512	103.17321	9.3448696	50.000000	571.29837
6	0.8391938E-02	68.570701	177.72890	2.6096747	-50.000000	-0.6146729E-05	431.37277
0 1	414.37731	-3029.5562	100023.79	741.52996	1968.5781	0.7895043	177.47620
4 2	3522.7790	78.845428	11765.594	36.513098	-0.5884197E 09	30.358381	166.91470
C 1	30437.817	15244.981	15192.837	4946.1429	432.88560	430.87543	-0
E 2	11.651497	5.8218654	5.8296312	24166.312	35.196968	35.260392	-0
N 3	58.805862	29.375102	29.430760	33.000000	57.119999	-420.43999	-282.19999
T 4	5.0470651	5.0456511	5.0484772	33.820000	59.860000	-420.39999	-282.00000
0*1	250.00000	435266.25	10.975747	27.526793	30300.625	-0.4397734E-01	0.1486163E-06
P 2	35213.154	0.2134592E 08	0.5734902	-76.975640	0	0	0.5602209E-03
1 3	70.168076	10866.446	16.334805	105.55305	9.5185270	0	0.9105591E 08
4	194.82420	10818.842	0	105.14015	9.5608044	0.8604904	5.1152771
5	4.1451632	12188.259	2.1920517	103.36429	8.4781723	50.000000	390.00946
6	0.6156828E-02	71.635612	194.81297	2.6140694	-50.000000	-0.6146729E-05	431.82921
0 1	434.85983	-3009.0737	97388.835	774.18913	1979.5040	0.7803188	177.58730
4 2	3524.1481	80.214600	12017.228	36.817497	-0.5851719E 09	30.369774	165.86344
C 1	30300.625	15182.346	15118.279	4829.0871	433.24712	431.43251	-0
E 2	11.699493	5.8376460	5.8618466	23581.490	35.023028	35.042048	-0
N 3	58.365584	29.185382	29.180202	33.000000	54.299999	-420.53841	-282.45365
T 4	4.9887277	4.9995121	4.9779879	34.138414	54.876218	-420.43840	-282.43048
0*1	257.08054	447577.75	11.611727	27.473195	30245.424	-0.3502165E-01	0.1263950E-06
P 2	34716.756	0.2135828E 08	0.5887685	-76.752222	0	0	0.4461357E-03
1 3	70.046470	11025.185	16.068350	105.69310	8.8502674	0	0.9105595E 08
4	207.15455	10977.519	0	105.26685	8.8890076	0.8712043	5.9174991
5	4.3758247	12349.831	2.3893758	103.50068	7.8945599	50.000000	315.14196
6	0.5186704E-02	73.661823	207.14204	2.6171255	-50.000000	-0.6146729E-05	431.79084

[redacted]

O 1	449.99542	-2993.9381	95555.925	798.10786	1987.5338	0.7735911	177.66752
4 2	3525.0722	81.138672	12198.255	37.041749	-0.5828078E 09	30.377746	155.82811
C 1	30245.424	15152.116	15093.308	4746.3542	433.25278	431.35229	-0
E 2	11.669594	5.8265517	5.8430421	23168.555	34.952796	34.990675	-0
N 3	58.273877	29.126244	29.147633	33.000000	54.299999	-420.58158	-282.62535
T 4	4.9936508	4.9988819	4.9884344	34.181588	55.523829	-420.48158	-282.68953
O*1	257.08054	447577.75	12.032666	27.473195	30245.424	-0.3502165E-01	0.1263950E-06
P 2	34716.756	0.2135828E 08	0.5899693	-76.752222	0	0	0.4461357E-03
1 3	70.046470	11025.185	16.489290	105.69310	8.8502674	0	0.9105595E 08
4	207.15455	10977.519	0	105.26685	8.8890076	0.8712043	5.9174990
5	4.3758247	12349.831	2.3893758	103.50068	7.8945599	50.000000	315.14194
6	0.5374279E-02	73.661823	207.14204	2.6174147	-50.000000	-0.6146729E-05	431.79084
O 1	449.99542	-2993.9381	95555.925	798.10786	1987.5338	0.7735911	177.66752
4 2	3525.0722	81.138672	12198.255	37.041749	-0.5828078E 09	30.377746	165.82811
C 1	30245.424	15152.116	15093.308	4746.3542	433.25278	431.35229	-0
E 2	11.669594	5.8265517	5.8430421	23168.555	34.952796	34.990675	-0
N 3	58.273877	29.126244	29.147633	33.000000	54.299999	-420.58158	-282.62535
T 4	4.9936508	4.9988819	4.9884344	34.181588	55.523829	-420.48158	-282.68953
O*1	260.00000	452448.75	12.273983	27.450719	30222.696	-0.3222992E-01	0.1190326E-06
P 2	34512.332	0.2136318E 08	0.5961880	-76.659141	0	0	0.4105722E-03
1 3	69.996423	11091.821	16.369209	105.75110	8.5862961	0	0.9105597E 08
4	212.29559	11044.133	0	105.31937	8.6236544	0.8757062	5.8496721
5	4.4718802	12417.543	2.4731668	103.55717	7.6637650	50.000000	291.78047
6	0.5044942E-02	74.463488	212.28246	2.6186705	-50.000000	-0.6146729E-05	431.77485
O 1	456.37928	-2987.5542	94809.732	808.14226	1990.9140	0.7707690	177.70023
4 2	3525.4486	81.515076	12273.387	37.136282	-0.5818183E 09	30.381002	165.81380
C 1	30222.696	15139.651	15083.045	4712.3033	433.25510	431.31894	-0
E 2	11.657274	5.8219734	5.8353001	22998.482	34.923838	34.969586	-0
N 3	58.236150	29.101864	29.134286	33.000000	54.299999	-420.59938	-282.69755
T 4	4.9956921	4.9986253	4.9927656	34.199389	55.790852	-420.49939	-282.79533
O*1	270.00000	468251.25	13.048091	27.372021	30141.116	-0.2521675E-01	0.9930830E-07
P 2	33813.290	0.2137906E 08	0.6169943	-76.336010	0	0	0.3212325E-03
1 3	65.811857	11325.752	15.937969	105.95088	7.7186623	0	0.9105601E 08
4	230.16096	11278.002	0	105.50047	7.7515440	0.8913978	5.5648281
5	4.8051593	12654.822	2.7713067	103.75188	6.9038305	50.000000	233.12387
6	0.4195839E-02	77.064244	230.14579	2.6229035	-50.000000	-0.6146729E-05	431.74780
O 1	478.98887	-2964.9446	92285.354	843.42516	2002.8385	0.7608450	177.81379
4 2	3526.6881	82.754608	12534.042	37.470423	-0.5783542E 09	30.392070	166.76573
C 1	30141.116	15098.049	15043.068	4595.9168	433.24208	431.28065	-0
E 2	11.620083	5.8044512	5.8156316	22416.857	34.828862	34.879996	-0
N 3	58.088776	29.024411	29.064365	33.000000	54.299999	-420.59999	-282.77983
T 4	4.9989984	5.0003712	4.9976282	34.199999	56.119354	-420.50000	-282.80000
O*1	280.00000	482726.75	13.741560	27.290613	30058.992	-0.2072963E-01	0.8544094E-07
P 2	33116.102	0.2139362E 08	0.6370021	-76.006117	0	0	0.2640717E-03
1 3	69.625302	11568.393	15.475000	106.15241	6.9062614	0	0.9105604E 08

[redacted]

4	248.42950	11520.597	0	105.68349	6.9350538	0.9076844	5.5372949
5	5.1451524	12900.330	3.0867792	103.94854	6.1902514	50.000000	195.76359
6	0.3632363E-02	79.446605	248.41201	2.6270229	-50.000000	-0.6146729E-05	431.72511
O 1	502.81140	-2941.1221	89807.845	880.17476	2015.3309	0.7505068	177.92960
4 2	3527.8503	83.916809	12799.978	37.821542	-0.5747692E 09	30.403003	166.71908
C 1	30058.992	15057.470	15001.522	4479.8987	433.21098	431.26894	-0
E 2	11.583764	5.7855200	5.7982442	21836.717	34.737692	34.784611	-0
N 3	57.938539	28.952172	28.986367	33.000000	54.845454	-420.64545	-282.80000
T 4	5.0017022	5.0042472	4.9991628	34.199999	56.154544	-420.50000	-282.84545
O*1	290.00000	495922.75	14.353967	27.206397	30040.191	-0.1771641E-01	0.7530461E-07
P 2	32420.193	0.2140690E 08	0.6561560	-75.669317	0	0	0.2256868E-03
1 3	69.602202	11819.904	14.978181	106.35574	6.1475830	0	0.9105607E 08
4	267.11119	11772.079	0	105.86847	6.1726561	0.9265883	5.4527053
5	5.4920262	13154.282	3.4201483	104.14723	5.5219212	50.000000	170.95995
6	0.3242609E-02	81.618387	267.09119	2.6310219	-50.000000	-0.6146729E-05	431.59829
O 1	527.95831	-2915.9752	87372.578	918.50116	2028.4469	0.7397229	178.04744
4 2	3528.9355	85.002014	13071.669	38.191364	-0.5710527E 09	30.413813	165.67376
C 1	30040.191	15055.292	14984.900	4364.1509	432.96376	431.26100	-0
E 2	11.552535	5.7616374	5.7908973	21257.586	34.752497	34.746706	-0
N 3	57.946669	28.990860	28.955809	30.345142	55.500000	-420.69999	-282.80884
T 4	5.0159268	5.0317049	5.0002284	34.199999	56.144247	-420.50000	-282.89999
O*1	299.99999	507889.25	14.879904	27.119271	30204.991	-0.1562717E-01	0.5757394E-07
P 2	31721.734	0.2141895E 08	0.6743311	-75.325445	0	0	0.1990722E-03
1 3	70.161183	12081.451	14.441556	106.56087	5.4422846	0	0.9105609E 08
4	286.21743	12033.611	0	106.05542	5.4639864	0.9521855	5.4021214
5	5.8459674	13417.888	3.7718242	104.34812	4.8988276	50.000000	154.14935
6	0.2964951E-02	83.587820	286.19476	2.6348918	-50.000000	-0.6146729E-05	430.50857
O 1	554.64419	-2889.2893	84967.431	958.65880	2042.2959	0.7284212	178.15527
4 2	3529.9475	86.013977	13350.536	38.583149	-0.5671804E 09	30.424551	166.62955
C 1	30204.991	15233.633	14971.358	4248.9923	430.82806	431.20937	-0
E 2	11.554576	5.7745224	5.7800539	20675.315	35.338721	34.719463	-0
N 3	58.503608	29.564199	28.939409	3.7964784	55.499999	-420.69999	-282.89734
T 4	5.0632412	5.1197652	5.0067715	34.199999	56.586725	-420.49999	-282.89999
O*1	309.99999	518680.50	15.320131	27.029113	30100.839	-0.1414827E-01	0.5179774E-07
P 2	31021.457	0.2142983E 08	0.6914930	-74.974297	0	0	0.1802328E-03
1 3	69.872808	12352.981	13.863675	106.76787	4.7883997	0	0.9105612E 08
4	305.76185	12305.137	0	106.24442	4.8070621	0.9703227	5.3789853
5	6.2072042	13691.139	4.1422172	104.55127	4.3194504	50.000000	142.71031
6	0.2763742E-02	85.363832	305.73631	2.6386232	-50.000000	-0.6146729E-05	430.79475
O 1	582.99083	-2860.9427	82591.483	1000.7466	2056.9382	0.7165735	178.28609
4 2	3530.8856	86.952087	13636.827	38.998830	-0.5631429E 09	30.435212	165.58642
C 1	30100.839	15146.084	14954.755	4133.7848	431.39890	431.21147	-0
E 2	11.489381	5.7154769	5.7739042	20091.275	35.089017	34.680792	-0
N 3	58.280428	29.373540	28.906888	10.256853	55.499999	-420.72418	-282.68229
T 4	5.0725472	5.1392982	5.0064717	34.199999	56.696757	-420.52419	-282.92418

[redacted]

[redacted]

0*1	319.99999	528346.75	15.682774	26.935817	30009.332	-0.1309064E-01	0.5719609E-07
P 2	30324.084	0.2143959E 08	0.7077163	-74.615703	0	0	0.1667597E-03
1 3	69.607484	12633.075	13.248624	106.97687	4.1821213	0	0.9105614E 08
4	325.75641	12585.238	0	106.43561	4.1980467	0.9896200	5.3781404
5	6.5759320	13972.662	4.5320452	104.75662	3.7805576	50.000000	135.04783
6	0.2617660E-02	86.954692	325.72764	2.6422095	-50.000000	-0.6146729E-05	431.12221
0 1	612.99194	-2830.9416	80254.376	1044.6652	2072.3684	0.7042071	178.40805
4 2	3531.7449	87.811340	13929.456	39.438478	-0.5589499E 09	30.445756	166.54454
C 1	30009.332	15071.270	14938.062	4018.9928	432.05341	431.21518	-0
E 2	11.475180	5.7072835	5.7678961	19509.724	34.862703	34.641782	-0
N 3	58.029305	29.155420	28.873886	17.738150	55.499999	-420.74912	-282.45785
T 4	5.0569409	5.1084583	5.0059649	34.199999	56.796507	-420.54912	-282.94912
0*1	329.99999	536934.50	15.967553	26.839264	29944.231	-0.1233998E-01	0.5355009E-07
P 2	29629.136	0.2144827E 08	0.7229590	-74.249497	0	0	0.1571972E-03
1 3	69.403937	12922.012	12.594182	107.18790	3.6217136	0	0.9105615E 08
4	346.21263	12874.192	0	106.62902	3.6351843	1.0106342	5.3964978
5	6.9523463	14262.770	4.9415132	104.96425	3.2808657	50.000000	130.22561
6	0.2512369E-02	88.368053	346.18053	2.6456427	-50.000000	-0.6146729E-05	431.44860
0 1	644.80652	-2799.1270	77952.200	1090.5504	2088.6662	0.6912831	178.53197
4 2	3532.5259	88.592407	14228.936	39.904628	-0.5545884E 09	30.456191	166.50383
C 1	29944.231	15014.903	14929.328	3904.1780	432.70792	431.21885	-0
E 2	11.494216	5.7292584	5.7649575	18930.621	34.679706	34.621232	-0
N 3	57.806722	28.950448	28.856274	25.219447	55.499999	-420.77406	-282.23341
T 4	5.0292009	5.0530881	5.0054617	34.199999	56.896258	-420.57406	-282.97406
0*1	339.99999	544494.00	16.173365	26.739332	29902.255	-0.1190553E-01	0.5039468E-07
P 2	28935.853	0.2145593E 08	0.7371728	-73.875502	0	0	0.1515628E-03
1 3	69.254409	13220.260	11.897462	107.40098	3.1056299	0	0.9105618E 08
4	367.14335	13172.463	0	106.82470	3.1169109	1.0333977	5.4640782
5	7.3366597	14561.963	5.3714932	105.17424	2.8192425	50.000000	128.55267
6	0.2455184E-02	89.612187	367.10760	2.6489155	-50.000000	-0.6146729E-05	431.77403
0 1	678.62950	-2765.3040	75680.254	1138.5727	2105.9299	0.6777531	178.65757
4 2	3533.2303	89.296814	14535.948	40.400392	-0.5500421E 09	30.466533	166.46420
C 1	29902.255	14973.026	14929.229	3789.0369	433.36238	431.22249	-0
E 2	11.536289	5.7709401	5.7653488	18353.510	34.530699	34.620711	-0
N 3	57.615120	28.759758	28.855362	32.700743	55.500000	-420.79900	-282.00897
T 4	4.9942508	4.9835482	5.0049638	34.199999	56.996009	-420.59900	-282.99900
0*1	349.99999	551075.50	16.299187	26.635892	29900.835	-0.1171735E-01	0.4802881E-07
P 2	28243.364	0.2146261E 08	0.7503148	-73.493521	0	0	0.1492656E-03
1 3	69.248932	13528.299	11.155601	107.61616	2.6322775	0	0.9105620E 08
4	388.56235	13480.532	0	107.02269	2.6416121	1.0586849	5.5526294
5	7.7290984	14870.750	5.8223440	105.38667	2.3945036	50.000000	129.47973
6	0.2435217E-02	90.695363	388.52271	2.6520196	-50.000000	-0.6146729E-05	431.78767
0 1	714.67823	-2729.2553	73434.398	1188.9137	2124.2688	0.6635651	178.78462
4 2	3533.8593	89.925751	14851.176	40.929260	-0.5452936E 09	30.476800	166.42559
C 1	29900.835	14972.787	14928.048	3673.6541	433.36658	431.24554	-0
E 2	11.538388	5.7708454	5.7675422	17777.434	34.529812	34.616120	-0

[redacted]

[redacted]

N 3	57.607545	28.758967	28.848578	33.000000	55.499999	-420.81578	-282.20526
T 4	4.9926859	4.9834929	5.0018841	34.136841	57.031578	-420.64736	-283.03157
0*1	359.99999	556730.00	16.344107	26.528803	29901.009	-0.1164718E-01	0.4611076E-07
P 2	27550.874	0.2146837E 08	0.7623504	-73.103342	0	0	0.1483717E-03
1 3	69.249238	13846.633	10.365777	107.83347	2.2000113	0	0.9105622E 08
4	410.48451	13798.903	0	107.22303	2.2076254	1.0853013	5.6499439
5	8.1299144	15189.662	6.2949374	105.60162	2.0054092	50.000000	131.74395
6	0.2427364E-02	91.625974	410.44072	2.6549476	-50.000000	-0.6146729E-05	431.78828
0 1	753.19675	-2690.7368	71210.943	1241.7681	2143.8054	0.6486636	178.91293
4 2	3534.4139	90.480408	15175.317	41.495187	-0.5403243E 09	30.486996	166.38793
C 1	29901.009	14974.191	14926.818	3558.2695	433.34367	431.26932	-0
E 2	11.538532	5.7687299	5.7698020	17201.357	34.534878	34.611362	-0
N 3	57.607707	28.766148	28.841559	33.000000	55.499999	-420.83223	-282.41908
T 4	4.9926375	4.9865652	4.9987087	34.071052	57.064473	-420.69670	-283.06447
0*1	369.99999	561509.75	16.308485	26.417917	29901.179	-0.1168324E-01	0.4455676E-07
P 2	26858.380	0.2147326E 08	0.7732695	-72.704739	0	0	0.1488311E-03
1 3	69.249545	14175.589	9.5261331	108.05295	1.8068981	0	0.9105624E 08
4	432.92567	14127.900	0	107.42578	1.8129997	1.1132901	5.7558708
5	8.5393680	15519.048	6.7896323	105.81915	1.6504326	50.000000	135.30266
6	0.2429653E-02	92.412620	432.87751	2.6576927	-50.000000	-0.6146729E-05	431.78881
0 1	794.43434	-2649.4992	69007.909	1297.3104	2164.6649	0.6329989	179.04257
4 2	3534.8954	90.961884	15508.875	42.102290	-0.5351175E 09	30.497131	165.35119
C 1	29901.179	14975.595	14925.585	3442.8835	433.32076	431.29298	-0
E 2	11.538665	5.7666129	5.7720518	16625.279	34.539944	34.606602	-0
N 3	57.607881	28.773331	28.834550	33.000000	55.500000	-420.84867	-282.63289
T 4	4.9925951	4.9896414	4.9955460	34.005262	57.097368	-420.74604	-283.09735
0*1	379.99999	565465.75	16.192800	26.303082	29901.347	-0.1181791E-01	0.4333957E-07
P 2	26165.883	0.2147733E 08	0.7830703	-72.297477	0	0	0.1505466E-03
1 3	69.249855	14515.543	8.6349239	108.27466	1.4510069	0	0.9105626E 08
4	455.90250	14467.899	0	107.63101	1.4557848	1.1427604	5.8703361
5	8.9577359	15859.305	7.3073517	106.03934	1.3280392	50.000000	140.15595
6	0.2440328E-02	93.063693	455.84962	2.6602500	-50.000000	-0.6146729E-05	431.78930
0 1	838.67477	-2605.2588	66823.342	1355.7315	2186.9899	0.6165164	179.17362
4 2	3535.3050	91.371429	15852.395	42.755290	-0.5296550E 09	30.507209	166.31535
C 1	29901.347	14976.998	14924.349	3327.4962	433.29785	431.31652	-0
E 2	11.538786	5.7644933	5.7742926	16049.200	34.545009	34.601848	-0
N 3	57.608070	28.780515	28.827555	33.000000	55.499999	-420.86512	-282.84670
T 4	4.9925590	4.9927225	4.9923959	33.939473	57.130262	-420.79538	-283.13026
0*1	389.99999	568649.75	15.997717	26.184131	29901.511	-0.1204661E-01	0.4238374E-07
P 2	25473.383	0.2148063E 08	0.7917593	-71.881308	0	0	0.1534600E-03
1 3	69.250173	14866.926	7.6905915	108.49865	1.1304188	0	0.9105628E 08
4	479.43237	14819.332	0	107.83876	1.1340504	1.1738331	5.9933235
5	9.3853109	16210.884	7.8488137	106.26223	1.0366926	50.000000	145.33860
6	0.2457714E-02	93.587712	479.37453	2.6626156	-50.000000	-0.6146729E-05	431.78970
0 1	886.24226	-2557.6913	64655.308	1417.2401	2210.9433	0.5991565	179.30627

[redacted]

[redacted]

4 2	3535.6443	91.710785	16206.456	43.459638	-0.5239167E 09	30.517229	165.28036
C 1	29901.511	14978.401	14923.110	3212.1078	433.27491	431.33994	-0
E 2	11.538896	5.7623726	5.7765238	15473.118	34.550077	34.597096	-0
N 3	57.608277	28.787704	28.820573	33.000000	55.499999	-420.88157	-283.06052
T 4	4.9925292	4.9958075	4.9892588	33.873683	57.163157	-420.84473	-283.16315
0*1	399.99999	571113.50	15.724190	26.060892	29901.671	-0.1236727E-01	0.4166295E-07
P 2	24780.879	0.2148321E 08	0.7993532	-71.455974	0	0	0.1575448E-03
I 3	69.250488	15230.228	6.6918684	108.72494	0.8432417	0	0.9105631E 08
4	503.53381	15182.687	0	108.04910	0.8458824	1.2066423	6.1248688
5	9.8223977	16574.291	8.4147359	106.48790	0.7748566	50.000000	153.91743
6	0.2480154E-02	93.993194	503.47069	2.6647887	-50.000000	-0.6146729E-05	431.79004
0 1	937.50871	-2506.4248	62501.893	1482.0645	2236.7121	0.5808541	179.44078
4 2	3535.9155	91.981934	16571.682	44.221638	-0.5178808E 09	30.527198	155.24522
C 1	29901.671	14979.804	14921.867	3096.7184	433.25197	431.36325	-0
E 2	11.538995	5.7602496	5.7787456	14897.034	34.555144	34.592346	-0
N 3	57.608494	28.794894	28.813600	33.000000	55.500000	-420.89802	-283.27433
T 4	4.9925053	4.9988970	4.9861340	33.807894	57.196052	-420.89407	-283.19604
0*1	409.99999	572906.50	15.373641	25.933180	29900.123	-0.1278011E-01	0.4114843E-07
P 2	24088.400	0.2148513E 08	0.8058801	-71.021197	0	0	0.1628039E-03
I 3	69.244528	15605.987	5.6379573	108.95360	0.5875883	0	0.9105633E 08
4	528.22615	15558.500	0	108.26208	0.5893822	1.2412659	6.2650645
5	10.269321	16950.076	9.0060418	106.71641	0.5409927	50.000000	162.99253
6	0.2506007E-02	94.288283	528.15753	2.6667715	-50.000000	-0.6146729E-05	431.80485
0 1	992.90128	-2451.0323	60361.250	1550.4534	2264.5110	0.5615383	179.57755
4 2	3536.1206	92.187103	16948.732	45.048604	-0.5115233E 09	30.537117	166.21289
C 1	29900.123	14979.724	14920.399	2981.3151	433.25482	431.39002	-0
E 2	11.542022	5.7607725	5.7812495	14320.989	34.554732	34.586796	-0
N 3	57.599506	28.793960	28.805547	32.809730	55.500000	-420.94756	-283.39513
T 4	4.9904173	4.9982810	4.9825814	33.704864	57.104864	-420.94756	-283.29513
0*1	419.99999	574079.75	14.948112	25.800805	29898.543	-0.1329603E-01	0.4082379E-07
P 2	23395.988	0.2148643E 08	0.8113810	-70.576698	0	0	0.1693762E-03
I 3	69.238495	15994.795	4.5286962	109.18465	0.3616114	0	0.9105636E 08
4	553.52989	15947.366	0	108.47775	0.3626871	1.2779340	6.4156298
5	10.726420	17338.846	9.6235514	106.94782	0.3335800	50.000000	173.81069
6	0.2535255E-02	94.481376	553.45538	2.6685710	-50.000000	-0.6146729E-05	431.81965
0 1	1052.9131	-2391.0204	58231.580	1622.6780	2294.5878	0.5411319	179.71712
4 2	3536.2625	92.328949	17338.303	45.949070	-0.5048184E 09	30.546988	166.18037
C 1	29898.543	14979.561	14918.982	2865.8783	433.25889	431.41555	-0
E 2	11.545103	5.7614650	5.7836377	13745.043	34.554029	34.581466	-0
N 3	57.590393	28.792564	28.797828	32.597044	55.522166	-421.00147	-283.50147
T 4	4.9882963	4.9974381	4.9791895	33.597044	57.002954	-420.99999	-283.40147
0*1	429.99999	574682.00	14.450082	25.663559	29904.085	-0.1390947E-01	0.4065447E-07
P 2	22703.502	0.2148717E 08	0.8159052	-70.122174	0	0	0.1771907E-03
I 3	69.258788	16397.374	3.3644529	109.41814	0.1635723	0	0.9105638E 08
4	579.46668	16350.006	0	108.69618	0.1640472	1.3171568	6.5756106

[redacted]

5	11.194056	17741.333	10.268239	107.18220	0.1511822	50.000000	185.42064
6	0.2564164E-02	94.580493	579.38586	2.6701998	-50.000000	-0.6146729E-05	431.77314
0 1	1118.1290	-2325.8046	56110.738	1699.0489	2327.2365	0.5195465	179.86019
4 2	3536.3439	92.410400	17741.216	46.933232	-0.4977363E 09	30.556815	165.14862
C 1	29904.085	14983.475	14920.610	2750.4658	433.19300	431.38775	-0
E 2	11.537398	5.7560848	5.7813137	13168.999	34.568322	34.587467	-0
N 3	57.618391	28.812237	28.806154	32.498521	56.261083	-421.05073	-283.55074
T 4	4.994054C	5.0055269	4.9826311	33.498521	57.101477	-420.99999	-283.45073
0*1	439.99999	574764.00	13.883083	25.521228	29909.664	-0.1461891E-01	0.4063148E-07
P 2	22010.812	0.2148738E 08	0.8195181	-69.657303	0	0	0.1862281E-03
1 3	69.279202	16814.521	2.1466908	109.65411	-0.8204460E-02	0	0.9105642E 08
4	606.05939	16767.215	0	108.91741	-0.8226395E-02	1.3588617	6.7431232
5	11.672609	18158.342	10.941028	107.41961	-0.7596970E-02	50.000000	200.92839
6	0.2589579E-02	94.593988	605.97211	2.6716798	-50.000000	-0.6146729E-05	431.72644
0 1	1189.2338	-2254.6997	53996.607	1779.9081	2362.8011	0.4966848	-179.99230
4 2	3536.3685	92.434937	18158.343	48.013179	-0.4902445E 09	30.566599	166.11762
C 1	29909.664	14987.430	14922.233	2635.1303	433.12674	431.35994	-0
E 2	11.529699	5.7507070	5.7789920	12592.675	34.582742	34.593462	-0
N 3	57.646504	28.832035	28.814469	32.399999	56.999999	-421.09999	-283.59999
T 4	4.9998273	5.0136504	4.9860718	33.399999	57.199999	-420.99999	-283.49999
0*1	449.99999	574373.50	13.252527	25.373579	29908.098	-0.1543048E-01	0.4074110E-07
P 2	21318.049	0.2148713E 08	0.8223094	-69.181749	0	0	0.1965667E-03
1 3	65.273376	17247.004	0.8787439	109.89259	-0.1553802	0	0.9105645E 08
4	633.33233	17199.762	0	109.14150	-0.1558065	1.4029465	6.9184417
5	12.162485	18590.650	11.643098	107.66010	-0.1441488	50.000000	217.55415
6	0.2609667E-02	94.529720	633.23823	2.6730448	-50.000000	-0.6146729E-05	431.74015
0 1	1267.0168	-2176.9168	51887.569	1865.6128	2401.6782	0.4724452	-179.83904
4 2	3536.3397	92.406158	18590.527	49.203040	-0.4823086E 09	30.576339	166.08738
C 1	29908.098	14986.320	14921.779	2519.8197	433.14576	431.36852	-0
E 2	11.532420	5.7525561	5.7798638	12016.253	34.578659	34.591719	-0
N 3	57.637957	28.826102	28.811855	32.250249	56.833611	-421.13327	-283.68319
T 4	4.9979065	5.0110076	4.9848674	33.316804	57.166721	-421.03328	-283.58319
0*1	459.99999	573558.75	12.565636	25.220370	29906.524	-0.1634866E-01	0.4096332E-07
P 2	20625.344	0.2148646E 08	0.8243897	-68.695161	0	0	0.2082632E-03
1 3	69.267533	17695.660	-0.4341294	110.13362	-0.2794800	0	0.9105648E 08
4	661.31117	17648.483	0	109.36850	-0.2802267	1.4499883	7.1019636
5	12.664111	19039.100	12.375577	107.90375	-0.2597589	50.000000	236.51301
6	0.2622234E-C2	94.395630	661.20985	2.6743450	-50.000000	-0.6146729E-05	431.75395
0 1	1352.4103	-2091.5233	49782.012	1956.5546	2444.3361	0.4467167	-179.67826
4 2	3536.2620	92.328430	19038.664	50.519737	-0.4738915E 09	30.586037	166.05788
C 1	29906.524	14985.206	14921.319	2404.4819	433.16480	431.37708	-0
E 2	11.535141	5.7544102	5.7807311	11439.916	34.574567	34.589967	-0
N 3	57.629393	28.820157	28.809236	32.100498	56.667221	-421.16655	-283.75639
T 4	4.9959849	5.0083598	4.9836664	33.233610	57.133443	-421.06655	-283.65639

[redacted]

O*1	469.99999	572367.75	11.831638	25.061342	29904.942	-0.1740756E-01	0.4130215E-07
P 2	19932.698	0.2148542E 08	0.8258895	-68.197164	0	0	0.2217524E-03
I 3	65.261674	18161.452	-1.7844561	110.37722	-0.3817987	0	0.9105652E 08
4	690.02307	18114.343	0	109.59847	-0.3827896	1.5002948	7.2982304
5	13.177936	19504.665	13.139644	108.15060	-0.3555040	50.000000	258.47943
6	0.2629723E-02	94.199616	689.91415	2.6756529	-50.000000	-0.6146729E-05	431.76753
O 1	1446.5368	-1997.3967	47678.056	2053.1762	2491.3384	0.4193736	-179.50777
4 2	3536.1400	92.206451	19503.771	51.983891	-0.4649509E 09	30.595687	166.02912
C 1	29904.942	14984.087	14920.855	2289.1169	433.18383	431.38559	-0
E 2	11.537864	5.7562685	5.7815954	10863.665	34.570467	34.588209	-0
N 3	57.620811	28.814198	28.806613	31.950748	56.500832	-421.19983	-283.84958
T 4	4.9940623	5.0057077	4.9824678	33.150415	57.100166	-421.09983	-283.74958
O*1	479.99999	570849.00	11.062591	24.896221	29903.353	-0.1860197E-01	0.4173956E-07
P 2	19240.111	0.2148406E 08	0.8269688	-67.687364	0	0	0.2369678E-03
I 3	65.255802	18645.435	-3.1616997	110.62344	-0.4633703	0	0.9105656E 08
4	719.49667	18598.394	0	109.83145	-0.4645405	1.5542184	7.5048231
5	13.704442	19988.400	13.936530	108.40072	-0.4322357	50.000000	283.59581
6	0.2628435E-02	93.949662	719.37980	2.6770721	-50.000000	-0.6146729E-05	431.78120
O 1	1550.7467	-1893.1868	45573.792	2155.9675	2543.3626	0.3902770	-179.32467
4 2	3535.9786	92.045044	19986.944	53.620656	-0.4554404E 09	30.605288	165.00110
C 1	29903.353	14982.967	14920.387	2173.7246	433.20288	431.39406	-0
E 2	11.540588	5.7581326	5.7824559	10287.500	34.566360	34.586444	-0
N 3	57.612215	28.808227	28.803988	31.800998	56.334442	-421.23310	-283.93277
T 4	4.9921383	5.0030502	4.9812724	33.067220	57.066887	-421.13310	-283.83278
O*1	489.99999	569053.25	10.274072	24.724713	29901.755	-0.1994227E-01	0.4226458E-07
P 2	18547.583	0.2148243E 08	0.8278259	-67.165344	0	0	0.2540417E-03
I 3	69.249912	19148.754	-4.5514878	110.87228	-0.5248852	0	0.9105661E 08
4	749.76260	19101.784	0	110.06749	-0.5261755	1.6121635	7.7220740
5	14.244136	20491.458	14.767722	108.65416	-0.4904909	50.000000	312.25831
6	0.2618145E-02	93.654119	749.63747	2.6787504	-50.000000	-0.6146729E-05	431.79485
O 1	1666.6790	-1777.2545	43467.263	2265.4718	2601.2311	0.3592730	-179.12514
4 2	3535.7832	91.849701	20489.371	55.461052	-0.4453084E 09	30.614836	165.97382
C 1	29901.755	14981.842	14919.914	2058.3051	433.22194	431.40250	-0
E 2	11.543315	5.7600009	5.7833139	9711.4205	34.562242	34.584671	-0
N 3	57.603598	28.802241	28.801357	31.651248	56.168053	-421.26638	-284.01597
T 4	4.9902129	5.0003883	4.9800784	32.984026	57.033610	-421.16638	-283.91597
O*1	499.99999	567033.00	9.4860085	24.546507	29900.150	-0.2143920E-01	0.4286560E-07
P 2	17855.113	0.2148057E 08	0.8287117	-66.630662	0	0	0.2731108E-03
I 3	69.244010	19672.664	-5.9346703	111.12378	-0.5665731	0	0.9105666E 08
4	780.85324	19625.766	0	110.30662	-0.5679264	1.6745976	7.9503224
5	14.797558	21015.100	15.634656	108.91097	-0.5303793	50.000000	344.90590
6	0.2600244E-02	93.321630	780.71960	2.6809010	-50.000000	-0.6146729E-05	431.80847
O 1	1796.3446	-1647.5890	41356.428	2382.2947	2665.9522	0.3261903	-178.90420
4 2	3535.5599	91.626373	21012.342	57.543761	-0.4344977E 09	30.624321	165.94729
C 1	29900.150	14980.714	14919.437	1942.8584	433.24099	431.41090	-0
E 2	11.546043	5.7618744	5.7841685	9135.4277	34.558119	34.582892	-0

[redacted]

[redacted]

N 3	57.594968	28.796244	28.798724	31.501497	56.001664	-421.29966	-284.09916
T 4	4.9882863	4.9977216	4.9788874	32.900831	57.000332	-421.19966	-283.99915
0*1	509.99999	564845.50	8.7235287	24.361272	29900.608	-0.2310286E-01	0.4352903E-07
P 2	17162.664	0.2147856E 08	0.8299531	-66.082849	0	0	0.2943039E-03
1 3	69.245779	20218.562	-7.2863024	111.37793	-0.5880375	0	0.9105672E 08
4	812.80340	20171.739	0	110.54889	-0.5894012	1.7421878	8.1898937
5	15.365286	21560.727	16.538870	109.17119	-0.5514288	50.000000	382.00975
6	0.2578608E-02	92.961614	812.66068	2.6838324	-50.000000	-0.6146729E-05	431.80405
0 1	1942.2441	-1501.6894	39239.054	2507.1183	2738.7793	0.2908358	-178.65509
4 2	3535.3144	91.380859	21557.296	59.917716	-0.4229440E 09	30.633738	165.92153
C 1	29900.608	14980.467	14920.141	1827.3996	433.24490	431.39819	-0
E 2	11.545677	5.7623549	5.7833222	8559.4679	34.557237	34.585543	-0
N 3	57.597103	28.794882	28.802221	31.416573	56.000000	-421.34171	-284.22513
T 4	4.9886293	4.9970685	4.9802207	32.691432	56.986095	-421.22780	-284.11123
0*1	519.99998	562557.50	8.0181000	24.168654	29901.077	-0.2494091E-01	0.4423736E-07
P 2	16470.197	0.2147644E 08	0.8320019	-65.521406	0	0	0.3177186E-03
1 3	69.247616	20787.993	-8.5743343	111.63473	-0.5880775	0	0.9105678E 08
4	845.64981	20741.245	0	110.79432	-0.5894012	1.8154641	8.4410487
5	15.947932	22129.888	17.482108	109.43487	-0.5524149	50.000000	424.04551
6	0.2560824E-02	92.585057	845.49762	2.6880068	-50.000000	-0.6146729E-05	431.79937
0 1	2107.5241	-1336.4094	37112.726	2640.7115	2821.2884	0.2529923	-178.36839
4 2	3535.0526	91.119080	22125.827	62.645649	-0.4105749E 09	30.643068	165.89655
C 1	29901.077	14980.224	14920.853	1711.9448	433.24856	431.38523	-0
E 2	11.545283	5.7628146	5.7824686	7983.4857	34.556385	34.588232	-0
N 3	57.599333	28.793570	28.805763	31.332303	56.000000	-421.38384	-284.35154
T 4	4.9889926	4.9964422	4.9815685	32.480758	56.972050	-421.25589	-284.22359
0*1	529.99998	560246.50	7.4086224	23.968272	29901.536	-0.2695679E-01	0.4495818E-07
P 2	15777.712	0.2147432E 08	0.8355277	-64.945801	0	0	0.3433986E-03
1 3	69.249438	21382.652	-9.7582853	111.89418	-0.5644503	0	0.9105685E 08
4	879.43183	21335.982	0	111.04293	-0.5656843	1.8951740	8.7039492
5	16.546154	22724.285	18.466062	109.70204	-0.5311241	50.000000	471.46148
6	0.2559883E-02	92.204715	879.26999	2.6941440	-50.000000	-0.6146729E-05	431.79464
0 1	2296.1947	-1147.7388	34974.876	2783.9406	2915.4875	0.2124148	-178.02995
4 2	3534.7803	90.846771	22719.694	65.809180	-0.3973092E 09	30.652289	165.97243
C 1	29901.536	14979.976	14921.560	1596.4940	433.25215	431.37225	-0
E 2	11.544891	5.7632675	5.7816238	7407.4813	34.555525	34.590914	-0
N 3	57.601548	28.792258	28.809290	31.248034	56.000000	-421.42598	-284.47794
T 4	4.9893538	4.9958219	4.9829063	32.270083	56.958004	-421.28398	-284.33595
0*1	539.99998	558007.25	6.9417977	23.759723	29901.985	-0.2914614E-01	0.4569142E-07
P 2	15085.209	0.2147227E 08	0.8416306	-64.355467	0	0	0.3712885E-03
1 3	69.251246	22004.432	-10.788577	112.15623	-0.5135746	0	0.9105693E 08
4	914.19186	21957.841	0	111.29470	-0.5146646	1.9822037	8.9785900
5	17.160655	23345.818	19.492835	109.97269	-0.4840651	50.000000	524.60949
6	0.2595918E-02	91.836182	914.01986	2.7034563	-50.000000	-0.6146729E-05	431.78985
0 1	2513.4603	-930.47327	32822.636	2937.7924	3023.9804	0.1688239	-177.61563

[redacted]

[redacted]

4 2	3534.5006	90.567078	23340.890	69.516543	-0.3830548E 09	30.661368	165.84922
C 1	29901.985	14979.722	14922.264	1481.0470	433.25566	431.35923	-0
E 2	11.544501	5.7637130	5.7807884	6831.4549	34.554659	34.593588	-0
N 3	57.603745	28.790946	28.812799	31.163764	56.000000	-421.46811	-284.60435
T 4	4.9897127	4.9952081	4.9842335	32.059410	56.943960	-421.31207	-284.44831
O*1	549.99998	555961.50	6.6695542	23.542572	29902.423	-0.3149096E-01	0.4636550E-07
P 2	14392.687	0.2147042E 08	0.8524352	-63.749793	0	0	0.4011587E-03
I 3	69.253037	22655.463	-11.608800	112.42079	-0.4302111	0	0.9105701E 08
4	949.97501	22608.951	0	111.54958	-0.4310961	2.0776100	9.2645793
5	17.792188	23996.623	20.564272	110.24680	-0.4061661	50.000000	583.62206
6	0.2696925E-02	91.499495	949.79250	2.7182942	-50.000000	-0.6146729E-05	431.78501
O 1	2766.2020	-677.73157	30652.775	3103.3984	3150.2082	0.1218987	-177.07233
4 2	3534.2145	90.280945	23991.687	73.914320	-0.3677059E 09	30.670241	165.82706
C 1	29902.423	14979.462	14922.962	1365.6039	433.25908	431.34619	-0
E 2	11.544112	5.7641508	5.7799608	6255.4065	34.553786	34.596252	-0
N 3	57.605927	28.789635	28.816292	31.079494	56.000000	-421.51025	-284.73075
T 4	4.9900702	4.9946013	4.9855514	31.848736	56.929914	-421.34016	-284.55067
O*1	559.99998	554265.00	6.6303288	23.316354	29902.852	-0.3395278E-01	0.4693437E-07
P 2	13700.148	0.2146892E 08	0.8733843	-63.128129	0	0	0.4325196E-03
I 3	69.254818	23338.146	-12.174349	112.68769	-0.3073568	0	0.9105711E 08
4	986.82995	23291.718	0	111.80743	-0.3079691	2.1826639	9.5615236
5	18.441562	24679.114	21.682682	110.52424	-0.2906551	50.000000	648.24969
6	0.2892082E-02	91.220287	986.63663	2.7446430	-50.000000	-0.6146729E-05	431.78010
O 1	3063.7125	-380.22107	28461.661	3282.0608	3298.8164	0.7126920E-01	-175.20901
4 2	3533.9204	89.986877	24674.676	79.205789	-0.3511411E 09	30.678781	165.80623
C 1	29902.852	14979.196	14923.656	1250.1647	433.26241	431.33312	-0
E 2	11.543725	5.7645812	5.7791443	5679.3364	34.552907	34.598911	-0
N 3	57.608093	28.788326	28.819767	30.995224	56.000000	-421.55238	-284.85715
T 4	4.9904247	4.9940012	4.9868571	31.638062	56.915870	-421.36825	-284.67303
O*1	569.99998	553119.50	6.6360809	23.080571	29903.270	-0.3646341E-01	0.4732365E-07
P 2	13007.591	0.2146799E 08	0.9341623	-62.489775	0	0	0.4645020E-03
I 3	69.256581	24055.311	-12.667566	112.95627	-0.1382647	0	0.9105721E 08
4	1024.8091	24008.967	0	112.06764	-0.1385317	2.2989063	9.8678923
5	19.109649	25396.130	22.850012	110.80445	-0.1309633	50.000000	717.62263
6	0.3112327E-02	91.031762	1024.6046	2.8149135	-50.000000	-0.6146729E-05	431.77514
O 1	3418.8083	-25.125244	26245.629	3475.3106	3476.2601	0.1652690E-01	-172.18346
4 2	3533.7119	89.778320	25392.216	85.681703	-0.3332173E 09	30.686596	165.78752
C 1	29903.270	14978.924	14924.346	1134.7294	433.26566	431.32001	-0
E 2	11.543340	5.7650049	5.7783356	5103.2448	34.552021	34.601562	-0
N 3	57.610241	28.787016	28.823226	30.910954	56.000000	-421.59452	-284.98356
T 4	4.9907773	4.9934070	4.9881536	31.427387	56.901824	-421.39634	-284.78539
O*1	573.09016	552912.25	5.3028592	23.005694	29938.184	-0.3723521E-01	0.4739453E-07
P 2	12793.592	0.2146785E 08	1.0963539	-62.289019	0	0	0.4743339E-03
I 3	69.334133	24284.583	-14.153330	113.03904	-0.7951450E-01	0	0.9105725E 08
4	1036.7813	24238.266	0	112.14796	-0.7966518E-01	2.3400893	9.9643199

[redacted]

[redacted]

5	19.320029	25625.372	23.220815	110.89108	-0.7535267E-01	50.000000	739.81087
6	0.2567923E-02	90.997653	1036.5732	2.9916047	-50.000000	-0.6146729E-05	431.79575
0 1	3531.4911	87.557587	25637.411	3538.3004	3538.3136	0.1928170E-02	-42.117909
4 2	3545.1360	101.20248	25538.734	87.986122	-0.3273735E 09	30.688514	165.78312
C 1	29938.184	14977.667	14960.517	1099.0266	433.90347	430.73166	-0
E 2	11.617187	5.8626166	5.7545708	4925.2665	34.498335	34.732800	-0
N 3	57.613947	28.635718	28.978229	21.514194	44.173146	-421.59999	-285.00000
T 4	4.9593714	4.8844603	5.0356890	21.800484	56.049031	-421.50000	-284.80000

[redacted]

[redacted]

0 1	TIME	ALTITUDE	ALPHA	GEOCENT LAT	THRUST FIXED	AXL FORCE	ATM PRESS
P 2	WEIGHT	RADIUS	BETA	LONGITUDE	THRUST CONTL	SIDE FORCE	DYNM PRESS
1 3	TOTAL FLOW	VEL E	PSI	AZI E	GAMMA E	NORM FORCE	HEAT PARAM
4	GRND RANGE	VEL R	PSIDOT	AZI R	GAMMA R	AXL LD FCTR	MACH NUMBER
5	THETA I	VEL I	CROSS RANGE	AZI I	GAMMA I	WIND VEL	RHO-VR CUBED
6	Q*ALPHA TOT	ALT	DOWN RANGE	PHI	EAST WIND	NORTH WIND	TOTAL ISP
0 1	SEC	FT	DEG	DEG	LBS	LBS	PSI
P 2	LBS	FT	DEG	DEG	LBS	LBS	LBS/FT SQD
1 3	LBS/SEC	FT/SEC	DEG	DEG	DEG	LBS	FT*LBS/FT SQD
4	N. MI.	FT/SEC	DEG/SEC	DEG	DEG		
5	DEG	FT/SEC	N.MI.	DEG	DEG	FT/SEC	LBS/SEC CUBED
6	DEG-PSF	N.MI	N.MI.	DEG	FT/SEC	FT/SEC	SEC
0 1	PERIGEE RAD	PERIGEE ALT	PERIGEE VEL	SEMI LAT REC	SEMI MAJ AXIS	ECCENTRICITY	TRUE ANOMALY
4 2	APOGEE RAD	APOGEE ALT	APOGEE VEL	PERIOD	ENERGY	INCLINATION	ASCEND NODE
0 1	NM	NM	FT/SEC	NM	NM		DEG
4 2	NM	NM	FT/SEC	MIN	FT**2/SEC**2	DEG	DEG
0*1	573.09016	552912.25	5.3028592	23.005694	17333.330	-0.3723521E-01	0.4739453E-07
P 2	12793.592	0.2146785E 08	1.0963539	-62.289019	0	0	0.4743339E-03
1 3	171.33000	24284.583	-14.153330	113.03904	-0.7951450E-01	0	0.9105725E 08
4	1036.7813	24238.266	0	112.14796	-0.7966518E-01	1.3548418	9.9643199
5	19.320029	25625.372	23.220815	110.89108	-0.7535267E-01	50.000000	739.81097
6	0.2567923E-02	90.997653	1036.5732	2.9916047	-50.000000	-0.6146729E-05	101.16926
0 1	3531.4911	87.557587	25637.411	3538.3004	3538.3136	0.1928170E-02	-42.117909
4 2	3545.1360	101.20248	25538.734	87.986122	-0.3273735E 09	30.688514	165.78312
0*1	573.27234	552902.00	5.3135678	23.001249	17333.330	-0.3726314E-01	0.4739804E-07
P 2	12762.379	0.2146784E 08	1.0963791	-62.277132	0	0	0.4746897E-03
1 3	171.33000	24292.512	-14.153330	113.04410	-0.7776642E-01	0	0.9105725E 08
4	1037.4906	24246.196	0	112.15288	-0.7791328E-01	1.3581553	9.9676880
5	19.332490	25633.298	23.242865	110.89609	-0.7369709E-01	50.000000	740.60809
6	0.2574828E-02	90.995966	1037.2823	2.9916047	-50.000000	-0.6146729E-05	101.16926
0 1	3531.9516	88.018036	25641.991	3540.4878	3540.5085	0.2416869E-02	-31.833172
4 2	3549.0654	105.13187	25518.343	88.068005	-0.3271706E 09	30.688560	165.78303
0*1	573.27234	552902.00	5.3135678	23.001249	17333.330	-0.3726314E-01	0.4739804E-07
P 2	12762.379	0.2146784E 08	1.0963791	-62.277132	0	0	0.4746897E-03
1 3	171.33000	24292.512	-14.153330	113.04410	-0.7776642E-01	0	0.9105725E 08
4	1037.4906	24246.196	0	112.15288	-0.7791328E-01	1.3581553	9.9676880
5	19.332490	25633.298	23.242865	110.89609	-0.7369709E-01	50.000000	740.60809
6	0.2574828E-02	90.995966	1037.2823	2.9916047	-50.000000	-0.6146729E-05	101.16926
0 1	3531.9516	88.018036	25641.991	3540.4878	3540.5085	0.2416869E-02	-31.833172
4 2	3549.0654	105.13187	25518.343	88.068005	-0.3271706E 09	30.688560	165.78303
	$$ INJECTION						

[redacted]

REFERENCES

1. Trajectory and Performance Data. Appendix B. General Dynamics/ Astronautics. Rept. No. 63-0495-19, Dec. 21, 1964.

2. Atlas-Centaur Flight Evaluation Report Vehicle AC-4 (U). General Dynamics/ Astronautics. Rept. No. BNZ-64-045, Feb. 1, 1965.

3. Centaur Unified Test Plan. General Dynamics/Astronautics. Rept. No. AY62-0047, vol. 3, rev. A, section 8.4, AC-4 ETR Test Plan. Nov. 2, 1964.

4. Gossett, John D.: Centaur Test Report (AC-4). Tanking (CTP-INT-0006E). First Attempt (Unsuccessful) Oct. 27, 1964. NASA Goddard Space Flight Center, Goddard Launch Operations, Atlantic Missile Range. Nov. 2, 1964.

5. Gossett, John D.: Centaur Test Report (AC-4). Tanking (CTP-INT-0006E). Conducted Nov. 6, 1964. NASA Goddard Space Flight Center, Goddard Launch Operations, Atlantic Missile Range. Nov. 12, 1964.

6. Gossett, John D.: Centaur Test Report (AC-4). Tanking (CTP-INT-0006G). Conducted Nov. 16, 1964. NASA Goddard Space Flight Center, Goddard Launch Operations, Atlantic Missile Range. Nov. 20, 1964.

7. Gossett, John D.: Centaur Test Report (AC-4). CTP-INT-0005C. Conducted Nov. 30, 1964. NASA Goddard Space Flight Center, Field Projects Branch, Atlantic Missile Range. Dec. 2, 1964.

8. Gossett, John D.: Centaur Test Report (AC-4). FACT (CTP-INT-0001F). Conducted Nov. 24, 1964. NASA Goddard Space Flight Center, Goddard Launch Operations, Atlantic Missile Range. Nov. 28, 1964.

9. Atlas-Centaur Launch Countdown Operations, AC-4 Launch (CTP-INT-0004G). Rept. No. AA63-0500-004-03G, Nov. 27, 1964.

10. Final Flight Test Data BET. AFETR Test No. 4373. RCA/AFETR, Data Processing Section, Patrick Air Force Base, Florida, Dec. 11, 1964.

11. Staff of Lewis Research Center: Postflight Evaluation of Atlas-Centaur AC-3. NASA TM X-1094, 1965.

12. Powers, Carol S.: Precision Determination of Vacuum Specific Impulse from Trajectory Data. Ballistic Missile and Space Technology, Vol. II, D.P. LeGalley, ed., Academic Press, Inc., 1960, pp. 111-126.

13. Pratt & Whitney Aircraft Division, Florida Research and Development Center, United Aircraft Corp.: Model Specification Engine, Rocket, Liquid Propellant: RL10A-3, Specification No. 2272B, Aug. 15, 1962.

14. AC-2 Postflight Analysis (U). Thompson Ramo Wooldridge/Space Technology Laboratories. Rept. No. 8414-6168-RC000. Feb. 28, 1964.

15. Beheim, Milton A.; Klann, John L.; and Yeager, Richard A.: Jet Effects on Annular Base Pressure and Temperature in a Supersonic Stream. NASA TR-R-125, 1962.

16. Baughman, L. Eugene; and Kochendorfer, Fred D.: Jet Effects on Base Pressures for Conical Afterbodies at Mach 1.91 and 3.12. NACA RM-E57E06, 1957.

17. Measurement of Circumferential Loads in the Insulation Panels on the AC-3 Centaur Vehicle. General Dynamics/Astronautics. Rept. No. 55E-3353, July 24, 1964.

18. Environmental Design and Test Requirements for Project Centaur Equipment. General Dynamics/Astronautics. Rept. No. 55-00200E. March 30, 1964.

19. AC-4 Post-Flight Analysis. Thompson Ramo Wooldridge/Space Technology Laboratories. Rept. No. 4222-6023-RC000. March 11, 1965.

20. Wallner, Lewis E.; and Nakanishi, Shigeo: A Study of Liquid Hydrogen in Zero Gravity. NASA TM X-723, 1963.

[redacted]

"The aeronautical and space activities of the United States shall be conducted so as to contribute . . . to the expansion of human knowledge of phenomena in the atmosphere and space. The Administration shall provide for the widest practicable and appropriate dissemination of information concerning its activities and the results thereof."

—NATIONAL AERONAUTICS AND SPACE ACT OF 1958

NASA SCIENTIFIC AND TECHNICAL PUBLICATIONS

TECHNICAL REPORTS: Scientific and technical information considered important, complete, and a lasting contribution to existing knowledge.

TECHNICAL NOTES: Information less broad in scope but nevertheless of importance as a contribution to existing knowledge.

TECHNICAL MEMORANDUMS: Information receiving limited distribution because of preliminary data, security classification, or other reasons.

CONTRACTOR REPORTS: Technical information generated in connection with a NASA contract or grant and released under NASA auspices.

TECHNICAL TRANSLATIONS: Information published in a foreign language considered to merit NASA distribution in English.

TECHNICAL REPRINTS: Information derived from NASA activities and initially published in the form of journal articles.

SPECIAL PUBLICATIONS: Information derived from or of value to NASA activities but not necessarily reporting the results of individual NASA-programmed scientific efforts. Publications include conference proceedings, monographs, data compilations, handbooks, sourcebooks, and special bibliographies.

Details on the availability of these publications may be obtained from:

SCIENTIFIC AND TECHNICAL INFORMATION DIVISION

NATIONAL AERONAUTICS AND SPACE ADMINISTRATION

Washington, D.C. 20546

[redacted]